



City Research Online

City, University of London Institutional Repository

Citation: Clarke, Timothy Alan (1991). Application of optical techniques to surveying. (Unpublished Doctoral thesis, The City University)

This is the accepted version of the paper.

This version of the publication may differ from the final published version.

Permanent repository link: <https://openaccess.city.ac.uk/id/eprint/17365/>

Link to published version:

Copyright: City Research Online aims to make research outputs of City, University of London available to a wider audience. Copyright and Moral Rights remain with the author(s) and/or copyright holders. URLs from City Research Online may be freely distributed and linked to.

Reuse: Copies of full items can be used for personal research or study, educational, or not-for-profit purposes without prior permission or charge. Provided that the authors, title and full bibliographic details are credited, a hyperlink and/or URL is given for the original metadata page and the content is not changed in any way.

**"APPLICATION OF OPTICAL TECHNIQUES TO
SURVEYING."**

By

TIMOTHY ALAN CLARKE.

A thesis submitted for the award of the degree of Doctor of Philosophy.

THE CITY UNIVERSITY.

**DEPARTMENT OF ELECTRICAL, ELECTRONIC AND INFORMATION
ENGINEERING.**

February, 1991.

TABLE OF CONTENTS.

Title page

Table of contents

List of Figures

List of Tables

Acknowledgements

Declaration

Abstract

Synopsis of thesis

1. INTRODUCTION.

- 1.1. General introduction.
- 1.2. Engineering surveys.
- 1.3. Optical triangulation features.
 - 1.3.1. Advantages.
 - 1.3.2. Disadvantages.
- 1.4. Conclusions.

2. A REVIEW OF 2-D & 3-D SPATIAL DATA ACQUISITION TECHNIQUES.

- 2.1. Synopsis.
- 2.2. Introduction.
- 2.3. Surveying.
 - 2.3.1. Introduction.
 - 2.3.2. Surveying procedure for location and measurement of points.
 - 2.3.2.1. Distance measurement.
 - 2.3.2.2. Angle measurement.
 - 2.3.3. Distance measurement by Tacheometry.
 - 2.3.4. Automated surveying equipment.
 - 2.3.5. Conclusion.
- 2.4. Metrology.
 - 2.4.1. Introduction.
 - 2.4.2. Contact methods.
 - 2.4.3. Non-contact methods.
 - 2.4.3.1. Position sensitive detectors.
 - 2.4.3.2. Charged coupled device detectors.
 - 2.4.3.3. Electro optic/mechanical sensors.
 - 2.4.4. Conclusions.
- 2.5. Photogrammetry.
 - 2.5.1. Introduction.
 - 2.5.1.1. History of photogrammetry.
 - 2.5.1.2. The connection with optical triangulation.
 - 2.5.1.3. Definition of the relevant area of photogrammetry.
 - 2.5.2. Close range photogrammetry.
 - 2.5.2.1. Introduction.
 - 2.5.2.2. Potential of close range photogrammetry.
 - 2.5.2.3. Future developments in close range photogrammetry.

- 2.5.3. History of tunnelling.
- 2.5.4. Measuring the profiling of surfaces.
- 2.5.5. The light sectioning method.
- 2.5.6. The future of photogrammetry.
- 2.5.7. Conclusion.

2.6. Machine vision.

- 2.6.1. Introduction.
- 2.6.2. Optical 3-D measurement techniques.
- 2.6.3. Incoherent light techniques.
 - 2.6.3.1. Optical triangulation techniques.
 - 2.6.3.2. Non-triangulation measuring systems.
- 2.6.4. Coherent light techniques.
 - 2.6.4.1. Homodyne techniques.
 - 2.6.2.2. Heterodyne techniques.
- 2.6.5. Conclusions.

2.7. Conclusion.

3. OPTICAL TRIANGULATION THEORY.

- 3.1. Synopsis.
- 3.2. Introduction.
- 3.3. Geometrical optical triangulation theory.
 - 3.3.1. Introduction.
 - 3.3.2. The optical triangulation configuration.
- 3.4. Theory of optical interactions.
 - 3.4.1. Prism.
 - 3.4.1.1. Derivation of the prism deviation equation.
 - 3.4.1.2. Characteristics of prisms.
 - 3.4.1.3. Conclusions.
 - 3.4.2. Filters.
 - 3.4.1.1. Introduction.
 - 3.4.1.2. Matching a filter to the light source and sensor.
 - 3.4.1.3. Filter characteristics.
- 3.5. Theory of CCD sensors.
 - 3.5.1. Features of CCD sensors.
 - 3.5.1.1. Introduction.
 - 3.5.1.2. Photosites.

- 3.5.1.3. Shift registers.
- 3.5.1.4. CCD shift register operation.
- 3.5.1.5. Charge transfer efficiency.
- 3.5.1.6. Dynamic range.
- 3.5.1.7. Spectral response.
- 3.5.1.8. Quantum efficiency.
- 3.5.1.9. Resolution.
- 3.5.1.10. Data rate.
- 3.5.1.11. Reliability.
- 3.5.1.12. Temperature considerations.
- 3.5.1.13. Non ideal performance.
- 3.5.2. Control of CCD sensor light requirements.
 - 3.5.2.1. Introduction.
 - 3.5.2.2. Linear array camera exposure controls.
 - 3.5.2.3. Laser beam size and modulation.
 - 3.5.2.4. Lens design and aperture control.
 - 3.5.2.5. Conclusion.
- 3.5.3. Modulation transfer function of a CCD sensor.
 - 3.5.3.1. Introduction.
 - 3.5.3.2. The MTF of the optics.
 - 3.5.3.3. The MTF of the sensor.
- 3.6. Laser theory.
 - 3.6.1. Laser operation.
 - 3.6.1.1. Spontaneous emission.
 - 3.6.1.2. Stimulated emission.
 - 3.6.1.3. Stimulated absorption.
 - 3.6.2. Semi-conductor diode lasers.
 - 3.6.3. Comparison between diode and gas lasers.
 - 3.6.3.1. Introduction.
 - 3.6.3.2. Technical requirement for optical triangulation.
 - 3.6.3.3. HeNe lasers.
 - 3.6.3.4. Diode lasers.
 - 3.6.4. Gaussian beam optics.
 - 3.6.4.1. Gaussian beam properties.
 - 3.6.4.2. Gaussian beam profile.

3.6.4.3. Propagation of a Gaussian beam.

3.7. Light scattering theory.

3.7.1. Surface reflections.

3.7.2. Laser speckle.

3.8 Signal processing theory.

3.8.1. Introduction.

3.8.2. Image formation.

3.8.3. Data processing.

3.8.4. Survey of techniques.

3.8.5. Algorithms for subpixel accuracy.

3.8.5.1. Centroid method.

3.8.5.2. Weighted centroid method.

3.8.5.3. Vernier method.

3.8.5.4. Interpolation method.

3.8.6. Differences between CCD and PSD sensors.

3.9. Calibration theory.

3.9.1. Calibration and interpolation methods.

3.9.1.1. Introduction.

3.9.1.2. Requirement for calibration and interpolation.

3.9.1.3. Numerical methods.

3.9.1.4. Piecewise linear interpolation.

3.9.1.5. Piecewise parabolic interpolation.

3.9.1.6. Cubic spline interpolation.

3.9.1.7. Lagrange interpolation.

3.9.1.8. Least squares.

3.9.2. Calibration equipment. (Appendix 1.)

3.9.2.1. Calibration tests.

3.9.2.2. Specification of interferometer.

3.9.2.3. Operation of interferometer.

3.9.2.4. Conclusion.

3.10. Conclusion.

4. PROTOTYPE DEVELOPMENT.

4.1. Synopsis of prototype development.

4.2. Introduction.

4.2.1. Research objective.

- 4.2.2. Specification for the measurement technique.
- 4.2.3. Choice of measurement technique.
- 4.2.4. The research objective.
- 4.3. Preliminary investigation.
 - 4.3.1. Introduction.
 - 4.3.2. Analysis of required components.
 - 4.3.3. Tests with CCD camera.
 - 4.3.4. Conclusion.
- 4.4. Prototype I.
 - 4.4.1. Mechanical design.
 - 4.4.2. Electronic design.
 - 4.4.2.1. CCD camera.
 - 4.4.2.2. IBM PC interface.
 - 4.4.2.3. Software design.
 - 4.4.3. Results.
- 4.5. Prototype II.
 - 4.5.1. Introduction.
 - 4.5.2. Mechanical design.
 - 4.5.3. Electronic design.
 - 4.5.3.1. Introduction
 - 4.5.3.2. CCD sensor.
 - 4.5.3.3. Signal conditioning.
 - 4.5.3.4. Laser diode circuit.
 - 4.5.4. Software design.
 - 4.5.4.1. Introduction.
 - 4.5.4.2. Manipulation of raw prototype data.
 - 4.5.4.3. Conversion of image data into distance data.
 - 4.5.4.4. Conversion of data into Cartesian coordinates.
 - 4.5.4.5. Display of data.
 - 4.5.4.6. Validity of data.
 - 4.5.4.7. Programming considerations.
 - 4.5.4.8. Conclusions.
 - 4.5.5. Results.
 - 4.5.5.1. Cross section data collection.
 - 4.5.5.2. Mechanical reliability.

4.5.5.3. Conclusions.

4.6. Prototype III.

4.6.1. Introduction.

4.6.2. Mechanical design.

4.6.3. Electronic design.

4.6.3.1. Computer.

4.6.3.2. Display.

4.6.3.3. Power supply.

4.6.3.4. Stepper motor drive circuit.

4.6.3.5. Exposure time control.

4.6.3.5. Keypad interface.

4.6.4. Software design.

4.6.4.1. Introduction.

4.6.4.2. Interfacing to the Sentel frame grabber board.

4.6.4.3. Calibration.

4.6.4.4. Cross section data collection.

4.6.4.5. Conversion to DXB format.

4.6.4.6. Conclusion.

4.6.5. Results.

4.7. Conclusions.

4.7.1. Introduction.

4.7.2. Speed.

4.7.3. Accuracy.

4.7.4. Dimensions and non-linearity.

4.7.5. Reliability.

4.7.6. Measurement of cross sections.

5. ANALYSIS OF ERRORS.

5.1. Synopsis.

5.2. Introduction.

5.3. Triangulation intrinsic errors.

5.3.1. Introduction.

5.3.2. Camera errors.

5.3.3. External errors.

5.3.4. Summary.

5.3.5. Results.

5.4. Survey errors.

5.4.1. Introduction.

5.4.2. Mechanical errors.

5.4.2.1. Introduction.

5.4.2.2. Laser alignment errors.

5.4.2.3. Angular measuring errors.

5.4.3. Survey errors.

5.4.3.1. Local errors.

5.4.3.2. Field surveying errors.

5.5. Conclusions.

6. RESULTS.

6.1. Synopsis.

6.2. Introduction.

6.3. Calibration tests.

6.3.1. Introduction.

6.3.2. Calibration test rig.

6.3.2.1. Optical benches.

6.3.2.2. Trolley.

6.3.2.3. Interferometer.

6.3.2.4. Target.

6.3.2.5. The prototype mount.

6.3.2.6. Atmospheric conditions.

6.3.3. Calibration procedures.

6.3.4. Calibration results.

6.3.4.1 Analysis of calibration data.

6.3.4.2. Large calibration file CALIB4.

6.3.4.3. Fitting an appropriate curve to the data.

6.2.4.4. Analysis of data collected over a small range.

6.3.4.5. Laser mounted close to the target.

6.3.5. Conclusion and interpretation of results.

6.4. Subpixel accuracy tests.

6.4.1. Introduction.

6.4.2. Discussion of methods for subpixel accuracy.

6.4.3. Discussion of performance of subpixel methods.

6.4.4. Experiments with simulated data.

6.4.5. Experiments with real data.

6.4.6. Image problems.

6.4.7. Conclusions.

6.5. Correction to triangulation non-linearity.

6.5.1. Introduction.

6.5.2. Discussion of solution to non-linearity.

6.5.3. Application to the triangulation system.

6.5.4. Derivation of an equation for the corrected system.

6.5.4.1. Angle between object and first element.

6.5.4.2. Angle of exit from first element.

6.5.4.3. Orientation of the sensor to the prism.

6.5.4.4. Analysis of the triangulation correction system.

6.5.5. Testing of correction to linearity.

6.5.6. Summary of the correction method.

6.5.7. Limitations of large apex angle prisms.

6.5.8. The design of a triangulation computer aided design program.

6.5.8.1. Introduction.

6.5.8.2. Description of the operation of the CAD system.

6.5.8.3. Conclusion.

6.6. Conclusions.

7. CONCLUSIONS AND SUGGESTIONS FOR FURTHER WORK.

7.1. Introduction.

7.2. Research achievements.

7.3. Further work.

7.3.1. Investigation into laser beam pointing stability.

7.3.2. Exposure time control.

7.3.3. Temperature compensation.

7.3.4. Compact system design.

7.3.5. Hardware implementation of image processing algorithms.

7.3.6. Rotation of the measuring system.

7.5. Conclusion.

APPENDIX.

REFERENCES.

GLOSSARY.

LIST OF FIGURES.

Chapter 1.

Fig. 1.1. Cross section of rail tunnel.

Fig. 1.2. Plan view of all cross sections.

Fig. 1.3. Cross section of laboratory.

Chapter 2.

Fig. 2.1. Data collected by AMT Profiler.

Fig. 2.2. Tacheometry parallactic angle.

Fig. 2.3. Configuration of PROTA 2.

Fig. 2.4. Optocator, basic configuration.

Fig. 2.5. Measurement principle of LAMBDA system and timing diagram.

Fig. 2.6. Rockset system.

Fig. 2.7. Improvement in overall performance due to selective window.

Fig. 2.8. Three dimensional measuring techniques.

Fig. 2.9. Reflectance variations.

Fig. 2.10. Basic triangulation configuration.

Fig. 2.11. Elimination of occlusion by two receivers.

Fig. 2.12. Block diagram of principle of EDM operation.

Fig. 2.13. Phase measurement using digital pulse counting.

Fig. 2.14. Frequency ramped modulation.

Chapter 3.

Fig. 3.1. Optical triangulation configuration.

Fig. 3.2. Calibration curve.

Fig. 3.3. Images of light reflected from surfaces S₁ and S₂.

Fig. 3.4. Simple optical triangulation.

Fig. 3.5. Configuration for small working range.

Fig. 3.6. General triangulation configuration.

Fig. 3.7. Non-linear relationship for triangulation.

Fig. 3.8. Geometry of the Scheimpflug condition.

Fig. 3.9. Graph of d against D.

Fig. 3.10. Configuration for equation.

Fig. 3.11. Measuring range for prototype III.

Fig. 3.12. Basic prism configuration.

Fig. 3.13. Deviation angles for a series of refractive indices.

- Fig. 3.14. Deviation angles for a series of apex angles.
- Fig. 3.15. Fresnel prism configuration.
- Fig. 3.16. Spectral response curve of silicon.
- Fig. 3.17. Cross talk between photosites.
- Fig. 3.18. Spectral characteristics of KG-1 filter.
- Fig. 3.19. Schematic of a CCD sensor.
- Fig. 3.20. Three phase shift register operation.
- Fig. 3.21. Spectral response of silicon.
- Fig. 3.22. Photo response non linearity.
- Fig. 3.23. Exposure times for CCD output.
- Fig. 3.24. Lens diagram.
- Fig. 3.25. Laser power output control by mark space ratio variations.
- Fig. 3.26. Photon absorption coefficient graph.
- Fig. 3.27. MTF graph for Fairchild sensor.
- Fig. 3.28. Diode laser optical power vs. forward current.
- Fig. 3.29. Diode laser relative output power vs wavelength.
- Fig. 3.30. Gaussian beam intensity distribution.
- Fig. 3.31. Gaussian beam.
- Fig. 3.32. Reflected light components.
- Fig. 3.33. Response curves for three material types.
- Fig. 3.34. Centroid calculation.
- Fig. 3.35. Vernier calculation parameters.
- Fig. 3.36. Gaussian interpolation functions.
- Fig. 3.37. The interpolated curve.
- Fig. 3.38. Block diagram of Hewlett Packard interferometer.

Chapter 4.

- Fig. 4.1. Configuration for simple optical triangulation.
- Fig. 4.2. Configuration of Prototype I.
- Fig. 4.3. The effect of a misaligned laser beam.
- Fig. 4.4. A-D converter circuit.
- Fig. 4.5. IBM prototype board 4 x 8 Bit parallel interface.
- Fig. 4.6. Interface card circuit.
- Fig. 4.7. Flow diagram for interface card.
- Fig. 4.8. Laser image and the effect of a bright light source.
- Fig. 4.9. Program menu.

- Fig. 4.10. Pascal library files and descriptions.
- Fig. 4.11. Calibration data from first prototype.
- Fig. 4.12. Effect of missing rotation steps.
- Fig. 4.13. Effect of systematic rotation error.
- Fig. 4.14. Partial cross section of corridor in 'A' building, City University.
- Fig. 4.15. The configuration of Prototype II.
- Fig. 4.16. Laser diode collimation and orientation.
- Fig. 4.17. Camera tilting focal plane design.
- Fig. 4.18. Mirror mount.
- Fig. 4.19. Block diagram of evaluation board and signal processing.
- Fig. 4.20. Data output from CCD camera.
- Fig. 4.21. Timing diagram for clamp and sample timing.
- Fig. 4.22. Block diagram of black level clamp.
- Fig. 4.23. Automatic black level control circuit.
- Fig. 4.24. Logic circuit for black level clamp.
- Fig. 4.25. Signal inversion circuit.
- Fig. 4.26. Block diagram of peak detection circuitry.
- Fig. 4.27. A-D conversion circuit.
- Fig. 4.28. Timing diagram for appropriate conversion timing.
- Fig. 4.29. D-A conversion circuit.
- Fig. 4.30. Image of illuminated spot imaged on a CCD sensor.
- Fig. 4.31. Flow diagram for peak detection.
- Fig. 4.32. Comparison circuit.
- Fig. 4.33. Optical power output vs forward current.
- Fig. 4.34. Laser diode control circuit and diode LC protection.
- Fig. 4.35. Single cross section of a corridor.
- Fig. 4.36. Multiple cross sections of a corridor.
- Fig. 4.37. Cross section of a laboratory.
- Fig. 4.38. Profile of a model boat hull.
- Fig. 4.39. Multiple views of the boat hull.
- Fig. 4.40. Alternative configuration for cross section measurement.
- Fig. 4.41. Cantilever configuration adopted.
- Fig. 4.42. Finlux EL display.
- Fig. 4.43. Opto-isolator circuit for stepper motor.
- Fig. 4.44. Intensity display of complete array.

Fig. 4.45. Magnified image of the laser beam reflection.

Fig. 4.46. Manikin.

Fig. 4.47. Model boat hull.

Fig. 4.48. Model roof structure.

Fig. 4.49. Polyhedron.

Fig. 4.50. Laboratory.

Fig. 4.51. Corridor.

Chapter 5.

Fig. 5.1. The general optical triangulation system.

Fig. 5.2. Camera sources of errors.

Fig. 5.3. Image location error.

Fig. 5.5. Expansion of the sensor.

Fig. 5.6. Camera image distance change with temperature.

Fig. 5.7. Internal error sources.

Fig. 5.8. External error sources.

Fig. 5.9. Refracted ray diagram.

Fig. 5.10. The deviation of the laser and reflected rays due to temperature.

Fig. 5.11. Image location errors.

Fig. 5.12. Laser conic section.

Fig. 5.13. Setting up procedure for rotation of the laser in a plane.

Fig. 5.14. Establishing a starting angle.

Fig. 5.15. Starting position error.

Fig. 5.16. Bearing errors.

Fig. 5.17. Survey errors.

Fig. 5.18. Location of the measuring axis.

Chapter 6.

Fig. 6.1. Trolley design for target movement.

Fig. 6.2. Configuration of the calibration system.

Fig. 6.3. Calibration data from CALIB2 and line fit error data.

Fig. 6.4. Calibration curve for CALIB6.

Fig. 6.5. Residuals from curve fitting algorithm on CALIB6 data.

Fig. 6.6. Subpixel accuracy plot for CALIB6.

Fig. 6.7. Calibration plot of CALIB4.

Fig. 6.8. Plot of residuals after curve fit.

Fig. 6.9. Ji curve fitted to CALIB6.

Fig. 6.10. Error sets, ERR17-ERR24.

Fig. 6.11. Error sets ERR25-ERR31.

Fig. 6.12. ERR18, calibration and interpolation and error data at 2.5 metres.

Fig. 6.13. ERR23. Calibration, interpolation and error data at 3.5 metres.

Fig. 6.14. ERR23 data showing interpolation data and best fit straight line.

Fig. 6.15. ERR30, error data with laser 150 mm from target.

Fig. 6.16. Absolute values of ERR16 data plotted against distance.

Fig. 6.17. Error graphs for centroid method with noise.

Fig. 6.18. Error graphs for weighted centroid method with noise.

Fig. 6.19. Error graphs for vernier method with noise.

Fig. 6.20. Errors caused by changes in spatial resolution.

Fig. 6.21. Data set 1.

Fig. 6.22. Data set 2.

Fig. 6.23. Data set 3.

Fig. 6.24. Data set 4.

Fig. 6.25. Error frequency for data set 3.

Fig. 6.26. Gaussian curve fit to data set 7.

Fig. 6.27. Gaussian curve fit to data set 8.

Fig. 6.28. Angular deviation for seven prism apex angles.

Fig. 6.29. Triangulation configuration diagram number 1.

Fig. 6.30. Lens and sensor configuration.

Fig. 6.31. Range 1-2 metres, 1 metre base length.

Fig. 6.32. Range 1-3 metres, 1 metre base length.

Fig. 6.33. Range 1-4 metres, 1 metre base length.

Fig. 6.34. Range 1-2 metres, 0.5 metre base length.

Fig. 6.35. Range 1-3 metres, 0.5 metre base length.

Fig. 6.36. Range 1-4 metres, 0.5 metre base length.

Fig. 6.37. Comparison between double and single prism corrections.

Fig. 6.38. Plot of residuals for linearity comparison.

Fig. 6.39. Triangulation CAD screen.

LIST OF TABLES.

Chapter 1.

Table 1.1. Comparison of measurement times for four techniques.

Chapter 2.

Table 2.1. Comparison of Lambda system to other triangulation systems.

Table 2.2. Four options possible in a (FMCW) system.

Chapter 3.

Table 3.1. Vernier accuracy for differing signal to noise ratios.

Table 3.2. Comparison of subpixel methods.

Chapter 4.

Table 4.1. Data from tests with black felt.

Table 4.2. Calibration data for Prototype I.

Table 4.3. Curve fitting coefficients.

Table 4.4. I/O address assignments

Chapter 5.

Table 5.1. Laser performance comparison.

Table 5.2. Definition of terms.

Table 5.3. Deviation of light beam in a temperature or pressure gradient.

Table 5.4. Theoretical errors in distance measurement.

Table 5.5. Parameters for calculations.

Chapter 6.

Table 6.1. Subpixel results for data set ERR18.

Table 6.2. Subpixel results for data set ERR23.

Table 6.3. Subpixel results for data set ERR30.

Table 6.4. Subpixel data sets.

Table 6.5. Standard deviations for data sets 1-4.

Table 6.6. Subpixel accuracies for data set 7.

Table 6.7. Subpixel accuracies for data set 8.

ACKNOWLEDGEMENTS.

The mistakes that may be found in this thesis are likely to be my own, and if any insight is gained through reading it, then I have to acknowledge the help of those mentioned below and many others, too numerable to record here, who have given practical assistance and helped in the gathering of information and ideas.

I wish to acknowledge the help given to me by those who have supervised this project. Norman Lindsey, whose generous gift of time on a regular, sometimes daily basis, meant a much easier passage through to the completion of this thesis than would otherwise have been the case. Ken Grattan, whose organisational and management skill was invaluable in the practical promotion of the product of this thesis.

Other names deserve mention are: Geoff West for his late night enthusiasm, Mike Phillips for his interest and objectivity, Robin Croft for initiating the project, and many others with whom I have been privileged to be in contact over the last three years. These people freely gave their help and I am grateful for their generosity which made the task of learning easier to bear.

The assistance of British Technology Group in providing some early funding and Patent expertise, and that of Thames Water for financial assistance, and in particular David Jones, for his enthusiasm for the project.

Lastly, and by no means least, I acknowledge the assistance of my wife, Alison, who has been the inspiration for my efforts and without whose financial support none of this would have been possible.

DECLARATION.

The circulation of this thesis is restricted until February 1993.

ABSTRACT.

This thesis addresses the problem of acquiring spatial data concerning points on the surface of structures such as underground tunnels and sewers. These data can usefully provide knowledge of deformation, shape, area, volume, and position of structures. Such data can be further analysed to give insight into clearances, deterioration, flow rates and in-fill volumes or can be used to give knowledge of the present state of structures and their position.

Few systems address the problem of reliably acquiring this data in a manner that is fast and accurate while remaining flexible, adaptable and robust. This thesis considers a solution to the problem of fast and accurate spatial data acquisition concerning commonly found structures using the technique of optical triangulation with a linear array camera and diode laser light source.

Optical triangulation is a technique that has not fully matured for medium range measurement with few systems having been developed and little research material produced. However, the research carried out for this thesis shows that providing all the factors that contribute errors of measurement are understood, then a fast, robust and high accuracy system can be developed.

The development of the optical triangulation technique for use in surveying was addressed through a programme of prototype development, testing, and refinement. Three prototypes were built that demonstrated the reliability, accuracy, speed and robustness of this technique.

The errors associated with the a triangulation measuring system when applied to surveying application is considered from the intrinsic errors which are the same for any triangulation system and the extrinsic errors which are particular to the use of this system in surveying situations.

A calibration bench was constructed for consideration of the triangulation system which was automatic and used an interferometer to provide high accuracy measurement of the performance of the triangulation system. Calibration and interpolation trials were conducted and the results analysed. An analysis of the subpixel accuracy achieved with the discrete pixel CCD imagers has been performed and an analysis made.

One of the main disadvantages of optical triangulation when applied to the range 0-5 metres is that of non-linearity. A method of correction has been developed and analysed which is believed to be novel and makes a significant improvement to the measuring system.

The conclusion of this research is that an improved system of measurement has been produced which has a number of novel features. Trials show that the measuring system could be developed commercially to provide a solution to measurements of structures within the range of the device and with greater accuracy than comparable equipment designed for the same purpose.

SYNOPSIS OF THE THESIS.

The context of the research is thoroughly reviewed and a historical perspective of the development of distance measuring equipment from the areas of surveying, metrology, photogrammetry and machine vision. Contributions from these areas to the measurement system presented herein is acknowledged and the position of the research is established.

The theory necessary for a full understanding of the constituent parts of the optical triangulation system is given such as the theory of the laser, sensor, light interactions and signal processing.

The development of three prototypes is presented with particular reference to the mechanical, electronic and software design, the results of each of these methods is shown.

A comprehensive analysis of errors in triangulation systems when used for surveying is made.

Results of the research undertaken to establish the errors in subpixel resolution, the testing of the triangulation system through a number of calibration and interpolation trials, the development of a method of correcting the non-linearity of triangulation systems and finally a computer aided design software system is explained.

1. INTRODUCTION.

1.1. GENERAL INTRODUCTION.

The phenomenal rate of technological change in the equipment used in field surveying, photogrammetry and remote sensing has been noted by several observers (Jones, 1987; Vancans, 1987; Kennie, 1990). These changes have been stimulated by developments in optics, laser technology, microprocessors and electronics. However, although Kennie notes the progress made in *automatic recording* of field data, he states that little progress has been made in the area of *automated field measurement* and that 'clearly there is a need for such devices, since they would enable more emphasis to be placed on the structuring and classification of field measurements rather than on observational procedures.'

This thesis addresses the requirement for *automated field measurements* in the form of a fully, or partially, automated device for measuring the cross sections of structures in the range 0.1 to 30 metres. The measurement technique investigated differs from the coaxial, light based measurement systems within, or attached to, angle measuring theodolites, instead a camera is used to measure the angle from the known base of a right triangle to a point illuminated by a light source. If this angle and the base length are known, trigonometric methods can be used to calculate the distance from the base of the triangle to the illuminated point. This technique, called 'optical triangulation', has been applied in many mechanical tacheometers but few electro-optic systems have been developed for surveying purposes.

The objective of the research described in this thesis was the development of a piece of surveying equipment which could be used for the rapid measurement of structures. These structures may be man made or natural. Typical structures of interest are: tunnels, shafts, cavities, buildings, offshore oil rigs, storage tanks, ships, industrial structures such as car bodies, and machined parts. There are many reasons for measurement such as: checking manufacturing or construction tolerances, monitoring

deformation, acquiring structure detail for research purposes, assisting planning and for long term record purposes.

In the past these measurement tasks have been carried out by time-consuming and expensive manual methods or frequently not at all. The demand for spatial information is increasing encouraged by the knowledge of the ability of relatively cheap computer workstations to be programmed to analyse such data. However, using existing methods, surveyors may have to accept working periods of several days to measure a structure such as a car body or to monitor the deformation of engineering structures such as railway tunnels.

The objective of acquiring spatial data is shared with many recent measuring systems, these are reviewed in chapter 3, under the headings of surveying, photogrammetry, metrology and machine vision. Most of these methods do not entirely satisfy the requirement for speed and accuracy to reduce the time taken for the measurement process to be completed.

An ideal measurement system would use a narrow collimated beam of light directed to a small unique point on a given surface. The measurement would be highly accurate, take very little time to occur and take place along a single line of sight. It is likely that in the next ten years a laser distance measuring technique will be developed to meet this specification. This will happen because of the increases in: the speed and sensitivity of electro-optic components, the sophistication of laser technology and understanding of the available techniques. However, until such a fast coaxial laser range-finder is produced, with data acquisition speeds in MHz, and high accuracy, there will continue to be a requirement for alternative methods and techniques to measure distance. One such method is based on optical triangulation using a linear array sensor which has benefits which can be realised with current technology having data recording rates of kHz and reasonable resolution with subpixel accuracy.

Optical triangulation with linear sensors has been widely used to determine distances in industrial metrology (range less than 200mm, relatively high accuracy) and robotics (range up to 10m, relatively low accuracy). However, this technique has not received the same attention for close range applications in surveying and industrial measurement where a range of up to ten metres and medium accuracy might be required.

The principle of an optical triangulation system is that with the fixed parameters of camera angle, triangle base length and a narrow light beam source acting as a pointer

to a discrete position on a structure, the camera can be used to measure the angle between the reflected laser light from the structure and the base of the triangle. The distance of that point on the structure from the base line can be determined by calculation using the known parameters or by calibration and interpolation.

The structures and cavities encountered in civil engineering, and the large work pieces produced in mechanical engineering present a growing demand for specialist measurement techniques. The subjects vary in size from a few tens of millimetres to a few tens of metres, often demanding sub-millimetre accuracy with a high data recording and processing rate. In practice, for many applications there are no robust general purpose systems available or suitable to provide a rigorous general purpose solution. Optical triangulation systems have an excellent reputation for being quick, robust, reliable, and accurate in operation, the obvious limitations being occlusion and non-linearity.

1.2. ENGINEERING SURVEYS.

Surveying in the engineering environment is often required to determine the shape of a surface or the coordinates of unique points on a structure to ascertain correct construction, or monitor the structure over a period of time to determine possible movement and/or change of shape. Usually the surveying investigation is required to be carried out quickly with an equally rapid analysis of the data.

Surveys required for this type of work have usually involved observations being taken from a network of well established and coordinated instrument positions to clearly defined points of detail, e.g. corners of stone, bricks, window frames etc., or easily visible targets fixed to the fabric of the structure. Such observations have been made with tapes, levels, theodolites and electro-magnetic distance measuring devices. In many instances, because of the time involved on site to gather the data, only a limited number of points may be observed, consequently, surface shapes are obtained by interpolation (a practice used extensively in car body shell measurements) while construction control and movement detection is limited to a few, well chosen, points often restricted in value by sighting and identification demands.

Photogrammetry has been used in the quest for rapid data collection, as the method requires only a short time on site and affords measurement of almost any point recorded in the photography. However, the resulting photography requires processing and analysis on expensive instrumentation, with little reduction in the control survey work.

A variant of traditional photogrammetry has been examined at City University for some time in which the feature of interest, a cross section, is illuminated with a narrow plane of light and photographed. With the use of metric cameras or adequate control in the scene, the spatial data concerning the cross-section of a given structure may be obtained in the office for discrete points along each line. This is illustrated by Fig. 1.1, which shows a typical profile plotted from one such set of coordinates out of over seventy recorded in a tunnel system which are also shown in their correct spatial position.

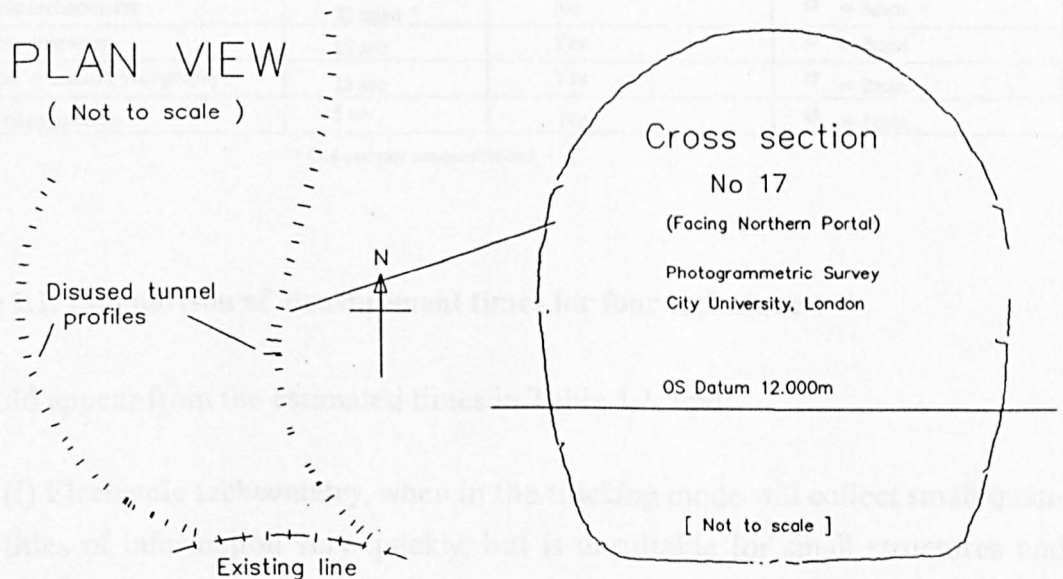


Fig. 1.1. Plan view of cross sections and cross section number 17.

The plan position of each profile is obtained by observing at least two points on each profile using observations of angle and distance from survey instruments fixed in position from a suitable control network. Such limited observations can be performed simultaneously with the photography and hence do not unduly extend the site occupation.

Optical triangulation measurement systems are, as is any optical method of measurement, dependent on clear lines of sight and may suffer non-linearity. However, the optical triangulation technique will perform measurements more rapidly and accurately than alternative methods, with the results being presented fully analysed, if necessary, on site. The number of points recorded will depend on the nature of the surface under examination which can vary from smooth newly installed concrete to soot-caked broken brick linings or sludge covered rock in a mine-shaft.

It is of interest to compare the performance of each system. If the problem is to, say, measure 5000 points on a grossly irregular surface at a range of 1-4m, see Table 1.1. The number of points required will depend on the nature of the surface since interpolation will give a distorted representation of a surface if insufficient data are obtained.

Method	Data acquisition time	Post processing	Accuracy
Electronic tacheometry	33 mins *	No	$\sigma = 3\text{mm}$
Stereo photography	15 sec	Yes	$\sigma = 3\text{mm}$
Light line + mono Photography	15 sec	Yes	$\sigma = 2\text{mm}$
Optical triangulation	5 sec	No	$\sigma = 1\text{mm}$

* 0.4 sec per measurement

Table 1.1. Comparison of measurement times for four techniques.

It would appear from the estimated times in Table 1.1, that:

(i) **Electronic tacheometry**, when in the tracking mode will collect small quantities of information very quickly, but is unsuitable for small structures and artifacts at close range.

(ii) **Photogrammetry:**

(a) **Stereo**, this techniques gathers a lot of data very quickly on site, the quality is good and there is the added advantage that the negative, stored in archive, may be measured as often as required. However, the films have to be processed and the analysis is time consuming, especially for a lot of data, in addition good quality control is required in each stereo pair. A useful advantage of this system is that the pairs of photographs can be viewed stereoscopically for detailed examination of the subject.

(b) **Mono** - this system is as fast on site as stereo, it requires processing and analysis, which is a little faster than for stereo, provides a good archive, and is less demanding on control. The best results are obtained when the subject has targetted points.

(iii) **Optical triangulation**, is able to compete favourably in this situation being comparable to photogrammetry, with regard to speed of measurement, and is better than electronic tacheometry in terms of accuracy and speed.

An example of data collected by an optical triangulation system is shown in Fig. 1.3, which is a cross-section of the laboratory at City University.

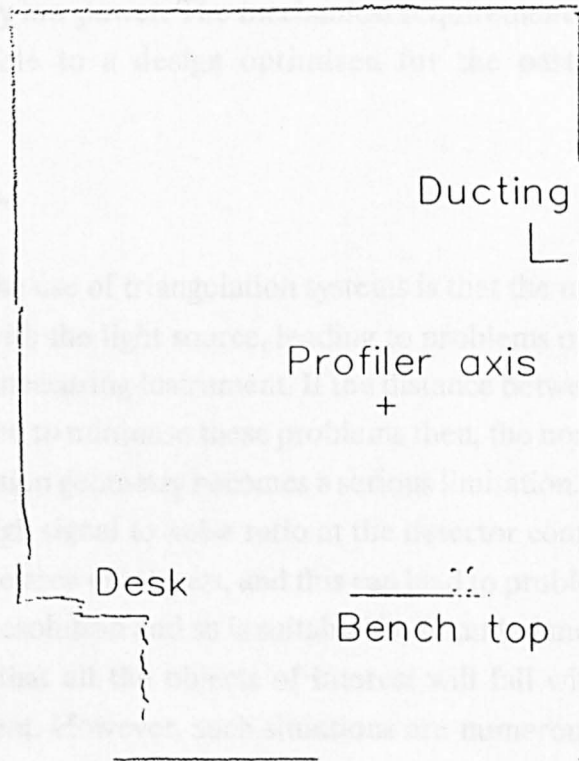


Fig. 1.3. Cross section of laboratory.

1.3. OPTICAL TRIANGULATION FEATURES.

1.3.1. Advantages.

The advantages of an optical triangulation measuring system are: speed (data rates up to 10,000 measurements per second are possible) and accuracy (resolution of 2,000:1 to 20,000:1). When such a system is rotated about a central axis, it is possible to measure structures which are relatively large with reasonable speed and accuracy for most practical purposes. In many situations this speed of measurement is an important economic consideration as the measurement process is usually only one step in an overall engineering process.

The typical working environment for a measurement system can vary enormously from the clean research environment, to that encountered in a mine-shaft where there are draughts, local temperature and humidity variations, surface wetness, occluded surfaces, and an environment hazardous to the operator. Any measurement system may be required to cope with this very wide range of conditions. The triangulation scheme discussed herein is robust, as all the electronic components are solid state and operates at relatively low power. The mechanical requirements for the triangulation system are amenable to a design optimised for the particular measurement requirements.

1.3.2 Disadvantages.

A disadvantage of the use of triangulation systems is that the measurement does not take place coaxial with the light source, leading to problems of occlusion and in the physical size of the measuring instrument. If the distance between the sensor and the light probe is reduced to minimise these problems then, the non-linearity inherent in the simple triangulation geometry becomes a serious limitation. The light source used has to maintain a high signal to noise ratio at the detector compared to the ambient light reflection in the area of interest, and this can lead to problems of eye safety. The system has a finite resolution and so is suitable for bounded measurement situations where it is known that all the objects of interest will fall within the range of the measuring equipment. However, such situations are numerous e.g. rail, sewer, and road tunnels. The speed of measurement is limited by the time it takes (a) to collect enough light and (b) the time taken to clock the data from the array and process it, this implies a maximum data rate of 10kHz for a 2048 pixel CCD sensor typical of what is available commercially. However, there are alternatives such as "tapped" arrays which overcome some of these problems. The lens system and laser launching system may present problems in dirty environments to ensure clear optical surfaces.

1.4. CONCLUSIONS.

The conclusion reached through the research carried out for this thesis is that the optical triangulation is able to offer some significant advantages over current technology and that such improvements are required in many areas. The optical triangulation technique has not been thoroughly investigated for surveying applications and there are a number of key problems that require solution and other areas where improvements may be made.

2. A REVIEW OF 2-D & 3-D SPATIAL DATA ACQUISITION TECHNIQUES.

2.1. SYNOPSIS.

The review examines the development the science of measurement in the areas of:

- (i) surveying,
- (ii) metrology,
- (iii) photogrammetry, and
- (iv) machine vision.

Each area is set in the perspective of its historical beginnings followed by a review of present day developments that are pertinent to this thesis. In doing so much is learnt about the progression of measurement techniques with advancing technologies such as optics, electronics, solid state electro-optics and computing. This review ensures that lessons that have been learnt in other areas, which have been reported in the research literature, are acknowledged and where appropriate made use of.

2.2. INTRODUCTION.

This thesis is concerned with the development and application of a fast and accurate method of distance and angle measurement to acquire 2-D and 3-D spatial data. The range of methods and techniques applicable to the acquisition of such data, which have been developed in the disciplines of surveying, metrology, photogrammetry and machine vision, are examined in this chapter. By reviewing the alternative methods, the technique that has been developed is compared and contrasted with both research and commercial work. Furthermore, the review brings together the experience and techniques built up in all of these disciplines to facilitate cross fertilisation of ideas and eliminates the possible reinvention of such techniques.

The review shows that machine vision is a growing area of research where the acquisition of spatial data for use in industrial inspection tasks has advanced considerably over the last twenty years. Solutions to some industrial inspection tasks, such as measurement of manufactured steel strip widths, are in regular use, while others task, such as robot vision, still require significant improvement in the technology before widespread application. The deficiencies in current technology provide a great stimulus for research funding and ideas. Consequently, many techniques, of varying merit, have been experimented with in the race to provide solutions to inspection tasks.

Industrial metrology is revealed as an area of research which has developed many techniques for the requirements of close range measurement with high accuracy. The range of techniques that have been developed and which are being continually improved through research include: holography, electronic speckle interferometry, interferometry, moiré techniques, optical triangulation and many contact methods.

The field of surveying has seen less development of the short range measurement techniques compared to those in machine vision and industrial metrology. Hence, few short range systems have been developed and reliance been placed on the traditional techniques of surveying and photogrammetry. For many years these techniques have been adequate to collect spatial data in a reasonable time and with sufficient accuracy for those who use them. It is, however, becoming increasing apparent that a number of situations exist where these traditional methods are no longer acceptable and new solutions need to be devised. It is for this reason that the active development of systems in machine vision and metrology are of particular interest. However, any application in the areas of surveying traditionally catered for by photogrammetry, does require research to adapt and modify the techniques available for maximum efficiency.

2.3. SURVEYING.

2.3.1. Introduction.

Surveying has been carried out from the earliest civilised times. The necessity for surveying exists when:

- (i) knowledge is required about a existing structure or terrain, for example the floor plan of a building or civilian or military maps, and

(ii) the position of a new structure or surface relative to an existing structure or surface is required.

The objective of a survey is generally the location, relative to some local or global datum, of some arbitrary point in space, constrained by some measurement scheme. It is immaterial to this objective which method, or methods, are used, but a knowledge of the accuracy with which the measurements are made is of extreme importance. Thus the whole of surveying may be reduced to the aim of locating one point with respect to another with a known accuracy of measurement. This simple objective does not trivialise the task of surveying, as adding two binary numbers does not trivialise the operation of a computer, because from such data vastly complex knowledge can be acquired about buildings, countries, and planets. The context of this research within this global picture is the acquisition of spatial data concerning points within a 0-10 metre range from the measuring instrument at millimetre or sub-millimetre accuracy.

2.3.2. Surveying procedure for location and measurement of points.

Of the four branches of surveying: geodetic, topographic, cadastral and engineering, it is latter that is of interest to the research carried out for this thesis. The data collected for analysis may, however, relate to data collected during the course of the other types of survey. Rail tunnel cross sections can be related to a land survey of the area, or each cross section may be related to a similar cross section recorded at the same location in the past to facilitate deformation monitoring, hence, requiring no information from other methods of surveying.

The methods used in engineering surveys to acquiring knowledge about the spatial coordinates of points of interest fall into a number of categories, two of the most widely used methods are:

(i) tape (steel band) or chain surveying. This is the simplest method of obtaining spatial data being cheap, robust and simple to use. This method is suitable to survey the dimensions of a room (Garner, 1976) if it can be assumed that the room square or is some other easily defined geometrical shape. However, if the room is not square or is complex in shape then the tape is not so suitable for this task, and

(ii) Theodolites and Electro-magnetic Distance Measurement (EDM). These are able to measure angles and distances respectively and are combined in the

Electronic Tacheometer where angles and distances are both read and automatically recorded for subsequent processing, a major advance in the fast data acquisition recording and storage.

The development of EDM and its use with angle measuring theodolites has provided an important technique for acquiring spatial data. A review of its development is required as it could be viewed as an alternative to the technique of optical triangulation.

2.3.2.1. Distance measurement.

The measurement of distance by speed of light techniques is a highly developed and well understood technique which has been utilised to the full in the surveying field. The development of these techniques first used white light as the source of electromagnetic radiation and when diode light sources were sufficiently developed, the light emitting diode (LED) and latterly the diode laser (DL) were used which are essentially monochromatic.

(i) White light methods.

The development EDM as used for survey measurement originated with the work undertaken by Bergstrand of Sweden, who successfully determined the speed of light in air in the early 1950's and applied his research technology in the development of the Geodimeter family of distance measuring devices. These instruments used tungsten and mercury arc light sources with Kerr cells to modulate the beam. The phase delay system of measurement produced good accuracy over distances up to 15 miles with speedy determination in what was a light weight instrument.

A white light technique developed at the National Physical Laboratory (NPL), London, and tested initially by Hilger and Watt and later manufactured by KERN of Switzerland, under the name 'Mekometer' is described by K.D Froome and R. H. Bradsell in 1965. The system used a modulated light beam with a frequency in the region of 500 MHz, with specially designed cavity resonators to determine the modulation wavelength independent of a knowledge of the speed of light. The system required a retro-reflector (called a cats eye target) and achieved an accuracy of better than 1 part in 10^6 (Connel,1965).

The VEB Carl Zeiss Jena 'EOS' (Electro Optical telemeter System) appeared about 1965 (Strocsche,1965) with improved light transmission. This system used a light beam

to which was applied a sinusoidal modulation. This beam was reflected from the point to be measured and the modulation phase measured against the phase of the initial output beam. This system allowed the measurement to a integral multiple of a scale derived from the modulation frequency and light velocity. In summary a phase measuring scheme is used similar to the theodolite, but without the velocity of light compensation.

The advantage of being able to measure long distances without interference from the largely indeterminate atmospheric effects is advantageous in general surveying. This is not of such importance in close range measurement because the effect does not produce significant errors, see chapter 5, however, the white light method is interesting as a forerunner of EDM.

(ii) Diode and diode laser methods.

The development of EDM using a LED or DL stemmed from the invention of the MASER (Microwave Amplification by Stimulated Emission of Radiation) in the 1950's which prompted the development of the LASER (Light Amplification by Stimulated Emission of Radiation) in 1960. The importance of these events is in the nature of the laser as a source of light, it is highly directional compared to conventional light sources that radiate in all directions which ensures a high intensity of light which is also highly coherent and monochromatic. These features enable the laser to be used in interferometry and time of flight systems which can also make use of the speed of modulation that can be achieved. By 1965 some crude distance measuring devices had been experimented with. K. Harris, 1965, summarised the possible directions for development of EDM:

- (i) use of the high coherence length properties for interferometric methods,
- (ii) modulation of the laser with high frequency radio signal and phase measurement, and
- (iii) pulse modulation as in conventional radar.

He states that the latter was being used more successfully but predicted a modest accuracy of 300 mm. It can now be seen that each of these methods has been extensively developed with pulse systems able to measure distance with a standard deviation of 1-3 mm in commercial surveying instruments with a relatively short time delay between measurements (0.01 - 3 seconds). Initially the early systems relied upon a retro-reflector to return enough signal back to the measuring system for

measurements to be made, at a later stage the sensitivity of the receiver had improved sufficiently for reflectorless operation in suitable circumstances.

The development of a reflectorless EDM has been of prime importance in the development of surveying instruments suitable for measuring to the non-cooperative surfaces found in tunnels, cavern and slopes. Traditionally less measurements were been carried out than desirable because of the cost and time involved in placing the retro-reflecting target on the surface to be measured. With a reflectorless EDM this is not necessary and so time and cost savings can be made.

A comparison between the manual and automatic methods of profile acquisition made possible by reflectorless EDM is described by Hagedorn, 1986, in a paper on the use of the WILD Distomat TM DIOR 3001 EDM. The complete system is called the A. MT. Profiler 2000, operation is by rotation of the EDM to discrete position where the angle and distance are stored on a portable computer. This profiling system is analysed in detail as it is one of very few alternative profiling systems with which to compare the performance of the system developed in this thesis. The disadvantages of conventional profiling which were noted are:

- (i) manual methods are labour intensive,
- (ii) only selected profiles are measured because of the time factor,
- (iii) these profiles do not permit any representative judgment of the geometry of the structure as a whole, and
- (iv) the full extent of any under breaks in a railway tunnel are not measured with the purpose made measuring carriage.

The profiler was developed to meet the following conditions:

- (i) simple and quick operation,
- (ii) highly accurate,
- (iii) automatic data registration,
- (iv) evaluation possibilities with the aid of computers, and
- (v) suitability for use under the conditions of tunnelling.

The operation of the profiler is described in the advertising literature (AMBERG) the salient points of which are:

- (i) Positioning the profiler.

The position of the instrument station can be determined by: xy-method (e.g. determining the position by a visible line such as a laser beam or rail centre line), theodolite and prism mounted on the profiler, or by mounting a theodolite on the profiler.

(ii) Measuring the profile.

The system measures distance without a reflector from 0.3-50 metres depending on the surface reflectivity and structure. The accuracy is 5-10 mm depending on the measuring speed. A laser beam marks the measured point.

(iii) Operating the profiler.

Measuring angle intervals are adjustable from 0.1° to 99.9° , measurements can be programmed by remote control and are either automatic or manual.

(iv) Data recording.

The data is recorded by hand-held computer, up to 60 profiles of 100 measured points can be recorded on one cassette, each of which can be identified for future reference.

(v) Data evaluation.

The data can be transferred to the office where it can be plotted, compared with previous profiles, and evaluated for: over and under profile, distance computation, volume computation and computation of layer thickness.

An example of the data that can be collected using this system is shown in Fig. 2.1.

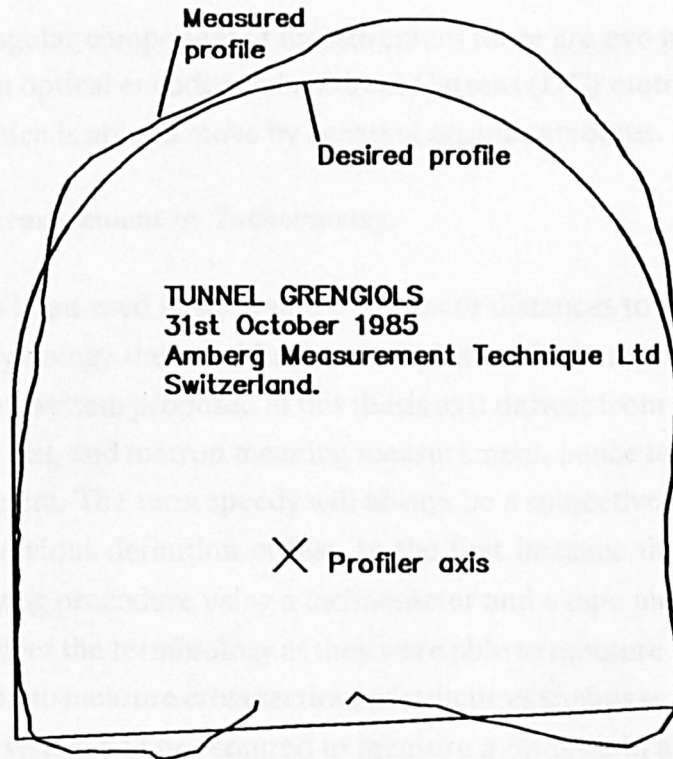


Fig. 2.1. Data collected by AMT Profiler.

Alternative systems, which use the same type of EDM, have been developed such as the EO Fennel FET 1 tunnel profile scanner (FENNEL), and Measurement Devices Limited tunnel profiler (MDL). However, none offers any significant advantage over the AMT profiler and so are not further discussed.

2.3.2.2. Angle measurement.

The complementary task to distance measurement, when gathering 2D and 3D spatial data, is that of angle measurement. In the past angles were measured using theodolites with glass or metal circles engraved with angular divisions, using this technique accuracies of a single second of arc have been achieved with rigorous procedures. Recent developments have enabled the automatic measurement of the same angles with the same accuracy but with relaxed and less time consuming methods.

It is not necessary to review the methods of angle measurement as the accuracies obtained are far in excess of what is required for the system under consideration in this thesis where angular accuracies of the same order as the distance measuring accuracy is required. As a result, the highest angular accuracy envisaged as being necessary is 20 seconds of arc. This is not a high requirement as resolutions of 0.5 seconds of arc are routinely achieved by the better quality theodolites.

To achieve the angular component of measurement there are two methods available first, the use of an optical encoder and a Direct Current (DC) motor and secondly, a stepper motor which is able to move by constant angular amounts.

2.3.3. Distance measurement by Tacheometry.

Tacheometry has been used in surveying to measure distances to known points on a structure. The etymology the word 'tacheometry' is useful in seeing the connection with the measuring system proposed in this thesis as it derives from two Greek words, tacheos meaning fast, and metron meaning measurement, hence tacheometry means speedy measurement. The term speedy will always be a subjective comparative term relative to the previous definition of fast. In the first instance the comparison was between a surveying procedure using a tacheometer and a tape measure, later EDM equipment took over the terminology as they were able to measure a distance in a few seconds. However, to measure cross sections of structures such as sewers or car bodies, a fast measuring system will be required to measure a distance in a few μ seconds to a few milliseconds to measure the complete structure in a few seconds.

There are many tacheometer systems described in the literature (Irvine,1988), the feature common to the optical triangulation system is the measurement of a small angle called the 'parallactic' angle which is measured by theodolite to a short base line defined on a staff. The distance between the theodolite and the staff is then a function of this angle. This simple system shown in Fig. 2.2. can be used as the basis of understanding the operation of a number of these systems which have an accuracies of 1:500 to 1:10000.

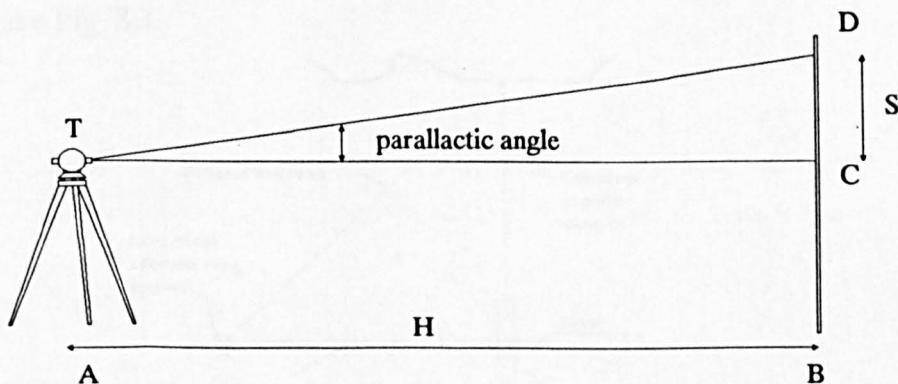


Fig. 2.2. Tacheometry parallactic angle.

In the triangle TCD as shown in Fig. 2.2, TCD is right angled, TC is the unknown distance H, DC is a known distance on the staff S, and the parallactic angle is θ . Hence,

the equation $H = S/\text{Tan}(\Theta)$ allows the distance H to be computed by either measuring S or Θ if the other is known.

The range of tacheometer methods are: tangential tacheometry, stadia tacheometry, horizontal staff tacheometry (subtense bar and optical wedge system) and self reducing tacheometers. They all rely upon the parallaxic angle variations with distance for a fixed base line, or the variation in base line length for a fixed angle.

The measurement principle of optical triangulation with a CCD camera differs from most of these systems as the operation is by measuring the parallaxic angle with a fixed base length. It is simpler for the mechanical tacheometer system to use a fixed parallaxic angle and read the distance from a variable base line which is calibrated for the purpose. A tacheometer with a variable base line is the Carl Zeiss (Jena) BRT 006 self reducing tacheometer that has a base line length of about 0.5 of a metre. The measured distance is read from the calibrated scale when a directly viewed image and an indirect image, viewed from a prism mounted along the base line, are brought into coincidence.

A variation on the BRT 006 tacheometer, which is currently on the market, is the 'PROTA' tunnel profiler manufactured by R.&A. ROST of Austria (Tunnel,1989; Rost,1989). This system uses both laser and traditional tacheometer technology to acquire point by point measurement of cross sections of tunnels. The measuring principle is 'Intersection by means of a laser beam via a right triangle with a variable base (Rost,1990).' In practice the laser light is imaged with a telephoto lens onto a ground glass plate. By changing the position of the adjustable laser mirror the image can be made to coincide with a division mark and the distance is then read off from a counter, see Fig. 2.3.

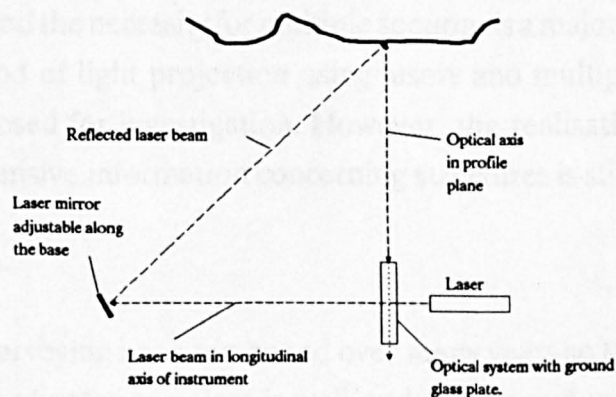


Fig. 2.3. Configuration of PROTA 2.

The claimed accuracy is ± 10 mm, the measuring range 1.6 - 11.25 metres, and some uses are: for checking the driving of tunnels, as a basis of accounting, for checking project execution, as proof of large deformations. However, a disadvantage must be the manual operation, no figures are quoted for the time to measure a point, but it cannot be very quick as there is no electronic data recording.

A similar system to the PROTA was the subject of a patent application FR 2468101 in 1981. The main difference is that both of the rays that enclose the parallax angle are formed by laser beams, these beams can be adjusted into coincidence, at this point the distance is recorded by a counter.

2.3.4. Automated surveying equipment.

A number of systems have been developed which utilise the accuracy of a theodolite with the flexibility of techniques from machine vision using electronic cameras to achieve an automated triangulation system. The KERN Space system is described by Kyle, 1989, and Gottwald, 1987, is based on a number of motorised theodolites with telescopes having built in CCD cameras. The system has the disadvantages of requiring either a recognisable target or a laser type pointer and for the theodolites to move to each target position mechanically with a high degree of precision. Hence, the system is only able to work relatively slowly and with cooperative structures or targets. However, to illustrate the importance of cross section profiling Kyle states 'In the field of applications, surface form is an important requirement. Here Kern is developing a general "Profiling" package based on a scanning laser spot.'

The limitations of point by point measurement, as performed by EDM profilers, are discussed by Foo, 1989, who concludes that the necessity to rotate through 360° to collect a profile, and the necessity for multiple sections is a major drawback of profiling systems. A method of light projection using lasers and multiple views with a CCD camera are proposed for investigation. However, the realisation of a system which gathers comprehensive information concerning structures is still a research problem.

2.3.5. Conclusion.

The practice of surveying has been honed over many years so that the measurements of the spatial coordinates of points is well understood and many methods exist for collecting such data. However, the invention of, and the improvements in EDM and the advantages of electronic data logging have made a great deal of difference to the speed of data capture. Further progress will continue to be made with advances in the

accuracy, speed and ease of use of such equipment. Although tacheometry has largely been superseded, the technique identified in this thesis, electronic optical triangulation, is closely related and may provide a number of advantages over the alternative techniques.

Over the next few years there are likely to be further improvements in the close range measurement area with techniques from metrology, photogrammetry, and machine vision merging to provide fast and accurate spatial data collection on a scale not yet contemplated. This will allow the 3-D mapping of structures and surfaces which will enable the next generation of computers to manipulate this data for a large variety of purposes. This close range data will compliment the data gathered by large scale surveying methods such as remote sensing, satellite positioning systems and traditional surveys. The development of the system described in this thesis forms part of the early development of such fast data gathering techniques.

2.4. METROLOGY.

2.4.1. Introduction.

The historical development of the science of metrology follows that of surveying but predates that of photogrammetry by many years, going hand in hand with the rapid changes of the Industrial revolution. The first mechanical metrology instrument may have been James Watt's micrometer of 1772. The use of optical techniques in metrology was promoted and advanced by Carl Zeiss of Jena, an early device (1920) was the 'Optimeter', a comparator, which was developed for gauge inspection and control (Hume,1980). From these early times the term Metrology covered measurement to an accuracy of microns. The micrometer is an example of the earliest metrology tool which has been refined over many years, in mechanical and electro-optic forms, which is still used today.

There has been a resurgence of interest in the application of optic techniques with the emergence of lasers, optical fibres, electronic sensors and the requirements of inspection techniques in manufacturing. This interest means that this subject has become a major research area with five international conferences taking place in 1986 (SIRA,1988). A summary of the techniques which overlap with optical triangulation is required for comparison. The metrology methods can be divided into a number of categories.

2.4.2. Contact methods.

There are many and various contact methods which range from the simple vernier callipers to the expensive Coordinate Measuring Machine (CMM) which uses a touching stylus as the point of contact. Contact methods have the advantages of relatively quick measurement and high accuracy when used with suitable objects and the disadvantages of expense if a high accuracy (CMM) is required which is not very flexible if measurement is required to objects which are too large or of complex shape.

2.4.3. Non-contact methods.

The non contact methods which have developed to circumvent the disadvantages of contact techniques and methods range from interference methods using such phenomena as Newton's rings to optical triangulation probes used with CMM's. The general applications of non-contact measurement which have been noted (SIRA, 1988) are to such diverse subjects as: multi-dimensional small components where a system of touch is impractical, plastic and non-metal components which could distort by using a touch technique, printed circuit boards, and integrated circuits. It is the field of non-contact measurement that is of greatest relevance to this thesis. A summary of the reported results of a number of authors follows.

2.4.3.1. Position sensitive detectors.

The use of position sensitive detectors (PSD) in this field has been particularly fruitful with a number of optical triangulation PSD based system being marketed such as the LAS-5010 Laser analogue displacement sensor sold by GWI Ltd (GWI,1990), for approximately 400 pounds in 1990. Anthony,1986, reports the use of lasers and PSDs in non-contact optical triangulation probes which are use used in place of a stylus in a CMM. He reports that these devices are more expensive than mechanical probes, but over the range of 4mm the accuracy was 10 microns in the model quoted.

2.4.3.2. Charged Coupled Device detectors.

The advantages of opto-electronic methods of measurement has been noted by Hantke,1986, as: non contact measurement, short measuring time, great number of measurements per object. The paper discusses the relative merits of Charged Coupled Devices (CCD) versus PSDs, and concludes that with correct calibration the accuracy of location on the CCD chip can be made to 0.1 μ m.

The use of mechanical probes is contrasted to that of non-contact probes by Warnnecke, 1987, who uses the optical triangulation principle with a CCD imager and 2.5 Watt HeNe laser. The magnification used was 30 times. An unusual feature of this system is an endoscope which is used to remotely collect the image because this allowed a compact design. One of the advantages of the non-contacting probe is the ability to measure previously undetected surface roughness because of the contact probe's relatively large dimensions.

2.4.3.3. Electro-optic/mechanical sensors.

K. Goh, 1986, reported on the applicability of a triangulation based probe for non-contacting inspection, the measuring system described, called the Optocator, was designed to eliminate the undesirable effects of a touch probe and improve the speed of operation of a CMM, see Fig. 2.4.

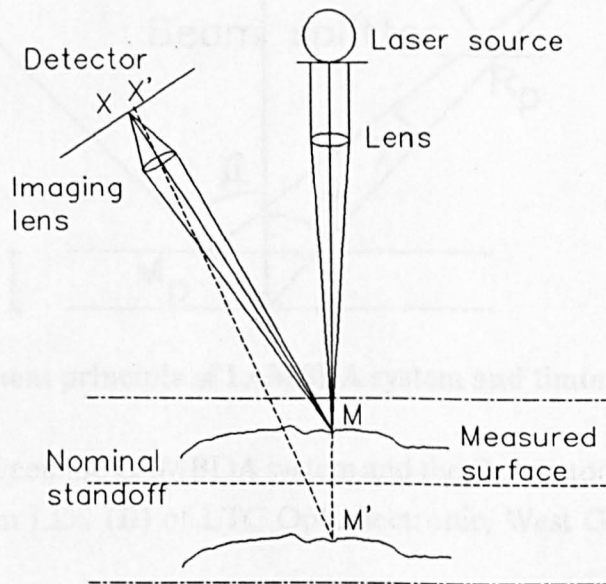


Fig. 2.4. Optocator, basic configuration.

Many early optical triangulation systems sought to improve the angular measuring capability, limited by the available sensor resolutions which were low, by various mechanical scanning techniques. One of these was a system described by Bodlaj, 1976, where a piezo-ceramic beam deflector was constructed and the beam was deflected by it as a function of the time of revolution so converting the angle measurement to one of time. These angle to time conversion systems are still used and a recent example is that of the LAMBDA (Vandenberg, 1990) sensor (LAMBDA is an acronym from German which could be translated 'non-contact measurement of distances using a

scanning laser beam'). This sensor is claimed to be up to ten times better than normal triangulation sensors over the same range. The operation of this system takes place by scanning a laser beam over the surface which is to be measured by the beam deflector. On each scan of the laser beam a reference angle is established followed by another angle which is dependent on the increase in angle required to gain a return signal from the surface to be measured. Hence, an angle to time system is effected where the inaccuracy in distance measurement is proportional to the error with which the timing interval is measured, see Fig. 2.5.

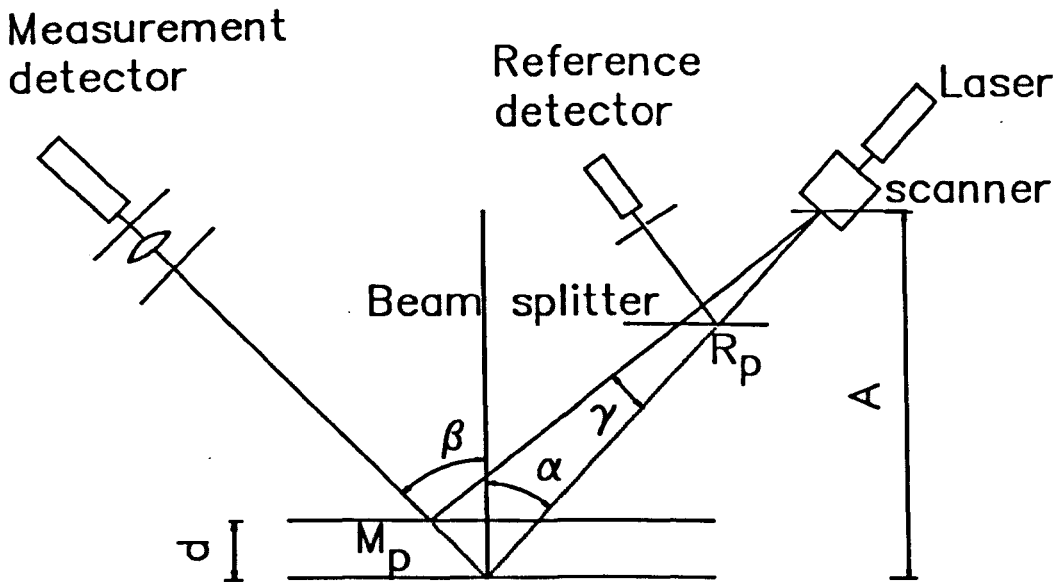


Fig. 2.5. Measurement principle of LAMBDA system and timing diagram.

A comparison between the LAMBDA system and the Optocator (A) described above and another system LDS (B) of LTC Optoelectronic, West Germany, is shown in Table 2.1.

	LAMBDA SENSOR	Triangulation sensors	
		A	B
Stand off (mm)	100 - 10000	55 - 80	95 - 1000
measurement range	25 - 10000	2 - 100	8 - 512
accuracy (%)	0.01	0.25	0.1
linearity	0.01	0.25	0.1
resolution	0.0015	0.05	0.025
temp. coeff. (ppm/K)	20	-	100

Table 2.1. Comparison of Lambda system to other triangulation systems.

2.4.4. Conclusions.

There is increasing use of triangulation systems to measure artifacts in the industrial environment with non-contact triangulation probes, in fact, the recent proliferation of suppliers for these systems suggests that they have now moved out of the experimental research environment into daily use as a 'black box' measuring system. There appears a high reliance on the PSD for this type of application which may be understood in terms of the closed environment of industrial inspection and the relatively high accuracies that are required over a small range. However, in some cases the slightly more expensive CCDs are able to provide the same, or better results with the addition of the digital readout of distance information rather than the analogue voltage that the PSD provides.

2.5. PHOTOGRAMMETRY.

2.5.1. Introduction.

2.5.1.1. History of photogrammetry.

The earliest photogrammetric use of photography was made by Arago, a geodesist with the French Academy of Science, who used photographic plates in topographic surveying. The earliest experimental work took place in 1849 leading to Colonel Aimé Laussedat presenting this work in 1859 for which he was later recognised as the "Father of Photogrammetry."

The term photogrammetry was first coined by Kersten in 1855, and used by Koppe in the first German textbook on photogrammetry. Many of the early uses of photogrammetry were initiated by military interest in gaining reconnaissance data. However, the close range photogrammetry applications are more recent so the historical development of the art of photogrammetry is not pursued in this thesis.

2.5.1.2. The connection with optical triangulation.

The American Society of Photogrammetry describes photogrammetry as 'the art, science, and technology of obtaining reliable information about physical objects and the environment through the process of recording, measuring and interpreting photographic images and patterns of recorded radiant electro-magnetic energy and other phenomena (American, 1979)'. The term 'photogrammetry' was introduced by

an architect, Albert Meydenbauer who made his first photogrammetric surveys in 1867 (Handbook of NTP, 1979). Historically photogrammetry has meant the use of a photographic image but today the post event processing can be eliminated by the use of solid state cameras which allow analysis of the data immediately following its collection.

The system described in this thesis concerns a solid state camera with a one dimensional array sensor which records and allows measurement and interpretation of *patterns of recorded radiant electromagnetic energy* with the end result of *reliable information about physical objects*. Hence, there is an overlap between the type of data recorded by photogrammetry and the information which is acquired as a final product. However, the intermediate data, a photographic image, is not kept in this case. Furthermore, the interest in the development of this measurement system arose because of the disadvantages experienced using a photogrammetric method of cross section measurement and the resulting information is identical.

To further strengthen the case for inclusion of this topic in the realms of photogrammetry remote sensing is considered. In the "Manual of Photogrammetry" 4th edition, 1980, it is reported that the science of photogrammetry was broadened to include the tool of remote sensing. The important new feature here, apart from the method and subject matter, is the inclusion of special purpose sensors and the widening of the spectral range of electromagnetic radiation covered. The CCD sensor generally used in remote sensing equipment is able to image both visible and infra-red radiation and is frequently a one dimensional linear sensor which scans the scene line by line. Hence, the CCD sensor is now commonly used in photogrammetry.

T. Luhmann, 1990, in a review of image recording systems for close range photogrammetry, states 'Triangulation systems with laser sources and passive imaging sensors can also be regarded as photogrammetric systems. Most appear to offer high speed processing, although the obtainable accuracy is rather poor'. The latter point may apply to most active measuring systems, but the linear type of sensor is generally more accurate than the area sensor.

The argument for the inclusion of the subject of this thesis in the realms of photogrammetry are: (i) a sensor, similar to that used in remote sensing, is used to collect image data concerning a scene perturbed by a laser spot, (ii) the data concerning this scene is processed to provide a selected part of the image, the laser

reflection, and (iii) the final result, spatial data concerning parts of a scene imaged by a camera, can be acquired by a number of alternative photogrammetric methods.

2.5.1.3. Definition of the relevant area of photogrammetry.

P. Wolf, 1983, describes two distinct areas of photogrammetry (i) metric photogrammetry and (ii) interpretive photogrammetry. It is the former category that is of interest in this thesis where the definition is in making 'precise measurements from photos and other information sources to determine, in general, the relative location of spatial points. This enables finding distances, angles, areas, volumes, elevations and the sizes of shapes of objects'. The area within metric photogrammetry that is of interest is that of 'close range photogrammetry' where the camera to object distance is less than 300 metres, sometimes known as 'non-topographic photogrammetry', the term 'terrestrial photogrammetry' is used for applications of photogrammetry which are non-mapping and have a camera to object distance of over 300 metres where usually the camera is ground mounted. The term *non-topographic photogrammetry*, has largely been superseded by *close range photogrammetry*, which is less confusing to the newcomer to photogrammetry.

2.5.2. Close range photogrammetry.

2.5.2.1. Introduction.

Close range photogrammetry is a term used to describe measurements where the object to camera distance is less than 300 metres (Handbook NTP, 1979). In the case of the investigation conducted here, the distance is further confined to less than 30 metres, but distances of 0.3-5.0 metres are of prime interest. This area is ever expanding and includes architecture (Badekas, 1975), biostereometrics, and industry (where the range of interest is very large e.g. automobile construction, machine construction, mining, shipbuilding, aircraft structures (Hall), buildings, and traffic engineering). However, the development of close range photogrammetry has only accelerated over the last twenty to thirty years despite early interest (Developments in CRP, 1980). As the pace of development increases the confines of the subject are being blurred by techniques from other disciplines which collect essentially the same type of data for the same purposes. In 1990 there was a conference titled 'Close range photogrammetry meets machine vision' which shows that there is a growing overlap of subjects of mutual interest between these two areas.

2.5.2.2. Potential of close range photogrammetry.

The justification for the application of photogrammetry to any task has always to be one of cost effectiveness. This factor is also important in the desirability of the technique described in this thesis, it has to be able to prove itself against the best of the alternative methods for it to be applied. This cost aspect of any technique is described succinctly in *The Handbook Of NonTopographic Photogrammetry, 1979*,: 'the fact remains that this technique will not gain general acceptance in industry unless it is cost effective and provides enough technical and economical advantages over other measuring techniques which are in use or under consideration'. The ability to do a task quickly is an important factor in choosing photography or optical triangulation that may be sufficient reason alone for its application.

The potential of close range photogrammetry has been described by Torlegard, 1980, where he summarises its advantages in twelve points which are given below with a comment in brackets comparing the use of optical triangulation for the same purpose.

- (i) The object is not touched during measurement. (Yes.)
- (ii) Data capture (acquisition) is rapid. (Yes.)
- (iii) The photographs store both semantic and metric data with very high density. (No photographs are taken.)
- (iv) The photographs are documents related to the time when they were taken and can be used in legal evidence. (No, although the cross section taken at the time could be.)
- (v) Not only rigid and fixed objects but also deformation and movement can be measured (Yes.)
- (vi) Time dependent parameters such as velocity, acceleration and frequency can be determined. (Yes, in some cases.)
- (vii) Evaluation of the metric photographs can be done at any time in the office and repetition and amendments are always possible. (No.)
- (viii) Photography and evaluation are flexible and can be easily optimised to the project requirements as, for example, in accuracy. (Yes)
- (ix) The invisible part of the spectrum can be used for creating images (Yes, though this feature does not give the same advantages as no image is recorded)
- (x) Complicated shapes and movement are easily measured. (Yes, but the same limitations of lines of sight apply)
- (xi) Stereoscopy is the basis for continuous contouring of irregular objects. (Contouring can be achieved from the data collected)

(xii) Analytical methods provide a means of integration with succeeding calculations and data handling. (Yes)

A number of drawbacks of photogrammetry are also cited by Torlegard, these show that the optical triangulation technique can make significantly improvements.

(i) The results of measurements are not immediately at hand, because time is needed for photographic processing and for evaluation. (No, the data can be seen and evaluated immediately if required.)

(ii) Except for the simplest problems, the need for specialised and expensive equipment makes the method expensive. (Yes, the equipment may be expensive, the method may not prove to be expensive when compared to the complete photogrammetric process.)

(iii) Errors during photography and development of the film can ruin the whole measurement project. (No, if there is any problem in the measuring system this is determined immediately.)

(iv) It must be possible to photograph the subject. (No, the system can operate where it is not possible to photograph, but clear lines of sight are needed.)

(v) Specialised instrumentation and personnel are not always available. (No, this equipment can work automatically or with non professional crews, although there are situations where specialists are required to collect additional data concerning the spatial position of the acquired data.)

2.5.2.3. Future developments in close range photogrammetry.

The emerging trends in close range photogrammetry have been analysed by Hyser, 1984, the pertinent predictions are listed below:

(1) Continuation of efforts to improve precision, accuracy, and reliability of close-range photogrammetric methods.

(9) Improvement and development of digital on-line photogrammetry and robotics.

(12) Study of ways and means of obtaining results more rapidly.

The development of the optical triangulation technique for close range photogrammetric applications appears to supply all of the predicted requirements for the specialised case of measurement of cross sections of structures.

2.5.3. History of tunnelling.

Tunnels have been built by man since Egyptian times who found that they could make tombs in the ground which are still self supporting today. Further tunnelling was carried out by the Romans, but the largest and most prolonged period of tunnelling began in the late 19th century and continues to this day (Harding, 1972). The earliest 'modern' tunnel was probably that constructed in 1692 for the Languedoc canal in South Western France which was 157 metres long, 6.7 metres wide and 8.2 metres high (Willet, 1979). In England, the first industrially important tunnels were constructed by D. Brindley to transport coal from Worsley Mill to Manchester in 1761, and the canal tunnel at Harecastle completed in 1777, which was 2,633 metres in length.

2.5.4. Measuring the profile of surfaces.

The development of the system described in this thesis came about as a direct consequence of the use of photogrammetry to acquire profiles of structures such as railway tunnels and mine shafts. The start of the development, by academic staff at Northampton College of Advanced Technology, of techniques to acquire spatial data concerning specific cross sections or profiles of structures such as railway tunnels for deformation, wriggle surveys or for general information concerning tunnels was as early as 1962 by Manton and Cheffins of Fairey Surveys Ltd (Lindsey, 1991).

The use of tunnel profiles in wriggle surveys (used to assess train clearances in curved track tunnels) and their acquisition by stereo-photography is discussed in a paper by Proctor and Atkinson, 1972, where they used a survey of the second Mersey tunnel, carried out in 1970, as an example. However, a number of problems were encountered that illustrate some of the limitations of the technique: (i) the bar supporting the cameras needs to be long and ideally purpose made, (ii) illumination is required internally for location of the fiducial marks, (iii) control points have to be placed on the surface to be measured, (iv) the cameras must be metric, (v) the post processing times experienced were longer than desirable, and (v) uniform illumination of the tunnel surface is required.

L.J. Rivett, 1973, discusses the use of stereo photogrammetry to measure cross-sections and profiles and concluded that no difficulty was experienced in producing profiles at one metre intervals over twelve metres. The stereo camera used was a Zeiss SMK 120 Stereometric camera.

2.5.5. The light sectioning method.

The use of light sectioning is described by Gates, 1980, as a method developed from the principle of Schmaltz microscope of 1934. The applications of this method include: single image photogrammetric methods used in Austria for the profiling and cross sectioning of railway, highway and street tunnels, the measurement of the abrasion of rock surfaces in Rumania and tunnel surveys carried out for the pumped storage system at Dinorwic, Wales.

The surveying of the Dinorwic pumped storage station is described in Tunnels and Tunnelling by S. Fellows, 1976, the method used the projection of a light plane using a flash light and photography with a Wild P32 terrestrial camera wide angle lens and 400 ASA film. The photograph was synchronised to the flash and the position of the plane of the profile was recorded by a Wild T2 theodolite with a laser eyepiece fitting. The work enabled profiles of tunnels at Dinorwic to be measured faster than would have otherwise been possible.

The contractors BKS Surveys Ltd (Anderson, 1984), experimented with tunnel sectioning from 1978 first of all using stereo photography and later in 1980 using a light plane generator. The experience using stereo confirms what Proctor and Atkinson discovered, that it is not easy, in the restricted visibility and poor conditions of tunnels, to get high accuracy profiles of the subject. The light plane generator used both halogen and ring flash to project a single plane of light onto the surface of the tunnel allowing a photograph of the profile to be taken for subsequent analysis. Scale was established by means of scale points which could be identified in the photograph. Anderson and Stevens note that the measurement of the cross section indicates one of three things:

- (i) The shape of the tunnel as built,
- (ii) changes in pressure during the life of the tunnel, which may have since stabilised, or
- (iii) changes in pressure still occurring.

A system of flash photography is marketed by ROCKSET under the name Photosect 40, the system uses a flash unit and a anodised aluminium disk to project the shadow of the disk onto the wall, this silhouette is photographed and the cross section is then drawn from the negative. A non-metric camera is recommended with a 60 x 60 mm format film, see Fig. 2.6.

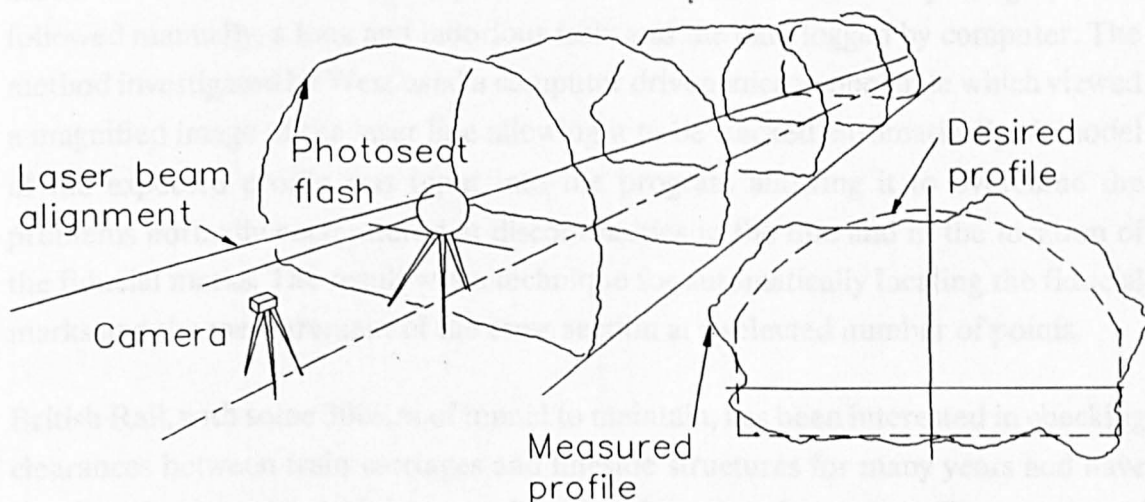


Fig. 2.6. Rockset system.

Care is taken to ensure that the flash unit is located along a straight line illuminated by a laser beam, scale is achieved with scale bars and level by spirit levelling. The accuracy is claimed to be 30mm and the rate of profile photography is 25-40 per hour. It was reported in *Tunnels and Tunnelling* in 1984 that this method was successfully used at the CERN nuclear laboratory project in Geneva.

The first developments in railway profiling were made by a member of staff of the then Northampton College of Advanced Technology in approximately 1962, and used stereo photography with a target at a set distance from the camera to indicate the plane of interest. Following this work, during the 60's and 70's, light flash was experimented with and later the projection of a rotating laser line was used as described by D. Stirling, 1990. This latter method was used successfully at a number of sites and proved a valuable technique in the acquisition of this type of data, but with

limitations. These are of the type indicated in 2.5.4. but also include the disadvantages of long exposure times as the relatively low power laser beam was spread out over a large area which also enforced that the measurements could only take place without the interference of extraneous light.

The problem of improving the collection of data from the photographic plates was addressed in a paper by G. West, 1987, of City University. The standard method of analysing the plates at the time of his investigation was by a stereocomparator in mono mode. The thin line which corresponded to the cross section on the photograph was followed manually, a long and laborious task, and the data logged by computer. The method investigated by West used a computer driven microscope table which viewed a magnified image of the laser line allowing it to be tracked automatically. A model of the expected profile was input into the program allowing it to overcome the problems normally encountered at discontinuities in the line and in the location of the fiducial marks. The result was a technique for automatically locating the fiducial marks and the measurement of the cross section at a selected number of points.

British Rail, with some 300Km of tunnel to maintain, has been interested in checking clearances between train carriages and lineside structures for many years and have developed a 'gauging train' to monitor the clearances between rolling stock and lineside structures such as tunnels (Edworthy, 1986). This system is designed to operate in the presence of conflicting lighting from street lights and to operate while moving. The system operates as a dual light stripe system with a flash. There are twelve TV cameras, forty seven tungsten halogen white light projectors and fourteen microcomputers. The operation of the system allows an average distance map to be constructed for each flash of light taken while the train is in motion. While fulfilling the requirements for gauging information, the necessity for deformation monitoring still exists which needs alternative techniques. This method is described as a photogrammetric method and as such must rank as a real-time photogrammetry application.

British Rail require not only gauging but the dimensions of rails to check for wear. Small, 1986, discusses the use of light sectioning to measure the cross sections of rails. The proposed system was found to work at speeds of 80 Km/hr and with subpixel resolution of 1/10 and accuracy of better than 0.3mm.

It was as a result of continuing interest in the field of measurement of cross sections of structures that the present research project was started. The aim was to investigate

the use of a CCD sensor and optical triangulation techniques to collect the same data quickly, efficiently and with comparable or better accuracy.

2.5.6. The future of photogrammetry.

D. Stirling, 1990, notes the directions in which photogrammetry may develop in the future with a move to what is called 'real time photogrammetry', this is the area which the system described in this thesis fits. He notes that the major research work to date (El Hakim, 1986; Haggren) has the drawback of low resolution, even with cooperative objects. This difference can be as high as a factor of 100, as resolution in the image plane may be of the order of 1:200,000 with photogrammetry but only 1:2000 with CCD sensors used in real time systems. The reason for the low resolution is because of the use of area cameras, which at the present time, and in the near future, are not expected to achieve significantly better resolution. However, the system described herein is able to better these figures because it uses a line scan sensor which uses a selective window of view operating at high speed with higher resolution than area camera systems, see Fig. 2.7.

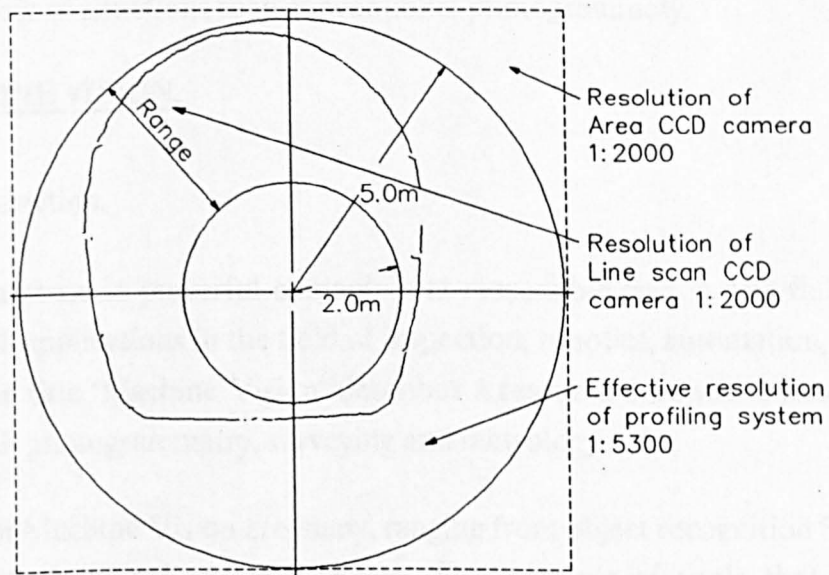


Fig. 2.7. Improvement in overall performance due to selective window.

The use of a window of measurement that is rotated to survey the whole of a cross section gives a significant improvement to the use of an area camera alone. With some configurations which have a narrow range it would be possible to equal the resolution and accuracy of photogrammetry.

2.5.7. Conclusions.

The use of photogrammetry, with or without additional techniques such as light sectioning, has been successfully applied to the field of data acquisition of close range structures such as tunnels. The problem of the time taken to acquire the data, the required environmental conditions, and the post processing time makes this method less attractive as a general purpose technique compared to other techniques. In some instances the data acquired can serve more than one purpose, long term record and provision of spatial data, which may be an advantage over comparable techniques. The method can often provide more spatial data than required, for example a British Rail tender, 1988, for tunnel profiles requires only 40 points to be measured compared with the thousands available photogrammetrically.

The optical triangulation technique which may be described as a selective, electronic, photogrammetric technique, is able to offer the possibility of improved speed of data acquisition with accuracy comparable with that achieved photogrammetrically. It is evident from the cost effectiveness argument of 2.5.2.2. that such a system is desirable and because of the additional features of triangulation systems it may be used in a larger number of situations than conventional photogrammetry.

2.6. MACHINE VISION.

2.6.1. Introduction.

With the increase in powerful computers at reasonable cost, a new field has been created with applications in the field of inspection, robotics, automation, and quality control. The title 'Machine Vision' describes a research area which has substantial overlap with photogrammetry, surveying and metrology.

The goals of Machine Vision are many, ranging from object recognition for robots to defect analysis of rolled steel sheets. The number of tools that have been experimented with, in the search for faster and more efficient tools, is vast. There is a great deal of research work that must be studied to determine the overlap in knowledge and learn from the successes and failures of similar work already conducted.

Within the field of robotics, machine vision is required of: (i) man made structures which are easily described by planes, cylinders, cones, ellipses etc., and (ii) natural structures which are not so easy to describe such as trees, rivers, lakes, landscapes etc.

In applying vision systems to manufacturing there are three main categories: (i) visually guided manipulation, (ii) visual inspection, and (iii) Computer Aided Design (CAD)/ Computer Aided Manufacturing (CAM). D. Nitzan, 1988, describes the techniques for measuring three dimensional information in a tree form, see Fig. 2.8.

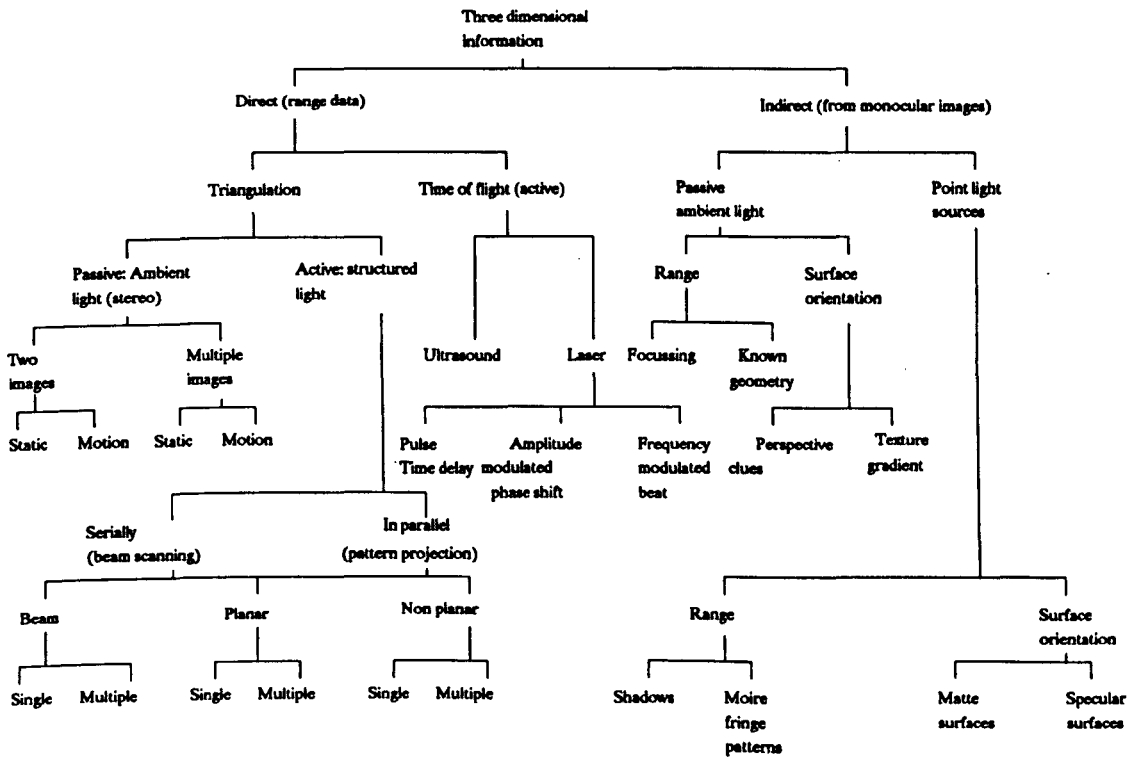


Fig. 2.8. Three dimensional measuring techniques.

Some of the measurement techniques illustrated in Fig. 2.9, are well known and have been exploited commercially while others are relatively obscure and are not suitable for general use. The specification for fast and accurate measurement in the range 0-10 metres excludes many potential methods which are more suitable to provide qualitative information than the quantitative information demanded.

2.6.2. Optical 3-D measurement techniques.

Three dimensional information can be acquired in many ways. Mundy, states that 'The formulation of three-dimensional descriptions of perspective images is a major goal for machine vision research'. The perspective views are generally obtained by use of

one or more electronic area cameras. Although these techniques are undoubtedly important they are not of primary interest here unless further techniques are added such as light sectioning. Jarvis, 1983, notes that most of the techniques which are image based 'are really geometric triangulation techniques of one kind or another'.

In a review of optical 3-D measurement techniques Tiziani, 1989, divides the subject into two areas depending on the coherence of the light source.

(i) Incoherent techniques, such as: triangulation, structured light illumination, Moiré techniques, image plane locating systems and line of sight ranging, time of flight measurement and phase measurement.

(ii) Coherent techniques, such as: (a) homodyne techniques of interferometry, holography, moiré and speckle, (b) heterodyne techniques of single and multiple wavelength interferometry.

An alternative categorisation uses the distinction between 'active' and 'passive' techniques. In the following review the headings, based on coherence, are used with the incoherent techniques section subdivided into active and passive techniques, and coherent techniques, which are (by definition) all active, used as the last section.

2.6.3. Incoherent light techniques.

2.6.3.1. Optical triangulation techniques.

The optical triangulation technique is a fundamental means of range finding, occurring naturally in the depth perception of the human vision system. Hallert, 1960, describes the two triangulation mechanisms that are used human vision as those of convergency and stereoscopic vision, it is the former type that this thesis is concerned with.

Nitzan, 1988, succinctly describes the triangulation scheme, 'Triangulation techniques are based on elemental geometry. Given the baseline of a triangle, i.e. the distance between two of its vertices, and the angle of these vertices, the range from one of the vertices to the third one is computed as the corresponding triangle side'. However, the baseline, which is essential to the triangulation measurement is also the source of one of major problems of triangulation systems that of occlusion, often described as the 'missing parts' problem because, in some circumstances, parts of an object are

obscured. J.P Brady, 1989, comments on the problem of missing parts in the triangulation scheme when compared to coaxial beam methods concluding that the solution is to bring the camera and light source closer together, but this is at the expense of error 'introduced due to the small angles involved in the triangulation calculation'. The trade off between the desire to have a small base length, to avoid the missing parts problem, and the additional errors that this produces is one of the major considerations in optical triangulation design. In comparing optical triangulation schemes to the alternatives Brady also concludes that the coaxial laser schemes using 'time of flight' have not produced results very quickly compared to the triangulation method.

(i) Passive triangulation techniques.

The distinction between active and passive triangulation techniques is in whether any energy is transmitted to a surface under inspection, if so, the technique is an active technique. There is a grey area which covers the placement of targets on the structure to be measured which should be included in the active techniques although no energy is transmitted to the subject.

(a) Range from stereo.

This technique relies on the passive ambient light and two or more cameras positioned to mutually view a given surface. The steps to obtain meaningful data are: the electro-optical recording of the image, the preprocessing of the data, and feature extraction and interpretation to provide the required information. The main problem in stereo vision is the 'correspondence problem', which is the problem of matching features in the images. A major drawback of this method is the inability to form a range map of featureless portions of the image, for instance a plane or slightly curved surface. Hence, there are portions of any image about which no reliable information can be gained which may, unfortunately, be the areas about which precise information is required e.g. the shape of a concrete pipe. For this reason, many stereo systems are active, rather than passive.

(b) Range from focussing.

Range can be deduced from an assessment of when an portion of an image is in focus. A small window is used to provide spatial resolution in the image plane and distance is computed from information concerning the adjustment required for sharp focus. The technique is limited because focus must be obtained for each region of interest,

and the measurement is increasingly inaccurate with increasing range. A description of this technique has been given by Grossmann, 1987, but no results given to show that this method has any promise as an analytical tool.

(ii) Active triangulation techniques.

In active triangulation, light is 'structured' in order to illuminate the object of interest at specific points or planes. This active illumination provides the means of non-contact measurement at high data rates and allows the measurement of featureless planes and curved surfaces. A number of methods are used to project a pattern of light on the surface of interest, these include holographic gratings, interference gratings, white light projectors and laser scanners. If an active scheme is used then, with good design, the operation can be made largely independent of the external lighting conditions, as systems for robot welding have shown (Browne, 1983). However, if no allowance is made for reflectance variations the performance may be less than optimum for surfaces with wide variations in reflectivity over the field of interest. In some cases the reflectance variations can fool the system making the measurement, this is described by Mundy for the case of an edge, see Fig. 2.9.

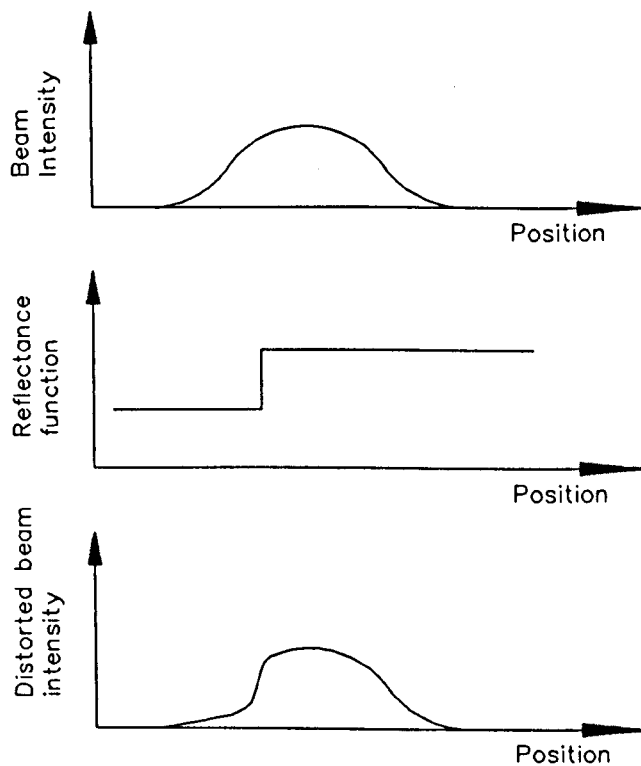


Fig. 2.9. Reflectance variations.

Tiziani, 1989, comments on the optical triangulation technique, 'Triangulation is a very robust method for 3-D measurements point by point. It is particularly appropriate in a hostile environment'. The reason for the robustness of the technique is because, in the basic configuration, it only involves the use of a light source and a sensor held in some fixed configuration for measurements to be made. The basic configuration is shown in Fig. 2.10.

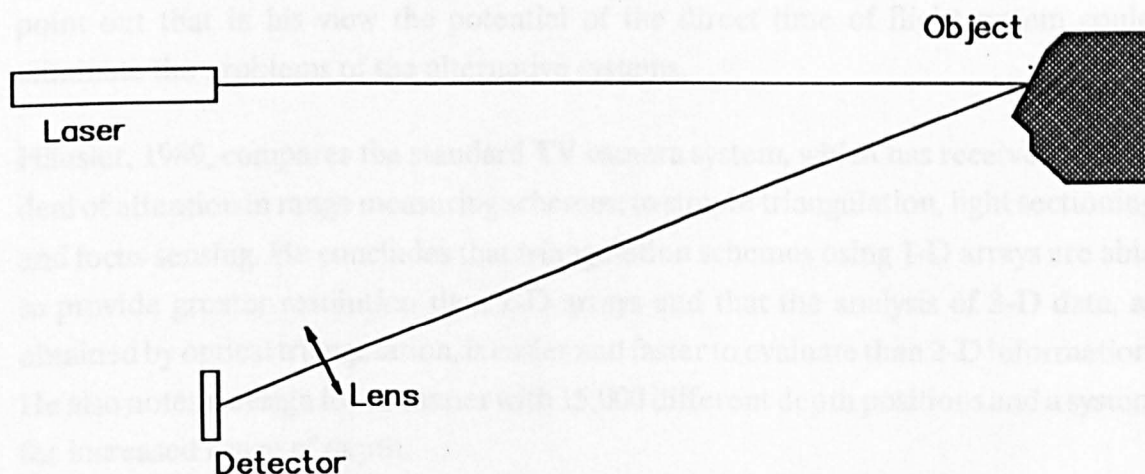


Fig. 2.10. Basic triangulation configuration.

The simple triangulation scheme was chosen as the subject for investigation for this PhD thesis, consequently a more detailed examination of this concept is presented in section (a).

(a) Structured light spot and simple triangulation.

Weise, 1989, discusses the choice of laser triangulation probes for high speed inspection, showing how such systems can be used for both dimensional and non-dimensional inspection tasks. He argues that it is not good enough for a system such as this, to be superior to comparable techniques, it must also survive normal plant/industrial environments and require little maintenance. He concludes that laser triangulation probes have been successfully used in:

- (i) gauging the thickness of hot slabs in a steel rolling mill,
- (ii) profiling lumber in a saw mill,
- (iii) checking dimensions of a finished tire in a tire grinding machine,
- (iv) measuring the level of molten metal in a mould or pouring vessel, and
- (v) as a substitute for weighing, i.e. measure the profile of bags.

He further states that 'Laser triangulation probes can be reliably applied in areas where high temperatures as well as high levels of shock and vibrations are expected'.

Jarvis, 1983, states that 'Perhaps the most obvious method of absolute range finding is to use simple one spot at a time triangulation.' and concludes his review of the range-finding techniques 'from the view point of sheer simplicity, it is hard to improve on triangulation schemes involving one point at a time'. He does, however, go on to point out that in his view the potential of the direct time of flight system could eliminate the problems of the alternative systems.

Häusler, 1989, compares the standard TV camera system, which has received a great deal of attention in range measuring schemes, to simple triangulation, light sectioning and focus sensing. He concludes that triangulation schemes using 1-D arrays are able to provide greater resolution than 2-D arrays and that the analysis of 3-D data, as obtained by optical triangulation, is easier and faster to evaluate than 2-D information. He also notes a design for a scanner with 15,000 different depth positions and a system for increased range of depth:

M. Rioux, discusses the triangulation technique and concludes that a typical configuration will use an angular separation of 30° between the camera optical axis and the source of radiation, which means that the device is bulky. The system developed by Rioux had an angular separation of 10° and used a rotating polygonal mirror and PSD sensor. However, the system was designed under the relaxed requirement of object recognition which is 1% in each axis. However, the system was able, by virtue of its special scanning design, to operate at a response time of 1ms. Rioux chose optical triangulation because it was likely to provide a low cost 3-D camera. This measuring system is now being used in space for location of artifacts on a space station (Maclean, 1990).

Nimrod describes the use of simple triangulation with a synchronised rotating and transmitting mirror of compact construction with a typical precision of 0.1% of the range at 30mm to 0.07 % of the range at one metre. This system uses a photodetector to detect the position of the mirror when the incident light is imaged, then the timing is used to compute distance with a reported scan rate of 1.23ms.

Various systems have been developed which use optical triangulation for guidance of automated welding systems, Smati, 1984, used a PSD. The idea of using a PSD for the sensor to probe objects and extract their features was explored by Ishii, 1976, who developed a 'hand eye' system which was able to select edges in an object and scan

the boundary to determine the shape of the object prior to a robotic task, such as moving the object. The use of PSD's in 3-D Vision is explored by Chen, 1987, who used two receivers to collect the light, partially eliminating the problems of occlusion, see Fig. 2.11.

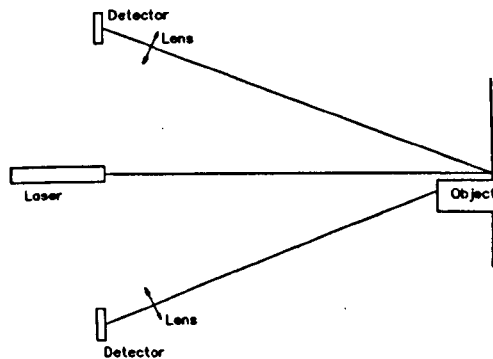


Fig. 2.11. Elimination of occlusion by two receivers.

However, the use of two receivers adds to the cost, weight and size of any complete system.

Verbeek, 1985, discusses a new sensor for use in optical triangulation systems which is a PSD array sensor, combining the advantages of the PSD with those of the CCD array. The authors claim that their sensor allows the construction of a 'video speed range camera system on the basis of triangulation with a light plane which generates successive object depth profiles at video line frequency.'

The use of optical triangulation has been shown to be a well known and reliable technique which can be used in many circumstances to provide measurements of structures with a high degree of accuracy and speed. The fact that many systems have been used in industrial environments shows that there is a lot to commend this technique and that the investigation carried out in this thesis is justified if it can be applied to the measurement of structures such as sewers, mine shafts and tunnels.

(b) Structured light & Moiré.

Moiré fringe range contours are obtained in a number of ways, the active scheme is as follows: A scene is illuminated by light which is modified by a grating to produce a light pattern this is viewed via a second identical grating by a camera which is displaced laterally from the projection system. An interference pattern is the result where the contours represent equidistant displacements.

(c) Structured light and ratio image depth sensor.

The scheme uses the image of a scene illuminated by the projection of a beam of light that varies monotonically in intensity from one side to the other, followed by another image with illumination of uniform intensity. The two images are divided pixel by pixel, the resulting image then contains only information about the location of surfaces in the 3-D scene as factors which affect the intensity of the reflected light.

Bastuscheck, 1985, comments in their paper on an experimental implementation of a ratio image depth sensor that 'the amount of accurate spatial information which can be extracted from an image such as is made by a camera using ordinary illumination is distinctly limited.' They proposed a system for forming a 512x512 depth image in thirty seconds using standard components. The claimed average random deviation was about +/- 0.7% of the depth of the workspace.

(d) Structured light and light patterns.

To overcome the correspondence problem of passive stereo techniques, structured light is projected onto the scene to be measured. The light pattern may be a light stripe or a serial sequence of patterns such a Hamming, Gray's, or a binary code, in each case the projection allows the unique identification of points of interest. Problems of this technique are those of specular reflections causing the camera to see the multiple reflections of the projected pattern, and the problem of the speed restriction placed on the system because multiple frames each with a unique code are required of the same scene. The restrictions relating to the light stripe identification reported by Jarvis, 1983, are:

- (i) the image should contain parts of the supporting plane surface,
- (ii) shadows cause line interruptions,
- (iii) top surface lines should be distinguishable from ground plane lines, and
- (iv) scenes with more than one object should not have hidden object planes.

He notes that this last point would appear to affect nearly all types of ranging. The problem of requiring multiple frames in a coded projection pattern scheme has been addressed by Vuylsteke, 1990, who reported a single binary encoded light pattern that enabled the identification of any grid point by the signature of a 2x3 pixel window. This system was therefore able to offer significant speed advantages over standard

coded systems making it applicable to moving scenes such as found in robotic assembly.

(e) Structured light attached to object of interest.

O'Connor, 1990, reports some experiments using a PSD with a LED attached to a PUMA robot. The system was able, after calibration, to accurately locate the position of the LED with respect to the PSD camera. He makes the comment 'Judging by the scarcity of published material, the position sensitive detector (PSD) appears, at least until recently, to have been regarded as insufficiently precise for applications in robot coordinate measuring systems.'

(f) Range from brightness.

Jarvis, 1984, describes the use of brightness variations in a scene to obtain range data about the scene from a monocular viewpoint, so eliminating the missing parts problem, but restricting its use to lambertian scattering objects without secondary light reflections. Duda, 1979, also describes the use of range and reflectance data to find planar surface regions. The aim of such systems is the 'extraction of low-level representations of surfaces for subsequent three dimensional scene analysis'. It is unlikely that this method is sufficiently robust or accurate enough for general use.

2.6.3.2. Non-triangulation measuring systems.

There are many non-triangulation non-contact distance measuring systems from the ultrasonic to microwave, however, only the light based systems have the required spatial resolution to measure objects to an accuracy of 1mm in x,y and z. The main distance measuring technique is that of the time of flight of light and can be both coherent and incoherent techniques.

The coherent techniques which also use time of flight, are covered in section 2.6.4. The incoherent techniques use the time of flight system in two basic ways first in the time for the pulse-echo round trip, and second in the modulation of the signal to provide a phase method of gaining the time of flight of the signal. The advantages to the incoherent techniques are the avoidance of the problems particular to coherent systems such as coherence loss and gross degrading of the signal due to speckle effects with non cooperative targets as explained by Joynes, 1975. Other advantages of the pulse-echo technique are that while accuracy may not be high, the electro-optic system

can be made into small and relatively low cost units, and the pulse technique may be the only solution to provide enough power over long distances.

(i) Pulse-echo techniques.

The time of flight laser range finder system measures the time delay from the sending of a very short pulse of light to its echo return. Because the speed of light is approximately constant, distance measurement can be achieved. The measuring beam can be scanned over the surface to be measured to build up a 3-D range map.

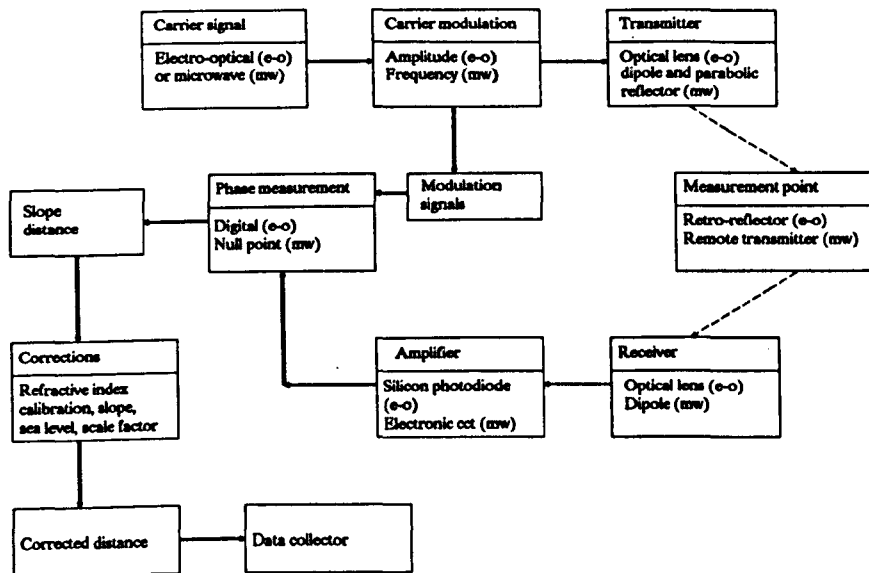
The use of a laser time of flight range scanner for robotic vision is explored by Jarvis, 1983, in an often quoted paper. He comments that many of the systems that indirectly gain information about a scene such as lighting, depth from focussing, range from brightness, all suffer by being computationally expensive, have diminishing accuracy with range and many suffer from the 'missing parts' problem. Direct time of flight is therefore superior to these methods if the speed of measurement and accuracy obtained is comparable or better.

Kaisto, 1983, reported an optical range-finder for 1.5 - 10.0 metres distance measurement of reasonable accuracy with a measurement time of 10 msec. He states that the phase shift method is not usually fast enough and so investigated the transit time of light pulses. He reports standard devices are able to provide the required resolution of 10 mm, but are not quick enough. With a high pulse repetition rate, averaging, and an efficient time to amplitude converter, improvements were achieved.

Two other methods are possible: Amplitude Modulated (AM) phase shift between the returned beam compared to that sent, and Frequency Modulated (FM) method which measures the phase difference between the sent and the returned beam.

(ii) Phase measurement.

The use of phase measurement in a laser distance range-finder has been discussed by Grattan, 1990, who also reviews the alternative techniques and concludes that a laser range-finder of high resolution may be constructed with the latest techniques and components. In the field of surveying many EDM systems use the phase measurement system, the technique has been extensively reported in the literature (Burnside, 1982; Price, 1989; Rueger, 1990) and will not be covered in detail except to point to limitations and to allow comparison.



The principles of operation of a typical EDM instrument are shown in Fig. 2.12. reproduced from the book 'Engineering surveying technology.' (Kennie, 1990).

Fig. 2.12. Block diagram of principle of EDM operation.

The carrier measurement of the phase difference between the outgoing and incoming signal can be measured digitally by counting the number of accurate timing pulses to occur between the positive going zero crossing of the two waves, see Fig. 2.13.

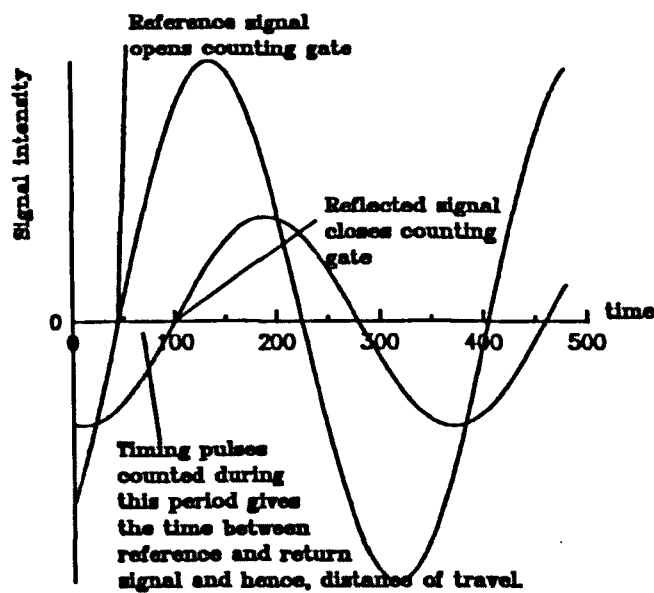


Fig. 2.13. Phase measurement using digital pulse counting(Burnside, 1982).

For continuous wave modulation techniques, intensity or polarisation methods may be used. Joynes, 1975, comments that with non-cooperative targets the intensity modulation technique is to be preferred because the polarised light gets depolarised

in the back scattering process. The method used compares the instantaneous phase difference between transmitted and received signals.

The precision laser measurement system (Eagle, 1988) produced by Digital Optronics Corporation, U.S.A. has developed equipment for accurate measurement of Radar/Microwave dishes, but the producers hope that it may find uses in other areas such as: inspection of rivets on aircraft structures, surface waviness of aircraft panel assemblies, tooling fixture alignment verification and general purpose non-contact measurement. The specification is as follows:

Accuracy 0.038mm (R.M.S.)

Range 1.54m to 4.57m

Measurement field of view 80x80 degrees

angular resolution +/- 10 seconds

maximum no of point measurements per session 64k

maximum speed of measurement 2 seconds

range of reflectivity allowable 100% to 10%

method of operation is by continuous wave frequency modulated radar type

power output of laser 30 mW

wavelength 840 nm

class of laser = IIIb

The system is very accurate, but slow, immobile, and has a limited field of view for profiling applications, but illustrates that short range, high accuracy time of flight systems can be built.

(iii) Frequency ramp.

Frequency ramping is a means of distinguishing the time between the reference and reflected beams. This system has been described by Kobayshi, 1988, Shinohara, 1989 and Hymans, 1960, the latter describing the application to conventional RF Radar and the former two are concerned with laser techniques. The principle of the system is the production of a continuous wave signal of constant amplitude that has a ramped frequency of modulation. See Fig. 2.14.

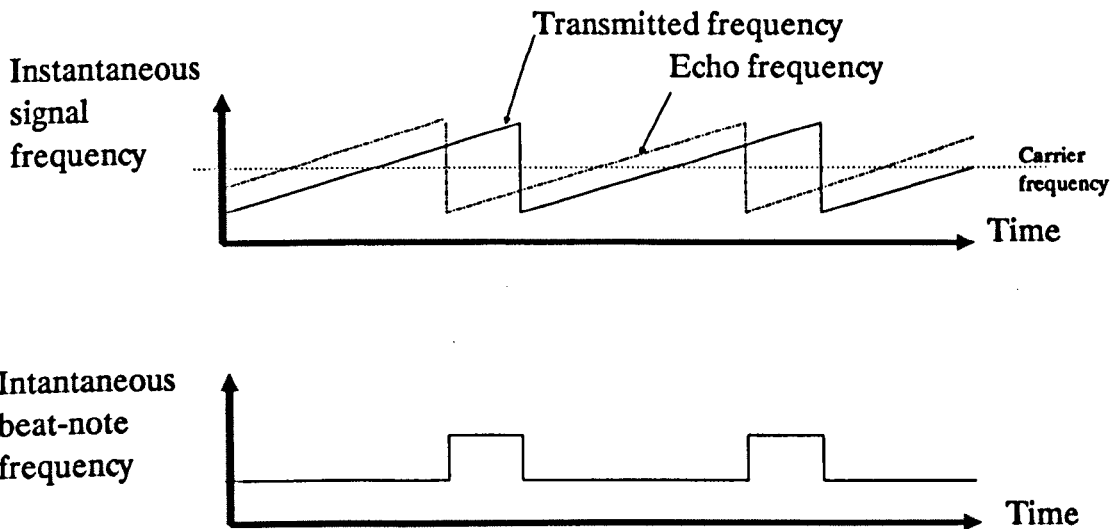


Fig. 2.14. Frequency ramped modulation.

The production of a frequency ramped signal is achieved by modulating the current to laser diode by a saw tooth wave form. The frequency of the laser output is approximately linearly related to the current, hence, given the current waveform, the diode laser is frequency ramped.

The principle of operation is the same as most of the time of flight systems, the measurement (delayed) signal is compared to the reference (undelayed) signal. In the scheme identified by Hymans the measurement is conducted in the frequency domain. In the system developed by Kobayashi the target range is obtainable by measuring the total phase shift of the beat signal, accuracies as high as $7\mu\text{m}$ were obtained. The options available for frequency ramped systems are described by Economou, 1986, and are shown in Table 2.2.

METHOD DOMAIN	Measure small path length changes by monitoring the phase of the beat frequency (non-variable interferometer)	Measure absolute path length by monitoring the beat frequency (variable interferometer)
TIME DOMAIN	Lock to or follow a selected location of the time domain output signal	Measure the wavelength of the beat frequency in the time domain
FREQUENCY DOMAIN	Demultiplex the sidebands of the beat frequency	Determine the peak of the $\sin(x)/x$ sideband spectrum

Table 2.2. Four options possible in a Frequency Modulated Continuous Wave (FMCW) system.

Economou also summarises the sources of error in FMCW systems as (a) non linear frequency ramp effects, (b) laser drift noise, (c) (1/f) noise, and (d) Phase noise. The reliable use of this technique has yet to be established, but there grounds for the view that this technique could be important in distance measurement in the future.

(iv) Optical inverse square law displacement sensor.

This invention (Howe, 1987) uses the back scattered light from a surface to calculate the distance from the sensor. The method of operation is to project a spot of light onto the surface to be measured and measure the difference in light intensity by two sensors (A & B) at the same solid angle from the spot but at different distances.

2.6.4. Coherent light techniques.

The accuracy achieved by the coherent techniques is much higher than that achieved by most methods of distance measurement by virtue of the short wavelength of light. It is possible to measure to fractions of a wavelength of the light making measurements to sub micron distances possible. However, these techniques are generally unsuitable for non-cooperative targets.

2.6.4.1. Homodyne techniques

A novel technique recently reported by Rarity, 1990, is that of single photon range-finding using parametric down-conversion. This technique uses the spontaneous parametric fluorescence of two photons created from one pump photon. The operation of this technique is based upon the near simultaneous (100 fs) creation of two photons. The means of operation is to take one set of photons around a controlled path and let the others go to the target and back, the measure the difference in time. In these experiments retro-reflective targets were used. The advantages of this technique are in the low light levels used (nWatts), and that accuracy of the order of millimetres may be obtained. The technique has importance in military application in the avoidance of range finding detection by the enemy which is liable to happen with more powerful probes.

2.6.4.2. Heterodyne techniques

Heterodyne techniques involve the production of two light beams of slightly different frequencies. In the Hewlett Packard Interferometer this is achieved by magnets which are placed near to the gas discharge tube causing Zeeman splitting, the two beams

which have differing polarisations are split optically. One beam is used as a reference and the other is reflected back from the target and optically mixed with the reference beam. The Doppler shift in the measuring beam allows the counting of fringes to occur and hence the measurement of distance. The technique is only useful in measuring to a mirror like surface or corner cube reflector, and the distance measured, although accurate, is only referenced to a count starting position. Dual wavelength heterodyne techniques are being researched which may provide 0.1 mm resolution over 10 metres (Tiziani, 1989).

2.6.5. Conclusions.

Several techniques for distance measurement have been surveyed. The techniques which are of most relevance to the simple optical triangulation system investigated in this thesis are the area camera techniques which promise large quantities of information per field of view and the laser ranging systems which promise high accuracy measurement to non-cooperative targets.

The area camera approach to 3D data acquisition, used in light stripe, coded shading, moiré, shadows, is inadequate to collect spatial data concerning cross section of objects for several reasons:

- (i) the camera resolution is low,
- (ii) the area of interest is large, and
- (iii) the time for collection of each frame or frames is high.

The laser ranging techniques are the most promising because of the elimination of the missing parts problem, the high potential data rates and high resolution. However, the requirements of a robust, accurate and fast system have not yet been met.

The triangulation system using a single spot and CCD sensor remains a system that is computationally simple, is robust in its basic design, fast in operation and capable of meeting the resolution requirements of many applications. However, there is still the missing parts problem, the inherent non-linearity and the disadvantage of the physical size of the resulting equipment due to the size of base of the measuring triangle required.

2.7. CONCLUSION.

The field of data acquisition of range data which can be built up into 3-D range data has been considered and the techniques have been analysed, a technique from among these, active optical triangulation, was chosen for investigation because it provided a faster and more accurate measuring system than comparable techniques, it had seldom been applied in this situation, and it is robust.

This technique is similar to that used in optical tacheometry and surveying triangulation. It has not been tested in surveying applications to any great extent but has received widespread use in machine vision especially in metrology where many optical triangulation sensors are available commercially.

The lessons learnt in surveying, metrology, photogrammetry, and machine vision are all of value in the development of the understanding of the technique. This thesis brings together this knowledge to contribute to the understanding of an optical triangulation system when applied to the measurement problems of industry and engineering.

3. OPTICAL TRIANGULATION THEORY.

3.1. SYNOPSIS.

The theory developed in this chapter is subsequently used in the analysis of the development of the prototypes in chapter 4, the error analysis of chapter 5, and the results of practical tests and theoretical simulations reported in chapter 6.

The following topics are considered:

- (i) Geometrical optical triangulation theory.
- (ii) Theory of optical components: lenses, prisms, filters etc.
- (iii) Theory of CCD sensors.
- (iv) Theory of laser light propagation.
- (v) Light scattering theory.
- (vi) Signal processing theory.
- (vii) Calibration theory.

3.2. INTRODUCTION.

This chapter describes the optical triangulation theory as applied to a measuring system. There are a number of possible configurations for optical triangulation systems (section 3.3), but the principle of operation remains the same, that is, a light source (section 3.6) identifies a point on a surface to be measured. The reflections of this light (section 3.7) will radiate in a variety of directions, a small proportion of which is collected by a lens (section 3.4) and focussed on a sensor (section 3.5) which provides the means to distinguish (section 3.8) the, relatively high intensity, peak from the background illumination and record its position. This position is related to a prior calibration (section 3.9) from which a distance can be computed. This system is held together in a fixed configuration so that a multiplicity of such measurements can be made.

An understanding of theory is vitally important for the efficient design of electro-optic systems, a small oversight can have very large consequences. For instance, the filter that is sometimes glued to a standard CCD sensor (to provide a spectral response curve similar to the human eye) will also block out most of the light from a diode laser of a wavelength of 780nm.

3.3. GEOMETRICAL OPTICAL TRIANGULATION THEORY.

3.3.1. Introduction.

A typical configuration for optical triangulation measurement is shown in Fig. 3.1. This comprises a laser pointer, lens, sensor and mechanical components to provide a stable configuration.

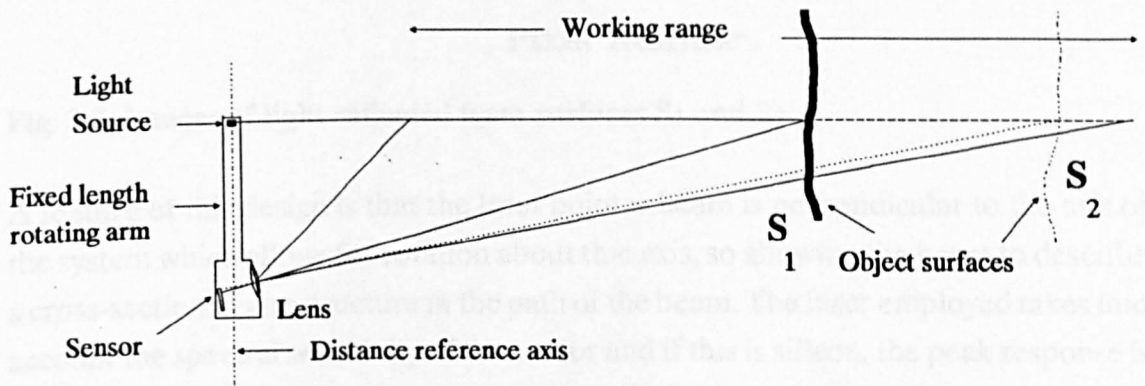


Fig. 3.1. Optical triangulation configuration.

The relationship between distance from a structure and image position on the sensor is shown graphically in Fig. 3.2, the image position variation for two distances is illustrated with reference to Fig. 3.3.

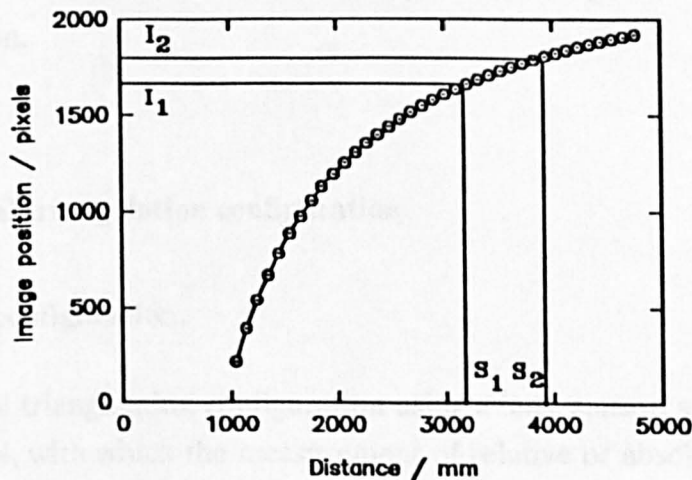


Fig. 3.2. Calibration curve.

The images that is formed from surfaces S_1 and S_2 are shown in Fig. 3.3.

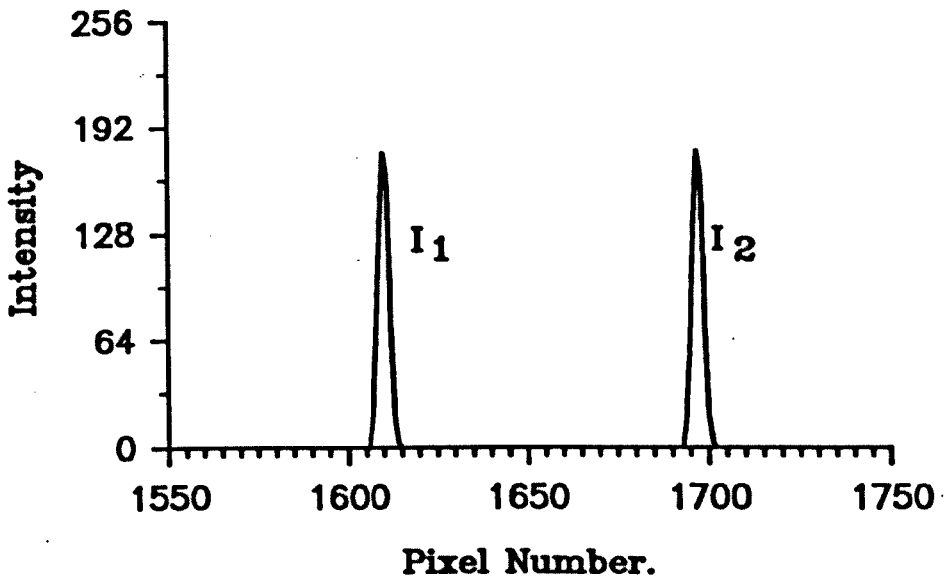


Fig. 3.3. Images of light reflected from surfaces S_1 and S_2 .

A feature of this design is that the laser pointer beam is perpendicular to the axis of the system which allows for rotation about that axis, so allowing the beam to describe a cross-section of any structure in the path of the beam. The laser employed takes into account the spectral sensitivity of the sensor and if this is silicon, the peak response is in the near infra-red part of the spectrum. A diode laser source, such as one of those emitting at wavelength 670,750 or 780 nm is a suitable choice, the first being highly visible to the naked eye, the latter being only just visible in the dark but much cheaper than the other two and well matched to the detector peak sensitivity. If another type of laser is used, such as HeNe (632.8nm), then its physical size is an important consideration as the diode laser offers not only the advantages of small size but low voltage operation.

3.3.2. The optical triangulation configuration.

3.3.2.1. Simple configuration.

A simple optical triangulation configuration using a lens, sensor, and light source is shown in Fig 3.4, with which the measurement of relative or absolute displacement can be effected.

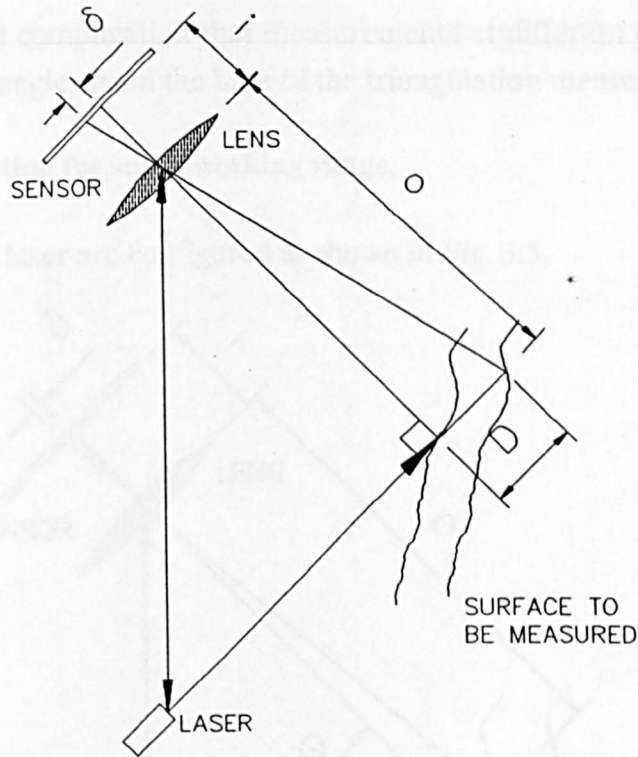


Fig. 3.4. Simple optical triangulation.

The relationship between object and image distances is given in Equ. 3.1.

Equ. 3.1.
$$\delta = \frac{iD}{o}$$

There is a linear relationship between object and image, the measurement of absolute distance can be effected by knowledge of three of the parameters. As 'i' is the focal length of the lens, 'o' the distance to the object from the central axis, then by measuring 'delta' on the sensor, the displacement 'D' is known. However, the accurate measurement of these parameters is not trivial, so a simple calibration will allow this system to be used to measure distance or alternatively relative measurement may be performed by comparison with a object of known dimension.

The main drawback of this configuration is that the base length is longer than the measuring distance, hence, the most suitable arrangement for measuring cross sections of structures is to make the axis of rotation perpendicular to the plane formed by the laser beam, base line and optical axis. This configuration has been used to measure cross sections of tunnels (Gallacher, 1987), but a obvious disadvantage is a very high moment of inertia for the system which makes it clumsy to transport and operate. A further disadvantage is that unless the laser beam is on the axis of rotation

there is the added complication that measurements at different distances also take place at different angles from the base of the triangulation measurement triangle.

3.3.2.2. Configuration for small working range.

If the camera and laser are configured as shown in Fig. 3.5,

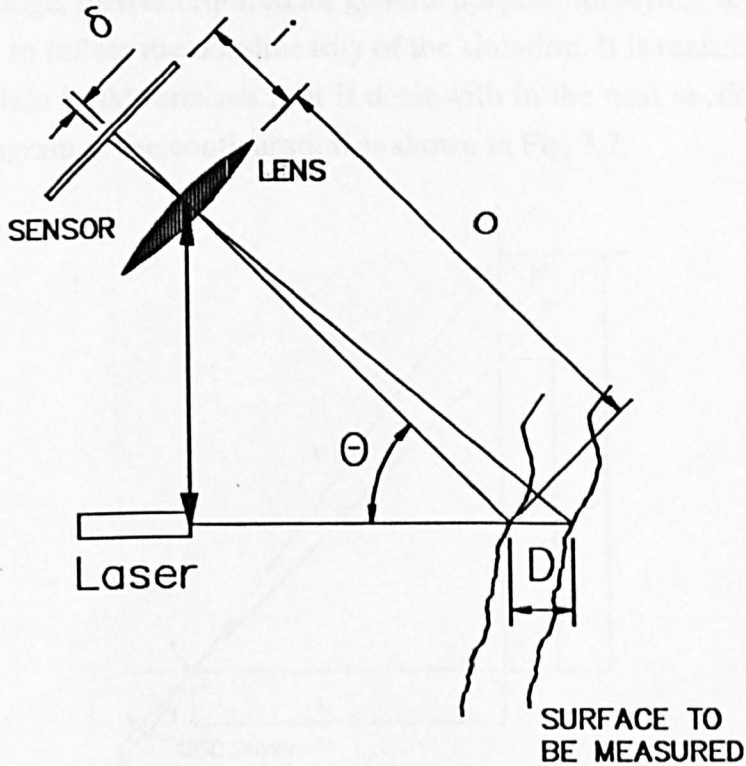


Fig. 3.5. Configuration for small working range.

where the camera and light source are no longer perpendicular to each other then provided 'D' is small and ' θ ' is constant the Equ. 3.1. is modified to Equ. 3.2.

$$\text{Equ. 3.2.} \quad \delta = \frac{iD}{o} \sin(\theta)$$

Over a small range the system is approximately linear and in some circumstances it may be an advantage to have a small range as it implies a higher resolution. Often, however, a larger range is required, in this case the configuration has the additional problem of requiring a large depth of field to keep the image in focus. It is also apparent from the geometry that, with the same base length, the resolution will decrease as the distance from the base-line of the system is increased. Unfortunately, with an extended range, the image of the laser pointer will be out of focus at certain

parts of the range, or a large depth of field (DOF) will be required. This is not always possible as a small DOF is achieved by a small aperture which reduces the amount of light able to reach the sensor from the object.

3.3.2.3. Non-linear equation for extended range.

Over a larger range, such as required for general purpose surveying, the equation has to be modified to reflect the non-linearity of the situation. It is reasonable to ignore the focus problem in this analysis as it is dealt with in the next section. Consider a generalised diagram of the configuration as shown in Fig. 3.7.

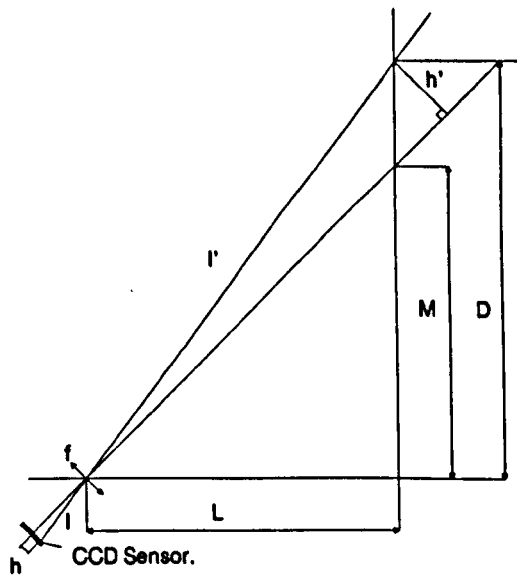


Fig. 3.7. General triangulation configuration.

If 'L' and 'M' are known, and 'D' is the Distance from the axis of the device to the profile surface being measured then the distance from the lens to this spot I' is given by Equ. 3.3.

Equ. 3.3. $I' = (L^2 + D^2)^{1/2}$ by Pythagorus.

By making use of the relationship between object/image distances and object/image heights as shown in Equ. 3.4.

Equ. 3.4. $\frac{I'}{I} = \frac{h'}{h}$

it is possible to write an equation for 'h' in terms of 'D', the desired distance, and the known parameters as shown in Equ. 3.5.

Equ. 3.5.
$$h = \frac{h'l}{l'}$$

Where 'l' is the focal length of the lens and by trigonometry h' is given by Equ. 3.6.

Equ. 3.6.
$$h' = (D - M) * \text{Sin}[\text{Tan}^{-1}(L/M)].$$

Hence, the equation linking 'h' to 'D' is given in Equ. 3.7.:

Equ. 3.7.
$$h = \frac{f * (D - M) * \text{Sin}[\text{Tan}^{-1}(L/M)]}{(L^2 + D^2)^{1/2}}$$

The relationship between 'h', the image position and 'D', the distance from the base line is plotted using Equ. 3.7, in Fig. 3.8. The parameters: M = 1.65m, f = 50mm, and L = 0.7m. were used.

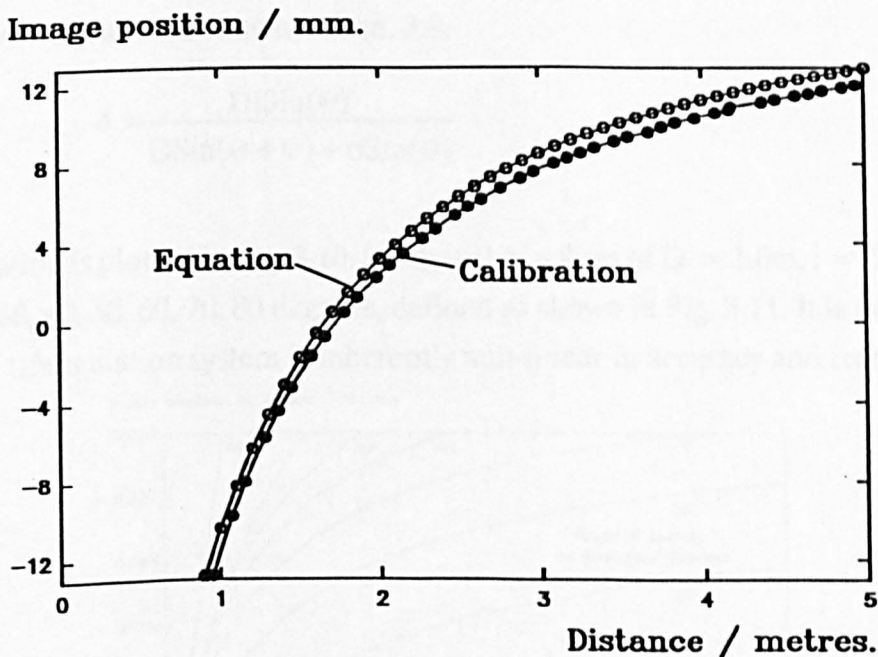


Fig. 3.8. Non-linear relationship for triangulation equation and calibration.

The results of this equation are compared to data from a calibration of prototype III, which had the same physical configuration. Apart from a small displacement there is very high degree of correlation between the two data sets.

3.3.2.4. Non-linear equation with perfect focus.

If a larger range of measurement is required while maintaining the favourable conditions of focus for the sensor, Ji and Leu, 1989, have derived an exact relationship between the object and image displacements with perfect focus throughout the range. This is achieved by making the sensor, lens and light source fulfil Scheimpflug's condition which states that 'for perfect focus, the image plane, the object plane and lens plane all must intersect along a common line' (Wolf, 1983), as shown in Fig. 3.9.

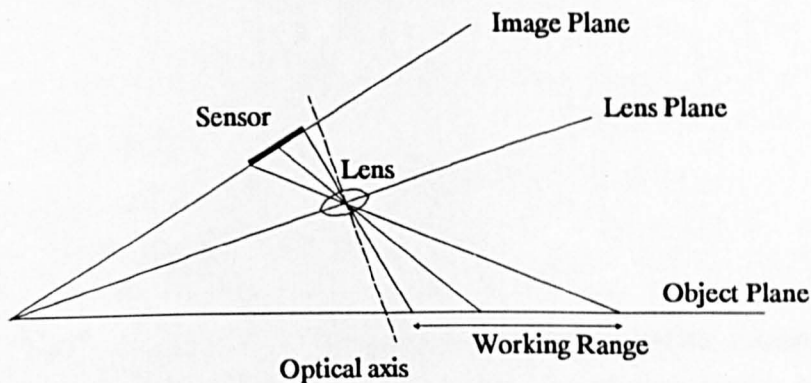


Fig. 3.9. Geometry of the Scheimpflug condition.

The derived equation is shown in Equ. 3.8.

Equ. 3.8.
$$\delta = \frac{Di \sin(\Theta)}{D \sin(\Theta + \Phi) + o \sin(\Theta)}$$

This equation is plotted in Fig. 3.10. for the set of values of $D = 1.0\text{m}$, $i = 50\text{mm}$, and $\Theta = 20, 30, 40, 50, 60, 70, 80$ degrees, defined as shown in Fig. 3.11. It is evident that the basic triangulation system is inherently non-linear in accuracy and resolution.

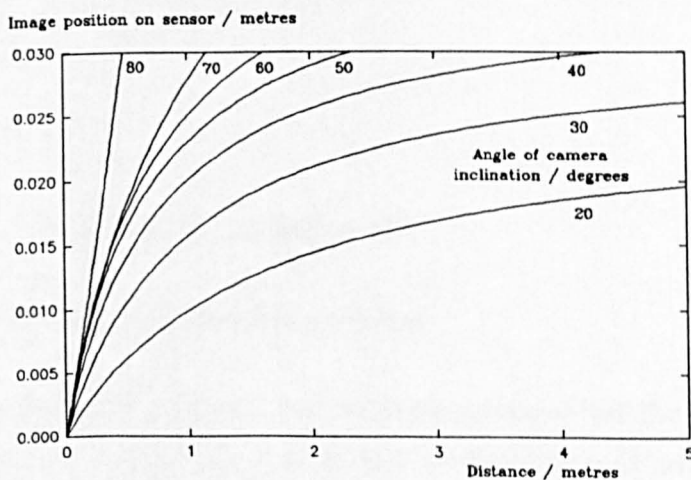


Fig. 3.10. Graph of δ against D .

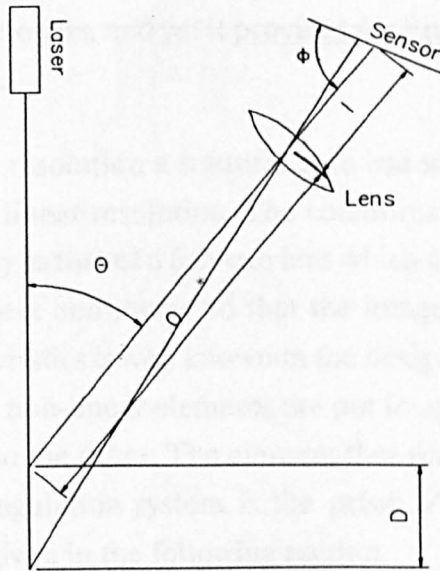


Fig. 3.11. Configuration for Equ. 3.8.

This equation shows the inherent non-linearity of triangulation systems which, for the same range, increases as the distance between the sensor optics and light source decreases. The effect of the non-linearity is that accuracy and resolution are not constant over the measuring range. An example of how onerous this variable resolution can be in a triangulation based measuring system is given in Fig. 3.12, half of the available resolution is used over the first 0.75 metres leaving the rest for the remaining 4.3 metres of the range. This was the configuration used for Prototype III.

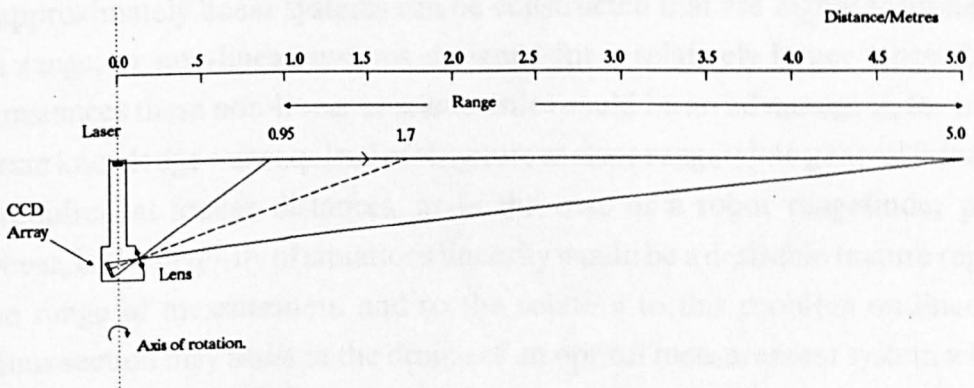


Fig. 3.12. Measuring range for prototype III.

3.3.2.5. Solution of the non-linearity problem.

Because ready-made components such as cameras come 'off the shelf', fundamental thinking about the appropriateness of the configuration is not often considered. However, in the case of optical triangulation, a detailed appraisal is required to gain optimum performance as, for example, the Scheimpflug condition has not been

spotted by all system developers, and yet it provides for little effort a great advantage over uncorrected systems.

In the case of non-linear resolution a solution is to use some form of correction to oppose its effect giving a linear resolution. The counteraction of the non-linearity is performed in a similar way to that of a fish-eye lens which changes the normally linear relationship between object and image so that the image is distorted. This type of correction of the characteristics is well known in the design of linear instrumentation (Doeboelin, 1983) where non-linear elements are put in opposition, so modifying the overall relationship one to the other. The element that was chosen to counteract the non-linearity of the triangulation system is the prism. A discussion of the theory concerning the prism is given in the following section.

A full analysis of the correction to the non-linearity problem is discussed in chapter 6. The geometrical analysis of the triangulation system assists in the design of a measurement system with a range that is suitable for a given requirement. However, for an assessment of the errors many other factors need to be taken in to account. These are analysed in the chapter 5.

3.3.3. Conclusions.

The implications of the inherent non-linearity in an optical triangulation system are that approximately linear systems can be constructed that are highly accurate over a small range, or non-linear systems designed for a relatively larger range. In some circumstances these non-linear characteristics could be an advantage if, for instance, accurate knowledge was required of structure at close range while general information was required at longer distances, as in the case of a robot rangefinder perhaps. However, in the majority of situations linearity would be a desirable feature regardless of the range of measurement and so the solution to this problem outlined in the previous section may assist in the design of an optical measurement system which has increased compactness and linearity.

3.4. THEORY OF OPTICAL INTERACTIONS.

To construct a optical triangulation system a number of components are used: a sensor, lens, prism and laser. The light generated by the laser interacts with the medium through which it passes (air) and the surfaces upon which it directly or indirectly impinges (surface to be measured, lens, prism and sensor). These interactions may bend the light beam, produce speckle patterns on the sensor and

modify the intensity distribution of the laser beam. The theory behind these interactions is given in the following sections.

3.4.1 Prism.

As suggested in the last section, the prism can be used as an important component in the correction of the inherent non-linearity of the triangulation scheme. Prisms are normally used in the dispersion of light and their use as linearity correctors is not well documented.

3.4.1.1. Derivation of the prism deviation equation. (Hecht, 1973; Southall, 1963)

Optical triangulation systems suffer from non-linearity in the relationship between image and object position. This can be a severe problem in the use of this technique as much of the available resolution and accuracy is wasted at one end of the measuring range. To correct this an opposing non-linear optical element is required.

A prism is often used for the way it disperses light so that component wavelengths can be identified. However, with a monochromatic source such as a laser, it is possible to use another feature of the prism; the angle of deviation has a non-linear relationship with the angle of incidence. A ray of light incident at the face of a prism will emerge having been deflected by an angle 'd' the 'angle of deviation', see Fig. 3.13.

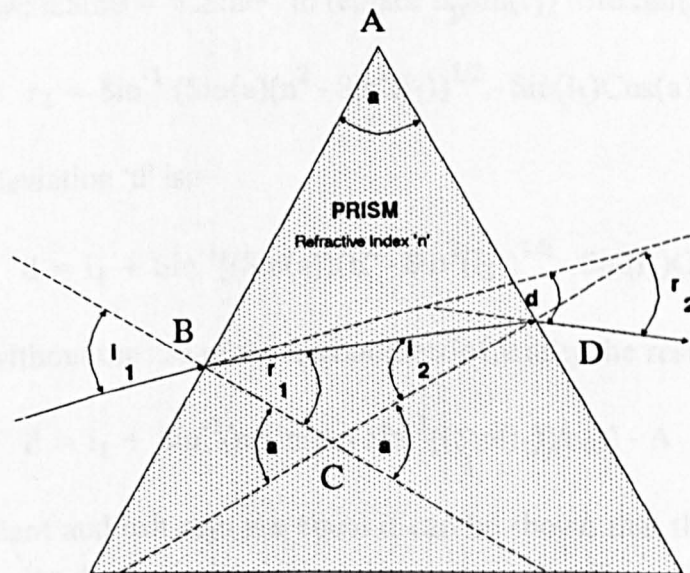


Fig. 3.13. Basic prism configuration.

The incident ray is deviated by an angle of $i_1 - r_1$ at the first interface, and by $r_2 - i_2$ at the second. The total deviation 'd' is then given by Equ. 3.9.

Equ. 3.9. $d = (i_1 - r_1) + (r_2 - i_2)$

Since the Polygon ABCD contains two right angles the angle BCD must be the supplement of the apex angle 'a'. Now 'a', being the exterior angle to triangle BCD, is also the sum of the alternate interior angles, see Equ. 3.10.

Equ. 3.10. $a = r_1 + i_2$

Therefore:

Equ. 3.11. $d = i_1 + r_2 - a$

It is required to write 'd' as a function of both the angle of incidence for the ray i_1 , and the prism angle 'a'. By Snells Law, assuming n_{air} to be approximately 1, and that n_p is known then:

Equ. 3.12. $r_2 = \text{Sin}^{-1}(n_p \text{Sin}(i_2)) = \text{Sin}^{-1}[n_p \text{Sin}(a - r_1)]$

Using $\text{Sin}(A - B) = \text{Sin}(A) \cdot \text{Cos}(B) - \text{Cos}(A) \cdot \text{Sin}(B)$ and replacing $\text{Cos}(r_1)$ by $(1 - \text{Sin}^2(r_1))^{1/2}$ it follows:

Equ. 3.13. $r_2 = \text{Sin}^{-1}[n_p \text{Sin}(a)[1 - \text{Sin}^2(i_1)]^{1/2} - n_p \text{Cos}(a) \text{Sin}(r_1)]$

Using Snells Law: $n \cdot \text{Sin}\theta = n' \cdot \text{Sin}\theta'$, to replace $n_p \text{Sin}(r_1)$ with $\text{Sin}(i_1)$ it follows that:

Equ. 3.14. $r_2 = \text{Sin}^{-1}(\text{Sin}(a)(n^2 - \text{Sin}^2(i_1))^{1/2} - \text{Sin}(i_1) \text{Cos}(a))$

Therefore the deviation 'd' is:

Equ. 3.15. $d = i_1 + \text{Sin}^{-1}[(\text{Sin}(a)(n^2 - \text{Sin}^2(i_1))^{1/2} - \text{Sin}(i_1) \text{Cos}(a))] - a$

Alternatively, without the use of the trigonometric identity the resulting equation is:

Equ. 3.16. $d = i_1 + \text{Sin}^{-1}(n \cdot \text{Sin}(A - \text{Sin}^{-1}((\text{Sin}(i_1))/n))) - A$

When the incident and exit rays are equal it can be shown that this is also point of minimum deviation d_{min} , that i_2 at this point is equal to $A/2$, and that the refractive index of a prism can be determined from equation Equ. 3.17.

Equ. 3.17. $n_2 = (\text{Sin}(A + d_{\text{min}})/2) / \text{Sin}(A/2)$

If the incident angle is plotted against deviation then a distorted 'U' shape is the result. The maximum deviation is the same either side of the point of minimum deviation, as a result of total internal reflection at the second interface and an incident angle of 90° , or greater, at the first.

3.4.1.2. Characteristics of prisms.

(i) **Wavelength.** The deviation 'd' increases with 'n', which is itself a function of frequency. For most conventional materials 'n' decreases as the wavelength increases across the visible spectrum. Hence, the deviation 'd' for red light will be less than for blue. The triangulation measuring system uses a wavelength greater than 632nm (as given by a HeNe laser) to optimise the efficiency of the detector.

(ii) **Refractive index.** For a series of prisms of the same apex angle and incident light of constant wavelength but with differing refractive indices, there will be a family of curves describing deviation against incident angle. The deviation of the beam is a non-linear function required to correct the inherent non-linearity of triangulation systems, see Fig. 3.14.

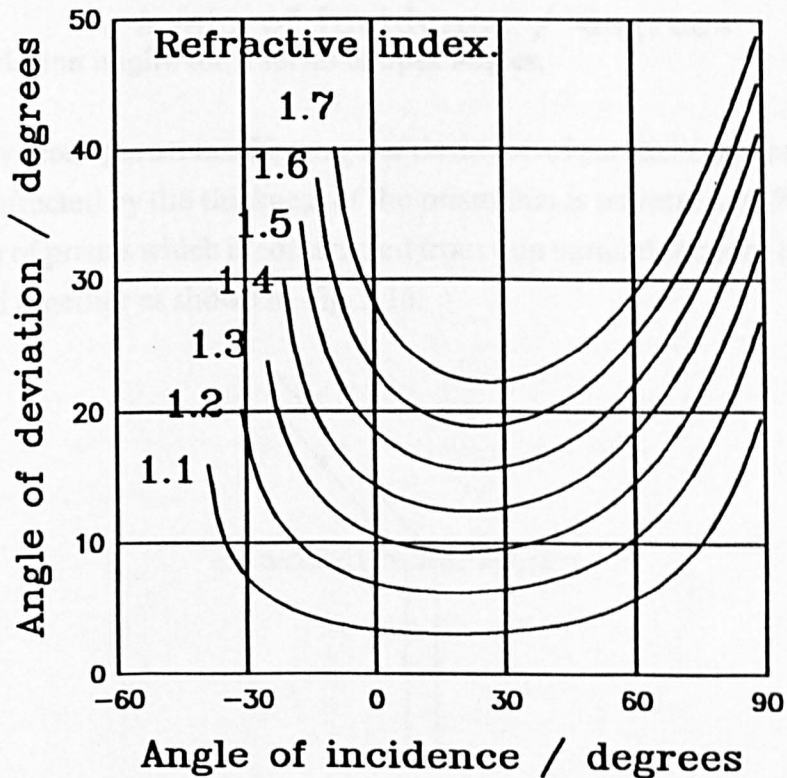


Fig. 3.14. Deviation angles for a series of refractive indices.

(iii) **Apex angle.** For a series of prisms of differing apex angle, monochromatic light and the same refractive index there will also be a family of curves which describe the deviation of the prism, see Fig. 3.15.

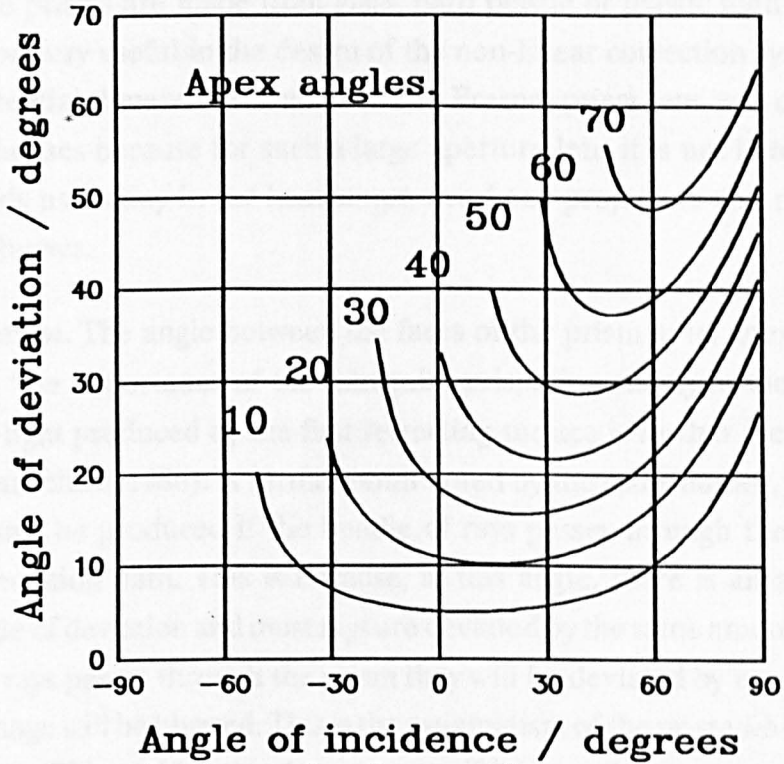


Fig. 3.15. Deviation angles for a series of apex angles.

(iv) **Alternative configurations.** The angular deviation of parallel rays passing through a prism is unaffected by the thickness of the prism that is traversed. A Fresnel prism is a collection of prisms which is constructed from thin parallel sections of the apex of prisms placed together as shown in Fig. 3.16.

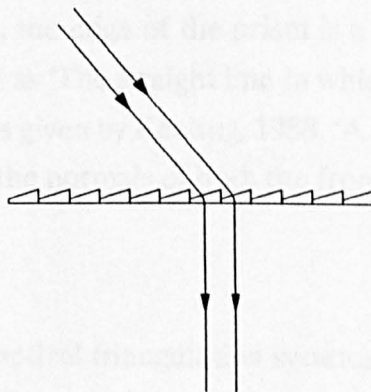


Fig. 3.16. Fresnel prism configuration.

The characteristics of the Fresnel prism are the same as for a single prism, the difference is that the prism is the same maximum thickness throughout. There is small loss in contrast with Fresnel prisms because of the boundaries where the prisms are joined. These prisms are made from glass, hard plastic or plastic membranes. Such prisms may be very useful in the design of the non-linear correction system because of the preferential dimensions available. The Fresnel prism lens was developed for use in light-houses because for such a large aperture lens it is not heavy. The same principle finds use today in car headlamps, overhead projectors and rear focussing windows on busses.

(iv) **Astigmatism.** The angle between the faces of the prism at its apex is called the *apical angle*, 'the importance of the triangular prism lies mainly in the fact that the deviation of light produced by the first refracting surface is further increased by the second' (Tunnacliffe, 1986). A further point noted by the same author, is that a clear image will only be produced if the bundle of rays passes through the prism at the minimum deviation path. This is because, at this angle, there is an approximately constant angle of deviation and most rays are deviated by the same amount. If a bundle of diverging rays passes through the prism they will be deviated by unequal amounts and so the image will be blurred. This is the astigmatism of the prism which is inherent in its geometry. This problem can be overcome if it is possible to arrange the incident pencil of rays to be parallel. A further problem of prisms occurs when the prism face is not perpendicular to the incident rays with respect to the parallel sides of the prism. In this case the prism will present a different apical angle to the bundle of rays and consequently a different deviation.

(v) **Definition of the principal section.** Southall, 1964, states that 'every section made by a plane perpendicular to the edge of the prism is a *principle section*.' where the edge of the prism is defined as 'The straight line in which the planes of the two faces meet'. A clearer definition is given by Keating, 1988, 'A principal section of the prism is the section that contains the normals of both the front and back surfaces'.

3.4.1.3. Conclusions.

Fortunately, in the case of optical triangulation systems with linear sensors, the light source is monochromatic, the principle section can be used, and the rays can be arranged to be approximately parallel. Hence, several of the unwanted side effects of the prism are negated.

If an appropriate prism is used in the optical path then it should be possible to correct the non-linearity of the profiler. There are two parameters available to adjust the degree of non-linearity: the apex angle and the refractive index. The desired result is an even distribution of resolution throughout the range of the profiler and with the parameters available it would appear that some correction to the overall linearity should be possible.

3.4.2 Filters.

3.4.2.1. Introduction.

A filter positioned in the optical path between CCD chip and object will modify the spectral sensitivity curve of the system. This may be desirable either to mimic the response of the human eye or to give an increased signal to noise ratio. The most frequent position for a filter to be found is mounted on the surface of the chip where it acts as a protective layer between the surface of the chip and the environment. In this position there is maximum throughput of optical energy as the filter saves an optical element which would reduce the amount of light finally incident on the sensor. Some CCD camera manufacturers, such as Fairchild, provide a filter as standard whereas other manufacturers, such as Texas, do not. If it is important to modify the incident light to CCD Chip then the side-effects of using a filter must be fully understood and taken into account in the design. These factors range from loss of overall light to the chip to loss of angular field of view.

3.4.2.2. Matching a filter to the light source and sensor.

To match a filter characteristics to those of the sensor an understanding of the characteristics and operation of silicon sensors is required.

(i) **Spectral response of silicon.** Silicon has a response curve that peaks at 750nm and is shown in Fig. 3.17. This is ideal for use with the diode laser used in an optical triangulation system as the wavelength will be in the range 670 nm to 780 nm.

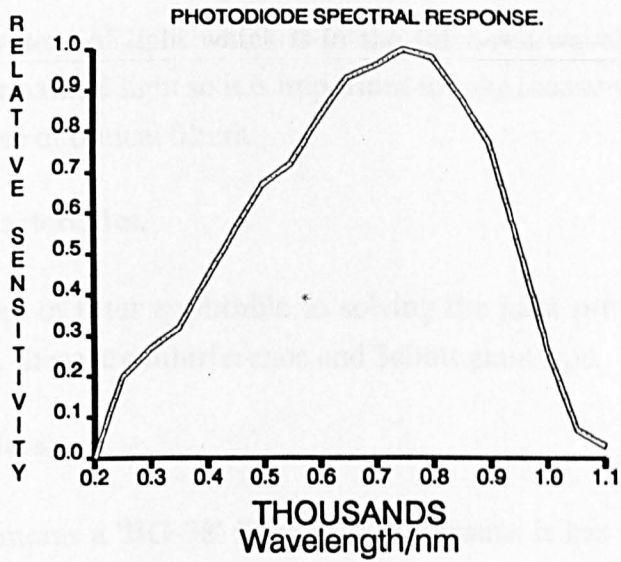


Fig. 3.17. Spectral response curve of silicon.

(ii) **Deep carrier cross-talk.** An important spectral characteristic of silicon photodiodes used in the CCD sensor is 'deep carrier cross-talk'. This effect results from the increasing absorption depth of photons at higher wavelengths which means that the probability that the photon generated charge will be collected by the appropriate sensing element decreases. The diffusion length can be as large as $25\mu\text{m}$ to $50\mu\text{m}$ depending on the process variables. In general, when the diffusion length becomes comparable with the centre to centre spacing of the pixels (typically $7\text{-}13\mu\text{m}$) there is a 10 - 20% chance of cross talk. The effect of this cross-talk is to cause blurring of the image. However, the absorption depths range from $0.1\mu\text{m}$ to $5\mu\text{m}$ over the visible range with any problems occurring further into the infra-red than necessary for optical triangulation systems, see Fig 3.18.

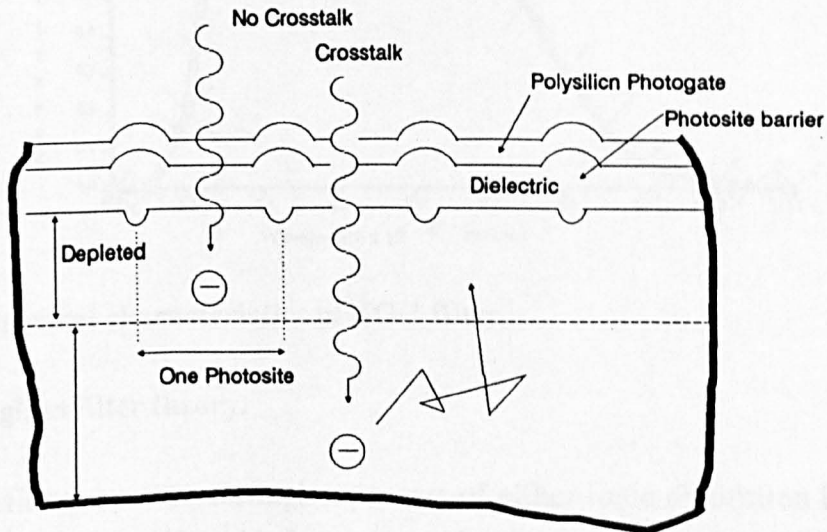


Fig. 3.18. Cross-talk between photosites.

There is a high content of light which is in the infra-red wavelength present in a tungsten sources or natural light so it is important to take measures to limit its effect, possibly with the use of optical filters.

3.4.2.3. Filter characteristics.

There are two types of filter applicable to solving the joint problems of noise and spectral selectivity, these are interference and Schott glass type.

(i) Schott glass filters.

In many Video cameras a 'BG-38' filter is used because it has a spectral response similar to that of the human eye. Although these have been used in linear array cameras this is not generally the case as the transmittance of this filter is only 5% at the wavelength of the diode laser light source (750nm).

The standard filter supplied by Fairchild is the KG-1 filter, the response of this filter is shown in Fig. 3.19. There is a great improvement in the 750nm wavelength region where approximately 40% of incident light is transmitted, however, this is still an unacceptable loss of light at this wavelength. This filter's characteristics when convolved with that of the silicon pushes the peak sensitivity down to about 650 nm.

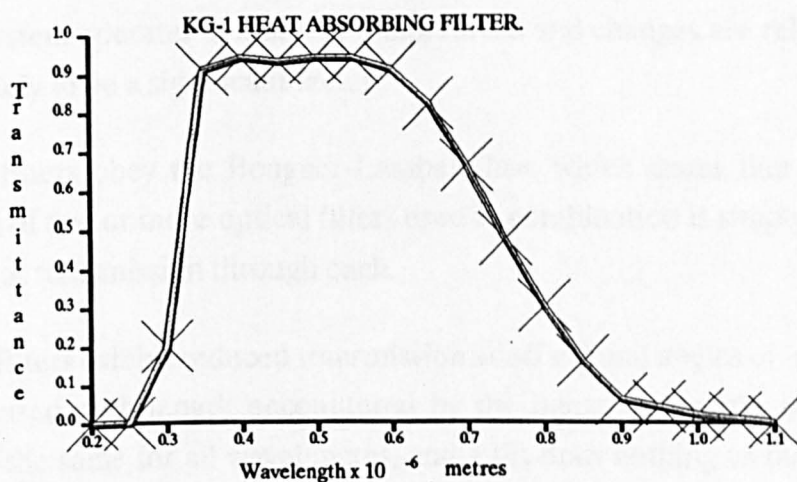


Fig. 3.19. Spectral characteristics of KG-1 filter.

(ii) Schott glass filter theory.

Solid glass filters operate through a process of either ionic absorption by inorganic material dispersed uniformly throughout the filter, or via absorptive scattering crystalites formed within the glass. In a colour filter, absorption predominates as the

primary wavelength selection process, as opposed to reflection which is important in interference filters.

Transmission 'T' through an absorption filter is given by Equ. 3.18.

$$\text{Equ. 3.18.} \quad T = (1-R)^2 \exp^{-xt}$$

where R = Reflection at the two air filter interfaces as given by Equ. 3.19.

$$\text{Equ. 3.19.} \quad R = \frac{(n-1)^2}{(n+1)^2}$$

and 'n' is the refractive index of the material, 'x' is a wavelength, material and pigment concentration dependent constant known as the 'extinction coefficient', and t = filter thickness. The term $(1-R)^2$ is known as the 'correction factor', and is especially important when considering Schott glass filters since the transmission curves represent internal transmission values, i.e. they ignore any influence due to reflection. The correction factors are available in the manufacturers literature.

To arrive at the absolute filter transmission then the transmission at a specific wavelength is multiplied by the correction factor to give the final percentage of transmission. These filters exhibit a wavelength shift with temperature, but as the measuring system operates at ambient temperature and changes are relatively small this is not likely to be a significant factor.

Absorption filters obey the Bouguer-Lambert law, which states that the spectral transmission of two or more optical filters used in combination is simply the product of the spectral transmission through each.

Absorption filters exhibit reduced transmission at off normal angles of incidence due to the increased path length encountered by the beam within the material. This reduction is the same for all wavelengths, and a tilt does nothing to the transmitted spectral distribution for angles below the Brewster angle (approx. 57°).

(iii) Interference filters.

An interference filter allows the transmission of spectrally selective images, in the case of the optical triangulation measuring system the reflected light from the laser light source is at a specific wavelength, other spectral information is not required. Hence, a filter improves the signal to noise ratio of the system.

(iv) Interference filter theory.

Interference filters are multilayer thin-film devices. Many of them may be described as all dielectric in construction but metallic layers may be present to provide auxiliary blocking, most of the depression of the peak transmittance below the 100% level can be attributed to these blocking layers. The sort of filter applicable here is the bandpass type which rejects wavelengths above and below the band of wavelengths which are transmitted. The process of selective transmittance is the result of interference between many thin film boundaries. This interference is constructive at some wavelengths and destructive at others. Band pass filters may be thought of as a thin, solid Fabry-Perot interferometer having a fixed spacing.

If the angle of incidence is not perpendicular to the filter face the path length of the transmitted light will change, for small angles of incidence the shift in spectral transmittance to shorter wavelengths is negligible, but at larger angles it increases. This feature can be put to good use in tuning the filter to a desired wavelength, but is not useful in optical triangulation systems as the light is required to be incident at a range of angles. However, the angle of incidence allowable without serious loss of signal can be calculated and the appropriate bandwidth filter used to give maximum signal transmission.

3.5. THEORY OF CCD SENSORS.

3.5.1. Features of CCD sensors.

3.5.1.1. Introduction.

A Charged Coupled Device (CCD) is a monolithic silicon integrated circuit which is essentially a shift register with very low loss on transferring charge, this charge is provided by photodiodes which respond to the amount of light received. The CCD sensor system is analogous to photographic film.

3.5.1.2. Photosites.

The packets of charge collected by each photosite are generated by photons liberating free electrons at the CCD surface which are accumulated as charge packets within the photosites. This happens because of the well known 'photo-electric effect'. This effect is explained by quantum theory which describes how incident light packets of ' hf ' (a

quanta) liberates an electron from an atom causing an electron hole pair. The pair are then separated in the electric field applied to the region.

3.5.1.3. Shift registers.

In the CCD sensor, whether area or linear, the packets of charge that are accumulated at each pixel site are transferred in parallel to a CCD shift register that is shielded from incident light. For reasons of speed and transfer efficiency there are usually two shift registers on either side of a linear array and the odd pixel numbers charge is transferred to one side and the even pixel numbers charge to the other. The array of charges are then sequentially clocked past a charge detector and output amplifier by the transport register input clocks. The amplifier then converts the charge packets into an analogue output waveform. This waveform is proportional to the light intensity across the whole CCD Chip. Advanced buried channel CCD technology allows linear sensors to offer excellent Charge Transfer Efficiency (CTE) at high data rates with low signal to noise ratios and relatively small sizes, see Fig. 3.20.

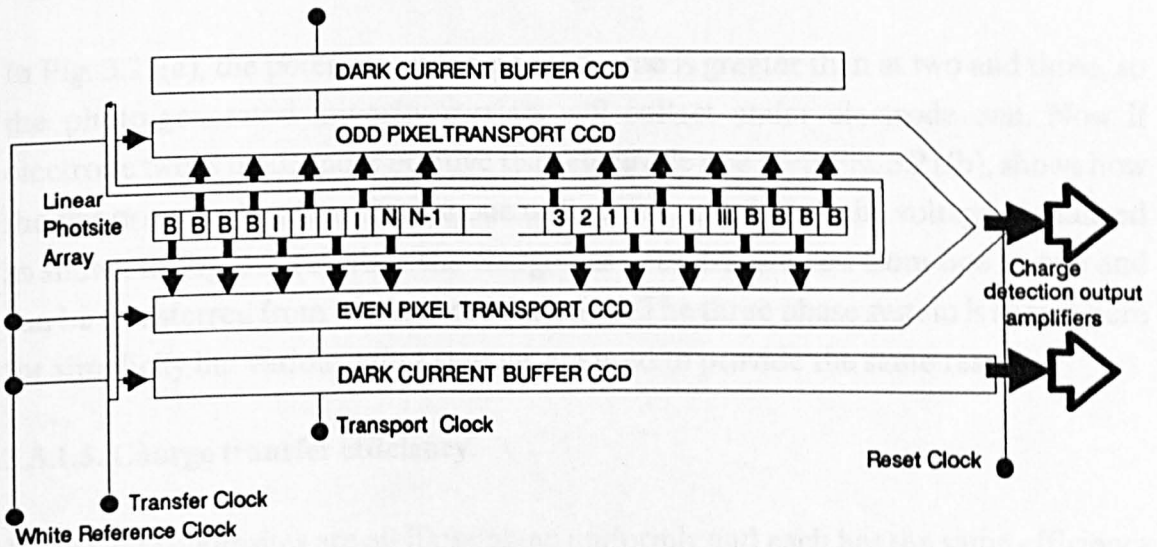


Fig. 3.20. Schematic of a CCD sensor.

3.5.1.4. CCD shift register operation.

The shifting of the photogenerated minority carriers can be understood by consideration of a p-type substrate of silicon with an array of metal electrodes deposited on the surface. The electrodes are connected in groups of three and operated with a three phase voltage supply to give direction to the transfer of accumulated charge, see Fig. 3.21.

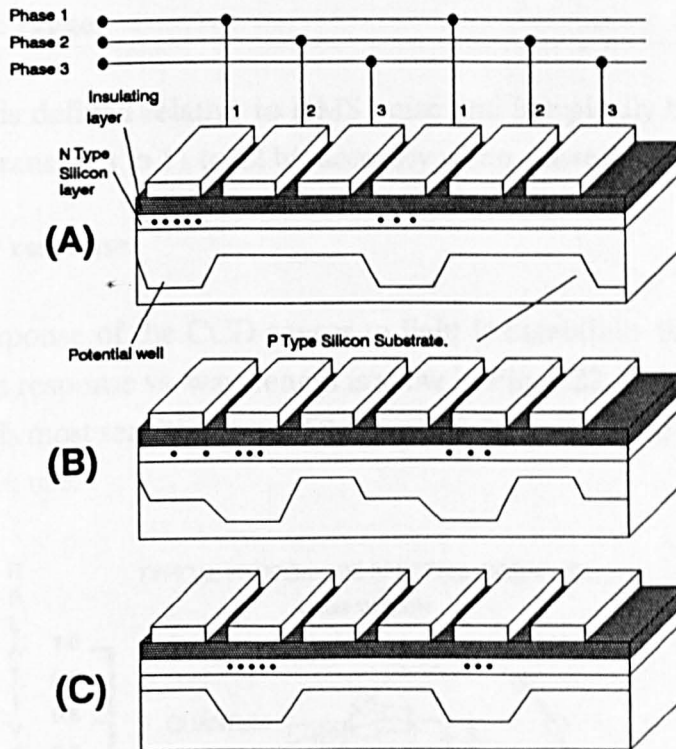


Fig. 3.21. Three phase shift register operation.

In Fig. 3.21(a), the potential under electrode one is greater than at two and three, so the photo-generated minority carriers will collect under electrode one. Now if electrode two is made more positive than electrode one then Fig. 3.21(b), shows how the minority carriers funnel from one well to the next. If now the voltage is changed as shown in Fig. 3.21(c), then the charge has been transferred from one to two and can be transferred from two to three and so on. The three phase system is shown here for simplicity but various other systems are used to provide the same result.

3.5.1.5. Charge transfer efficiency.

If the CCD photosites are all illuminated uniformly and each has the same efficiency there will still be a difference in voltage output at the end of the scan as opposed to the beginning because of the CTE.

The CTE /transfer can be calculated from the equation

$$\text{Equ. 3.20.} \quad \text{CTE/transfer} = (1 - n_e/V_{\text{out}})^{1/n}$$

Where n = total number of shift register elements = 2 times the number of pixels plus the number of additional registers for the end sites, V_{out} is the average output amplitude under uniform illumination, and n_e is the global CTE.

3.5.1.6. Dynamic range.

Dynamic range is defined relative to RMS noise and is typically between 1000 and 5000 to 1. This translates to 11 to 12 bit accuracy when converted to a digital output.

3.5.1.7. Spectral response.

The spectral response of the CCD sensor to light is essentially that of silicon. The graph of relative response vs. wavelength is show in Fig. 3.22. This figure shows that the photodiode is most sensitive in at 750 nm, which happens to be the wavelength of the laser diode in use.

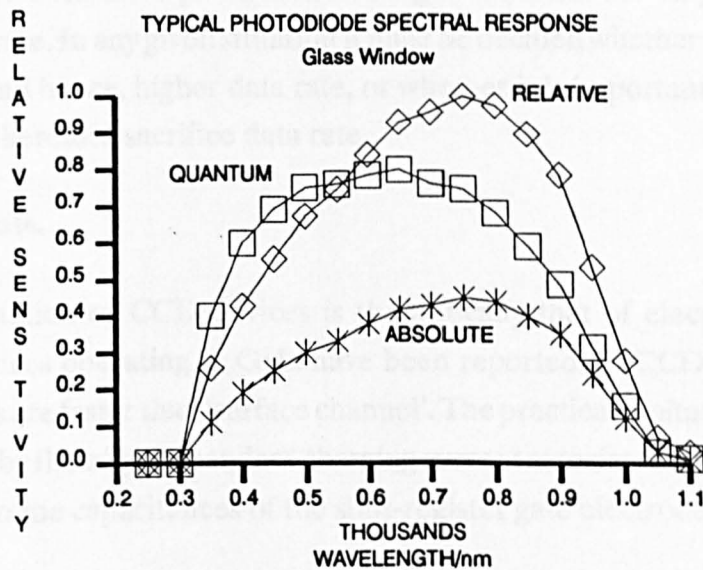


Fig. 3.22. Spectral response of silicon.

3.5.1.8. Quantum efficiency.

Quantum Efficiency (QE) is the efficiency of converting input photons of light to electrons. QE is related to spectral response, but not the same, as the spectral response is related to the silicon material, but quantum QE is related to wavelength because of the relation E_p (photon energy) = hc/λ , where h = Planks constant, c = speed of light, and λ = wavelength. If the spectral response is known, then the QE can be calculated from the relation $QE = E_p \cdot R/A$ where R is the spectral response in coul/joule/cm² and A is the pixel area in cm².

3.5.1.9. Resolution.

At present, CCD sensors with from 128 to 10,000 pixels can be purchased which can be split into several groups. In general low pixel number chips are used for Optical Character Recognition (OCR), medium resolution devices are used in many differing applications the main one being document FAX, large resolution devices have been devised for contact recording of documents.

One fundamental limitation to resolution is the sensitivity of silicon, to gain higher resolution the photosite has to be made smaller if the device is going to use readily available optics. This results in a lower area to receive incident light with consequently lower sensitivity. With more pixels it takes longer to collect the output so there is a decreased scan rate. In any given situation it must be decided whether to go for a faster line scan rate, and hence, higher data rate, or whether it is important to have greater resolution and therefore sacrifice data rate.

3.5.1.10. Data rate.

The speed limitation of CCD devices is theoretically that of electron mobility in silicon, and devices operating in GHz have been reported. In CCD devices 'buried channel' devices are faster than 'surface channel'. The practical limitation to operating speed is caused by the edge dependent charging current associated with delivering the clock voltages to the capacitances of the shift-register gate electrodes.

3.5.1.11. Reliability.

The materials used and the fabrication technology of CCD's are essentially the same as for NMOS LSI products, it follows that reliability is similar which is very high.

3.5.1.12. Temperature considerations.

A CCD sensor works best at low temperatures because thermally generated noise is at a minimum, but can work at full capacity in the range -55°C to 70°C .

3.5.1.13. Non -ideal performance.

(i) Cross-talk of deep carriers.

The longer the wavelength of incident light, the deeper into the silicon the photon travels before generating an electron because it has less energy. Since the photosite capture mechanism is at, or very near, to the surface, the deeper into the silicon an electron is generated the weaker the field strength is. Consequently it is more likely that the electron will wander randomly and be captured by another photosite other than the one it entered, as shown in Fig. 3.18.

(ii) Photo-response non uniformity.

Photo Response Non Uniformity (PRNU) is illustrated in Fig. 3.23, there are two phenomena shown: first, there is a low frequency non-uniformity which is the difference that can be seen from one end of the sensor to the other, and second, a high frequency non uniformity which manifests itself as single pixel offset, either positive or negative. However, these are both constant for a given chip and can be corrected if need be, furthermore these effects are very low in modern devices.

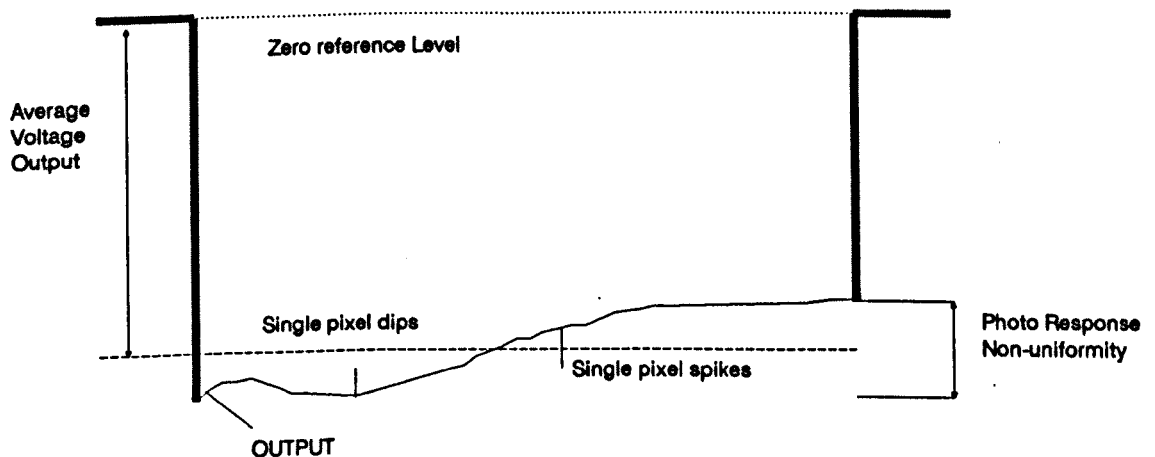


Fig 3.23. Photo response non linearity.

(iii) Dark signal.

Dark signal exists when no light is incident upon the chip and is caused by internally generated electrons which are gathered by the photosite capture mechanism. These

electrons are generated by: surface states, crystal imperfections, lattice defects, and general impurities. It follows that for longer integration times this effect is more significant. Furthermore, the dark signal is sensitive to temperature, doubling for every 5-10°C increase, and the dark signal generation may not be constant across the device.

(iv) Noise.

The basic CCD register is practically noiseless because it does not have the PN junctions as MOS and BIPOLAR devices do. Associated on chip devices, such as detectors and buffer amplifiers, do have PN junctions and so introduce some noise. Dynamic ranges of 10,000:1 have been achieved without cooling.

3.5.2. Control of CCD sensor light requirements.

3.5.2.1. Introduction.

The optical triangulation measuring system will be required to deal with changes in reflectivity of the surface to be measured over several orders of magnitude. The range of reflectivity is theoretically infinite as for a given amount of incident light the reflected light can range from 1 (say) from a perfect mirror surface to zero for a perfect black surface. In practice, it is sufficient to quote the range from 1 to the smallest intensity detectable by the system in question. Hence, the range of reflectivity to be considered is the range of the detector/light source combination.

There are a number of possible methods of controlling the range of reflectivity covered by the line scan camera, three will be looked at in detail.

- (i) Line scan camera data rate and exposure controls.
- (ii) Laser power and modulation frequency.
- (iii) Lens design and aperture control.

3.5.2.2. Linear array camera exposure controls.

The linear array camera used in Prototype III and its associated Sentel driver board electronics allow adjustment of the exposure time. Normally this is achieved by a set of switches called 'J2'. The board has been modified to allow the alteration of the exposure time via a parallel interface card. There are eight switches so one 8 bit port was used to obtain full control over this aspect of the camera.

The total exposure time T_{exp} is related to two factors, the data rate frequency f_{shift} and the exposure time factor 'm'.

(i) Data clock frequency.

Control over f_{shift} is achieved on the Sentel Cam + board by setting the switches J1, these switches allow the values $n = 1$ to 255 to be decoded giving a range of f_{shift} defined by Equ. 3.21.

$$\text{Equ. 3.21.} \quad f_{shift} = f_q / (2 * (1 + n))$$

where $f_q = 14.31818$ MHz. Putting $n = 1$ to 255 into Equ. 3.21, gives a range of f_{shift} frequencies of between 3.58MHz to 28 kHz for the Sentel system.

(ii) Exposure time.

The length of time for the data to be clocked off the CCD chip T_{chip} is given by Equ. 3.22.

$$\text{Equ. 3.22.} \quad T_{chip} = 2048 / f_{shift}$$

The Exposure time is then related to T_{chip} by Equ. 3.23.

$$\text{Equ. 3.23.} \quad T_{exp} = m * T_{chip}$$

where $m = 2$ to 255 giving a range of exposure times from 1.1 ms to 18.65 seconds, a factor of $1:1.7 \times 10^4$. However, it should be noted that under the circumstances of extended exposure times the noise from dark current and other sources would give a very poor signal to noise ratio. T_{chip} and T_{exp} are shown in Fig 3.24.

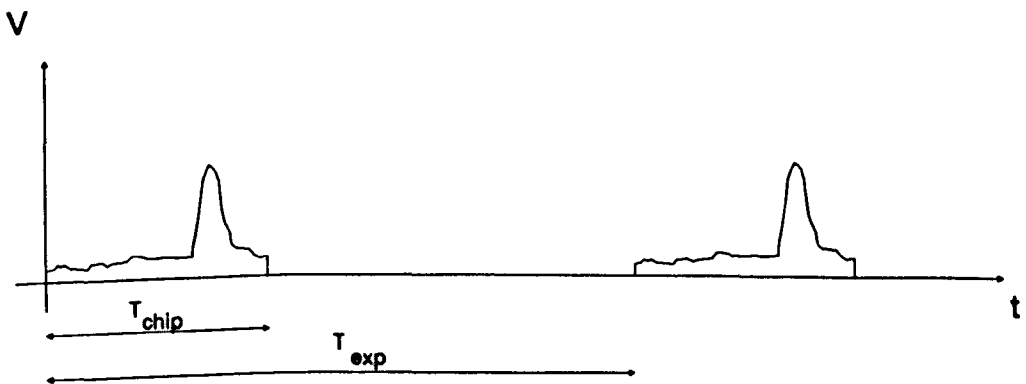


Fig. 3.24. Exposure times for CCD output.

3.5.2.3. Laser beam size and beam modulation.

(i) Control of laser beam size.

The power of the laser, dimension of the beam and modulation of the laser, all affect the total amount of light incident on the surface to be measured. The size of the beam must be as small as possible so that the image on the CCD sensor spreads over as few pixels as possible. Each pixel integrates over the exposure time and the resulting charge stored is directly related to the number of incident photons. Hence, for a given laser power the fewer the number of pixels which form an image of the laser the higher will be the charge stored, and for a given desired output voltage level the exposure time can be as small as possible.

The requirement for a small beam size must be met over the working range of the device, approximately 0.9 to 5.5 metres. The laser and collimating lens is designed to give the smallest possible beam divergence, the fundamental limitation is caused by diffraction. The quoted divergence of the laser collimators is less than 1.2 mrad, and the pointing stability is 0.1 mrad (D.O. Industries). This equates to a divergence of 6.6mm at a distance of 5.5 metres and if the initial beam size = 0.7mm then the final beam size = 7.3mm. For the lens system being used the equations Equ. 3.24, and Equ. 3.25, allow the size of the image to be computed, see also Fig. 3.25.

$$\text{Equ. 3.24.} \quad \frac{1}{l'} - \frac{1}{l} = \frac{1}{f}$$

$$\text{Equ. 3.25.} \quad \frac{l}{l'} = \frac{h}{h'}$$

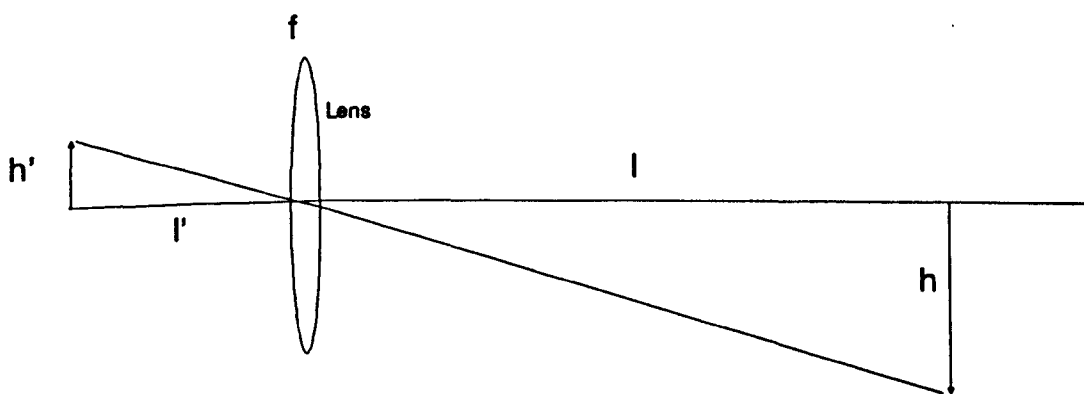


Fig. 3.25. Lens diagram.

Putting f and l into Equ. 3.24, gives l' , and inserting this and h into Equ. 3.25, gives h' , the image of the laser on the chip. For $l = 5.5\text{m}$, $f = 0.050\text{m}$ and $h = 0.0073\text{m}$ gives $h' = 67\mu\text{m}$. With a pitch of $13\mu\text{m}$, the number of pixels illuminated (ignoring imperfections in the lens) is approximately 5.

(ii) Control of laser power output.

For the laser system to meet eye safety regulations it is necessary that the power density per mm^2 is below a certain threshold value, this is either achieved with a low power laser of less than say, 0.5mW , or by expanding the beam. In each of these cases the signal to noise ratio is lowered considerably and the first requirement of the line scan camera is also not met. Because of the likelihood of poor surface reflectivity, it is not desirable to use a laser with less power output than about 1mW without serious degradation of speed performance, and noise problems. This power output would be above the limit allowed for 'safe operation', it follows that it would not make any difference to the classification if a higher output laser is used. Laser diodes can be obtained with power outputs in the range 1 to greater than 30mW . The output power of these lasers is variable over a small range, but it is preferential to keep the laser at the same power output, hence, the modulation of the laser output provides a means of controlling the output power while keeping the laser at the same power output level.

Modulation of the output of the laser has been described by Weise, 1989, to compensate for the reflectivity and lighting variations, in this case the laser beam is pulsed on and off at a rate of 16kHz or greater. When the laser is 'off', the probe/camera detector measures the level of the background light. The information is then used to compensate the measurement value during the probe 'on'. He notes that this technique works well because the background light level changes are slow compared to the frequency of the probe (16kHz).

Another way of altering the total power output from the laser is to switch the laser off when enough light has been collected. Rather than try and link the laser on/off cycle to the line scan camera, it is easier to use a square wave modulation and vary the mark space ratio, this enables a fine control over the laser output power to take place, see Fig. 3.26.

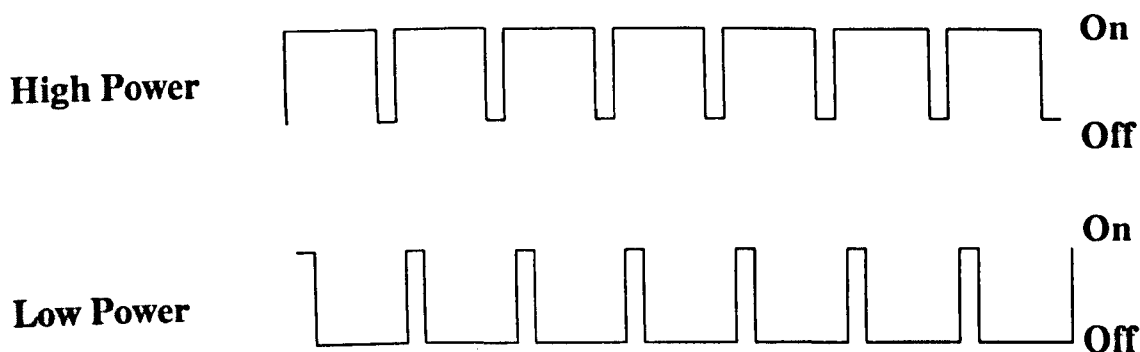


Fig. 3.26. Laser power output control by mark space ratio variations.

This method could be arranged to be transparent to the camera system as it could take place during the exposure time. A simple circuit could be built to change the mark space ration by a n-bit word from the computer. The range of values of 'n' would depend on the degree of control desired by the system. Alternatively, this function could be altered via a feedback diode which would look at the laser image and make the alterations in exposure control necessary.

3.5.2.4. Lens design and aperture control.

The size of lens used by the system will dictate the light collecting power of the system. It is an advantage to make the lens as large as possible from the speckle and depth of field point of view, but this has to be weighed against other disadvantages such as the expense and image degradation caused by larger lenses.

Changes in the aperture affects the field of view, this would normally be an unacceptable feature but if optics obey the Scheimpflug condition then this is not a problem as the camera will always be optimally focussed. Hence, it is possible to vary the aperture by an automated diaphragm to compensate for lack of light and range of reflectance in the surfaces of interest. The aperture will allow light into the system proportional to the square of the aperture diameter, this is convenient because as well as reflectance variations, the system also has the inverse square law variations in light received by the lens area according to the distance of the target from the lens.

If the lens/laser system is designed so that the image sensor is obscured from seeing all of the laser image at close range while gradually revealing all of the image as the distance from the target is increased, this will provide a means of control on the quantity of light incident on the sensor.

3.5.2.5. Conclusion.

There are three main factors available for controlling the amount of light perceived to be received by the sensor system: (i) the CCD chip itself has a wide dynamic range in excess of 1,000:1, (ii) the laser power output can be controlled, and (iii) the aperture of the lens can be changed to accommodate more or less light. The most attractive of these is the laser power control as this could be performed with either software or hardware.

3.5.3. Modulation Transfer Function of a CCD sensor.

3.5.3.1. Introduction.

The mathematical definition of Modulation Transfer Function (MTF) (Marescaux, 1989; Hopwood, 1980; Melles Griot) is: 'the Modulus of the Fourier Transform of the point spread Function', which is similar to the impulse response of an electrical system. The resolution of a solid state imaging system is affected by the overall MTF which may be defined in many different ways.

This definition of a system is useful because the overall MTF of the system is the product of the MTF of the individual components of the system, i.e. the MTF of the lens * MTF of the filter, etc. The evaluation of the systems MTF can not only predict performance but also give valuable insight into the interrelated optical and electrical functions. The system as a whole can be split into three separate areas: the optics, the sensor and the processing circuitry.

3.5.3.2. The MTF of the optics.

For a perfect lens the MTF would be '1' and would represent 100% contrast to all subject spatial frequencies. The closer to this a real lens can attain the better the performance of this system.

The MTF of a lens is dependent on the wavelength of illumination, the aperture of the lens and the magnification ratio. As an aid to evaluating lenses, the MTF is often shown as a curve plotting the contrast against distance for a given aperture, spatial frequency and magnification ratio. By comparing the MTF's of the various components of the optical system it is found that the frequency response is sensitive to even slight aberrations. As the MTF is increased from zero, a detectable degradation is required before the size of the central disk of a diffraction pattern shows

a perceptible increase (the high frequency content is displaced well away from the central components containing mainly low frequency). However, it does show the difficulty in noting the degradation of the system using diffraction patterns which are complex, as opposed to MTFs, which are essentially simple to analyse.

In practice, a designer of an optical system will use an off-the-shelf lens, and in general, there will be no published MTF for the lens, so several lenses need to be compared to evaluate the best for the given task.

3.5.3.3. The MTF of the Sensor.

The MTF of a line scan camera array is determined by two factors (i) The spacing of the sensing element and (ii) optical cross-talk.

(i) Spacing of the sensing elements.

This factor may be considered analogous to sampling theory in digital signal processing. Each of the pixel sites collects a charge which is proportional to the light intensity at that site, the result is a sampled light intensity waveform. For such a waveform Nyquist's sampling theorem states that the highest frequency that can be reproduced from the sampled data is twice the sampling frequency. This gives a maximum frequency f_n of:

$$\text{Equ. 3.26.} \quad f_n = 1 / 2 \cdot \text{Pixel Pitch.}$$

For the chip (Fairchild, 1989) used in testings with a $13\mu\text{m}$. pixel spacing, the maximum number of Lines per mm that can be resolved = 38.5.

(ii) Cross-talk.

Cross-talk of the deep carriers results as a consequence of less energetic photons of higher wavelength penetrating further into the substrate than the more energetic ones. If photons are absorbed away from the depletion region the probability that this charge will be collected by another pixel site increases as the charge moves by diffusion, see Fig. 3.18. The photon absorption coefficient versus wavelength is shown in Fig. 3.27.

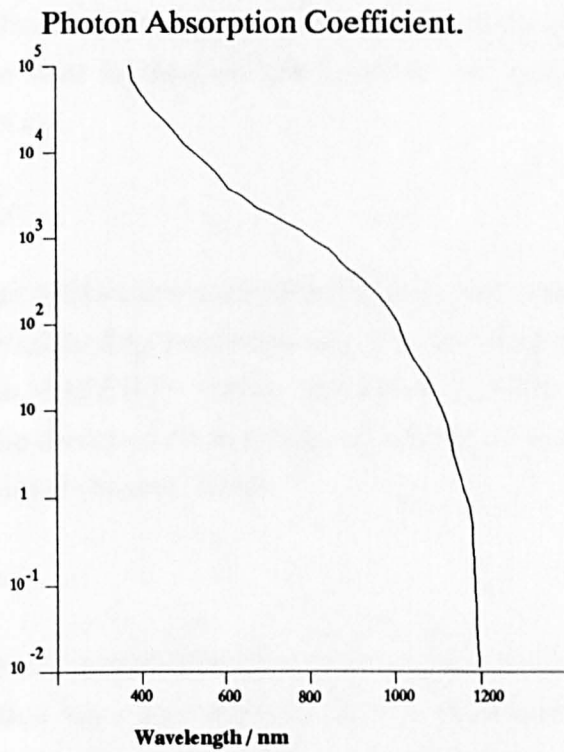


Fig. 3.27. Photon absorption coefficient graph.

As cross-talk is a function of wavelength, a filter is often used in the optical path to reduce its effect. The MTF of the Fairchild CCD143A, 2048 element line scan camera is shown in Fig. 3.28.

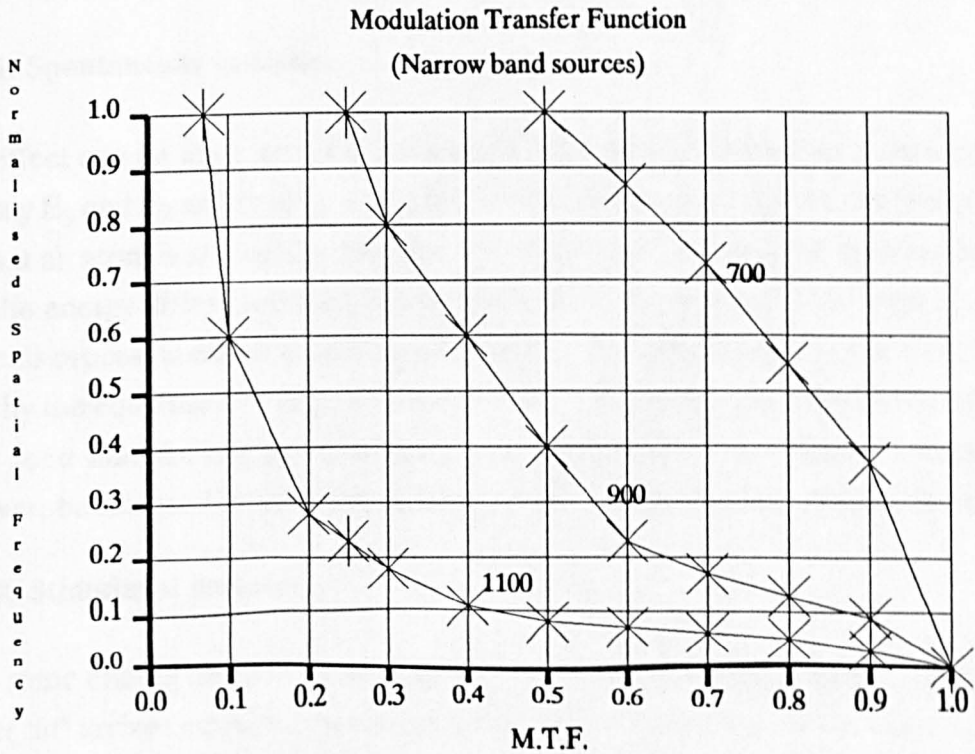


Fig. 3.28. MTF graph for Fairchild sensor.

The processing of the line scan data can also degrade the MTF of the overall imaging system because as the data is sampled quantisation and non-linearity errors are introduced into the system.

3.6. LASER THEORY.

The first successful laser operation was achieved by T. H. Maiman, in 1960 with a Ruby laser, this result was predicted by Schawlow and Townes two years earlier following the development of the MASER by Townes and others in 1954. (The MASER was a microwave system). The theory of the existence of stimulated emission was predicted by Einstein in 1917 (Meyer-Arendt, 1984).

3.6.1. Laser operation.

The operation of the laser is possible because of three types of interaction that Electro Magnetic (EM) radiation has with matter: (i) Spontaneous emission (ii) Stimulated emission. (iii) Stimulated absorption. These interactions can be understood by considering a two level energy system which is a gross simplification of common energy systems that are highly complex and occupy so many levels that changes in energy are seen as continuous (as defined by Newtonian mechanics). However, by careful selection of materials, energy levels only slightly more complex than the example are used in laser systems where the quantum nature of energy is used.

3.6.1.1. Spontaneous emission.

This effect can be understood if we consider two energy levels that a material may have say E_1 and E_2 and that $E_1 < E_2$. It is convenient to take E_1 to be the ground level and that an atom is at level E_2 . Because the atom (or molecule) will decay to level E_1 then the energy difference must be released, when this is done in the form of an EM wave this process is called spontaneous emission. The frequency 'f' of the wave is then given by the equation $f = (E_2 - E_1)/h$ where 'h' is Planks constant. It can therefore be easily seen that the energy is released in a quanta 'hf'. The release of energy can however, be released in the form of kinetic energy to the surrounding molecules.

3.6.1.2. Stimulated emission,

If the same energy levels are assumed and the atom is initially at level 2, and a wave packet 'hf' arrives equal to the energy difference between the levels, there is a high probability that there will be a radiative emission from the atom again of 'hf' so

combining with the original wave packet. Unlike the case of spontaneous emission where no information concerning the direction or phase of the emission, in this case the direction and phase will be the same as of the incident wave.

3.6.1.3. Stimulated absorption.

If an atom is initially at Energy Level 1 and an EM wave of frequency 'f' is incident on the material then there is a finite probability that the atom will be raised to level 2. This is a process called absorption.

The process of laseing is caused by the creation of a 'population inversion', i.e. there is a higher population in energy level 2, than in 1. This condition can be promoted by stimulated absorption. There will then be a preference for spontaneous emission to normalise this situatio. As this happens, the random emission will cause stimulated emission of the rest of the population down to the lower level. Thus, a flash of light is produced where there is coherence radiation of photons with the same frequency (Wilson, 1983). This is the operation process of the early Ruby lasers that used flash tubes to pump the ruby rod to produce the population inversion and so produce the flash of laser light. However, more complex energy schemes are required for efficient operation and so new materials with better energy bands were devised to produce continuous and flash type operation. The operation of the laser is also dependent on the design of the laser cavity and the size of the active material or gas. For the production of the laser action three elements are required: an energy source to raise the system to an excited state, an active medium which can achieve population inversion, and an optical cavity to provide the feedback for oscillation.

3.6.2. Semi-conductor diode lasers.

The physical size of the conventional laser is determined by fundamental limitations so that typical devices are too large for many applications. They also require high voltage (kV) and current to operate. Lasers produced from semi-conductors are not dissimilar to Light Emitting Diodes (LED), being small and conveniently packaged.

The design of the diode laser is such as to provide population inversion in a narrow zone called the active region. The optical feedback is provided between the cleaved faces of the laser diode which reflect some 30% of the light back from the face. The Power output vs. current characteristic is shown in Fig. 3.29, where the threshold point that distinguishes between the spontaneous emission and the stimulated emission can be seen.

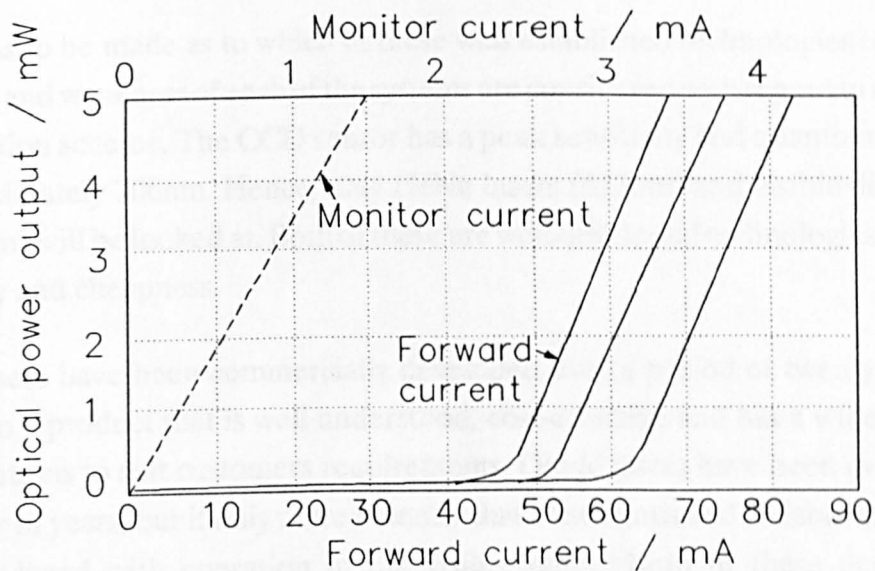


Fig. 3.29. Diode laser optical power vs forward current.

The Power output as a function of frequency is shown in Fig. 3.30. where the fine frequency band width of the laser source is shown.

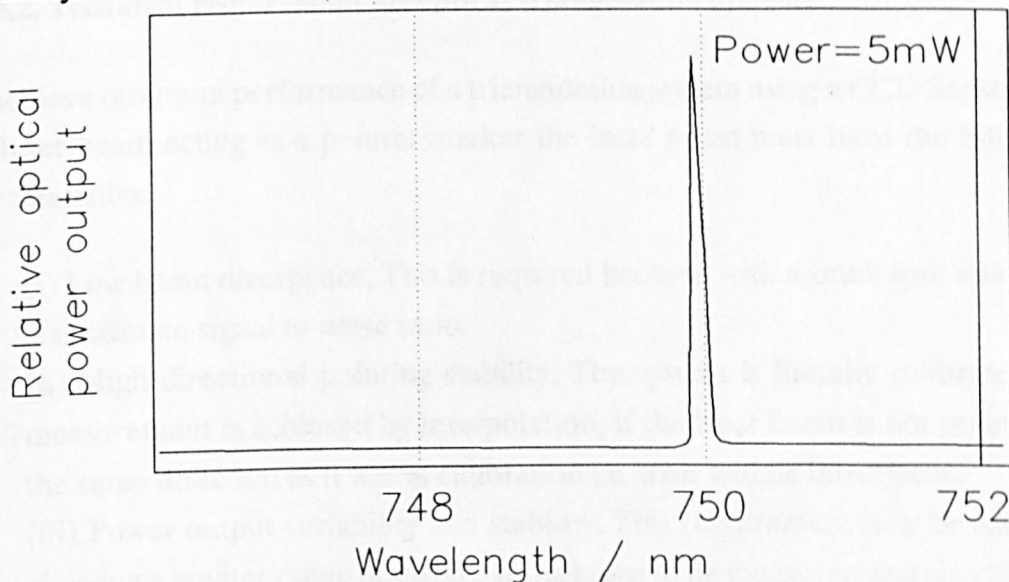


Fig. 3.30. Diode laser relative output power vs. wavelength.

3.6.3. Comparison between diode and gas lasers (Smith, 1989; Bobb, 1988; Wilson, 1983; Wheeler, 1990)

3.6.3.1. Introduction.

Both diode and gas lasers are available for use as a highly collimated light sources in applications requiring a pointer/marker such as optical triangulation systems. A

choice has to be made as to which of these well established technologies to use. The strengths and weakness of each of the systems are considered with regard to the optical triangulation scheme. The CCD sensor has a peak sensitivity and quantum efficiency at approximately 700nm. Hence, only HeNe lasers (632nm) and visible diode lasers (> 670nm) will be looked at. Both of these are well developed technologies providing reliability and cheapness.

HeNe lasers have been commercially developed over a period of twenty five years leading to a product that is well understood, cost-effective and has a wide variety of configurations to suit customers requirements. Diode lasers have been available for a number of years, but it only more recently that continuous and reliable diodes have been produced with operation in the visible range. Both of these devices have limitations because of the physics of their operation and examination of these will allow a sensible choice of laser for the requirements of an optical triangulation measuring system.

3.6.3.2. Technical requirement for optical triangulation systems.

To achieve optimum performance of a triangulation system using a CCD Sensor with the laser beam acting as a pointer/marker the laser beam must have the following characteristics:

- (i) Low beam divergence. This is required because with a small spot size there is maximum signal to noise ratio.
- (ii) High directional pointing stability. The system is initially calibrated and measurement is achieved by interpolation, if the laser beam is not pointing in the same direction as it was at calibration an error will be introduced.
- (iii) Power output variability and stability. This requirement may be useful in allowing a greater range of surface reflectance to be measured and also to allow for prediction of the exposure level based on a previous exposure level, clearly this would not be possible if the power output changed between exposures.
- (iv) High reliability. The system will be used in a range of temperatures, humidity and pressure, and for long periods of time, the laser must be reliable if the system is to be trustworthy.
- (v) Low cost. Each component in an optical system will contribute to it's overall cost and the laser is likely to be a significant cost in the development of the system.

3.6.3.3. HeNe lasers.

The Helium Neon (HeNe) gas laser has been commercially developed over the last 25 years to produce a product that is both highly reliable and sophisticated. The essential features of the design are two mirrors of 6-8 mm diameter which are aligned parallel to each other and 125 to 450mm. apart. Between these mirrors is a borosilicate glass tube 15 - 38mm. in diameter with a narrow bore capillary tube of 0.6 to 2.0mm. mounted coaxially. Situated inside the space between the two borosilicate tubes is a metal cylindrical cathode with the anode being the mirror mount at one end. In operation the HeNe gas is pumped by gas discharge caused by the high potential between the anode and cathode. This creates the desired 'population inversion' and subsequent decay with resultant photons of characteristic wavelength being emitted. In the preferential conditions of the tube these photons are allowed to traverse the cavity resulting in a coherent beam emitted from the 0.99% transmittance of the mirror at one end. The construction of the HeNe laser is important in its operational characteristics.

The Gaussian beam waist should be situated at the output couple, a positive meniscus lens, and the far field divergence, full range in radians, can be simply stated in Equ. 3.27.

$$\text{Equ. 3.27.} \quad \text{Divergence} = 1.27\lambda/d$$

where d is the spot size, λ is the wavelength. The divergence of the laser is proportional to the wavelength of the laser. The laser light will appear to come from a point source behind the lens.

The Power output of the laser is affected by discharge tube length and bore size (which also introduces more modes, which may not be desirable). A higher power laser will be longer than a low power laser. The longer tube has the beneficial effect of reducing modes that sweep through shorter lasers during start up causing power fluctuations.

Beam alignment is important at the manufacturing stage to ensure a Gaussian, 1mrad divergence, well collimated beam, and this is routinely achieved.

3.6.3.4. Diode lasers.

Diode lasers have been constructed since about 1963. They were at first unreliable and operated in pulse mode, they had a reputation of such high failure rates they were

sometimes referred to as 'flash bulbs'. However, much development has taken place to produce a wide range of high efficiency, reliable, low cost diodes at a variety of wavelengths for numerous applications.

The construction of a laser diode is not unlike a LED and before laseing action takes place they do operate as an LED. A diode laser construction will vary depending on the power output and wavelength. A simple laser will consist of a chip constructed of several layers to provide a region where the desired population inversion can take place and the resultant wave train is guided preferentially between the cleaved end faces which act as mirrors. Unlike He-Ne lasers, the gain is much higher over one length of the cavity and a power reflection of 30% is enough to ensure laseing action. Above the laseing threshold close to 100% of injected carriers recombine by stimulated emission and facet efficiency may attain 40% per face. On both sides of the chip an astigmatic beam which is highly divergent is produced but can be collimated on one side and used to provide feedback to a monitor diode for power control on the other.

The main spur to the development of diode lasers has been in optical communications and in compact discs and laser printers. It is the compact disc that has pushed the wavelength available from the diode laser down to its present commercial limit of 670nm (in the human visible range).

3.6.4. Gaussian beam optics (Hecht, 1973; Bridges, 1989).

3.6.4.1. Gaussian beam properties.

The Gaussian beam intensity distribution provides the optical engineer with an important exception to the normal rules for defining the object-image relationship at discrete points in the optical path. Usually, to define all intervening patterns at intermediate distances between object and image it would be required to solve the Fresnel integral which for many optical systems can be simplified to Equ. 3.28.

$$\text{Equ. 3.28.} \quad E(Y,Z) \cong \iint_{\circ}^{\infty} E_s(y,z) \exp \frac{i2\pi Zz}{x} * \exp \frac{i2\pi Yy}{x} dydz$$

where $E(Y,Z)$ is the electric field at a distance $x = X$ away from a source plane, E_s is the source field. However, with Gaussian beam intensity distributions with a radially symmetric field distribution given by Equ. 3.29, the situation is eased.

Equ. 3.29. $E_s = E_0 \exp(-r^2/w_0^2)$

Equ. 3.29, has the interesting property that its Fourier Transform is also a Gaussian distribution. The implication in this equation is that the phase is uniform in 'r'. And, if the Fresnel integral is solved it is found that 'a Gaussian source distribution remains Gaussian at every point along its path of propagation through the optical system (Bridges, 1989)'. The size of the beam will of course vary as it propagates through mirrors or lenses, the intensity is also Gaussian and may be written as in Equ. 3.30.

Equ. 3.30. $I_s = \eta E_s E_s^* = \eta E_0 E_0 \exp(-2r^2/w_0^2)$

The usefulness of this information is in its application to the Gaussian beam profile obtained from lasers. The method of generation of the laser beam and the nature of the Gaussian beam distribution means that it is the preferred distribution of the light as it is reflected back and forth in the laser cavity.

3.6.4.2. Gaussian beam profile.

The Gaussian beam has no well defined boundaries to be measured by, hence the diameter is arbitrarily decided. It is useful to have a definition to work with and this is achieved with a diameter at which the intensity has fallen off by some predefined amount as in the case of 'half power' definitions used in electrical and electronic fields.

The parameter w_0 usually called the 'Gaussian beam radius', is the radius at which the intensity has decreased to $1/e^2$ (0.135) of its value on the axis. Other useful definitions are the radius at half maximum intensity which is $0.59 w_0$ and also $2w_0$ where the intensity is 0.0003 that on axis. This final point may be of interest in signal processing of the signal intensity as this is similar in magnitude to the least significant bit of a 12 bit A-D Converter.

The output of a typical HeNe laser may be defined by the distribution of Equ. 3.31, and shown plotted in Fig. 3.31.

Equ. 3.31. $I(r) = I_0 \exp(-2r^2/w_0^2)$

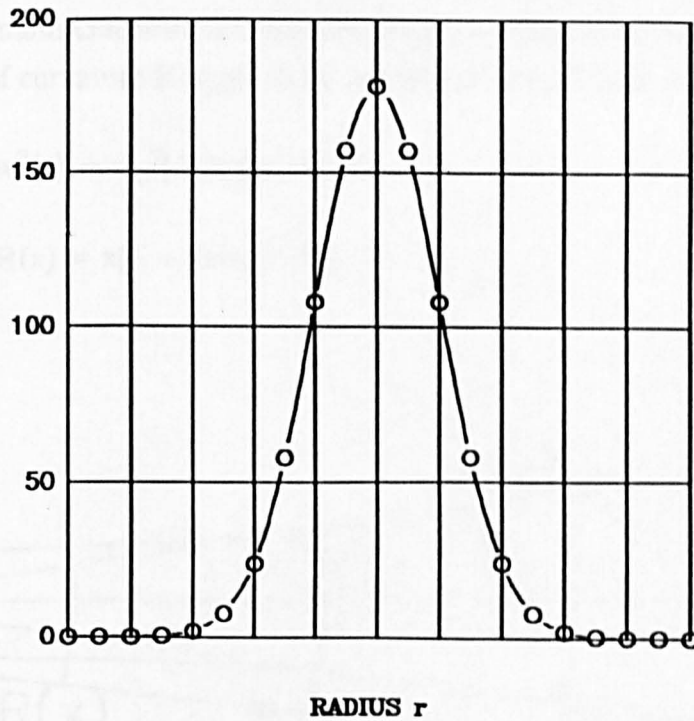
INTENSITY I

Fig 3.31. Gaussian beam intensity distribution.

The Power contained within a radius 'r', is obtained by integrating the intensity distribution from 0 to r as shown in Equ. 3.32.

Equ. 3.32.
$$P(r) = P(\infty)[1 - \exp(-2r^2/w_{02})]$$

From this equation it can be shown that: Nearly 100% of the power is contained in a radius of $2w_0$ and 50% of the power is contained in $0.59 w_0$. The power from 0 to Infinity is typically quoted by manufacturers when referring to output power of lasers. It is related to on axis intensity by, $I(0)(\text{Watts/m}^2)$ by Equ. 3.33.

Equ. 3.33.
$$P(\infty) = (w_{02} \pi/2)I(0)$$

Care must be taken not to cut off the Gaussian Distribution by using too small an aperture, $3 - 4w_0$ will have negligible effect.

3.6.4.3. Propagation of a Gaussian beam through an optical system.

Once a definition is used for the Gaussian beam profile its propagation through the optical system can be described at other points without resorting to solving the Fresnel integral or otherwise solving the wave equation.

If the beam diameter is defined as $2w_0$ with the origin of the beam waist is at $x = 0$, then the beam remains Gaussian as it expands in a spherical wave with Gaussian radius $w(x)$ and radius of curvature $R(x)$ given by Equations 3.34, & 3.35, see Fig. 3.32.

Equ. 3.34. $w^2(x) = w_0^2[1 + (\lambda x/\pi w_0^2)^2]$

Equ. 3.35. $R(x) = x[1 + (\pi w_0^2/\lambda x)^2]$

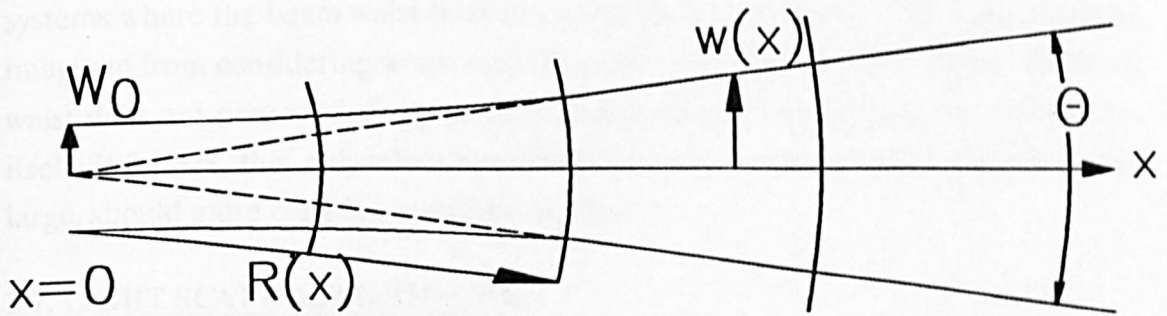


Fig. 3.32. Gaussian beam.

It can be noted from these equations that at large distances ($x > w_0^2$) from the beam waist the beam appears as a spherical wave from a point source located at the centre of the beam waist. The beam has a total angular width, defined by the $1/e^2$ points of:

Equ 3.36. $\Theta = 4\lambda/2\pi w_0$

Where the approximation $\Theta = \tan\Theta$ has been used and the origin has also been taken to be a point source. Referring to Fig. 3.32, it can be readily seen that:

Equ. 3.37. $\Theta \cong D/f = \text{f-number of the lens.}$

Using equations 3.36, and 3.37, gives the equation for the beam waist diameter in terms of the input beam diameter.

Equ. 3.38. $2w_0 = (4\lambda/\pi)(f/D)$

The focal spot diameter is approximately equal to wavelength times f-number of the lens. If Depth Of Focus (DOF) is defined arbitrarily as the distance between the values of x where the beam is two times larger than at the beam waist, then using the equation for $w(x)$.

Equ. 3.49. $DOF = (8\lambda/\pi)(f/D)^2$

Therefore, the DOF is approximately 2.5 times the wavelength times the square of the f-number. An exception to the general rules given above is for weakly focussing systems where the beam waist does not occur at the focal length. In fact, as can be imagined from considering weakening the power of a lens until it is plane, the beam waist does not occur at infinity as geometrical optics would predict but at the lens itself. It follows, that only when beam diameters are small, or when f-numbers are large, should more complex equations be used.

3.7. LIGHT SCATTERING THEORY.

The scattering of light by interaction with matter is a complex process that does not occur only when the light impinges upon the surface of interest, but also as it passes through the medium between the triangulation system and the subject surface. Fortunately, this latter form of scattering, caused by a process of interaction between the light and matter (in this case the atmosphere) is minimal at longer wavelengths and over the distances that this thesis is concerned with. The blue sky and red evening sun are caused by this phenomena (Meyer-Arendt, 1984).

3.7.1. Surface reflections.

The optical triangulation scheme, as an active technique, relies critically upon the outgoing light spot causing enough reflected light for the camera to distinguish this spot from the background lighting. Fortunately, only the perfectly specular or transparent surfaces do not reflect a reasonable proportion of thier light diffusely. The reflected light components are shown in Fig. 3.33.

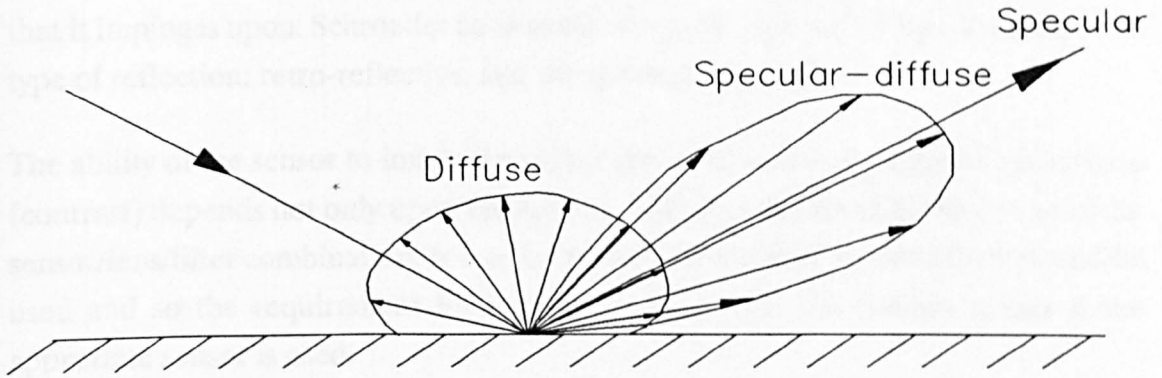


Fig. 3.33. Reflected light components (Page).

Page states that 'In practice, the amount of scattered light and the relative magnitudes of the specular, specular-diffuse, and diffuse components are dependent on the radiation wavelength, surface composition, and surface roughness.' The general shapes of response curves for some engineering materials are shown in Fig. 3.34.

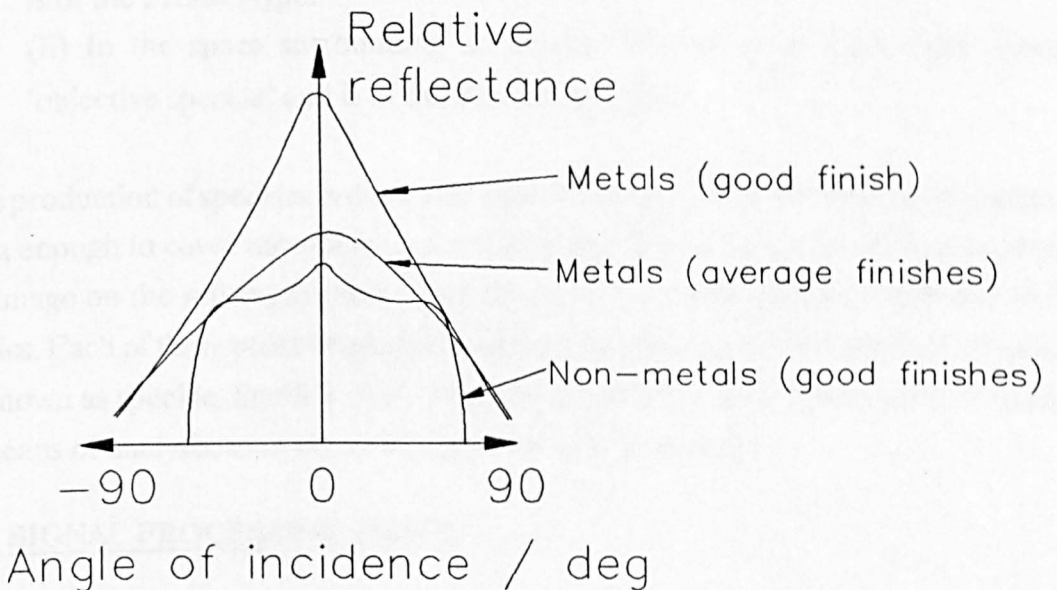


Fig. 3.34. Response curves for three material types (Page).

An encouraging feature of these diagrams is that there is a reasonable quantity of light being reflected at high angles of incidence from most materials.

Shroedrer describes a characteristic that is common to all machine vision systems, that of obtaining feature information from a scene. The term used to describe this

condition is 'contrast'. In the case of the triangulation system what is important is the contrast of the identifying light spot with respect to the intensity of the background that it impinges upon. Schroeder adds to the simple list given by Page, the additional type of reflection: retro-reflective, and the spectral selective.

The ability of the sensor to image the object spot with sufficient signal to noise ratio (contrast) depends not only upon the surface, but upon the spectral selectivity of the sensor/lens/filter combination. It may be assumed that a narrow band filter would be used and so the requirement for good contrast at that wavelength is met if the appropriate sensor is used.

3.7.2. Laser speckle (Svelto, 1982; Jones, 1983).

When a laser beam is viewed from a distance, the scattered light appears to consist of a random collection of alternately bright and dark spots (or speckles).

The phenomena known as speckle occurs in two ways:

- (i) On the surface of an imaging sensor. This is termed 'subjective speckle' and is of the Fresnel type.
- (ii) In the space surrounding an object illuminated by laser light, termed 'objective speckle' and is of the Fraunhofer type.

The production of speckles is due to the coherence of a laser beam which is generally long enough to cover the whole surface to be measured. Each object point produces an image on the sensing surface which is essentially a diffraction pattern due to the optics. Each of these point images is capable of interfering, it is the result of this which is known as speckle. Speckle may either be undesirable, as in holography, or used as a means of analysis, as in electronic speckle interferometry.

3.8. SIGNAL PROCESSING THEORY.

3.8.1. Introduction.

The only object of interest to the camera in a triangulation scheme is the laser spot which has a Gaussian intensity profile. The camera lens system also imposes onto the image its own point spread function (PSF), which, for most purposes is also a Gaussian distribution. The convolution of two Gaussian functions is a Gaussian function. The requirement of the triangulation system is for this Gaussian intensity profile to be

located as accurately as possible with respect to the CCD chip. The combination of electronic sensors and digital signal processing can be utilised to achieve a greater degree of flexibility and higher accuracy than would at first appear to be available from the sensors used.

A review of the methods contained in the literature (West, 1990) enables the correct choice of algorithm for this application. Subpixel techniques have been used in many areas of application such as: star tracking, satellite and space probe imaging and in measuring dimensions of products such as rolled steel strip and manufactured components i.e. position of edges and objects. In each application, knowledge of the physical nature of the scene imaged onto the sensor is used e.g. the edge of a steel sheet may be considered a unit step. This is modified by the electronics, optics, lighting, surface reflectivity and diffraction, to form a sampled intensity map of the edge from which the position of the edge can be recovered. Objects such as stars and laser spots may have a known shape, allowing subpixel registration with the model by computation of the position of the centroid or peak position after interpolation.

3.8.2. Image formation.

Subpixel accuracy can be achieved because the imaging process can be accurately modelled. The *a priori* knowledge of the intensity distribution of an object, such as a star (a point source), is essential for obtaining subpixel accuracy, and enabling a decision as to whether the data is valid for subpixel treatment. However, for a full understanding of the data recorded by the imaging system, further knowledge of the characteristics of the optics, sensor and signal conditioning electronics is required.

3.8.3. Data processing.

The spatially sampled analogue signal from the sensor is processed to produce a stream of digital information. Noise is generated by quantisation (in A-D conversion), amplification, black level clamping and signal restitution. Of these, quantisation noise is the most important, especially as most sensor arrays have a higher dynamic range than the typical A/D converter used (8 bits).

3.8.4. Survey of techniques.

The desire for some method of obtaining subpixel accuracy has occurred in many disciplines including photogrammetry, automatic inspection, remote sensing and computer vision. A large number of techniques have been proposed that fall into a

number of categories. These are centroiding, interpolation, correlation, edge analysis and shape-based. Most techniques fall into one of these categories. However, in some cases, more than one technique is used.

Subpixel accuracy is necessary because the data collected is a digital representation of an analogue signal that has been sampled onto a discrete array (usually 1-D or 2-D rectangular) and each data point is quantised to a finite number of levels (usually 256). Apart from the quantisation errors other factors need to be accommodated including noise and the system response of the lens and array as well as application dependent factors such as speckle.

3.8.5. Algorithms for subpixel accuracy.

3.8.5.1. Centroid method.

This method has been described by many authors (Brook, 1979; Salomon, 1979; Lange, 1986; Ho, 1986; El Hakim, 1986; Deng, 1987), and may be explained by use of Equ. 3.49, where δx is the position of the image to subpixel accuracy.

$$\text{Equ. 3.49.} \quad \delta x = \frac{\sum_{j=1}^n (1/M) * j * g_j}{\sum_{i=1}^n g_i}$$

where $M = \sum_{i=1}^n g_i$

and g_i is the intensity value of each pixel, and n is the number of pixels in the window of interest. The process is shown graphically in Fig. 3.35, for a Gaussian shaped image covering seven pixels.

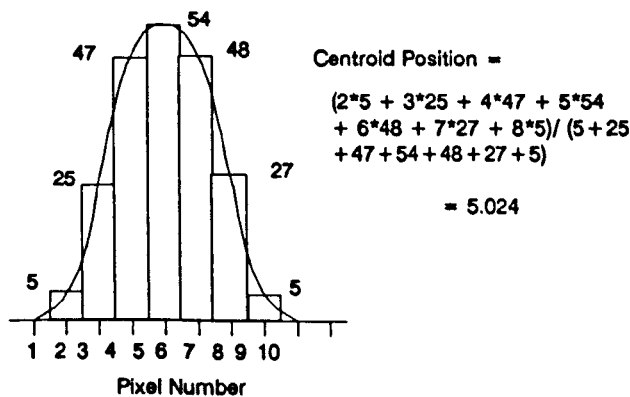


Fig. 3.35. Centroid calculation.

3.8.5.2. Weighted centroid method.

This method (Trinder, 1989) uses a weighting corresponding to the intensity value to multiply each successive point. This squaring of the intensity values places greater weight on those pixels that of greater value which are the stronger and more accurately measured values. This scheme is defined in Equ. 3.50.

$$\text{Equ. 3.50.} \quad \delta x = \frac{\sum_{j=1}^n (1/M) \cdot j \cdot g_j \cdot g_j}{\sum_{j=1}^n g_j \cdot g_j}$$

where the other symbols have the same meaning as before.

3.8.5.3. Vernier method.

This method (Overington, 1987) can be called a Vernier method because like the readout on a pair of Vernier callipers first the coarse position is computed then the small addition or subtraction quantity is computed to give an increased overall accuracy. The Vernier distance ' δx ' is shown in Fig. 3.36.

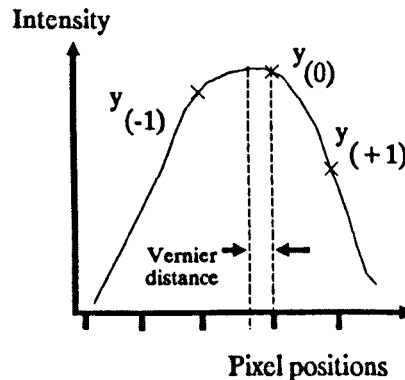


Fig. 3.36. Vernier calculation parameters.

Subpixel accuracy is achieved in this method by fitting a Gaussian curve to the three largest intensity values in the image. The function to be fitted is given by Equ. 3.51.

$$\text{Equ. 3.51.} \quad y(x) = y_0 \exp[-(x - \delta x)^2 / 2]$$

which expanded, neglecting terms in δx^2 , expanded again with $x = -1, 0, \& 1$, yields Equ. 3.52.

$$\text{Equ. 3.52.} \quad \delta x = \Gamma \cdot [(y(+1) - y(-1)) / (2y(0) - y(+1) - y(-1))]$$

where $\Gamma = \sigma^2[\exp(1/2\sigma^2) - 1]$ which is approximately equal to $0.5 + 0.125\sigma^2$.

Hence, this method is computationally simple, and claimed to be 'robust against random additive noise'. The author reports the following accuracies for a range of signal to noise ratios in Table 3.1.

SNR	VER
∞	0.02
6.6	0.09
3.3	0.17
2.0	0.26

Table 3.1. Vernier accuracy results.

It is possible to adjusted the algorithm to fit a quadratic by altering Γ to 0.5. This method has been described by others, such as Tian, 1986, where this method is described as 'correlation interpolation' and concludes that 'the accuracy of this estimator depends on how well a correlation function around the peak approximates to a parabola.' Some of the results obtained for this method compared to other methods are shown in Table 3.2.

	Intensity interp	Difference	Corr Interp	Phase corr
xerror	0.0029	0.013	0.045	0.092
yerror	0.006	0.010	0.052	0.127

Table 3.2.

3.8.5.4. Interpolation method (Castleman, 1979; Hou, 1978; Smith, 1985).

This method is defined as follows:

- (i) An interpolating function is generated which may be a Sinc, square, triangle, cubic B spline, bell or Gaussian shape, with a distinct width. The function may be continuous or discretely sampled.
- (ii) The interpolation function is multiplied by the intensity value at each pixel.
- (iii) The original waveform is recovered, with a faithfulness dependent on the type of interpolating function, by the summation of the components from each of the interpolating functions at discrete points between the intensity value positions.

The performance of the interpolation functions has been analysed by Castleman in 1979, with the conclusions that the Sinc function gives perfect results, followed in accuracy by the Gaussian function and the cubic B spline. Of these functions the cubic B spline is the best for practical implementation as it is not a continuous function as the Sinc and Gaussian are.

The operation of the interpolation procedure is illustrated in Fig. 3.37, and Fig. 3.38. The first figure shows the interpolation functions that were used to interpolate between one reflected image of the laser beam. The interpolation function is Gaussian of a set width and of maximum height of the intensity value of the image which is marked on the graph. Each of the Gaussian shaped interpolation functions was evenly distributed over 2000 points. The interpolation curve, shown in the Fig. 3.38, is the result of summing the contributions of each of the interpolations functions at each point along the horizontal axis.

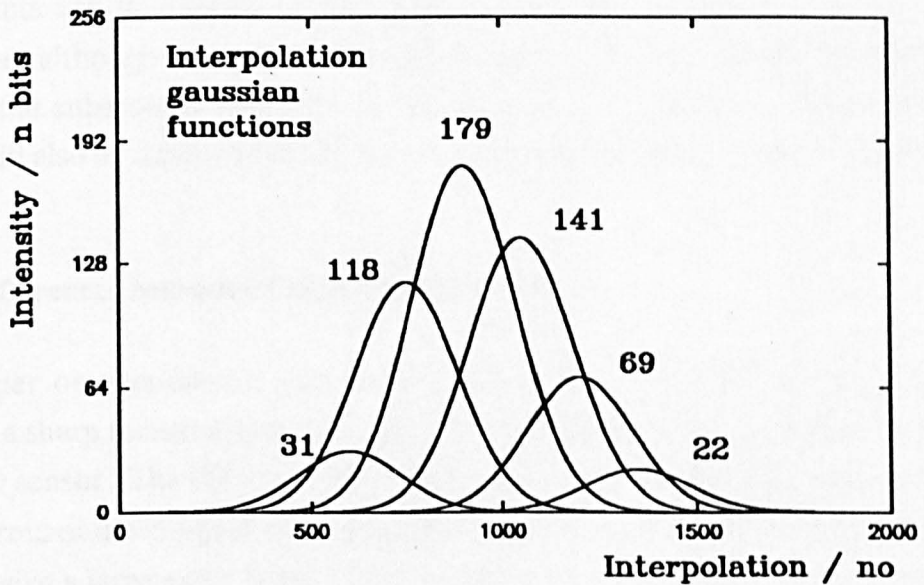


Fig. 3.37. Gaussian interpolation functions.

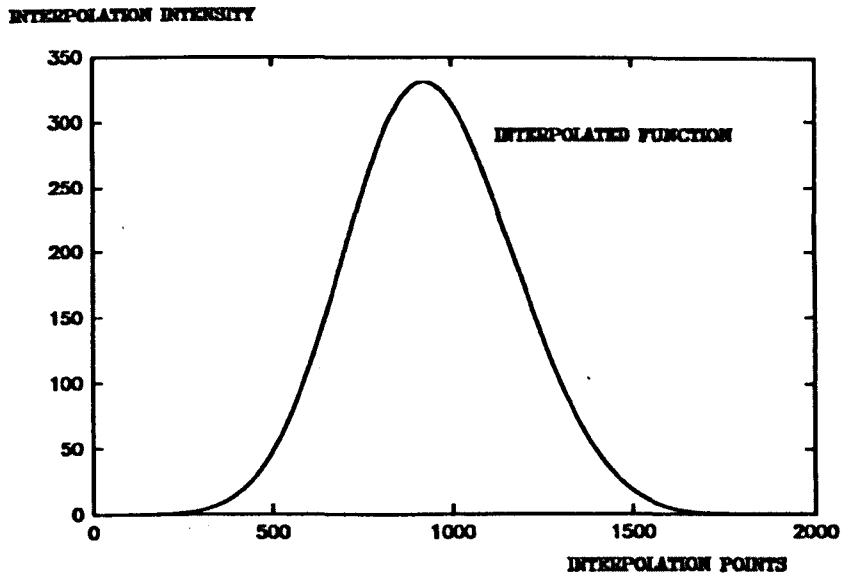


Fig. 3.38. The interpolated curve.

Two points are of interest to this project: first, this method is computationally expensive, although accurate in its representation of the original waveform, and second, the subsequent detection of the peak or the correlation with an accurate model will also be time consuming, and the technique would not work well with noisy images.

3.8.6. Differences between CCD and PSD detectors

In a paper on non-contact microprofilometry Warneke, 1987, states that CCDs 'require a sharp focussed spot' and that the 'conditions are far less restrictive in case of a PSD sensor'. The PSD does not require such a high degree of focussing because the centroid of the image is what is 'computed' by the chip and so a defocussed image will not give a large error because of the symmetry of the image shape. Chen, 1987, points out that CCD sensors require 'precise focussing' and that the PSD is 'insensitive to defocussing and the output signal gives the centroid of the focussing point.'

3.9. CALIBRATION THEORY.

3.9.1. Calibration and interpolation methods.

3.9.1.1. Introduction.

The process of optical triangulation demands a method of relating laser image positions with respect to the CCD chip to a distance measurement. This is achieved

via a calibration routine and a subsequent interpolation between calibration points. Several methods of calibration and interpolation are described.

3.9.1.2. Requirement for calibration and interpolation.

To operate any method of calibration and interpolation implies that the same method of laser image location with respect to the CCD chip is used. This may be to subpixel accuracy or otherwise. The task of the calibration and interpolation is to provide a computationally simple way of arriving at a distance measured from the profiler to the laser spot.

If the number of resolvable points along the length of the CCD chip is known then it is possible to calibrate a distance for each of these points with no requirement for interpolation. However, as each calibration point and corresponding distance has to be stored as a real number, typically requiring 6 bytes, and the number of resolvable points is likely to be 20,000 then the total storage of data would be greater than 240Kb. This presents both problems in data storage and calibration.

However, if the system under calibration has a well defined relationship between the calibration points and distance, then other methods may provide a better solution. Such methods can be tested out and the best used in the actual measuring system implementation. The techniques range from fitting a function through all of the points or a best fit curve through the points, to piecewise linear, polynomial or cubic spline interpolation. These methods are reviewed here and their respective characteristic evaluated.

3.9.1.3. Numerical methods (Greenspan, 1988; Hultquist, 1988; Boorland, 1988).

Discrete function definitions:

Definition 1. A function $y = f(x)$ that is defined only on an R_{n+1} set is called a *discrete function*.

Definition 2. If $y_i = f(x_i)$, $x_i \in R_{n+1}$, is a discrete function, then the set of points (x_i, y_i) , $i = 0, 1, 2, \dots, n$ is called the *graph* of the function. Where ' $x_i \in R_6$ ' is used in the customary mathematical way to mean ' x_i is an element in the set R_6 '.

If there is a discrete function $y_i = f(x_i)$ on a R_{n+1} set then, in general, interpolation is the process of approximating y at a point x which is between two points x_i and x_{i+1} .

In the case of the optical triangulation scheme x defines the image position with respect to CCD Chip and y is the interpolated distance with respect to two previous calibrated distances.

3.9.1.4. Piecewise linear interpolation.

Given a discrete function $y_i = f(x_i)$ $i = 0, 1, 2, \dots, n$. on a R_{n+1} set, then the piecewise linear interpolating function $L(x)$ of y_i is the function whose graph consists of straight line segments joining consecutive pairs of points.

$$\text{Equ. 3.53.} \quad L(x) = y_i + \frac{y_{i+1} - y_i}{h}(x - x_i), \quad x_i < x < x_{i+1}, \quad i = 0, 1, 2, \dots, n-1$$

If the error introduced as a result of use of this method because the continuous function is a curve, then a piecewise parabolic interpolating method may be used.

3.9.1.5. Piecewise parabolic interpolation.

With the piecewise linear interpolation it was sufficient to have just two points to interpolate between, if a parabola of the quadratic form Equ. 3.54, is used then three points are required.

$$\text{Equ. 3.54.} \quad y = a + bx + cx^2$$

For a discrete set as defined in the 3.9.1.4, with the restriction of 'n' being even, a parabolic interpolating function $P(x)$ is defined where the graph consists of a piecewise parabolic arcs through consecutive triplets of points, $(x_{i-1}, y_{i-1}), (x_i, y_i), (x_{i+1}, y_{i+1}), i = 1, 3, 5, 7, \dots, n-1$ given by:

$$\text{Equ. 3.55.} \quad P(x) = y_i + \frac{y_{i+1} - y_{i-1}}{2h}(x - x_i) + \frac{y_{i+1} - 2y_i + y_{i-1}}{2h^2}(x - x_i)^2$$

$$x_{i-1} < x < x_{i+1}, \quad i = 1, 3, 5, \dots, n-1.$$

One of the limitations of this method for producing a curve through a set of discrete points occurs when there is a sharp change in gradient which may not be representative of the type of data represented in the graph. However, in the context of the calibration

and interpolation this limitation is not a problem as the characteristic of the triangulation system, the characteristic relationship is slowly changing.

3.9.1.6. Cubic spline interpolation.

It is assumed that there are three points available, as in the former case, the x axis points to be interpolated between are evenly spaced, and the first derivative, y' , is known at the first point. Given this data the cubic spline interpolating equation is given by Equ. 3.56, and Equ. 3.57.

$$\text{Equ. 3.56. } y(x) = y_0 + y'_0 x \frac{8y_1 - 7y_0 - y_2 - 6hy'_0}{4h^2} x^2 + \frac{3y_0 - 4y_1 + y_2 + 2hy'_0}{4h^3} x^3$$

$$\text{Equ. 3.57. } y'_2 = y'_0 + 2 \frac{y_2 - 2y_1 + y_0}{h}$$

Using this method it is necessary to know the first derivative at the first point which is not always available, but, having gained the first interpolating cubic spline it can be seen that from Equ. 3.57, that the rest of the cubic splines for the whole data set can be constructed. There are also numerous variations on this method with differing criteria such as one ensuring that the second differential at the start and end points is zero. If these requirements are a problem then Lagrange interpolation may be considered.

3.9.1.7. Lagrange Interpolation.

In the previous examples there is a progression from piecewise linear, to quartic and then cubic, this can be continued by what are known as Lagrange polynomials which can be constructed relatively easily and can realistically cover a range of points up to about a hundred.

The general Lagrange Interpolating formula of degree k is denoted by $p_k(x)$, is given as follows. Consider the distinct points $(x_0, y_0), (x_1, y_1), \dots, (x_k, y_k)$ with $Q_j(x)$ defined by Equ. 5.58.

$$\text{Equ. 3.58. } Q_j(x) = \frac{(x-x_0)(x-x_1)\dots(x-x_{j-1})(x-x_{j+1})\dots(x-x_{k-1})(x-x_k)}{(x_j-x_0)(x_j-x_1)\dots(x_j-x_{j-1})(x_j-x_{j+1})\dots(x_j-x_{k-1})(x_j-x_k)}$$

then $p_k(x)$ is given by Equ. 5.59,

$$\text{Equ. 3.59. } p_k(x) = \sum_{j=0}^k y_j Q_j(x)$$

where, except in degenerate cases, $p_k(x)$ is a polynomial of degree k . This formula will allow a piecewise determination of the graph over the whole set of data, but in this case it will allow interpolation over any range of points required.

3.9.1.7. Least Squares.

In the previous methods the interpolating functions all contained the discrete points upon which the interpolation methods were based. However, if the data set is noisy this may not be the best way of obtaining interpolation. The method of least squares allows for the fitting of a given function (linear, cubic, sine, etc.) to the set of data and obtain a best fit. The data collected in calibration and interpolation is generally of this type, slowly changing but with some additive noise. The method of least squares is described generally as follows:

Let $y_i = f(x_i)$, $i = 0, 1, 2, \dots, n$ be a discrete function as in the previous cases, and let $y = g(x)$, x_0, x, x_n , be a continuous function to fit the given data by least squares, assume $g(x)$ contains the independent parameters a_1, a_2, \dots, a_m , then the requirement is to minimise Equ. 3.60,

$$\text{Equ. 3.60. } E = [g(x_0)-y_0]^2 + [g(x_1)-y_1]^2 + \dots + [g(x_n)-y_n]^2$$

by solving the system:

$$\frac{E}{a_1} = 0, \quad \frac{E}{a_2} = 0, \quad \dots, \quad \frac{E}{a_m} = 0$$

to yield the desired values of a_1, a_2, \dots, a_m .

3.9.2. Calibration equipment.

To analyse subpixel techniques and calibration/interpolation methods to establish their respective accuracies, a standard of measurement had to be used which was much higher than that able to be achieved by the triangulation system. An interferometer was used for this purpose which was highly accurate. The operation of this measurement system and its characteristics are described in Appendix 1, where the same numbering system is continued.

3.10. CONCLUSION.

The theory of all the important features of optical triangulation systems has been considered in this chapter.

4. PROTOTYPE DEVELOPMENT.

4.1. SYNOPSIS OF PROTOTYPE DEVELOPMENT.

The aim of the research carried out for this thesis was an investigation of the optical triangulation technique for measuring structures in the range 0-10 metres. To compliment the work described in chapter 5 on errors and the theoretical and simulation work in chapter 6, a programme of research by prototype development was carried out and is described in this chapter.

Using prototypes had a number of benefits to the research as hardware and software techniques were tested and a valuable proof of principle was available for engineers and surveyors. Three prototypes were developed which are described fully in this chapter. The initial investigations are outlined followed by an analysis of the mechanical, electronic, and software design necessary for the development of each prototype.

4.2. INTRODUCTION.

4.2.1. Research objective.

The research objective identified at the beginning of the research programme was to address the problem of measurement of full or partial cross-sections of structures. Two possibilities were available.

- (i) Investigate and improve the method in occasional use at City University, a light-sectioning photogrammetric technique. The objective would be to: (a) substantially decrease the data collection time by putting the process as 'on-line' as possible, (b) improve the accuracy, and (c) eliminate the disadvantage of the large camera to object distances required.

Such improvements would have necessitated improvement to the photographic process i.e. exposure time, and lighting conditions - not a very promising area of work.

(ii) Starting from first principles, design a measuring system to obtain the same type of data, using a non-contact measuring technique. The large range of available techniques is described in chapter 2. The advantage of this 'clean sheet' approach is that with the specification already known, the possible candidates are, to an extent, self selecting, the most suitable choice being made between the time of flight and optical triangulation techniques.

4.2.2. Specification for the measurement technique.

A high accuracy requirement is imposed when attempting to improve on the photogrammetric method because of the vast quantity of data collected in a photograph and its availability for measurement. A photograph has the equivalent of greater than 10^{10} pixels, which compares with the 10^7 current maximum from electronic cameras, hence, an improvement of 10^3 is required to compete on a like for like basis. However, the photograph is often the first step in a data reduction process in which selected information is removed for analysis, this relaxes the criteria for a comparable electronic system as only this reduced data need be collected. Hence, the same results can be produced with a system which records point by point, at a relatively low resolution. Furthermore, as the photogrammetric technique has the disadvantage of being over specified for the cross section measurement task, much of the available measuring surface of the film is wasted. Therefore, if a fast, directional, single point measuring system is used to collect spatial data about discrete points, then the requirement of an on-line system is met, and the film processing and post processing stages are eliminated.

The review of distance measurement techniques in chapter 2, showed that only a few were realistically able to provide better than millimetre accuracy at a greater than kHz measuring rate. The first, a laser range finder, was judged to be the best technique, but considered to be an unlikely goal to achieve with the currently available technology. This projection proved to be correct. In spite of much research work in this area over the time of the work conducted for this thesis, there is no commercially available system to meet this specification. The second technique, a laser triangulation range finder, appeared to offer a number of the required features with current

technology. Furthermore, the technique had not been researched in detail for use in the area of surveying which provided a good criteria for original research, and it was likely that this line of research would produce a fast, accurate, reliable and robust measuring system. A third option, an improved photogrammetric system along the lines of the British Rail gauging train, was considered feasible but likely to be expensive to construct and would probably be limited to specific applications.

The desired specifications considered adequate for surveying applications were:

- (i) millimetre accuracy range measurement,
- (ii) rapid measurement at greater than 1kHz,
- (iii) a compact, portable, tripod mounted instrument,
- (iv) robust and safe equipment, and
- (v) fast complete cross section measurement and recording.

4.2.3. Choice of measurement technique.

As a result of a thorough literature survey, it was decided to examine the development of an optical triangulation measuring system because it held out the promise of meeting parts of the specification such as speed of measurement, while still requiring development in the areas of robustness and accuracy. A further reason for this decision was the apparent lack of research in this area. However, there was ample evidence of its capability in other fields of application.

A close examination of the requirements of the surveying industry was conducted in a market survey (Clarke, 1989) which showed that there exists a wide demand for the acquisition of cross sectional data of structures. This demand was confirmed by the experience of the Photogrammetry Unit of the University in regularly undertaking work in this field. Searches in a number of computer data bases did not reveal any alternative solutions.

4.2.4. The research objective.

One method of research used to pursue the goal of an on-line cross section measuring system was by building and testing prototypes. Such an approach was likely to show up short comings of any system and enable solutions to be found. In addition this approach would be supplemented by theoretical analysis (chapter 6) and consideration of the nature and magnitude of likely errors (chapter 5).

The design of such a measuring system was likely to include the problems of:

- (i) maintenance of the configuration in a robust way,
- (ii) directing a laser beam to the point of interest,
- (iii) collecting the data from the sensor and processing it,
- (iv) eye safety,
- (v) rotating the measuring arm,
- (vi) compact design,
- (vii) tripod mounting without occlusion,
- (viii) non-linearity,
- (ix) accuracy and resolution,
- (x) calibration and interpolation,
- (xi) real time software, and
- (xii) measurement to diffuse and non-cooperative subjects.

Having defined the objectives of the project, the type of data required, and the expected environment a schedule of research was embarked upon, and is described in this chapter.

4.3. PRELIMINARY INVESTIGATION.

4.3.1. Introduction.

To establish whether the optical triangulation technique was sufficiently promising to proceed with, some preliminary investigations were carried out. The essential components of the optical triangulation system using a CCD linear array camera and laser pointer are shown in Fig. 4.1.

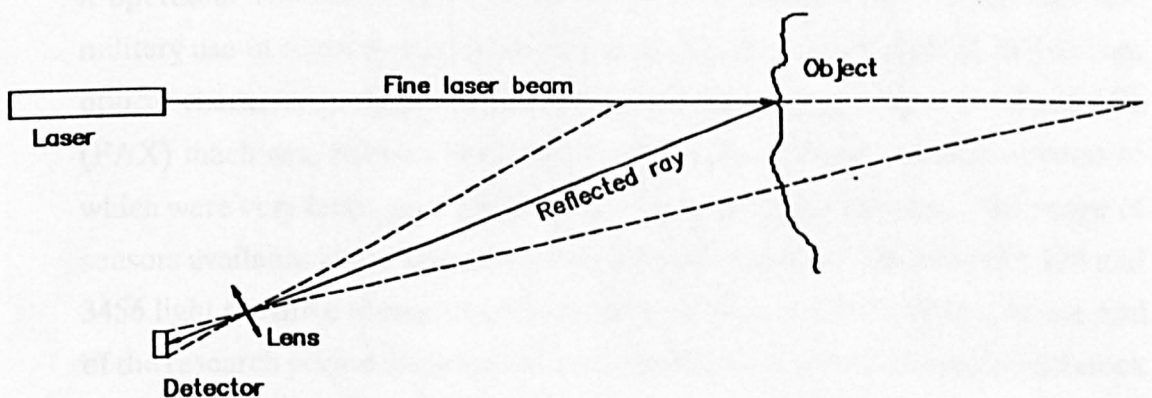


Fig. 4.1. Configuration for simple optical triangulation.

The laser illuminates a point on the object surface, this spot is imaged by the lens onto the sensor at a position which is related to the distance of the measuring system from the object surface. The configuration can be varied in a number of ways.

4.3.2. Analysis of the required components.

To investigate the potential of this system it was necessary to examine its constituent parts which are: the light source, mechanical configuration, lens and sensor.

- (i) The production of the light spot did not appear to be a problem with many systems available, HeNe and diode lasers being well developed technologies.
- (ii) The rotation of the mechanical configuration was of conventional design with no requirement for very fast movement. However, the mechanical configuration stability is of prime importance in maintaining a calibration configuration and would require investigation.
- (iii) The optics would be conventional and not require any new techniques.
- (iv) The sensor was an item where performance was considered to be of critical importance in obtaining a high speed of measurement, ensuring repeatability and in the obtaining the desired spectral and light response characteristics. Twenty two manufacturers of CCD devices were contacted for information concerning CCD line scan cameras. The major manufacturers were EEV Reticon, Fairchild, Hitachi, Texas, Thompson, and Toshiba. (The only significant addition to this list, during the development period, has been that of Dalsa). The information obtained provided a clear picture of the device and how it operated. The manufacturers reasons for production ranged from civil and military use in remote sensing, optical character reading, industrial inspection, optical character recognition and the rapidly expanding market for Facsimile (FAX) machines. Sensors were tailored for each of these markets, several of which were very large, giving high reliability, and reasonable cost. The range of sensors available at the beginning of the research period had between 128 and 3456 light sensitive elements with clock rates between 10-20MHz. (At the end of the research period sensors with up to 6000 light sensitive elements and clock rates of 40Mhz began to appear)

These initial investigations confirmed that the components for an optical triangulation system were readily available. There remained areas which would require research that would be particular to the use of this technique for the measurement of cross sections.

4.3.3. Tests with CCD camera.

Before ordering a sensor, tests were considered necessary to become familiar with the operation of CCD sensors, lasers and the triangulation configuration. These tests were made using a Fairchild CCD1500C CCD line scan camera, Fairchild 1320 camera control unit, and a HeNe 5mW laser. The camera control box allowed changes to the clock rate and exposure time of the sensor and visual inspection, with an oscilloscope, of the analogue voltage train which shows the response to incident light.

Tests were devised to assess whether a signal could be obtained from a dark surface similar to that found in a railway tunnel and whether the relationship proposed between image and distance could easily be established. The results of tests using a piece of black felt as a target are shown in Table 4.1.

Clock rate / MHz	Aperture / f number		
	Distance between laser and camera/metres		
	1.0	1.5	2.0
0.6	22	22	16
1.25	22	22	11
2.5	16	8	8
5.0	11	8	8
10.0	8	22	3.5

Table 4.1. Data from tests with black felt.

These results were encouraging showing that a high clock rate could be achieved in each case if the aperture was great enough to allow enough light to register on the sensor.

Additional tests were carried out to verify that a relationship existed between the image and distance of the target object from the camera, and that the angle of the target area with respect to the camera or laser did not reduce the reflected light unduly. These tests lead to the conclusion that, the sensor and light source could operate with standard components and normal surfaces, at a wide range of orientations.

4.3.4. Conclusion.

As a result of these preliminary tests it was decided to make a working prototype to investigate the configuration required to measure a corridor cross section of dimensions 2.0 metres wide by 3.0 metres high.

4.4. PROTOTYPE I.

The requirement for Prototype I was to provide a proof of principle. Therefore, it was intended that the design should be flexible and allow for a variety of configurations, both in the camera angle, and the base length.

4.4.1. Mechanical design.

The prototype was constructed from components that were readily available: a Fairchild CCD1300 Line scan camera (2048 pixel sites), a Fairchild CCD 1320 control unit, a Spectra-physics stabilite model 120 5mW HeNe laser, and two stepper motor rotation stages with an associated control box. These components were constructed as shown in Fig. 4.2.

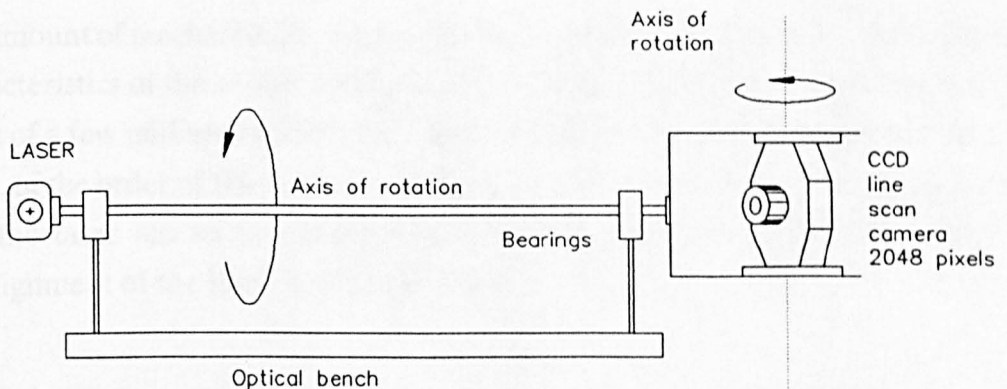


Fig. 4.2. Configuration of Prototype I.

The design allowed rotation of the system about the camera/laser axis by a stepper motor driven rotation stage, this enabled measurement to any point within the range of the camera that was not occluded by the apparatus itself. The adjustment of the parameters of importance was achieved by altering the angle of the camera to the rotation axis, and by altering the length of the base line of the triangle.

The design ensured that for set base line lengths, calculated values of the camera optical axis angle could be implemented easily allowing adjustment to the range. Several configurations were experimented with at differing base lengths. It was found

that in each, it was possible to maintain the reflected image of the laser beam on the sensor, at varying distances. The indication of the position of the laser image was initially possible by putting the output of the CCD sensor onto an oscilloscope and monitoring the analogue output of the camera. This enabled the image position, with respect to the beginning of the scan period, to be observed. Hence, an estimate of the feasibility of the location of this signal as a means of distance measurement was achieved.

The ability of the design to be configured in a number of ways was achieved at the expense of some difficulty in obtaining, and maintaining, the mutual alignment of the camera and laser. It was found that small knocks would cause the system to go out of alignment and even the changes in stress as the camera and laser were rotated would cause problems. The reasons for this sensitivity were first, by the small size of the sensor active elements which meant that small angular changes were enough to cause misalignment from the narrow laser beam, and second, by lack of sufficient rigidity in the mechanical design. Hence, although the ability to adjust the parameters of the system was desirable, it also meant difficulty in maintaining the mechanical configuration.

The amount of mechanical instability of the first prototype can be calculated from two characteristics of the sensor and light source. First, the light source produces a small beam of a few millimetres diameter, and second, the active area of the sensor is very small, of the order of $10\mu\text{m}$. Thus, when this is translated into the object space it means that the laser has to be accurately aligned for maximum effect. The effect of a misalignment of the laser is shown in Fig. 4.3.

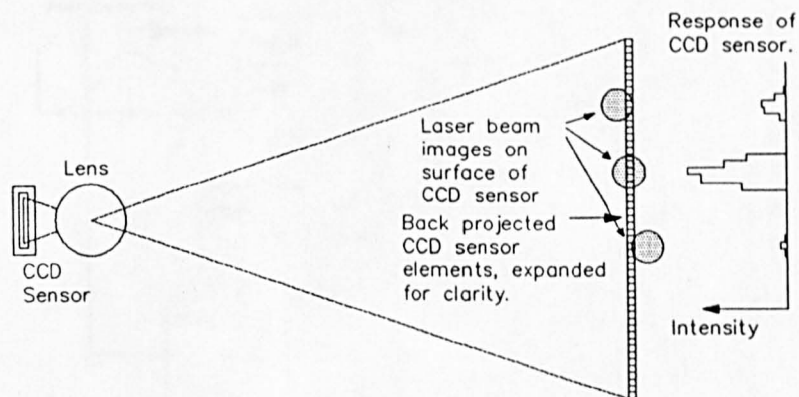


Fig. 4.3. The effect of a misaligned laser beam.

If a 50mm lens is used, with the reflected laser two metres away from the lens, the $10\mu\text{m}$ square sensor elements translate to a 0.4mm. wide stripe in the object space, assuming perfect optics. The laser beam has to be aligned as accurately as possible to fall in the centre of the sensor elements over the whole of the sensor. The need for mechanical stability was not met in the first prototype.

4.4.2. Electronic design.

To make use of the data that is available from the camera system at a number of orientations of the measuring arm, various electronic circuits are required. Few such circuits existed in off the shelf units, so the design and building of electronics circuits had to take place. The primary requirements were for collecting the intensity values from the camera and gaining access to them from a computer for processing.

4.4.2.1. CCD camera.

To use the optical triangulation components as a measuring system, the data that is produced by the CCD camera must be analysed for information concerning the position of the image of the laser spot. The data from the camera is initially contained in an analogue signal. The conventional approach is to convert the data to digital form and apply digital signal processing techniques which are flexible, and tolerant of noise and faults. To do this a circuit design is required to retrieve the intensity values as recorded by the Analogue to Digital (A-D) converter. An existing A-D convertor, with a sample and hold circuit was used from previous experiments and a new circuit was designed to read the data into a RAM chip, which could be interrogated by a computer. This circuit is shown in Fig. 4.4.

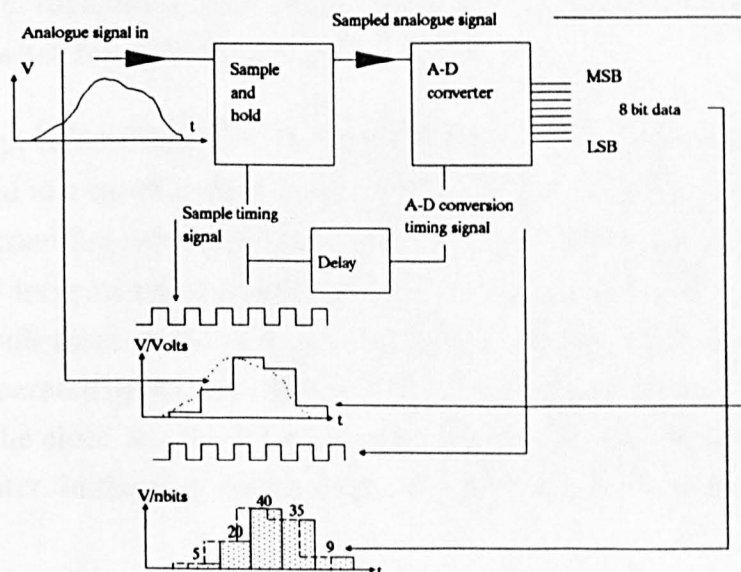


Fig. 4.4. A-D converter circuit.

The operation of this circuit is explained by analysis of the timing diagrams and the output corresponding to each stage of the circuit. The timing signal for correct operation of the circuit was provided by the CCD control box.

The overall sequence of events, of which the previous circuit is a part, is as follows:

(i) A timing signal called 'Video Valid', indicates the beginning of the CCD intensity data output from the sensor which is a constant number of clock cycles after this signal.

(ii) When the analogue voltage corresponding to the intensity of light, which has been built up by an individual sensor, arrives at the CCD output amplifier, a cycle of events takes place that will cause the corresponding digital value to be written into RAM. This cycle is made up of a number of individual events which take place during each clock period: (a) sample and hold of the analogue voltage, (b) conversion of this voltage into a digital number in the range 0-255 by the A-D converter, and (b) storage of this number in a position in RAM.

Hence, at the end of a complete cycle, the 2Kb RAM will have 2048 bytes stored in it corresponding to the light response of the sensor at that time.

The process of filling the RAM with data was a continuous process, which could be interrupted by a request from the computer to read out the information. The circuit had to allow the filling of the RAM to stop at the end of a cycle and the cessation of the fill cycle, in order that the data held in the RAM could be systematically read out by the computer for analysis of this data in digital form. This was achieved by causing the RAM to switch from READ mode to WRITE mode.

The RAM chip, HITACHI HM6116 P-4 (Hitachi), required addressing so that each byte was stored in a specific place in the RAM. This was achieved by using counters which started counting each clock cycle at the beginning of the read/write cycle, hence, producing an incremental address for each successive byte. The counters were constructed with three 74193 counter chips each of 4 bits. The clock for the first counter was operated by the main clock which generated addresses up to 2^4 , the fourth bit operated the clock for the second counter, its fourth bit operating the clock for the third counter. In this way unique addresses of 2^{12} were achieved.

To write the data out of the RAM, a logic circuit stopped the camera clock from operating the counters and a readout clock signal was generated by the computer parallel interface described in the next section. The computer was then able to read out the data from the RAM synchronously. The logic and timing was generated by various components e.g. a JK flip flop, monostable, inverter, NAND gates and buffers, a full description of these and the timing detail is not required here.

This circuit placed a restriction on the speed at which the CCD camera was able to work because of the maximum speed of the A-D converter and sample and hold circuits. However, this was not a major problem as data rates of up to 2MHz were possible, and the circuit worked satisfactorily.

The data stored in the RAM buffer required analysis, two possibilities were available: to directly analyse the data with another circuit or place the data into a microprocessor or computer for analysis by a computer program. This latter approach was decided upon, but implementing it required an interface to retrieve the data from the RAM. The design of a parallel interface to do this is the subject of the next section.

4.4.2.2. IBM PC parallel interface.

To retrieve the data from its storage in RAM, it was necessary to build a interface which would both read and write from the computer, there were three possible approaches.

- (i) A serial interface could have been constructed using standard components to comply with the RS-232 protocol as interfaces of this sort are common in computer systems. However, this was thought to be too slow as a maximum realistic speed would be 19,200 bits per second which means a byte of data is transferred in least an eighth of this. Whereas, the data transfer rate of a parallel interface was likely to exceed 5,000 bytes per second.
- (ii) Most computers do have a parallel interface capability which is reserved for printers which could be used for interfacing, but is not sufficiently flexible.
- (iii) Build a parallel interface using the specification for a prototype card specified by IBM. This method was adopted as it offered the greatest flexibility.

The parallel interface was constructed using a prototyping adapter, the design of which is specified in the technical reference for the IBM Personal Computer XT and AT range of computers (IBM Technical Manual, 1984). The purpose of the prototype adapter is to allow interfacing to the Input/Output (I/O) channel connectors which are a fundamental part of the IBM PC system. The design for the prototype adapter has been copied by various manufacturers, such as VERO, 1989, who provide boards with the basic interfacing circuits ready for other components and wire wrap circuits to be built on the rest of the board. At the time there were no ready made interfacing plug in boards or circuit designs available, so an interface card was designed and built to enable two eight bit inputs, and two eight bit outputs. These prototype boards had the advantages of being relatively cheap, easily software addressable and quick to construct. The block circuit diagram for one of these boards is shown in Fig. 4.5.

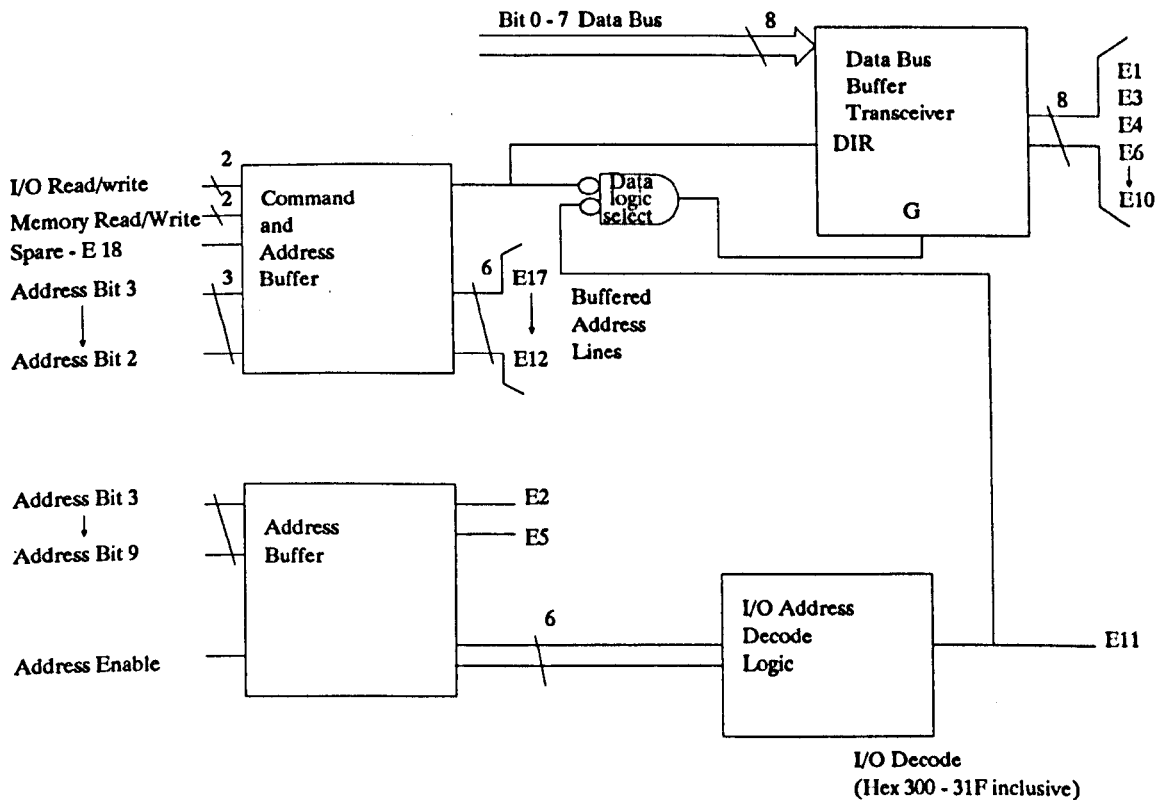


Fig. 4.5. IBM prototype board 4 x 8 Bit parallel interface.

The operation of this interface circuit is as follows:

The interface board provides the necessary buffering between the I/O channel of the computer and the circuits built onto the board. They also provide some of the decoding necessary for passing signals to and from the I/O bus.

A thirty seven way connector was provided by the board with several address signals, and an eight bit data I/O channel. The design for the parallel interface card is shown in Fig. 4.6, where these components and signals are shown. Buffers (74374) are used to hold data that is being read in or written out by the computer. The other components were required for timing and logic addressing.

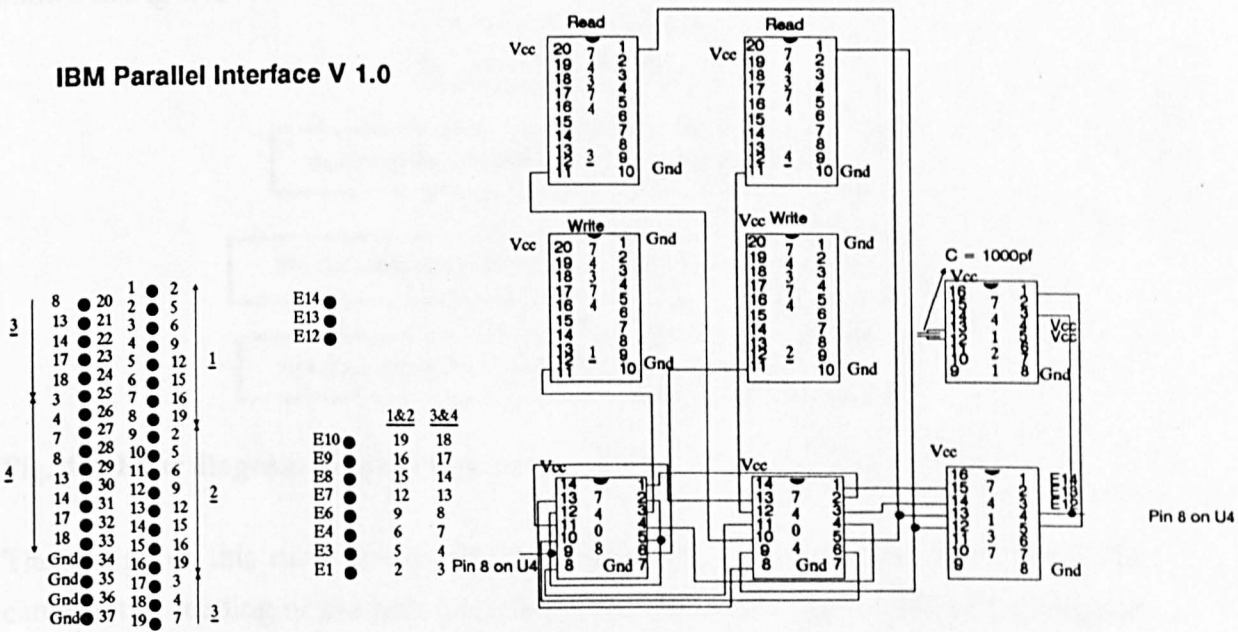


Fig. 4.6. Interface card circuit.

The design allowed the use of several address lines, three of which were required to differentiate between the four processes required and provide a unique enable signal to either (a) read the contents of one of the two 74374 buffers into the computer or (b) write data from the computer out to the other two 74374 buffers.

The addresses allocated in the design of the computer for Prototype board purposes were \$300-\$3FF. It was decided to start from the lowest address and decode it from the prototype board to cause the first operation, writing data out, to take place. When an operation is performed to this address, such as writing data out from the computer, the buffers can be made to accept this data which can then be used outside the

computer. For example, the statement 'port[\$300] := 7' in Turbo Pascal would cause the address lines into the state '1', which would allow the data on the data bus to be placed into the first buffer. In this case the data would make bits no 1-3 = logic one and bits 4-8 = logic zero. Alternatively, for the case of reading data into the computer, the statement 'temp := port[\$302]', where 'temp' is a variable, would cause the state of the data in the buffer number three to be read into 'temp'. In this way it is possible to control equipment, and read data into the computer for later analysis.

The time taken for a read or write cycle was approximately 8 μ sec, making operations by this method acceptably quick. A flow diagram for the operation of this interface is shown in Fig 4.7.

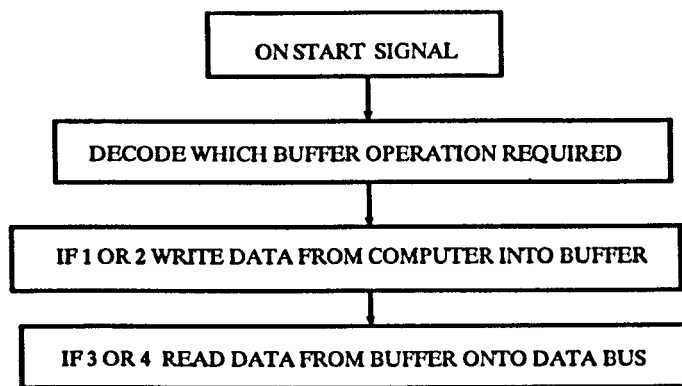


Fig. 4.7. Flow diagram for interface card.

The design of this card allowed the control of the data collection from the CCD camera, the reading of the same data from the RAM and the control of the stepper motor for rotation of the measuring system. The speed of operation was satisfactory.

4.4.2.3 Software design.

To operate the parallel interface, and hence, the camera system and stepper motor, software was required. There were a number of options for the language that could be used for this purpose: Fortran, Basic, Pascal, or Assembly language. Compared to compiled languages, Assembly language was considered too time consuming and the speed increases that would be gained would not be required as the compiled languages were very fast and allowed portions of machine code to be run from within the programs. The interpreted language, Basic, would be much slower due to the code being interpreted at the time of operation. Hence, a compiled language was the first choice. Turbo Pascal offered the greatest advantaged being a strongly 'typed' language which encourages good programming practise and a convenient environment for programming which was better than most others available at the time.

The software to control the equipment was written in Turbo Pascal Version 3. on a Amstrad IBM PC, and had several tasks to perform.

(i) Data collection.

To collect the data concerning intensity values of one line scan from the electronic hardware the following procedures must be carried out:

- (a) Ensure the RAM has the data. The RAM must contain the intensity values of the previous scan so the readout process must be initiated by producing a signal to stop the camera writing to the RAM and await the read out process.
- (b) Take the data from the RAM. A signal is generated by the parallel interface that incrementally clocks the counters for the RAM to address each byte. The data are read from the output buffer by the parallel interface.

The data, when read by the computer, are stored in an array, displayed on the screen or written to a hard or floppy disk.

(ii) Image processing.

The position of the intensity peak, corresponding to the laser image with respect to the sensor array, has to be determined. The analysis of the data can be achieved by a computer program. The easiest means of locating the image is to find the location of byte of largest value, and note its position. However, this method is prone to the problem of bright sunlight and fluorescent tubes being brighter than the laser spot and therefore making the lasers contribution, either very difficult, or impossible to distinguish as shown in Fig. 4.8.

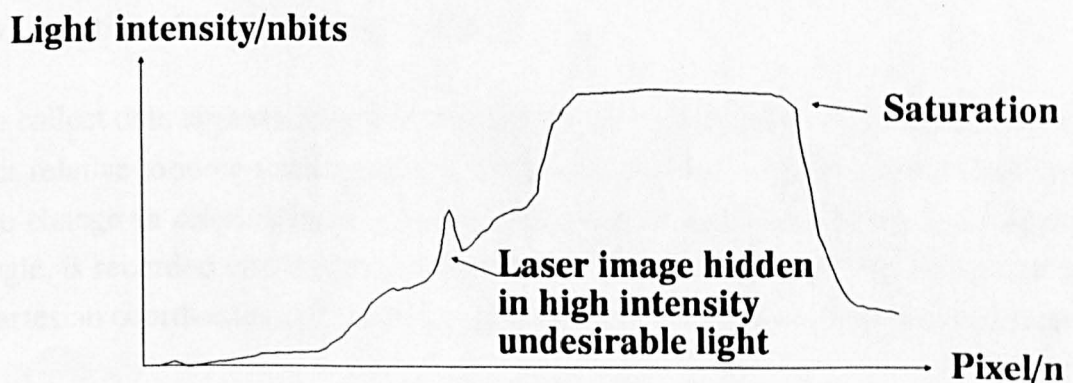


Fig. 4.8. Laser image and the effect of a bright light source.

This problem can be partially solved by using software matched filtering techniques and optical spectral filtering techniques. These techniques were not considered necessary for this prototype as data collection took place in a restricted environment.

(iii) Calibration and interpolation.

To relate the image position collected by the computer to an object distance from the base of the triangle system, a calibration procedure was required. Essentially this is performed by moving a target to a number of discrete positions over the angular field of view of the camera lens and noting the corresponding image position. The set of calibration data pairs was stored in a file for use with this particular configuration.

A consideration of the calibration/interpolation process is necessary. The data is required to reproduce a distance to match a given image position. Unfortunately it is not desirable to record a distance measurement for each unique image position (in this case 2048) as this would take a too long and would involve the storage of a large amount of information. However, the characteristic calibration curve given by plotting distance against image position is well behaved and can be represented by a polynomial without much loss of accuracy. Hence, the use of comparatively few calibration points (usually less than 30) was enough for the interpolation process.

Interpolation can be achieved in a number of ways, described in chapter 3. The method chosen at this time was to perform a least squares best fit of a polynomial (of appropriate degree) to the data and note the coefficients. The distance measurement is then computed from the equation for the polynomial using the coefficients and image positions. This calibration involves the storage of only the coefficients, typically 3-4, and is therefore efficient at the expense of a longer computation time because of the number of multiplications required.

(iv) Rotation of the measuring system.

To collect data appertaining to a cross section, the orientation of the measuring arm axis relative to some starting point is changed by a known angular amount. Following the change in orientation another measurement is taken which, together with the angle, is recorded and the process repeated. These data can then be converted into Cartesian coordinates and stored, or presented for viewing on a computer screen.

The amount of angular rotation must be variable, this is achieved with stepper motors which move in constant angular steps with a minimum increment determined by the

model design. Rotation was achieved by using the parallel interface, described in the preceding section, to give the TTL signals necessary to move the stepper motor in the required direction with an off-on-off signal per step. Hence, by keeping a record of the number of steps, and knowing the angle of rotation, the angle of movement is known. Stepper motors have very good linearity and the steps are repeatable to small tolerances and there is no cyclical error. The only problem with stepper motors is caused by the 'open loop' nature of the control, i.e. there is no feedback from the system to detect if a step is missed in an attempt to accelerate the motor too quickly. Further problems may be encountered if gearing is required, because of the relatively low angular resolution of stepper motors, in the form of gearing backlash.

The stepper motor used in Prototype I was manufactured by Oriel. Initially it was only possible to operate by use of switches on the control box, this was not acceptable to the requirement of computer control and so modifications were made to allow the parallel interface to operate the stepper motor directly from the parallel interface. Although the rotation stage geared down the stepper motor, backlash was small, and largely eliminated by rotation in one direction for collecting data and starting the data collection process against the backlash. The number of angular positions possible was 36,000 per revolution, 0.01 degrees per step.

(v) Support programs.

To ensure that the system under development had a professional appearance, could be understood by others, and was easy to use, the presentation of the program to the user (the user interface) was carefully considered. Several approaches are possible such as making a suite of programs to deal with each individual operation and presenting the user with a batch program that presents the choices and runs the programs at the users request. The method chosen for this prototype was a single program with a hierarchical menu system as shown in Fig. 4.9, by an edited version of the program used.

```
writeln(' ARRAY OPTIONS. ');
writeln(' 1. Display Array Right. ');
writeln(' 2. Display Array Left. ');
writeln(' 3. DISPLAY MENU. ');
{ Menu for Camera operations }
writeln(' CAMERA MENU OPTIONS. ');
writeln(' 1. Collect Line. ');
writeln(' 2. Collect Profile. ');
writeln(' 3. Display Maximum. ');
```

```

writeln(' 4. Display Dist Poly. ');
writeln(' 5. Display Dist Gauss. ');
writeln(' 6. Calibrate. ');
writeln(' 7. MAIN MENU. ');
{ Menu for moving data displayed }
writeln(' DISPLAY MENU OPTIONS. ');
writeln(' 1. Line display. ');
writeln(' 2. Bar chart display. ');
writeln(' 3. MAIN MENU. ');
{ Menu for Disc Operations on Numarray[j] }
writeln(' DISC MENU OPTIONS. ');
writeln(' 1. Load Array from Disc. ');
writeln(' 2. Save Byte Array. ');
writeln(' 3. Save Real Array. ');
writeln(' 4. MAIN MENU. ');
{ Menu for Data Creation by computer/keyboard }
writeln(' DATA MENU OPTIONS. ');
writeln(' 1. Keyboard input. ');
writeln(' 2. Computed data. ');
writeln(' 3. Display data. ');
writeln(' 4. MAIN MENU. ');
{ Menu for filter operations on Numarray[j] }
writeln(' FILTER MENU OPTIONS. ');
writeln(' 1. Averager. ');
writeln(' 2. Differencer. ');
writeln(' 3. Matched Filter. ');
writeln(' 4. Low Pass Filter. ');
writeln(' 5. High Pass Filter. ');
writeln(' 6. Band Pass Filter. ');
writeln(' 7. MAIN MENU. ');
{ Main Program via Menu Control. }
writeln(' MAIN MENU OPTIONS. ');
writeln(' 1. Disc Operations. ');
writeln(' 2. Data Creation. ');
writeln(' 3. CCD Camera. ');
writeln(' 4. Stepper Motor. ');
writeln(' 5. Display Array. ');
writeln(' 6. Manipulate Data. ');
writeln(' 7. Exit Program. ');

```

Fig. 4.9. Program menu.

The figure shows the number of individual procedures required in the research of the prototype. The software that was being used at this time allowed smaller universal programs to be written separately from the main program, the advantage being that several programs could share the same library of programs. If an improvement was

made to one of these library programs then all of the main programs would benefit from the change. The library programs used by the program are listed in Fig. 4.10, where comments follow the program name.

Cursorsw.psl - turn the flashing cursor off.
DoXaxis.psl - Draw the x axis for a graph.
DoYaxis.psl - Draw the y axis for a graph.
AnnXaxis.psl - Annotate the x axis of the graph.
AnnYaxis.psl - Annotate the y axis of the graph.
Waitkey.psl - Wait for a key to be pressed.
KeyArr.psl - Key in data to an array.
Bardisp.psl - Display data in bar chart format.
Linedisp.psl - Display data in connected line format.
SaveBarr.psl - Save a byte array of data to disk.
SaveRarr.psl - Save a real array of data to disk.
LoadArr.psl - Load data from disk into an array.
LoadRarr.psl - Load real data from disk into an array.
GetKey.psl - Note the key that was pressed.
GaussGen.psl - Generate a Gaussian shaped set of data.
Textbox.psl - Make a box to enclose menu options.
Camera.psl - Get data from the camera hardware into array.
Getccd.psl - Get data from the camera hardware into array.
Movestep.psl - Make camera move a specific number of steps.

Fig. 4.10. Pascal library files and descriptions.

The software written over the period of development was used to research into a number of methods of displaying and manipulating data, user interaction and profile collection techniques. This development was necessary to discover the most efficient methods for the large number of tasks that were undertaken such as: calibration, data collection, storage and display of the cross sections.

4.4.3. Results.

The prototype was set up on a bench and a target was mounted on a 1.5 metre optical bench. The measuring system was aligned so that the laser beam formed an image on the CCD array over the complete range of allowed distances, i.e. the laser beam and camera axis and array are required to be in the same plane. Data pairs were collected containing the pixel peak position and the distance from the camera axis. The results of one of the calibrations are shown in Table 4.2.

Distance / metres	Pixel number	Distance / metres	Pixel number
0.9	2036	1.6	771
1.0	1811	1.7	635
1.1	1601	1.8	511
1.2	1411	1.9	393
1.3	1236	2.0	279
1.4	1066	2.1	179
1.5	912	2.2	78

Table 4.2. Calibration data for Prototype I.

The same calibration data are shown in the graph Fig. 4.11.

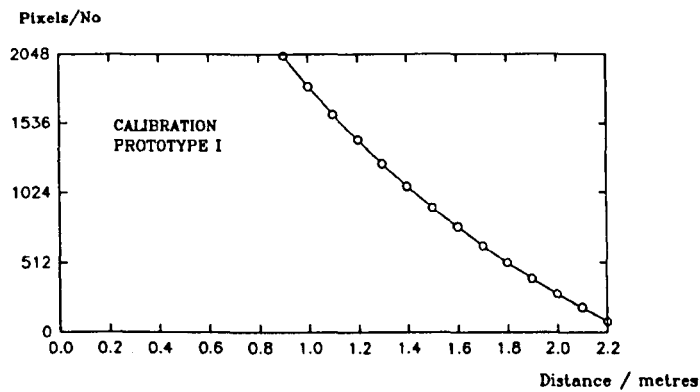


Fig. 4.11. Calibration data from first prototype.

The calibration data was manipulated by a least squares curve fitting program to determine the coefficients of the closest polynomial fit to the data. The coefficients used for one of the data sets are shown below in Table 4.3.

```

a := 0.860;
b := 4.219E-4;
c := 9.356E-8;
d := -7.407E-13;
e := 9.047E-15;
f := 0.0;

```

Table 4.3. Curve fitting coefficients.

The polynomial used to interpolate was of the form $f(x) = a + bx + cx^2 + \dots$, the constants were determined by the curve fitting program and the 'x' value is the position of the image on the sensor.

The calibration data shown in the previous three figures and data for new configurations of the system was used in testing the prototype. Software was written to record the image position, rotate the measuring system by a small increment and repeat the process until the desired number of measurements were taken. Other tests were carried out with the optical bench to check the sensitivity of measurement and accuracy.

The prototype was mounted on a trolley and a series of measurements were taken of a section of a corridor with an arched roof. To present the data, conversion to Cartesian coordinates was required, thus the starting angle of the first measurement was required to convert from the polar coordinate system. Initially it was very difficult to take enough measurements without the system going out of alignment. Fig. 4.12, shows the effect of missing rotation steps and positions where the system went out of alignment.

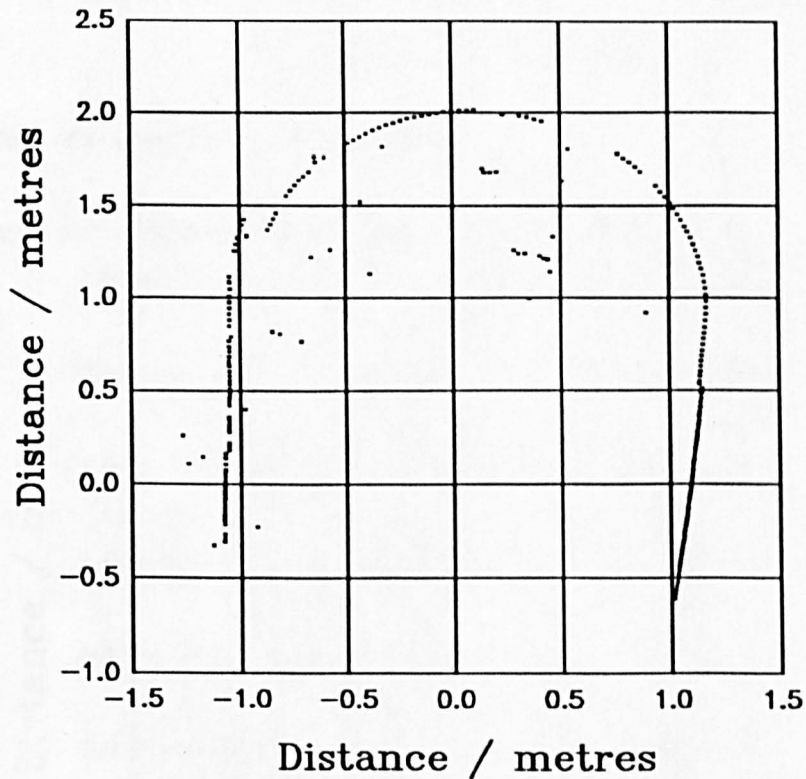


Fig. 4.12. Effect of missing rotation steps.

The profile shown in Fig. 4.13, illustrates the effect of a systematic error, a slight error in the amount of the rotation, which produced a distorted profile.

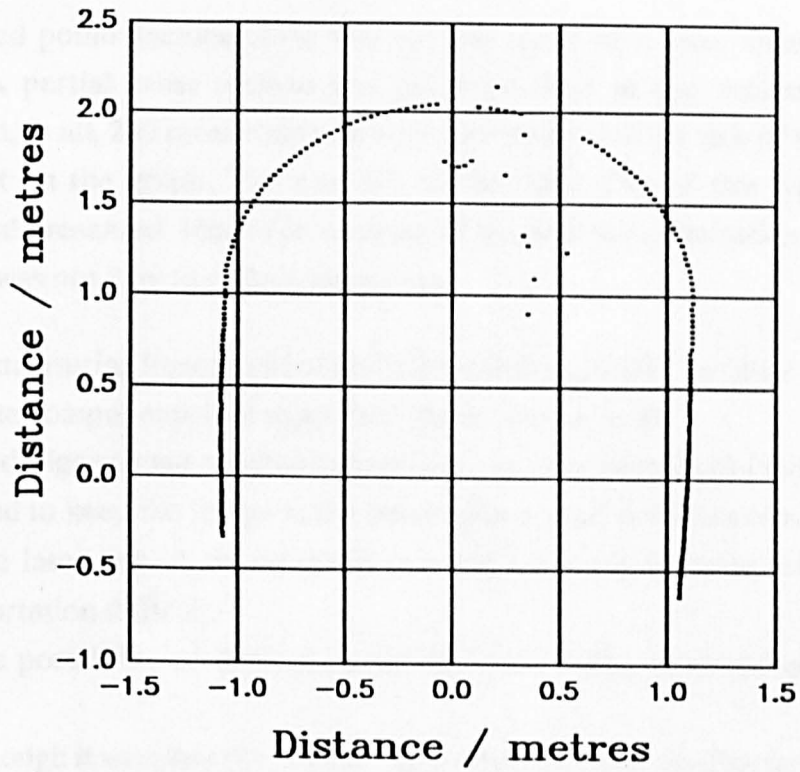


Fig. 4.13. Effect of systematic rotation error.

The best results collected with this prototype are shown in Fig. 4.14.

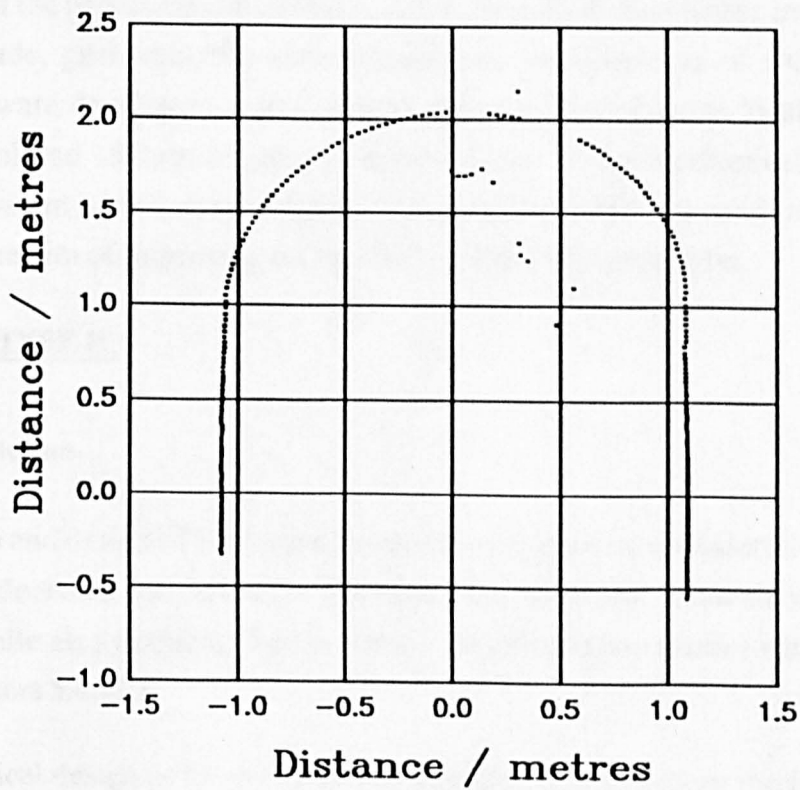


Fig. 4.14. Partial cross section of corridor in 'A' building, City University.

The measured points include some that are the result of a false measurement or occlusion. A partial cross section was taken because of the limitations of the configuration, in all, 230 measurements were attempted and the axis of the system is the 0,0 point on the graph. The exercise showed that data of this type could be collected, and presented. However, because of the following limitations of the first prototype it was not easy to collect more data:

- (i) the measuring head could not rotate fully through 360° because of occlusion from the components that supported the measuring arm,
- (ii) the design was not mechanically robust, constant tweaking of the camera was required to keep the image in the sensor plane at all positions of rotation,
- (iii) the laser was of considerable size and mass which made setting up and transportation difficult,
- (iv) the portability of the equipment was poor being mounted on an optical bench,
- (v) although it was possible to make some changes to the configuration, because of the fragility of the state of alignment, it was not a practical possibility, and
- (vi) the data rate was limited by the hardware.

The testing of the prototype was useful in that it: identified areas where improvements could be made, gave valuable understanding of the operation of CCD cameras, enabled software development to deal with the problems of image location, stepper motor control and calibration, and gave experience of the mechanical design of a measuring system of this configuration. A decision to build a second prototype was made with the aim of improving on the design of the first prototype.

4.5. PROTOTYPE II.

4.5.1 Introduction.

The research and design of Prototype I ensured that practical considerations were not ignored. A decision was taken to continue the practical research with another prototype while also pursuing the theoretical and simulation studies which are dealt with in chapters 5 and 6.

The mechanical design of Prototype II was intended to improve on the limitations of Prototype I, this demanded:

- (i) 360° rotation of the measuring arm,
- (ii) robust mechanical design,
- (iii) solid state laser,
- (iv) portability, and
- (v) ease of adjustment.

The design of Prototype II is shown in Fig. 4.15, the aim of the design was to keep the idea of a flexible configuration in the two most important areas of base length and camera angle. The object of the mechanical design was to make the setting up much easier and the fixing of components more reliable.

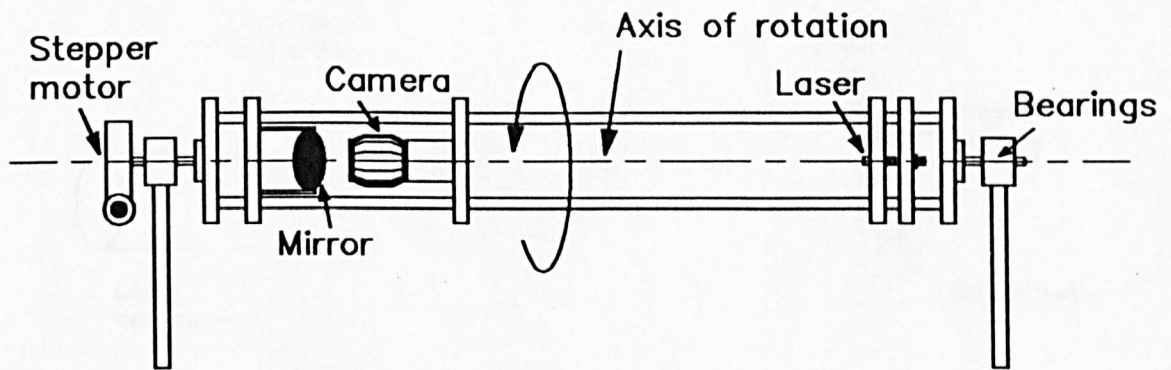


Fig. 4.15. The configuration of Prototype II.

The features of the design were:

(i) The laser beam alignment.

The light source, a SHARP LT030 series, 750nm wavelength, 3mW diode laser (Sharp) was chosen as it offered:

- (a) the advantages of sufficient power output for the CCD sensor without being too dangerous to the eye,
- (b) compact design,
- (c) DC operation at low power,
- (d) stable output of power and frequency,
- (e) low divergence with an appropriate collimator, and
- (f) low pointing angle variation.

A DO Industries 1-9118 collimator, provided the following beam conditioning with the Sharp diode laser:

- (a) beam size = $4.9 \times 2.2\text{mm}$,
- (b) beam divergence = 1.2 mrad, and
- (c) pointing stability = 0.1 mrad.

The collimator was mounted with its optical axis on the mechanical axis of the profiler and the beam from the laser was set up for parallel propagation. The cross section of the laser beam is approximately rectangular, so rotation about the axis of the profiler allowed any desired orientation of this beam to be maintained relative to the plane of the sensor. Further adjustment of the direction of propagation was controlled by a three axis mount with a right angle prism, see Fig. 4.16.

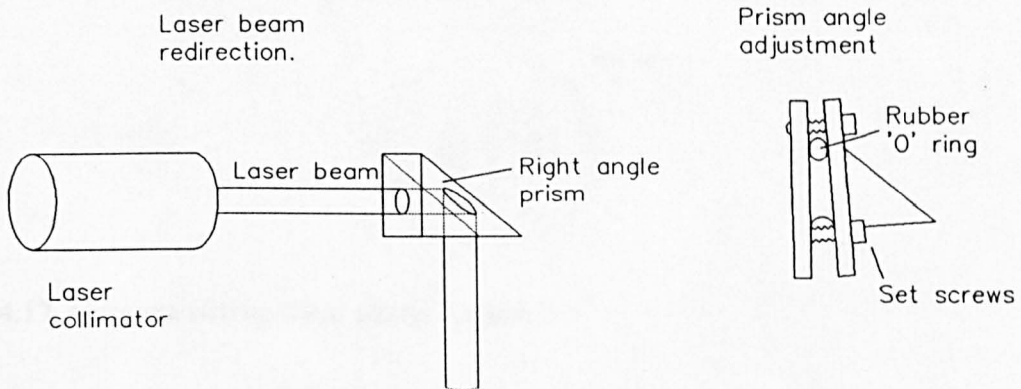


Fig. 4.16. Laser diode collimation and orientation.

The prism allows the redirection of the laser beam with minimal loss of optical power because the angle of incidence to the plane of the prism faces is approximately 90° and total internal reflection takes place at the 45° face. Hence, the direction and orientation of the laser beam could be fixed perpendicular to the axis of rotation, in the plane of the line scan camera optical axis, and parallel to the linear array.

(ii) The camera alignment.

The camera housing was mounted on the axis of rotation but allowed to rotate about the measurement axis to give adjustment to the correct orientation with respect to the laser and the two rods that held the components in a stable configuration. To achieve this, a mount was devised to allow rotation and fixing in this position. Additionally, the design of a tilted image plane was incorporated to improve the focus over the range of measurement. This tilting plane was engineered so that the axis of the tilt was as near as possible to the centre of the CCD Chip and that the axis of rotation was on the same level as the chip active area, see Fig. 4.17.

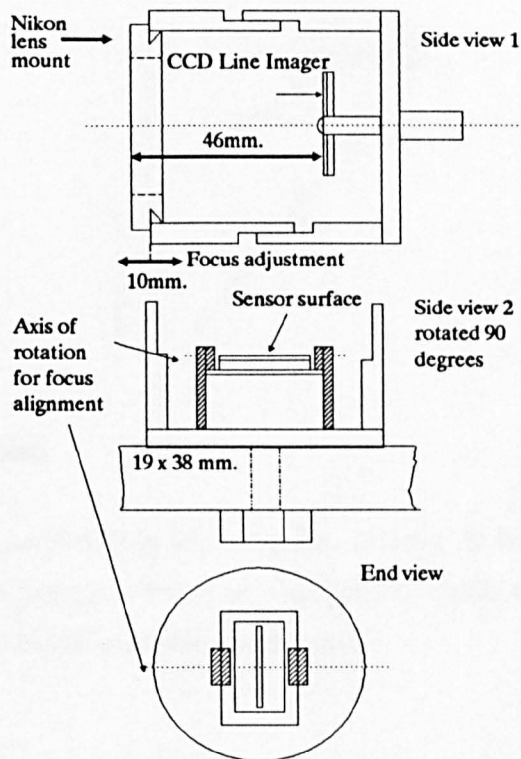


Fig. 4.17. Camera tilting focal plane design.

The lens mounting was achieved by a purpose made ring that could be retained in the camera body and which allowed the fitting of Nikon lenses.

(iii) Chip mount

To mount the chip within the camera meant that a 100mm. gap would have to be accepted between sensor chip and the drive circuitry. CCD sensors require good drive timing and clock signals. The output of the sensor is also susceptible to increased noise if removed from the PCB. Advice was sought from the manufacturers on this point who stated that 100mm was not likely to be a major problem.

(iv) Mirror mount.

Normally the camera would be physically pointed at the subject of interest, however, a decision was taken not to do this in favour of a more stable, adjustable design which allowed the mounting of the camera along the axis of the measuring system with a mirror to redirect the field of view of the camera. A mirror mounting was devised which would allowed the necessary adjustments in angle and orientation, see Fig. 4.18.

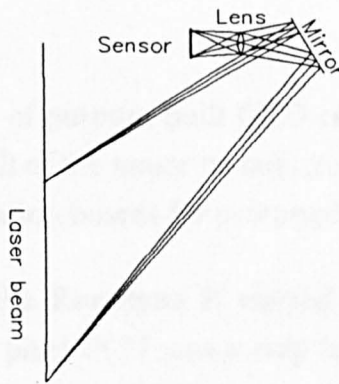


Fig. 4.18. Mirror mount.

This scheme worked successfully allowing the camera to be firmly fixed in position and giving a compact design. However, the optical losses and added complexity of using the mirror were significant disadvantages.

(v) Stepper drive

The stepper motor drive for the whole apparatus was initially the same as for Prototype I. The mechanical connection was made outside the main frame through the bearings. The wires from the laser and CCD camera were passed to the same end as the stepper motor and mounted close to the axis to minimise the torque demanded on the drive. Consequently only a single rotation was considered advisable.

(vi) Apparatus trolley.

The whole apparatus was then mounted on a trolley which enabled a complete 360° sweep with only a small 25mm connecting tube between the two ends which would be visible in any cross section. This tube could be positioned close to the floor so that only a small portion of a cross section would be lost.

4.5.3. Electronic design.

4.5.3.1. Introduction.

The new prototype required the design of a number of new circuits to control the laser power input, the stepper motor and the CCD data. The design of the electronics for the data acquisition from the CCD sensor was a major part of this work.

4.5.3.2. CCD sensor.

The limitations and expense of purpose built CCD cameras meant that alternative systems were investigated. All of the major manufacturers of CCD line scan sensors recognise the need for evaluation boards for prototyping.

The electronic design for the Prototype II started with the investigation of an evaluation board and a 2048 pixel CCD sensor chip from Texas Instruments, model numbers PC401 and TC103 respectively. The evaluation board only required a power supply to give all of the timing and clock signals necessary to operate the chip. The circuits necessary for making use of the outputs from the evaluation board are described in detail in application notes (Texas.1, 1986, Texas.2, 1986). In operation the evaluation board allows inspection of the output of the sensor on an oscilloscope, corresponding to the intensity of incident light onto the sensor, and a number of additional signals that allow the designer to use this output. The TC103 linear array sensor has the following characteristics:

- (a) high dynamic range,
- (b) 2048 sensor elements,
- (c) $12.6\mu\text{m} \times 12.6\mu\text{m}$ sensor elements,
- (d) $3.5 \text{ V}/\mu\text{J}/\text{cm}^2$ sensitivity,
- (e) 10 MHz data rate, and
- (f) peak spectral sensitivity @ wavelength 700nm.

The PC401 evaluation board has the following characteristics:

- (a) data rates from 0.2-2 MHz,
- (b) exposure times from 2-16ms,
- (c) adjustable clock voltages, and
- (e) dimensions of 110mm square.

The reason for using the CCD in the system is to provide an accurate method of locating the image of the reflected laser spot on the sensor and consequently to provide distance measurement via the calibration. The task is to locate this image with respect to the pixel locations given the index numbers of 1-2048. This method is valid because of the high dimensional stability and tolerances of CCD sensors.

The location of the pixel that has the highest intensity peak was considered the most sensible method of image location as, in tests, the image of the laser is the most dominant feature that the camera sees. This objective could be achieved in electronic hardware to have the advantage of high speed of operation at the expense of flexibility of image processing. Provided that the laser image is the brightest object in the field of view and reasonable focus has been achieved then peak detection gives pixel accuracy, which was considered to be reasonable if real time operation was to be achieved.

4.5.3.3. Signal conditioning.

(i) CCD output signal.

The analogue voltage signal from the CCD chip must be conditioned before the A-D converter is used because: the signal is inverted, it does not occupy the right voltage range, and there is noise present in the form of dark signal which it is possible to remove.

The block diagram for the circuit which does the signal conditioning is shown in Fig. 4.19. The circuit on the left hand side of the CCD chip shows all the functions necessary to operate the CCD chip which is provided by the Texas evaluation board. The circuits on the right hand side of the CCD chip shows the signal conditioning necessary to provide digital information that can subsequently be processed by the peak detection circuit.

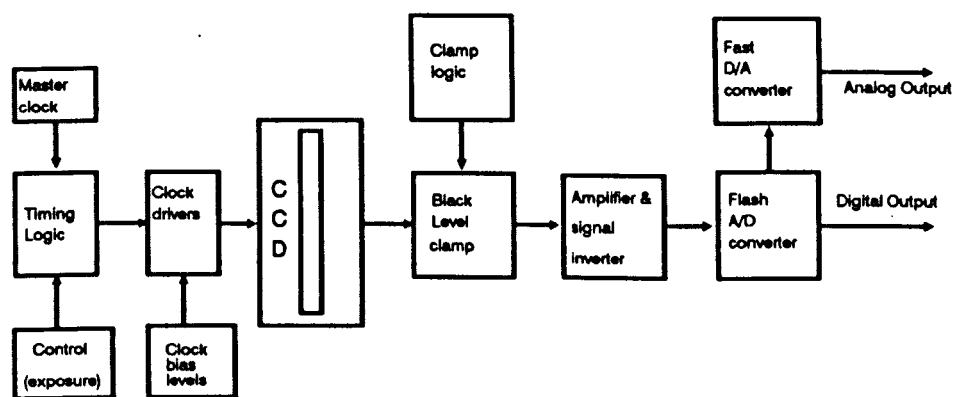


Fig. 4.19. Block diagram of evaluation board and signal processing.

The need for signal conditioning is because the unprocessed output from the CCD is a voltage pulse train in which the negative (lower) envelope represents analogue video and the positive (upper) envelope is the result of the reset clock. The upper envelope

is generally uniform and is representative of the zero or dark signal. The entire voltage pulse train is displaced from zero volts by the positive quiescent-output operating voltage of the charge detection amplifier. This means that the output level is above 5.0 Volts and less than V_{DD} the imager output amplifier supply voltage, approximately 16 Volts, see Fig. 4.20.

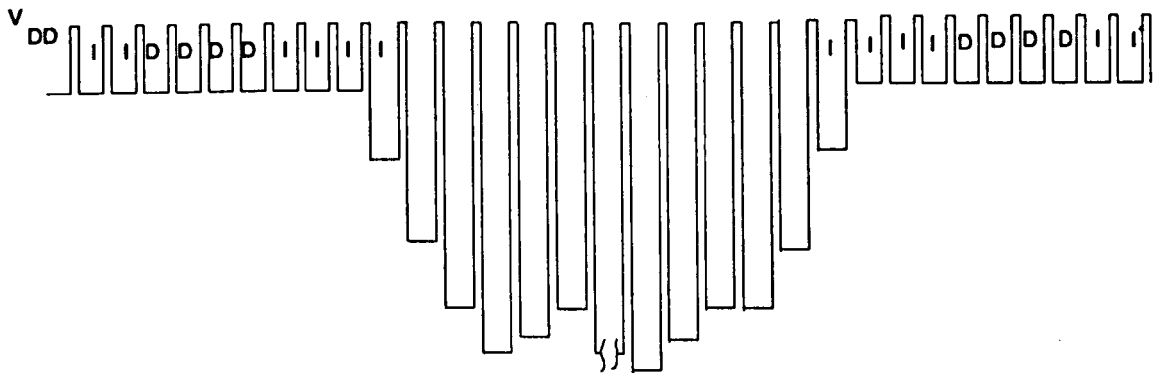


Fig. 4.20. Data output from CCD camera.

The input required by most A-D converters is a positive voltage. To limit the noise it is desirable that the black level output is less than 0.1 Volts, or less than the smallest voltage to record a '1' in the digital world. It follows that there are three requirements in the signal processing: (i) the analogue signal is inverted giving positive output, (ii) a stable reference voltage is established, and (iii) the output range suits the A-D converter.

(ii) Black Level Clamp.

The black level clamp is required because the signal DC operating voltage is variable, affected by both temperature and drain voltage variations. It follows that the signal must be capacitively coupled along the signal path which provides an opportunity to clamp the charge or voltage drop across a capacitor. This is done at a position in the CCD output signal referred to as the 'black reference pixels'. These pixels occupy four pixels which occur before and after the main signal envelope, see Fig. 4.21.

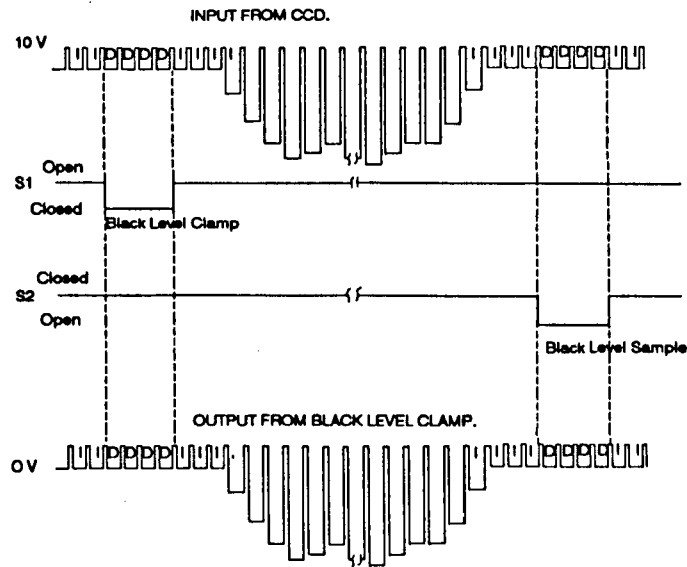


Fig. 4.21. Timing diagram for clamp and sample timing.

A simplified diagram of the black level clamp is shown in Fig. 4.22. The operation of this circuit is simple in that S2 opens whenever the dark reference pixels appears following the data stream, and a sample (black level sample) is taken. This is compared with an adjustable black level set voltage by the comparator. The comparator generates an error pulse output to the amplitude detector which corrects the voltage stored on capacitor C2 so that, when the voltage on C2 is applied via S1 to the capacitor C1, the output of the amplifier will be the desired value when no light is present i.e. Zero.

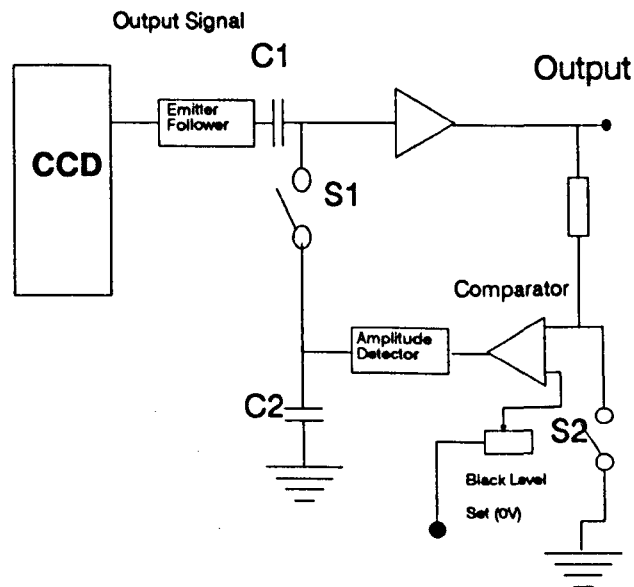


Fig. 4.22. Block diagram of black level clamp.

The block diagram given in the previous figure does not give all the details necessary to construct such a circuit. Fig. 4.23, shows the black level clamp built which was built.

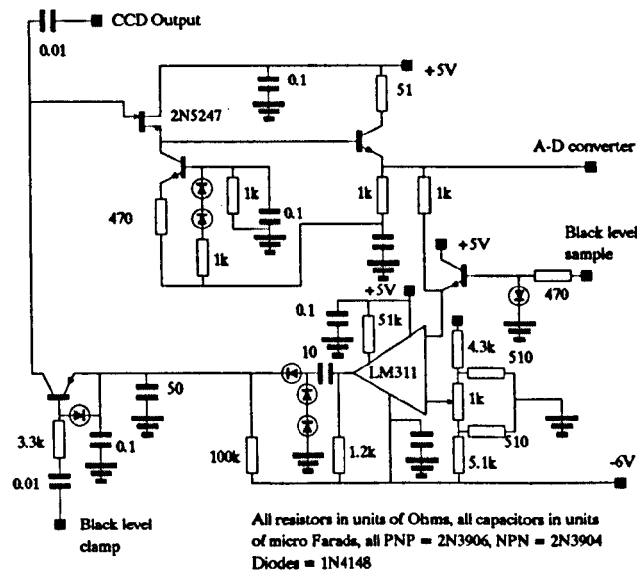


Fig. 4.23. Automatic black level control circuit (Texas.1, 1988).

The operation of this circuit is as follows:

The high input impedance buffer amplifier is a FET source follower with a constant current source load followed by a standard emitter follower. The FET operates at 6.3mA and the emitter follower at 6.0mA, giving a 0.95 gain and an output impedance of less than 25 Ohms.

The amplitude or peak detector gives a maximum of -2.5 Volts and occurs when there is no positive error signal from the LM311 comparator. The maximum negative output voltage of the positive peak detector is then produced by the forward biasing of three diodes. For the automatic black level circuit to function, the -1.9 volts input bias to the buffer FET of the amplifier must produce voltage equal to, or more negative, than that of the black level voltage desired at the output i.e. Zero. This input voltage is necessary so that, when the black level sample is taken, the comparator will produce a small positive voltage pulse output to be detected. This positive voltage will then be subtracted from the negative output of the detector to bring the input bias of the buffer amplifier to the correct level so that the output is the desired black level when the clamp switch is closed.

(iii) Black level clamp timing.

The black level clamp and the black level sample could be timed to occur at the same period in the data cycle, however, the black level clamp disturbs the signal causing errors to the black level sample, therefore the clamping and sampling take place at different times.

The timing of the clamp and sample can be timed by reference to the clock signal, the start of the readout cycle and use of TTL logic circuits. The logic is provided by three 74193 counters with 7404 inverters and two 7430, eight bit NAND gates. Correct timing is achieved by using programming the logic to initiate a clamp or a sample at specific numbers of clock cycles from the start of scan.

The position for sample, or clamp, is taken from the outputs of the down counters. The minimum down count is set by the minimum number of data reset clocks to be read to coincide with the four white reference output pixels. This count is $19 + N + 14$ (where N is the number of pixels in the CCD array). Assuming that $N = 2048$ there is 2081 down counts. However, the counter counts Transport Clock cycles (TCK) which are half the data frequency and so the nearest minimum whole number of TCK counts is 1041. This value is then programmed into the down counters as the number to count down from. The least significant bit of the counter is not used, therefore the next bit switches off and on at half the rate giving two pulses when the condition for a pulse output is met, and consequently creating the required pulse width of four.

The clamp timing is required to be initiated twelve counts from the beginning, the count position is $1041 - 12/2 = 1035$ and 1034 so 1034 is used. This can be achieved with the 8 input NAND gate and a 74103-bit NAND gate. The binary number required to be placed on the counters is 010 1000 0001. The sample timing is required to be initiated in a similar way to the clamp timing, 8 counts from the end of the down count, the logic required to input to the NAND gates is 000 0000 0100, see Fig. 4.24.

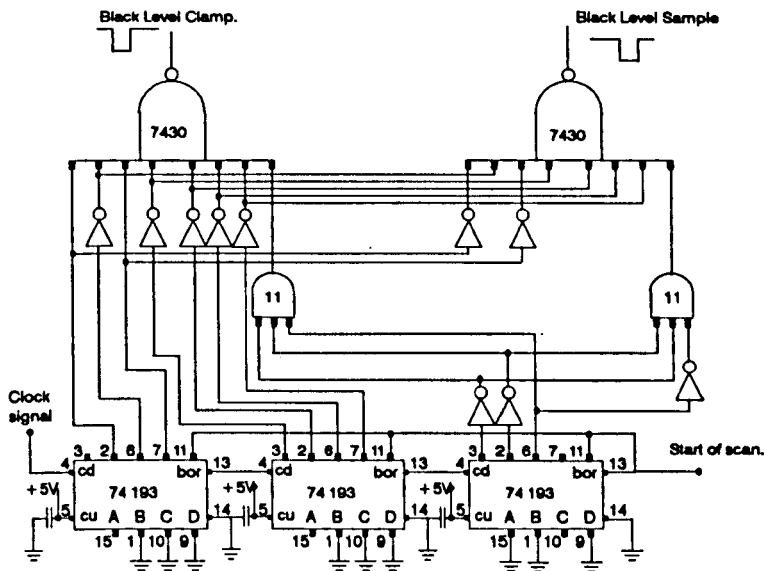


Fig. 4.24. Logic circuit for black level clamp.

(iv) Signal Inversion.

The output from the previous circuit is a negative voltage train that is which is at ground level if no light is incident on the sensor. Signal inversion is required for the A-D converter and can be achieved by using a fast operational amplifier (Chapman, 1982). The circuit for this is shown in Fig. 4.25.

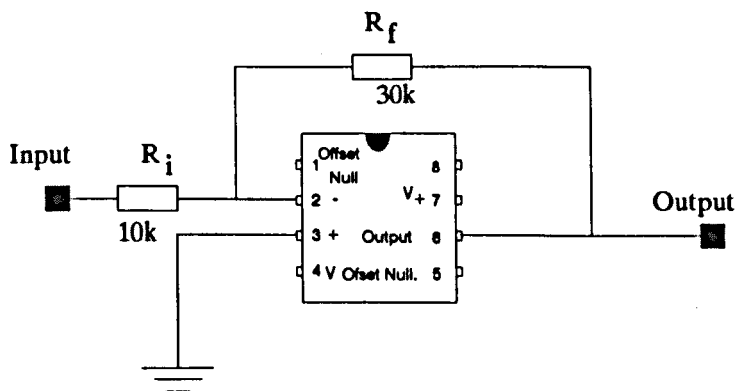


Fig. 4.25. Signal inversion circuit.

The signal, having been conditioned, is ready for digitisation so that the peak detection can take place. The block diagram which shows the relationship of the previous described circuits to the aim of a digital output of the laser image position is shown in Fig. 4.26.

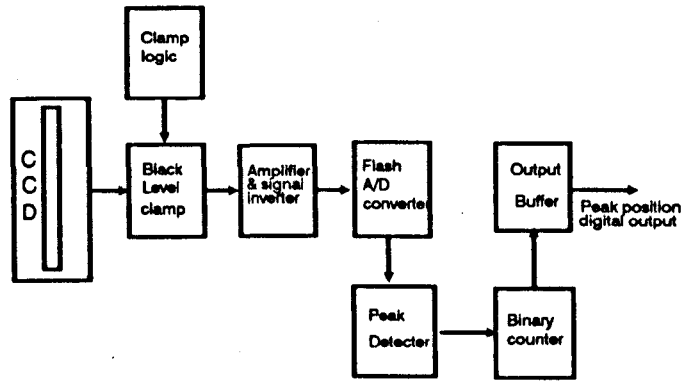


Fig. 4.26. Block diagram of peak detection circuitry.

(v) A-D Conversion.

The voltage level of the output from the amplifier can be adjusted, it is a positive voltage train representing the incident light intensity levels on the surface of the sensor. For the digital manipulation of this data, the voltage level that corresponds with each pixel must be digitised.

The A-D converter chosen was a 6 bit ‘flash’ A-D converter, R.S. 632-225 I.C. No. 3300. Six bits were sufficient for the peak detection and the converter also had the advantage of being cheaper than eight bit converters. The converter is able to operate at 15Mhz, in several different modes. The mode most suitable is the pulse mode because of the low power consumption and fast conversion speed, see Fig. 4.27.

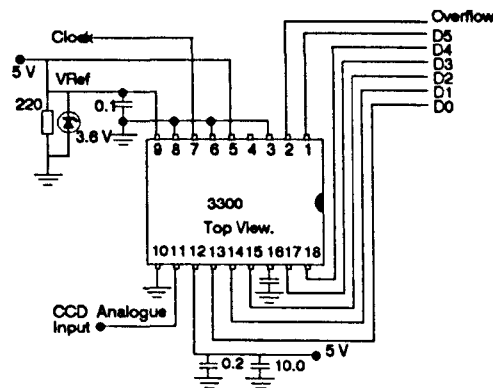


Fig. 4.27. A-D conversion circuit.

The converter requires a stable reference voltage which must be over 2.5 Volts and less than V_{dd} , the voltage supply to the converter, which is 5 Volts. The reference voltage defines the largest voltage that will be converted so must be the maximum output of the previous circuit. A value that can be achieved from standard components is 3.6 Volts with a Zener diode. These diodes have the characteristic of allowing a set

voltage drop for a large range of current over 5 mA. Therefore, the five volts supply is used to give enough current through a suitable resistor to enable the reference voltage to be used by the A-D converter. The clock determines the time at which the conversion of the data takes place and also when the data is latched onto the output of the converter, see Fig. 4.28.

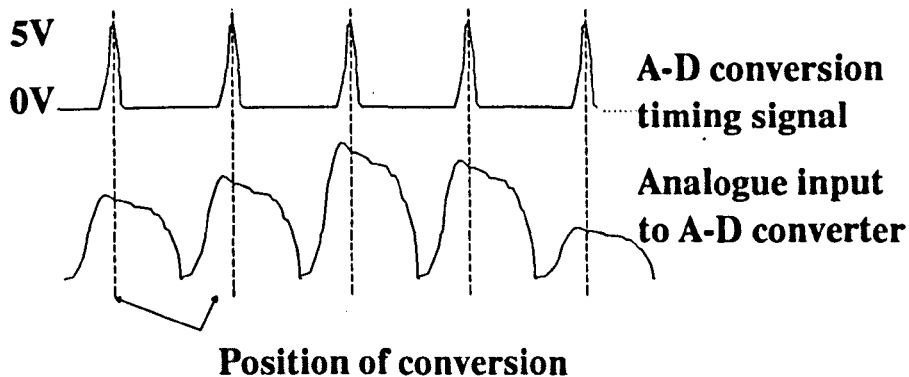


Fig. 4.28. Timing diagram for appropriate conversion timing.

It is important that the clock signal coincides with the time that the output of the Op-Amp is relatively stable. When clock signals are used for timing purposes the transition point between '0' and '1' or '1' and '0' is often used and is referred to as 'edge triggering'. This implies that the edge must coincide with the point at which it is required. This is not always possible and an alternative approach is used which takes the clock signal and delays it until the appropriate moment occurs, a 74121 monostable could be used for this purpose which produces a pulse of approximately 50ns after a programmable delay time. However, there is another signal, the reset clock (RCK), on the Prototype board that can be used directly and has the necessary timing. The signal must be taken from the output of a 3 input nand gate rather than a test point to get TTL levels. The signal has to also be inverted before use.

The A-D converter is able with the appropriate timing to coincide a flash conversion of the analogue voltage to a digital number at each clock pulse.

(vi) D-A conversion.

The A-D converter converts the signal but operation cannot easily be checked so a D-A converter is often used which reproduces the output of the converter in analogue form allowing visual inspection with an oscilloscope. The provision also gives a means of checking on the operation of the CCD sensor. The D-A converter is wired directly to the output of the A-D converter therefore giving the output data as seen by the

Peak detector. The D-A converter chosen is an 8 bit fast converter RS 632-203 IC 7518, see Fig. 4.29.

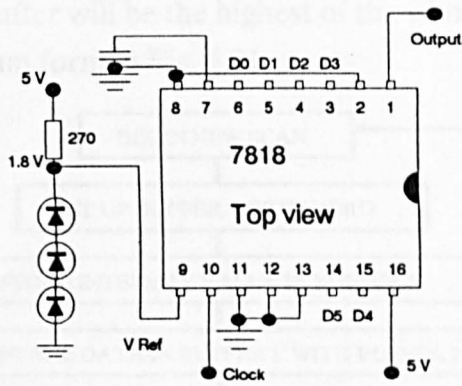


Fig. 4.29. D-A conversion circuit.

(vii) Peak detection.

The digital data output from the A-D converter will ideally be a series of zeros followed by a set of data that correspond to the image of the laser illuminated spot. Fig. 4.30. shows such an image.

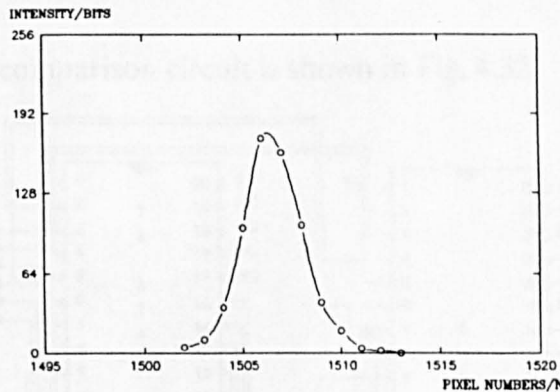


Fig. 4.30. Image of illuminated spot imaged on a CCD sensor.

The objective is to locate the pixel number that corresponds to the highest intensity value in the image, the highest digital number in the data. The peak detection can be achieved with an 8 bit comparator 74686N which is able to differentiate between two 8 bit numbers and signal the highest of the two which can be stored in a 74374 buffer.

The sequence of events for peak detection is to initially load the comparison buffer with zero, achieved by allowing the buffer to be loaded with the A-D converter output of the pixels that are shielded from the light. This number is then compared with the output of the A-D converter. The indication from the comparator that this number,

is higher than the stored number, results in the numbers being swapped, and the process repeated. Hence, when all of the numbers have been processed from one scan, the number left in the buffer will be the highest of the whole group. This sequence is illustrated in flow diagram form in Fig. 4.31.

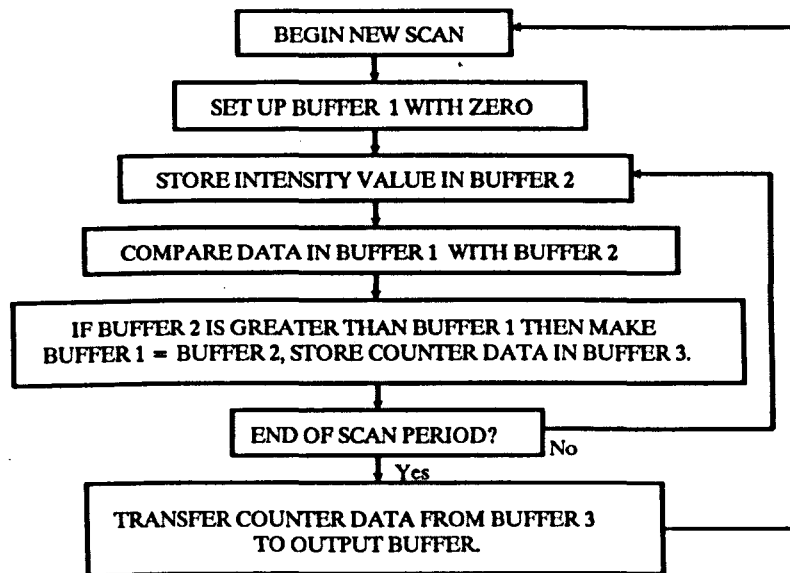


Fig. 4.31. Flow diagram for peak detection.

The diagram for the comparison circuit is shown in Fig. 4.32.

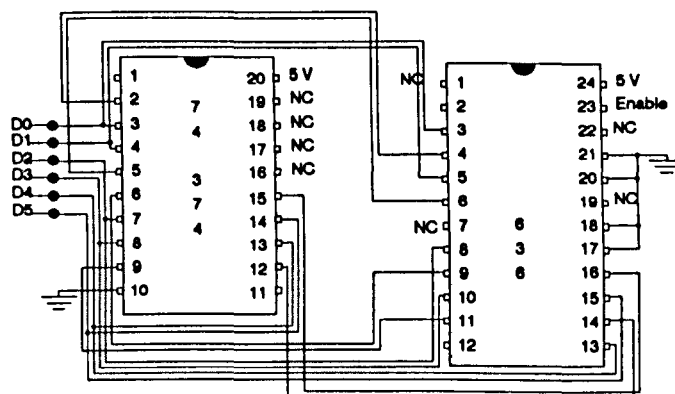


Fig. 4.32. Comparison circuit.

To locate the image position with respect to the pixel position the counter data for the timing of the black level clamp is used. Every time the comparator indicates a higher number, the number on the counter is placed into two 74374 buffers. At the end of the scan, this number will have stored the counter state (peak position) at the highest data value. The buffer containing the peak position is then placed into further 74374 buffers to be read by the parallel interface. Hence, the peak position is updated every scan and can be sampled at any rate provided that a value is not read twice.

The true pixel position will be offset by 19 pixels, as this is the set up period during each scan. Furthermore, the number that the counters start counting down from is 1041, or, if the lower bit of the counter is used, 2082. However, for the purposes of calibration this is not a problem as the offset is constant. The logic to control the output of the data on the 374's is given by the inverse of the black level sample.

(viii) Conclusion.

The circuits described worked satisfactorily, providing a stream of relevant data at 800 Hz, which equates to the rate of measurement. The problems of asynchronous data transfer between the prototype and the computer parallel interface were not significant as the parallel interface would have difficulty in reading the data quickly enough to repeat a reading of the buffer, and it was unlikely that the motor would have moved the apparatus to the next position.

A fundamental problem with the peak detection system is caused by CCD sensor saturation by the intensity of the reflected laser image from cooperative surfaces. This has the effect of offsetting the peak position. Further problems could be experienced if other sources of light were brighter than the laser spot in the field of view. The accuracy of the location of the image could be seen as another disadvantage as there is no flexibility in the design for improvement.

The speed of operation, although much faster than it is possible to use, was limited by the use of the Texas evaluation boards, which had a maximum data clock rate of 2MHz while the CCD sensor was able to be clocked at 10MHz.

4.5.3.4. Laser diode circuit.

The diode laser used, a Sharp LT030MD, at a wavelength of 750nm was the brightest available being just on the edge of the human spectral response. The diode was of relatively low power, because tests showed this output was more than sufficient to get a good signal to noise ratio. A further advantage was that although not considered eye safe for intraocular viewing, the reflected light from most surfaces would not be higher than the safe limit for the human eye to view (Sliney, 1989). The maximum power output of the laser was 5mW, but 4mW would be a practical maximum to preserve the lifetime of the laser. This equates to a beam of power of a little less than 3mW because of the optical losses in the collimator.

A circuit is necessary to control the power to the laser as the response time of the laser is so fast that even a small surge current is enough to optically destroy the laser. Such transient phenomena are likely to occur during powering up or down, while adjusting the power output level, or from surge currents which arise from outside of the control circuit from external sources. This destruction, or degradation of performance happens because too much optical power is allowed within the comparatively small chip. This quickly build up in the form of heat and the faces quickly degrade causing partial or total destruction of the chip. Even an open or short circuit, while the power is being supplied to the chip, can cause deterioration.

To achieve reliability a battery source was chosen as this would circumvent any mains borne spikes or voltage surges and eliminate any problems that occur when potentials develop between different circuits.

The diode laser is contained in a small metal can with three leads, one of which is earthed. The Laser requires a very precise current (50 - 100 ma) at about two Volts to start laseing, see Fig. 4.33.

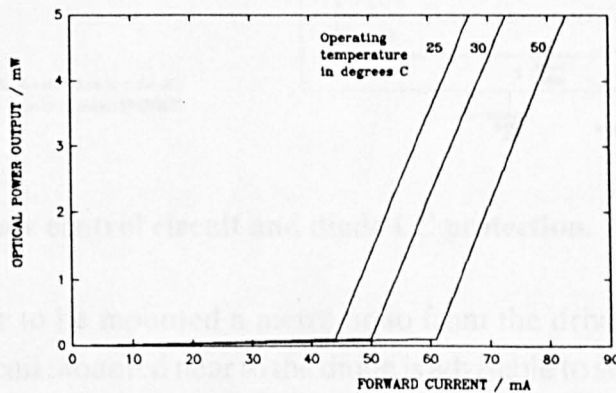


Fig. 4.33. Optical power output vs. forward current.

As soon as the chip starts laseing the chip will heat up as the process is not 100% efficient, and the current demand characteristic will change. This can lead to over powering the laser and failure. To stop this the manufacturers build into the chip a photodiode that monitors the current from the redundant chip face as light is produced equally from both faces. This monitor diode allows for a feedback circuit to adjust the current to a predetermined light power output.

A circuit manufactured by Sharp, the IR3C01, was available to control the current by the feedback from the monitor diode. A Printed Circuit Board (PCB) was built to supply the necessary voltage to the chip with a slow start up to avoid the introduction

of noise. The slow start up was achieved by a capacitor/resistor circuit with a long time constant. High frequency spike protection was provided with two additional lower value capacitors. It was not possible to obtain the desired -12 Volts and +5 Volts directly from batteries so three PP9 8.4 Volt NiCad rechargeable batteries were used providing -16.8 and +8.4 Volts. The regulation of the voltage to the desired level was achieved with two voltage regulators. A good quality wire-wound potentiometer was used to adjust the power output. The circuit is shown in Fig. 4.34.

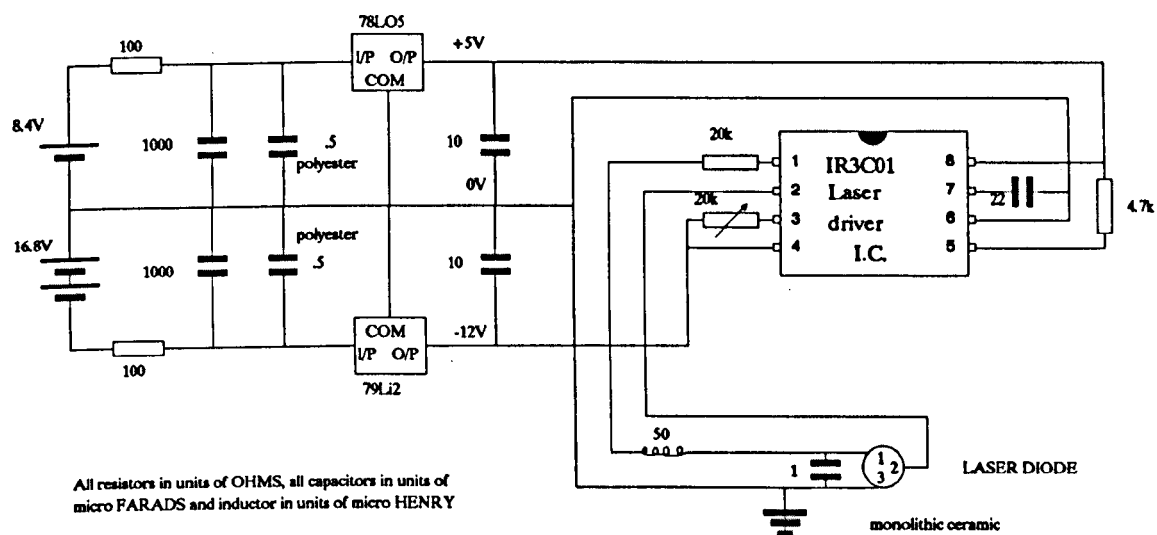


Fig. 4.34. Laser diode control circuit and diode LC protection.

To enable the laser to be mounted a metre or so from the drive circuit, a Inductor, Capacitor (LC) circuit mounted near to the diode is advisable to stop any noise picking up on the wires themselves.

To set up a diode laser system, the potentiometer is set to the minimum output position and the output from the laser monitored by a laser power output meter until it is at the desired working level. An important point that must be noted is that when a collimating lens is used the power output must be reduced by the amount of inefficiency of the lens system, sometimes as much as 40%.

The 750nm diode laser was set up in the manner described and mounted in a collimator to provide a small parallel beam of light. The reason for using a collimator is because the laser diode light output is diverging at angles of 30° in one plane and 11° in the other. A collimator is designed to take parallel light rays and focus them to a point, or the reverse, which is the case here. The use of the correct collimator is

critical in providing the desired beam characteristics, many collimators are also optimised for wavelength. The diode laser and collimator were set up by minimising the beam spread at a distance of 3-5 metres.

The 750nm laser and laser driver circuit were constructed and successfully used for over two years without failure showing that this circuit design achieved its objective of providing a reliable light source. A disadvantage of the 750nm laser was the lack of visibility in bright light which is: important to confirm laser operation, in setting up procedures, and in locating the position where the measurement takes place. A further disadvantage was the higher power requirement of the regulator circuits compared with the power requirement to drive the laser and the necessity for three batteries.

4.5.4. Software design.

4.5.4.1. Introduction.

The software developed for this prototype was different to that developed for the Prototype I, the image processing was eliminated by the electronic hardware but more emphasis became necessary on the speed of dealing with the data and presentation problems.

The simplified data acquisition requirements of this prototype were found to be very beneficial to the speed of data capture as the reading of the peak position via the parallel interface was a very quick operation. The only data required to be stored at the time of measurement was two bytes. In the case where the constant angle increment of angular rotation of the measuring arm and the starting angle is known, there is no requirement to store any more data as the angle is implicit in the sequence of the data index.

After data acquisition there must be manipulation of the data to regularise it for later use or presentation on the screen, or plotter. The procedure is to form the peak position from the two bytes from the prototype, and use an interpolation with the calibrations data to convert the image location data to a distance measurement. Finally, the angular data can be added and conversion from the Polar coordinates system to the Cartesian coordinate system, if required.

4.5.4.2. Manipulation of raw prototype data.

The data conversion procedure was programmed in the following lines of Pascal.

```
temp1 := port[io_base4];
{ collect high byte from parallel interface }
temp2 := port[io_base3];
{ collect low byte from parallel interface }
temp1 := ((temp1 and 15) shl 8);
{ only use four low order bits, shift the binary data 8
bits to the left }
Num2arr[index1,index2] := temp1 + temp2;
Num2arr[index1,index2] := angle;
```

4.5.4.3. Conversion of image data into distance data.

Further manipulation is required to convert the image data to distance data which is achieved by reference to the calibration data.

The calibration data is a collection of pairs of measured distances and image positions, typically 20-30 pairs. The total number of image positions is approximately equal to the number of pixel, 2048, so a method of interpolation is required. In the previous prototype a graph package was used to compute the coefficients of a polynomial that is the least squares best fit of a line through all of the points. A Pascal library routine (Boorland, 1988) was acquired to replace this package, and used to compute the coefficients of a polynomial from a stored calibration file and, hence, allow interpolation at points in between the calibration points.

4.5.4.4. Conversion of data into Cartesian coordinates.

To display the data on a computer screen, or plot it on a plotter, conversion of the polar coordinate data to Cartesian coordinates is required. This is achieved by use of the conversion equations: $y = \text{distance} * \text{Sin}(\text{angle})$, $x = \text{distance} * \text{Cos}(\text{angle})$.

The conversion procedure highlighted a problem of delay. If the processing took place before displaying on screen then a relatively long wait was required, or if the processing was completed at the time of display then that process took longer than seemed reasonable. The reason for this delay was the relative slowness of the Cosine and Sine routines, these are optimised for speed, but as the number of coordinates required was 4,800, the cumulated time was significant.

A solution to this problem was the establishment of Sine and Cosine tables which were held in the computers memory and could be looked up quickly. This was possible because the angles required were known and the tables computed in advance. The result was a significant improvement in the time take to compute the coordinates.

4.5.4.5. Display of data.

Following data collection and conversion the data was displayed on the screen to verify correct operation. The data had to be appropriately scaled for the screen or plotter and, if desired, the display enhanced by other techniques to show the data in perspective or hidden line views.

4.5.4.6. Validity of data.

The measuring system had no knowledge on the validity of the data collected, the laser could have been turned off during operation or obscured. Hence, the intensity peak position would correspond to the position of the highest noise or extraneous light source of higher intensity than the laser peak. A visual inspection of the measured cross section displayed on screen would be sufficient to confirm correct operation.

4.5.4.7. Programming considerations.

When the overheads of the program size, and complexity, were too great for the computer system, two approaches were adopted: first, the look up tables were assigned to RAM where they could be disposed of when not required (this approach saved the allocation of a fixed size of array), and second, the program was broken up into smaller parts which were only used when required.

During the development of software a number of hierarchical menu system were used which offered the operator a wide variety of choices concerning the analysis of the data or the presentation of the results. Some of the menu systems adopted were operated from the keyboard and others were mouse operated.

4.5.4.8. Conclusions.

A Prototype was developed which required little computing power to collect measurement data which produced significant advantages in the ease and speed of operation. The success of this aspect highlighted the need for further advances in the

software for handling and displaying the data. These advances were made by improving the methods by which computations were made and improving the user interface.

4.5.5. Results.

4.5.5.1. Cross section data collection

The prototype data collection was completely controlled from the computer for a complete or partial cross section gathering operation, provided that correct setting up took place, i.e. ensuring a sensible starting position. Following data collection the apparatus would generally be returned through the opposite rotation so that the wires would not get tangled.

The results of the use of Prototype II are shown in the following figures which demonstrate that a variety of shapes could be successfully measured and their 3-D topography mapped. The data rate was equal to the line scan rate of 800Hz. However, the rate at which the data could be read from the system, and the measurement arm moved to a new position, was always less than this.

Fig 4.37, shows a single cross section of a corridor.



Fig. 4.37. Single cross section of a corridor.

Artifacts that can be identified in the cross section are the piping and conduits, the skirting board, the walls, ceiling and floor. The cross section has been taken from the data used for drawing this cross section on the screen, consequently the data has been

quantised for screen display. A number of successive cross sections were measured with a displacement of 50mm between profiles, see Fig. 4.38.

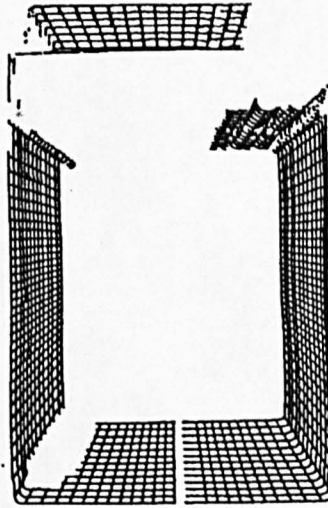


Fig. 4.38. Multiple cross sections of a corridor.

Fig. 4.39. shows a cross section of a laboratory.

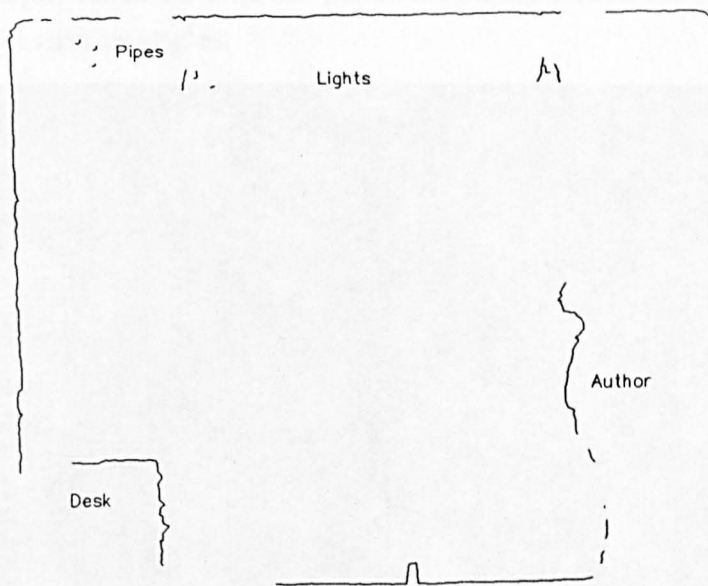


Fig. 4.39. Cross section of a laboratory.

A model boat hull used in early wind tunnel testing for the America's Cup yacht race was measured, the hull had dimensions of approximately 1.3metres x 300mm x 300mm. The hull was measured every 20mm over half of the surface and these results used to produce the complete hull because of the symmetry. The screen display is shown in Fig. 4.40.

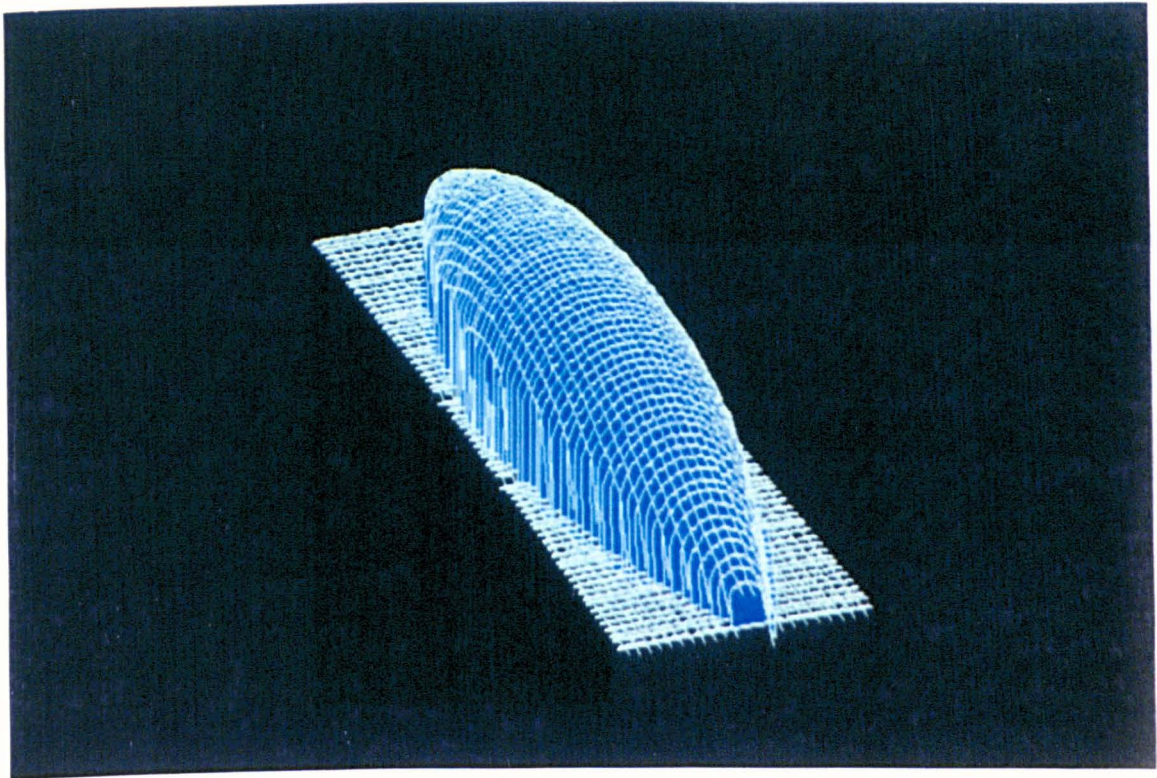


Fig. 4.40. Profile of a model boat hull.

By altering the way in which the data was produced on the screen the boat is perceived to be viewed from various angles.

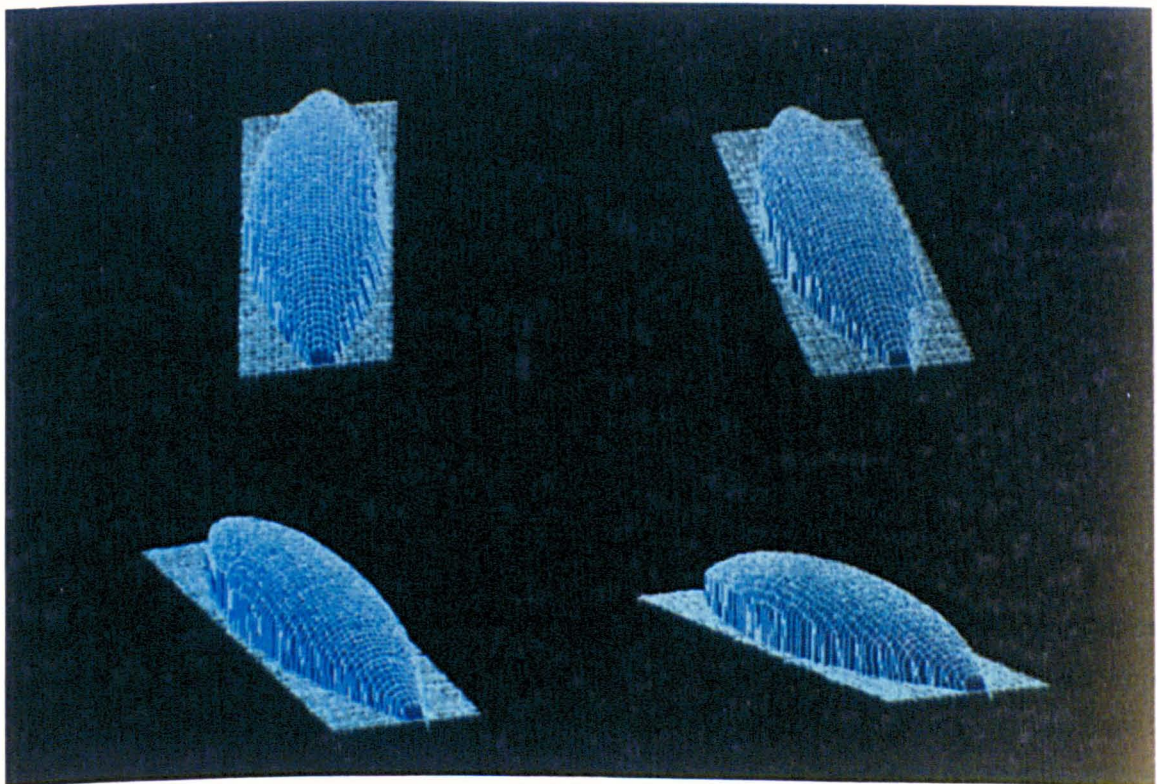


Fig. 4.41. Multiple views of the boat hull.

4.5.5.2. Mechanical reliability.

The mechanical design of prototype II was much improved on Prototype I, the evidence for this is shown in the number of successful cross sections acquired. The system, once set up, would continue to operate successfully for long periods of time even if transported over rough surfaces. Calibration was only required if the system was altered, or knocked out of alignment. The speed of measurement was very impressive, being limited only by the speed at which the data could be read, and the stepper motor moved to a new location. The limitations were that:

- (i) The system was supported at both ends making it unsuitable for profiling of some surfaces,
- (ii) as a result of the supported ends, the complete system was longer, and heavier, than necessary, and it did not look like a piece of surveying equipment,
- (iii) the electronic hardware, while operating very quickly, gave no opportunity to change the design,
- (iv) the rotation of the complete system was not ideal having a large moment of inertia, and
- (v) the mirror, while being the most compact and adjustable system, added to the number of items that could be misaligned.

4.5.5.3. Conclusions.

The development of this prototype gave experience of the speed of operation that could be expected, the type of data that would be collected and the problems of presentation and manipulation. However, the system did not look like a surveying tool and as such was unsatisfactory. A further prototype was therefore designed to tackle the problems of designing a system for general surveying.

4.6. PROTOTYPE III.

4.6.1. Introduction.

The lessons learnt from the construction, testing and software development of prototypes I & II were used in the design of Prototype III. Additional features were considered to be important in this model but the primary goal was to produce a surveying instrument for measuring cross sections i.e. mounted on a surveying tripod, easy to set up, portable, and battery powered. The design would have to be made

within the budget requirements which meant that compromises were made because of the equipment available. For instance, the camera was of fixed design and so no adjustment of the focal plane would be possible, however development in the hardware over this period meant that an 'off the shelf' camera interface could be purchased which would allow greater flexibility in the software design.

4.6.2. Mechanical design.

The specification for Prototype III differed from that of the two earlier models. Prototype I provided a proof of principle, Prototype II provided reliability, speed and accuracy. The objective of Prototype III, was to get as close as possible to a pre-production state. This prototype was considered to be the last that it would be possible to produce within the research period.

The design of Prototype III had to allow the system to be used in a site for demonstration purposes. It was recognised that such a system would not operate as quickly as the previous design, correct the linearity, or allow proper focus over the range. However, other areas would be explored, and a clear indication gained of the type of design required, while still allowing some basic research to be conducted using this model.

The main problem to be addressed in the design was, given the laser camera configuration, what is the most convenient layout. It was decided that for reasons of compactness, reliability and low moment of inertia, the axis of rotation chosen for the previous prototypes was to be preferred over an alternative described in the Patent application GB 2173301A (Gallacher, 1986) shown in Fig. 4.41.

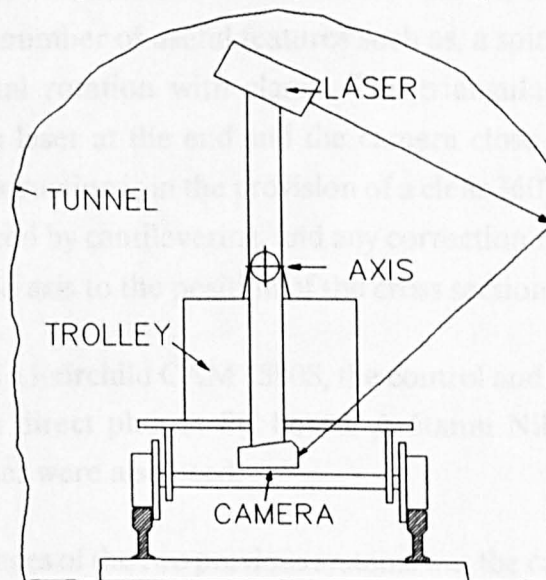


Fig. 4.41. Alternative configuration for cross section measurement.

The advantage of this configuration is that camera occlusion can only take place in the plane of the cross section, whereas the configuration employed in Prototypes I & II, the camera is occluded by objects in the field of view which are outside this plane.

Having decided on the axis of rotation, the mechanics of the configuration had to be decided. Both of the previous systems were supported at both ends which gave problems of a large overall size and occlusion by the support frame. A more convenient design is produced with a cantilevered measuring arm. One variant of this design puts the angle measurer and laser on opposite sides of the tripod e.g. the PROTA tunnel profiling system by ROST, 1989, which has the disadvantage of occlusion from the tripod legs. After looking at this, and other configurations, it was decided to cantilever both the camera and the laser, leaving the camera close to the tripod, and the laser extended on a light, rigid, thin bar. This configuration is shown in Fig. 4.42.

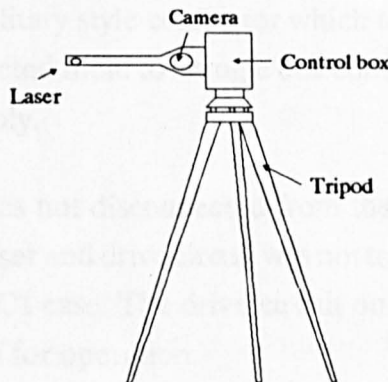


Fig. 4.42. Cantilever configuration adopted.

A Wild TC1 body was available and chosen as the base for the design, being tripod mounted, and with a number of useful features such as, a spirit bubble for levelling, and a 360° horizontal rotation with clamp. The triangulation system itself was cantilevered with the laser at the end and the camera close to the TC1 body. The advantage of this construction is in the provision of a clear 360° sweep, at the expense of the errors introduced by cantilevering, and any correction needed for the distance from the survey tripod axis to the position of the cross section measurement.

The camera used was a Fairchild CAM 1500S, the control and data storage board was made by Sentel as a direct plug in PC board. A 50mm Nikon lens and a 750nm wavelength diode laser were also used.

One of the disadvantages of the two previous systems was the cabling which was always heavy and inconvenient. The Wild TC1 body did have a clear tube which connected

between bearings, so this tube was used for the cabling, although this meant that the bearings were used without modification. This was not ideal, as they were not designed, indeed the TC1 body was not designed, for the pressure of the cantilever. A two part design was envisaged in which the measuring arm part could be disengaged from the rest for transportation, an advantage of this concept is that additional measuring arms could be constructed for use over different ranges and accuracies.

The cables were reduced to the minimum size and weight and threaded through the tube and fixed at the other end with enough slack to allow at least one rotation and probably three. One advantage of the length between the measuring arm and this connection was that the whole length of the tube would allow twisting to take place. The cables were routed through the case to a panel connecting all of the functions to the computer, power supply, stepper motor drive, etc. Initially these connections were made by individual connectors, depending on the function, but were later made more robust by using a single military style connector which took all of the required wires into the profiler and connected them to a single box containing the computer, control electronics and power supply.

To ensure that the laser was not disconnected from the laser driver circuit and that the distance between the laser and drive circuit was not too great, the laser drive circuit was mounted inside the TC1 case. The drive circuit only required the supply of the voltages from the batteries for operation.

The camera was mounted in a solid piece of Aluminium that had cable holes drilled into it for the camera and laser. The camera was a tight fit and held in place by a three grub screws. The angle calculated for the system was approximately 19° to the perpendicular to the axis. Being at a fixed angle guaranteed that this component would remain in its fixed position, yet allow setting up by rotation about its optical axis.

The laser fixing presented difficulty in the design of a satisfactory system of adjustment, as apart from the single adjustment of the camera axis rotation, all the other adjustments must be made with the laser. This required movement about two axes: rotation about the measuring axis and adjustment to perpendicularity with this axis to enable a laser beam to describe a plane when rotated.

The complete prototype design ensured good control over all of the important features of the triangulation system and added features necessary for good survey control of the cross section measuring and location process.

4.6.3. Electronic design.

Prototype III required less electronic design compared with the previous prototypes because components were available that interfaced directly with the IBM PC. The method of prototyping with IBM PCs, compared to dedicated microprocessors, was considered to be of value because of the flexibility that it allowed to reprogram.

The requirement for the camera interface was met by a frame grabber board made by Sentel of West Germany with a piggy back interface that could be purchased to interface directly with a number of Fairchild camera systems. The camera had a number of features that allowed it to be separated from the control system by up to a metre and a half. This meant that the computer system could be mounted in a separate box at some distance from the measurement system. While this means that the bulky computer and ancillary parts are required within a metre or so of the measuring system, there is the advantage that the measuring process is unimpeded by the bulk of the computer. Hence, the main part of the electronic design was in the construction and testing of: the computer system, display, and associated parts for portability.

To ensure that the prototype could be taken to a range of sites, including sewers and rail tunnels, special consideration was given to the computer that would be used to control the equipment. This meant that a mains powered system would be unsuitable because of the difficulty and safety aspects of having 240 Volts AC power in remote locations.

4.6.3.1. Computer.

A survey of portable computers was conducted. The specification was a battery powered IBM PC compatible machine with at least two expansion slots. These computers were found to fall into a number of categories:

- (i) battery powered, very light weight, non-standard operating system, no room for expansion (e.g. Husky Hunter),
- (ii) battery powered, standard operating system, medium weight, small amount of expansion (e.g. Toshiba T1100),
- (iii) mains powered, standard operating system, medium to heavy weight, 1 - 2 expansion slots (e.g. Toshiba T3100), and
- (iv) mains powered, lunch box style, standard operating system, several expansion slots, heavy weight (e.g. NEC Powermate portable).

None of these met the specification so another approach was considered which was made possible by the appearance on the market of the first 'Passive backplane computers'. This system uses the standard expansion I/O slots found on the standard IBM AT or XT and instead designing the computer on the backplane with the I/O slots, the computer is constructed on a full size I/O card which is plugged into the passive backplane, allowing expansion cards to operate as normal. This particular design has a number of advantages:

- (i) a purpose built system could be made,
- (ii) with CMOS technology the computer power requirement was low (only 2.6 Amps at 5 Volts),
- (iii) the computer had the functions built in that would have required three expansion cards, and
- (iv) two or more cases could be built specifically for laboratory or field work, with the only additional expense being that of another passive backplane.

A 80286 based system was purchased from Diverse Technology, and a case built to contain the passive backplane as no enclosures were available at the time because the technology was only just finding acceptance. At the present time there is full support for these systems with enclosures, many alternative suppliers of the technology, and cheaper costs. A mainstream supplier of computers has designed a conventional computer around these parts and industrial users are making widespread use of these, because of the ease with which a computer system can be repaired with just the insertion of another card. A laboratory mains powered version was the first objective to test the technology and then a battery powered version was planned for field work.

Because the computer had all of the features required for operation as a complete computer: hard disk controller, two floppy drives, two hard disk drives, two serial ports, one parallel port, one keyboard port and colour EGA or monochrome EGA display, a four slot passive backplane was purchased. This allowed one slot for the computer, one for the camera board, one for the parallel interface and one spare. This would then occupy the minimum space. The laboratory version was built and tested using a 180 Watt power supply, floppy disk drive and keyboard.

The testing and evaluation of the computer showed that this system was suitable for building into a special purpose computer, as it allowed a large variety of configurations. An important feature was that the computer could be programmed to ignore certain faults such as a missing keyboard. However, the use of this technology

left the research programme very exposed in the case of a breakdown of the passive backplane computer card, this unfortunately happened twice, leaving long periods where this system could not be used. To ensure reliability and continuity, another approach was taken towards the end of the research period which was to use standard computer components. The developments in the size, speed and power requirements of the motherboards used in conventional computers meant that at the end of the research period it was possible to replace the passive backplane computer with a high speed (12MHz) XT motherboard which had similar low power requirements and low cost. The supporting parts, being XT technology, now several years old, were also cheap. The overall price differential was approximately 6:1 in favour of the XT version because of the move away from leading edge technology. The complete system was not much slower than the passive backplane approach, but much cheaper for replacement parts, and easier to repair.

Two computer systems were used which were successful in collecting data from the prototype system and met the requirement for low voltage, portable equipment.

4.6.3.2. Display.

To meet the requirement for a portable system, the type of display had to be considered as most computer monitors are mains powered and are not suitable for hazardous environments. The requirement for the monitor was: no high voltages, solid state electronics, 640x350 pixel resolution for adequate display of a cross section, and low power consumption.

The monitor used in the vast majority of computer systems is the Cathode Ray Tube (CRT), flat screen technology being relatively new because of problems in design and fabrication. Three types of flat screen display have emerged as contenders for replacement of the CRT, the main application which has driven this research is in portable computer displays. These are: the Liquid Crystal Display (LCD), the Electro Luminescent Display (ELD), and the Plasma display.

(i) **CRT.** This display has dominated the market in the last twenty years being both cheap (a monochrome monitor can be purchased for £80 or less) and capable of displaying colour to a high degree of resolution and clarity. However, the operation of the CRT requires high voltages for the emission and control of an electron beam with sufficient energy to cause fluorescence at the phosphor screen target. A further disadvantage is that the a vacuum tube is fragile.

(ii) **LCD.** The advantages of the LCD are low power consumption, e.g. 0.392 Watts for the 600x400 pixel Seiko Model G644F, adequate resolution, relative cheapness. The disadvantages are: the necessity for back lighting which generally requires a high voltage supply, poor contrast, restricted viewing angle, slow screen update causing blurring with a mouse pointer or scrolling, and no interface available for direct connection to a computer.

(iii) **Plasma.** Plasma displays which have only recently been introduced into small portable computer systems, and are also popular in military applications because they have an active display. They have the disadvantage of requiring high voltages for display, low contrast ratios and have a high power requirement. Resolution is similar to that of the LCD. No Plasma display system was available at the time the survey was carried out.

(iv) **ELD.** Electro luminescent displays have very high edge definition compared to CRT and Plasma displays, and are similarly active. However, apart from the most recent developments, they are monochrome and often only have three levels of grey. The advantages are the high viewing angle of 140° , low screen flicker and reliability. The operation of the EL display is achieved by applying an electric field to a luminescent film. This film is often ZnSb which emits light at a broad band yellow colour centred on 580nm. A direct plug in system was available.

Having looked into the availability and technical merit of these displays, the two main contenders were the LCD and the EL displays because both were commercially available and could be operated with relatively low voltages and current, with high resolution. The choice of display was in favour of the EL display because it was possible to build an EGA display with a DC power supply without the requirement for a separate driving card.

A Finlux MD650.350 display that could be powered from 12 Volts was purchased, and an enclosure altered to allow the display to be protected and stand at a number of angles. The system was tested and adjusted for use. A photograph of the display is shown in Fig. 4.43.

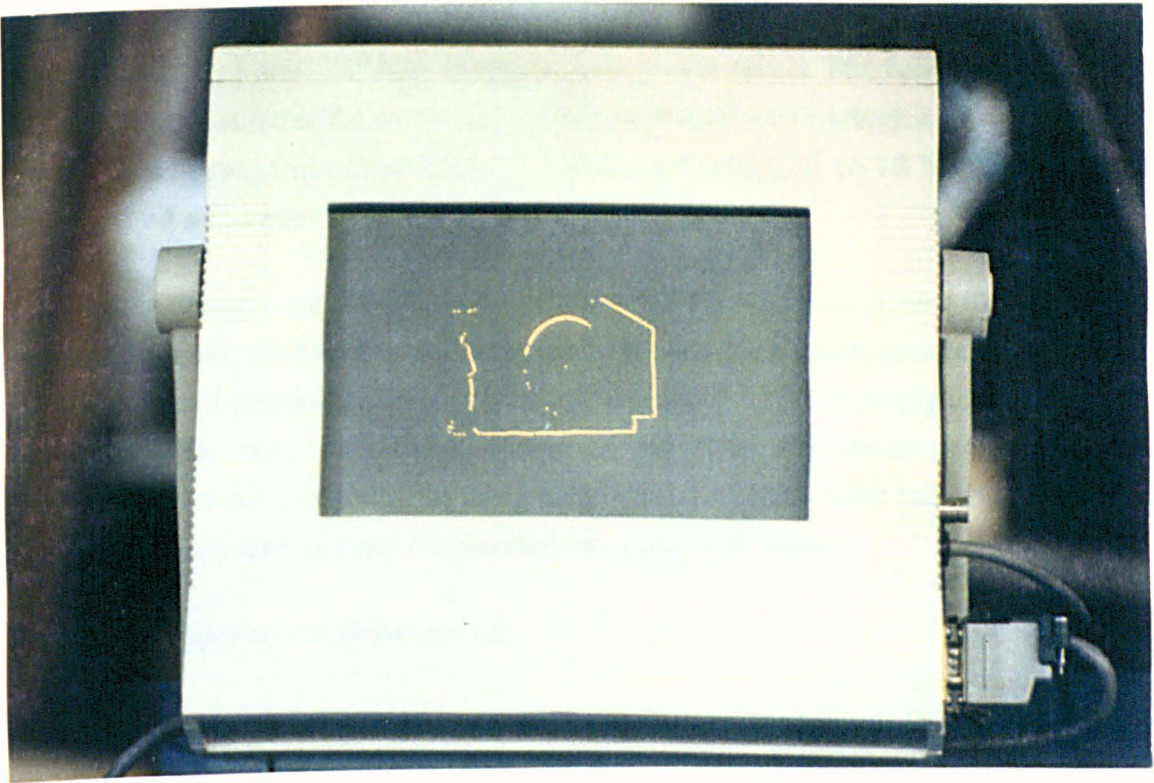


Fig. 4.43. Finlux EL display.

4.6.3.3. Power supply.

Initially the passive backplane computer was mains powered, this required a power supply to give regulated voltages of 12, 5, -5, and -12 Volts. A supply was ordered and wired up to supply these with a filter to suppress mains voltage spikes.

After the development and testing of the computer in a mains powered version it was required to make the system portable. A 'gel' type 12 Volt battery, made by Exide, was purchased to avoid the problem of accidental acid spillage. A 12 Volt battery was considered to have the maximum size and Voltage allowed in a sewer environment. Several precautions were taken to ensure safety.

- (i) The battery was encased in a box.
- (ii) The supply from the battery passed through a thermal overload cutout to protect in case of a short circuit in the cable.
- (iii) The thermal overload allowed isolation of the battery by a switch.
- (iv) The cable connectors were of military specification, polarised and retained with twist fit retaining collars.

A 60 Watt DC-DC converter, manufactured for Amplicon, was purchased to provide a regulated 12, 5 and -12 Volts at appropriate power levels. The requirement for a 12 Volt DC output from the converter is because a lead acid battery is unregulated and typically will range in output from 13.5 Volts fully charged, to 10 Volts when nearly discharged and under load.

A further demand on the power supply was the provision of power for the stepper motor drive circuit. The demand from the board was for a supply greater than 15 Volts, the method of providing this supply was to use the +12 Volt supply from the battery and the -12V from the DC-DC converter. However, this made problems for the control of the stepper motor as the ground of the circuit would then be at -12 Volts compared to the logic from the parallel interface of 0 Volts.

4.6.3.4. Stepper motor drive circuit.

The stepper motor drive board, required a semi-regulated supply in the voltage range 15-30 Volts. As discussed in the previous section, the supply that was available was 24 Volts, semi-regulated, but this led to a problem in the controlling of the stepper motor board as the ground for the stepper motor logic was at -12 Volts with respect to the parallel interface. The solution to this problem was to use opto-isolators between the parallel interface and the stepper motor system, this allowed the logic levels to float with respect to the ground of the driver board, see Fig. 4.44.

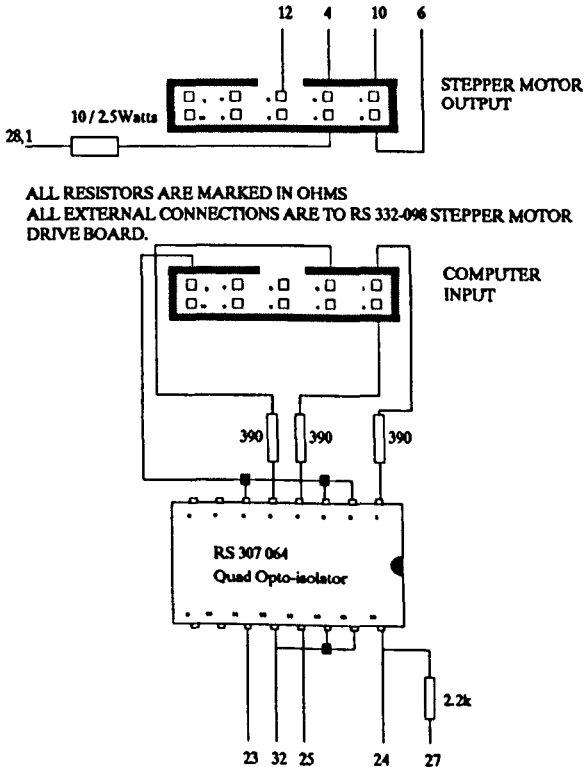


Fig. 4.44. Opto-isolator circuit for stepper motor.

The control of the stepper motor is by three means: (i) step pulse, the frequency at which this pulse is provided determines the speed of rotation of the stepper motor, (ii) forward / reverse logic levels, and (iii) full step / half step logic levels.

To provide the correct current to the windings of the stepper motor, a resistor has to be placed in series with the windings to limit the current that is drawn by motor. This circuit was tested and was found to work satisfactorily, allowing the board to be mounted within the computer enclosure so that all of the functions necessary for operating the system were within one box.

4.6.3.5. Exposure time control.

The Sentel PC board for control of the line scan camera allowed adjustment of the exposure time by a series of switches. However, this method of control was considered unsatisfactory as the only variability in the system would be the dynamic range of the CCD device, so a means of dynamically configuring the system was considered. This involved removing the exposure control switches, including the pull up resistors and replacing the connections with a ribbon cable connected to one of the ports of the parallel interface card. This arrangement meant that it was possible to dynamically change the exposure time, allowing better subpixel accuracy, and a wider range of surface reflectivities to be measured. A problem with this approach is that the exposure time is not designed to be adjusted in this way because it could be changed during a sensing cycle. Later systems were able to offer this feature built into the board which is a better solution. The operation of the exposure time control is considered in detail in chapter 3.

4.6.3.5. Keypad interface.

Both the computers used accepted a normal keyboard which is good for development of the software used in testing, calibration and general experimentation in the lab. However, such a keyboard would be a nuisance in the field and undesirable. Therefore, a 16 key pad was purchased which interfaced to a universal keyboard encoder RS Stock No. 350-765. The use of the encode allowed the key pad to be used in place of the keyboard. In use the key options can be drawn on the screen and the program written to read the keyboard and activate the various options which may be to collect a profile, save the profile data, display a profile, etc.

An alternative to the keypad was considered which was a touch screen integrated into the display, while this arrangement would be ideal, the cost of such an arrangement

was expensive, and required an additional interface in the computer, which was not considered desirable.

4.6.4. Software design.

4.6.4.1. Introduction.

A considerable amount of software was written for use with Prototype III because of the accessibility of the data from the camera. This software served two different purposes, first the testing and analysis of the performance of the prototype through the calibration rig, and second, the collection of cross sections of structures.

4.6.4.2. Interfacing to the Sentel frame grabber board.

To collect line scan data from the Sentel board a software program was written, the resulting program, once developed, was used in all subsequent programs. The Sentel documentation (Sentel) gave all the details for interaction with the camera interface. The software was written in Pascal.

The control of the Sentel board and camera system is achieved by reading and writing to port addresses on the IBM PC, there are eleven addresses provided, starting from a selectable base address. The method of operation is identical to that used in the parallel interface, but in this case the individual bits are decoded or written to in a way specified by the designers of the board. The eleven register relative addresses and descriptions are:

- 0: timer register 0
- 1: timer register 1
- 2: timer register 2
- 3: set status timer register
- 4: voltage reference negative register
- 5: voltage reference positive register
- 6: status of camera control unit register
- 7: camera control unit mode register
- 8: camera control unit select register
- 9: camera control unit page register
- 10: colour look up table register

The registers are all 8 bits wide and each of the bits may be defined as a flag to signal a state within the board, or to provide a means of selection a particular operation. A complete understanding of the setting of the computer and camera are required to

set up and use these registers. The control and use of the registers in the context of the line scan camera is described by reference to the program written to interface system from the IBM PC. The program is not reproduced completely, only the parts that are relevant to this section are shown. Comments that are additional to the program are in bold, comments that are an integral part of the program are enclosed in { } or { * * } brackets.

```
program collect_data;
```

Define the register addresses to be used.

```
const
  timer_0           = $340;
  timer_1           = $341;
  timer_2           = $342;
  set_status_timer = $343;
  v_ref_neg         = $344;
  v_ref_pos         = $345;
  status_ccu        = $346;
  ccu_mode          = $347;
  ccu_address_select = $348;
  ccu_page          = $349;
  clut              = $34A;
```

Define the variables, buff is the array that the line scan camera data is placed into.

```
var
  buff           : array[0..$8FF] of byte;
  camera_mode    : byte;
  status         : byte;
```

This procedure sets the camera up for use with the line scan camera.

```
procedure initialise;
```

Set up the flags that are required.

```
var
  select_camera_flags : byte;
  shoot_flag          : byte;
  rs0_flag            : byte;
  rs1_flag            : byte;
  repeat_flag         : byte;
  on_off_flag         : byte;
  ram_flag            : byte;
  value               : byte;
```

```

win_seg_flag      : byte;
mem_flag         : byte;
block_flag       : byte;
arr_lin_flag     : byte;
page             : byte;

begin

(* Set up A/D converter *)

port[v_ref_neg] := 0;      (* note can define binary window
by making      *)
port[v_ref_pos] := 255;   (* the difference = 1. Neg Pos
of course      *)

(* Set up flags for camera mode *)

select_camera_flags := 0; (* bits 0,1    00 for camera 1.*)
shoot_flag := 0;         (* bit 2    0 = don't shoot, 1
= shoot      *)
rs0_flag := 0;           (* bit 3    for clut
programming  *)
rs1_flag := 1;           (* bit 4    0,1 = color vals
clut reg     *)
repeat_flag := 1;       (* bit 5    0 = repeat, 1 = no
repeat      *)
on_off_flag := 0;       (* bit 6    0 = offline, 1 =
online monitor *)
ram_flag := 0;          (* bit 7    0 = RAM enable, 1
= RAM disable *)

(* Now do it *)

camera_mode := select_camera_flags
               or select_camera_flags shl 1
               or shoot_flag shl 2
               or rs0_flag shl 3
               or rs1_flag shl 4
               or repeat_flag shl 5
               or on_off_flag shl 6
               or ram_flag shl 7;
port[ccu_mode] := camera_mode;

(* set up address select *)

win_seg_flag := 0; (* bit 4 0=$D000,1=$A000 in DOS memory *)
mem_flag := 0; (* bit 5 0 = mem enable,1 = mem disable *)

```

```

block_flag := 0;          (* bit 6      0 = 256K window, 1 =
32K window      *)
arr_lin_flag := 0;      (* bit 7      0 = line scan, 1 =
area scan      *)

```

```
(* Now do it *)
```

```

value := win_seg_flag shl 4
        or mem_flag shl 5
        or block_flag shl 6
        or arr_lin_flag shl 7;
port[ccu_address_select] := value;

```

```
(* set up memory segment to map into PC *)
```

```

page := $00;
port[ccu_page] := page;
end;

```

This procedure grabs a line of data from the camera which is placed at a memory location for subsequent analysis by the software program.

```

procedure grab_line;
var
    shoot_flag      : byte;
    ram_flag        : byte;
    action_flag     : byte;
    temp            : byte;
    loop            : integer;
begin
    shoot_flag := 1;
    ram_flag := 1;
    action_flag := 1;
    temp := camera_mode or shoot_flag shl 2 or ram_flag shl 7;
    port[ccu_mode] := temp;

    (* wait for the correct time *)

    repeat
        until port[status_ccu] shr 3 and action_flag = 1;

    (* initiate the data transfer into the computers memory *)

    port[ccu_mode] := camera_mode;
end;

```

End of program.

The data can be read into an array 'buff' by reading from the correct memory location in the following way:

```
for loop := 0 to 2047 do
  buff[loop] := mem[$D000:loop];
```

This program reads the successive bytes stored in memory locations from \$D000 into the array 'buff', from where the data can then be manipulated by the computer.

4.6.4.2. Display of camera data.

The preceding section described the acquisition of the camera data, once this had happened verification of correct operation was required. This was achieved in by displaying the complete intensity profile graphically on the screen of the computer monitor and then allowing the position where the laser image was situated to be zoomed in for closer inspection. The complete intensity display is shown in Fig. 4.45.

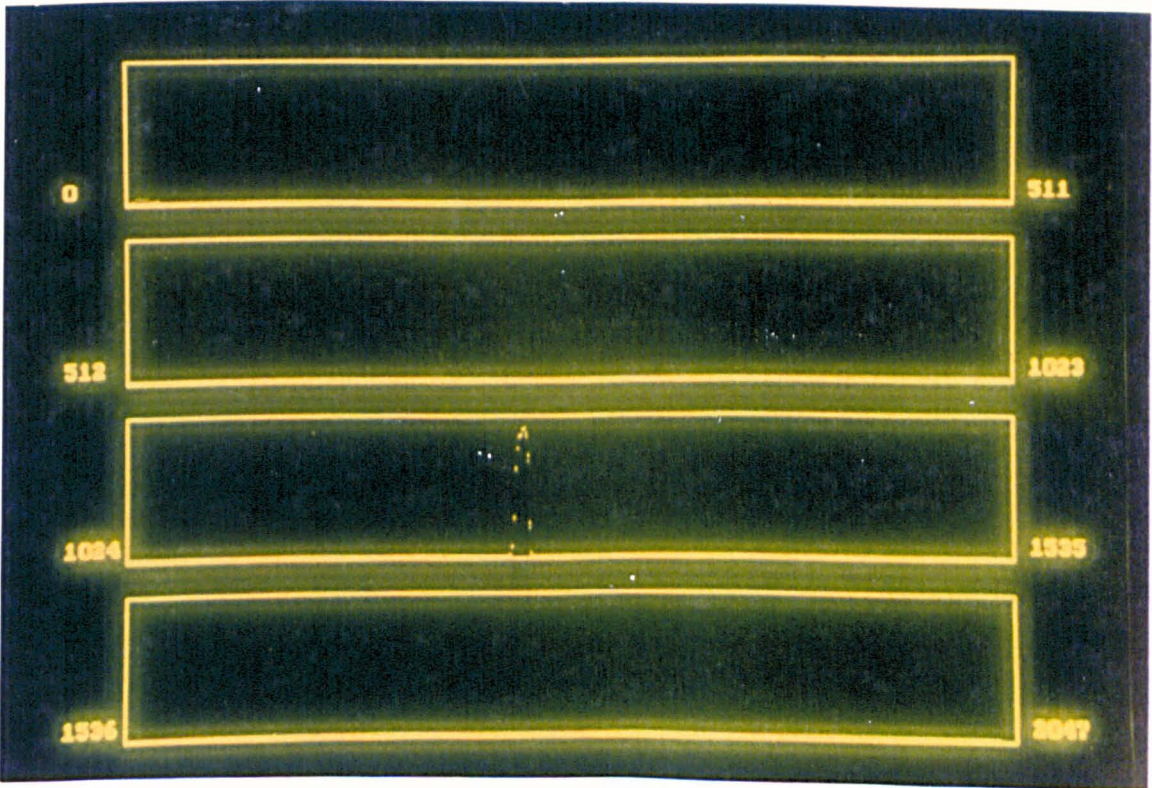


Fig. 4.45. Intensity display of complete array.

To display the magnified section of the array the position of the peak had to be determined. The screen display of the intensity peak caused by the laser is shown in Fig. 4.46.

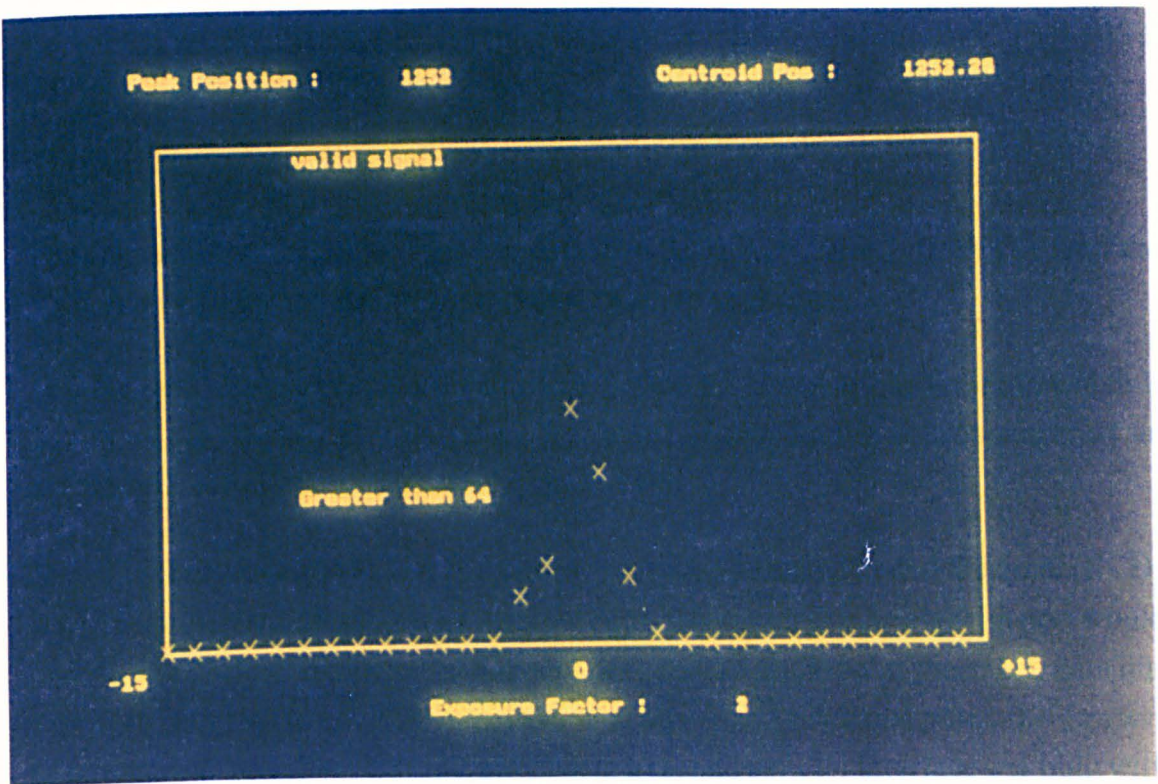


Fig. 4.46. Magnified image of the laser beam reflection.

The display of the intensity peak also allowed the experimentation on the peak location by other algorithms such as the centroid and Vernier methods (described in chapter 3), and control over the exposure time. The result of this work was the successful adjustment of the exposure time to allow the scaling of the intensity peak to optimise the use of the A-D converter.

4.6.4.3. Calibration.

The initial experiments that were carried out with the system were calibration tests. The profiler system was mounted on a fixed granite bench and a six metre optical bench track was constructed with movable trolley. The trolley was stepper motor controlled with a target mounted on it, the target was used both by a laser interferometer and the triangulation system. Hence, control of the position of the target, collection of data from the interferometer and operation of the triangulation system was required.

The calibration, and subsequent interpolation procedure, was also required to be automated to collect enough data to be analysed statistically. Without this automation,

the process of calibration would have taken a great deal of time, even with a reduced quantity of data collected.

(i) Decoding the interferometer.

The operation of the interferometer is described in Appendix 1. In this section the problems of gathering the interferometer data are addressed.

The Hewlett Packard Interferometer has a port for printing out the data which is shown on the display. This provided the means of tapping the data to construct an automated calibration and interpolation test bed.

The data that was available on the printer port was in Binary Coded Decimal (BCD) which requires four data bits for a decimal digit, this meant that an eight bit port would enable two decimal digits to be read and decoded. In addition to the seven data bits that were required to get 9999 mm, 2 decimal places and a decimal point, the sign was also required. To collect this amount of data a second parallel interface was built with a different address to enable four eight bit ports to read the data. The assignments for all of the ports are shown in Table 4.4. where W = Write and R = Read.

```
io_base1= $304; { W1 Stepper motor drive           }
io_base2= $305; { W1 Exposure control internal connection }
io_base3= $306; { R1 BCD 1 }
io_base4= $307; { R1 BCD 2 }
io_base5= $310; { W2 Printer port command }
io_base6= $311; { W2 Set up interferometer via AUX }
io_base7= $312; { R2 BCD 3 }
io_base8= $313; { R2 BCD 4 plus status }
```

Table 4.4. I/O address assignments.

The interferometer also allowed the remote setting up of its operating mode, this was achieved by connections to the parallel port. The program for collection and decoding the data from the interferometer is shown with comments in the next section, unnecessary parts of this program have been deleted and the comments are made in bold.

```
procedure Set_up_interferometer;
```

Set up the front panel of the interferometer by resetting.

```
begin
port[io_base6] := 254;
port[io_base6] := 255;
port[io_base6] := 251;
port[io_base5] := 0;
port[io_base5] := 4;
end;
```

```
procedure close_interferometer;
```

Reset the interferometer again.

```
begin
port[io_base6] := 254;
port[io_base6] := 255;
port[io_base6] := 251;
end;
```

```
procedure get_dist_pos;
```

```
var
    temp1,temp2,temp3,temp4,temp5,temp6,temp7,temp8 : byte;
    data1,data2,data3,data4 : byte;
begin
```

Ask for print out of distance

```
    port[io_base5] := 4;
```

Collect data from printer port into parallel interface.

```
    data1 := port[io_base3];
    data2 := port[io_base4];
    data3 := port[io_base7];
    data4 := port[io_base8];
    port[io_base5] := 0;
```

Analyse each byte for two BCD numbers.

```
    temp1 := (data1 and 1) + ((data1 and 32) shr 3)
            +(data1 and 2) + ((data1 and 64) shr 3);
    temp2 := ((data1 and 4) shr 2) + ((data1 and 128) shr 5)
            +((data1 and 8) shr 2) + ((data1 and 16) shr 1);
```

```

temp3 := (data2 and 1) + ((data2 and 32) shr 3)
        +(data2 and 2) + ((data2 and 64) shr 3);
temp4 := ((data2 and 4) shr 2) + ((data2 and 128) shr 5)
        +((data2 and 8) shr 2) + ((data2 and 16) shr 1);
temp5 := (data3 and 1) + (data3 and 2)
        +((data3 and 32) shr 3) + ((data3 and 64) shr 3);
temp6 := ((data3 and 4) shr 2) + ((data3 and 128) shr 5)
        +((data3 and 8) shr 2) + ((data3 and 16) shr 1);
temp7 := (data4 and 1) + (data4 and 2)
        +((data4 and 32) shr 3) + ((data4 and 64) shr 3);

```

Compute the distance.

```

distance := temp1 * 0.001 + temp2 * 0.01 + temp3 * 0.1
          + temp4 + temp5 * 10 + temp6 * 100 + temp7 * 1000;
end;

```

(ii) Moving the target trolley.

The trolley needed moving after each measurement of distance by the interferometer and triangulation system. A stepper motor drive system was used to move the trolley, the program for its operation is given next.

```

procedure motor_drive(direction : byte; steps : integer);
const
  motor_3 = 4; { other motors */2 }
  Clock   = 64;
  Set_up  = 128;
  { 0 = toward the Interferometer, 1 = away }
begin
  if direction = 1 then direction := 4
  else
    direction := 0;
    port[io_base1] := direction;
    delay(3);
    port[io_base1] := motor_3 or set_up;
    delay(3);
    port[io_base1] := direction;
  for loop1 := 0 to steps - 1 do
    begin
      delay(speed);
      port[io_base1] := motor_3;
      delay(speed);
      port[io_base1] := motor_3 or clock;
    end;
  end;
end;

```

(iii) Calibration.

Data concerning the interferometer distance, and the image distance were collected to provide a calibration file. The interferometer had to be reset at a starting position and the distance between the interferometer axis and the starting position added to the calibration data as an offset. The data collection procedure involved the following processes:

- (a) collect image position from the prototype measuring system,
- (b) collect distance data from the interferometer,
- (c) move target to new position, and
- (d) wait for target to settle and repeat process.

The image position was liable to alter during the image position measurement due to noise and so multiple measurements were used to improve the statistical accuracy of this measurement. The data was collected at a number of distances between calibration points, over the range of the system. The process could take up to an hour to complete depending on the number of calibration points and the settling time allowed.

(vi) Interpolation.

Interpolation tests were possible with the interferometer in the same configuration as the calibration to check the accuracy of the triangulation system. In this case the position of the interpolation places had to be varied to provide a good test. The random number generator in Turbo Pascal was used to move the target by random distances over a set range. The error, which was the difference between the reported distance from the profiler and the actual distance given by the interferometer, was saved in a file for subsequent statistical analysis.

The methods of interpolation used were Lagrange interpolation and piecewise linear interpolation. The latter method was the simplest to implement and gave results that were very similar to that of the more complex Lagrange interpolation.

4.6.4.4. Cross section data collection.

Following the period of calibration and interpolation trials (described in chapter 6), the prototype was taken off the bench and set up on a tripod to collect data concerning the cross sections of structures. To do this software was developed to collect data

concerning full or partial cross sections and save this data to disk or write the data in the Data Exchange Format (.DXF extension filenames) for later evaluation by AutoCad. The presentation of the results in real time was also achieved.

(i) Cross section data collection process.

The method of data collection was essentially the same as for the previous prototypes, the measurement had to start from a known point, the distance was measured, the measuring arm was rotated to a new position and the process repeated. The data are either presented for confirmation of operation or saved for later analysis. A new feature that was developed was dynamic exposure control which was evaluated by experiments varying the exposure control in accordance with the reflected light intensity.

(ii) Conversion to DXF format.

The DXF format (AutoCAD, 1989, Jones, 1989) provides a reliable and virtually universal means of data transfer between CAD systems allowing measured data concerning a profile, or series of profiles, to be input into a CAD program such as AutoCAD. The ASCII character files are simple to write out to a file and easy to view for confirmation of correct operation. The data output was achieved by the following section of program:

```
procedure GetOutputFile(var outfile : text);
var
  FileName : String[100];
begin
  { DXF creation }
  begin
    getoutputfile(outfile);
    writeln(outfile,'0');
    writeln(outfile,'SECTION');
    writeln(outfile,' 2');
    writeln(outfile,'ENTITIES');
    for loop := 1 to last do
      begin
        writeln(outfile,' 0');
        writeln(outfile,'POINT');
        writeln(outfile,' 8');
        writeln(outfile,'0');
        writeln(outfile,' 10');
        str(data_buffer2[loop,1]
          *sin(data_buffer2[loop,2]*pi/180):3:4,s);
```

```

writeln(outfile,s);
writeln(outfile,' 20');
str(data_buffer2[loop,1] *
cos(data_buffer2[loop,2]*pi/180):3:4,s);
writeln(outfile,s);
writeln(outfile,' 30');
str(z_coord:3:4,s);
writeln(outfile,s);
end;
writeln(outfile,' 0');
writeln(outfile,'ENDSEC');
writeln(outfile,' 0');
writeln(outfile,'EOF');
close(outfile);
end;

```

One of the features of this procedure was that it allowed the writing of the data to a device called 'outfile' where the device could be the screen, the printer or a file on disk. The advantage of this approach was that one program did all three tasks which meant that the operation of the DXF output could be monitored for correct operation.

The data output from this procedure was successfully imported into AutoCAD for closer examination, editing, measurement and analysis. The data was also successfully imported into another CAD system called EasyCAD.

4.6.4.5. Conversion to DXB format.

The disadvantage of the DXF format is that it is not compact, and files can become very large. The DXB format, supported only by AutoCAD, is a binary format which can result in large reductions in the size of data file and the size of the resulting AutoCAD file if the data is saved as a '.DWG' drawing file. The saving in space can be as great as 9:1, but a penalty is that this data can then only be used by AutoCAD. A further limitation that applies to both DXF and DXB files is that there is no easy alteration of the description of the data that is used, i.e. the data format used above is a 'point' description which cannot easily be changed to allow lines to be drawn between points.

4.6.4.6. Conclusion.

The prototype was very stable and data collection was reasonably quick, depending on the operations that were being performed. It was possible to pack the system into boxes and transport across London, set up again, and still achieve satisfactory results.

4.6.5. Results.

A number of test objects were systematically profiled. These included a corridor, a manikin, a model boat hull, a model roof structure, a model polyhedron, and the laboratory.

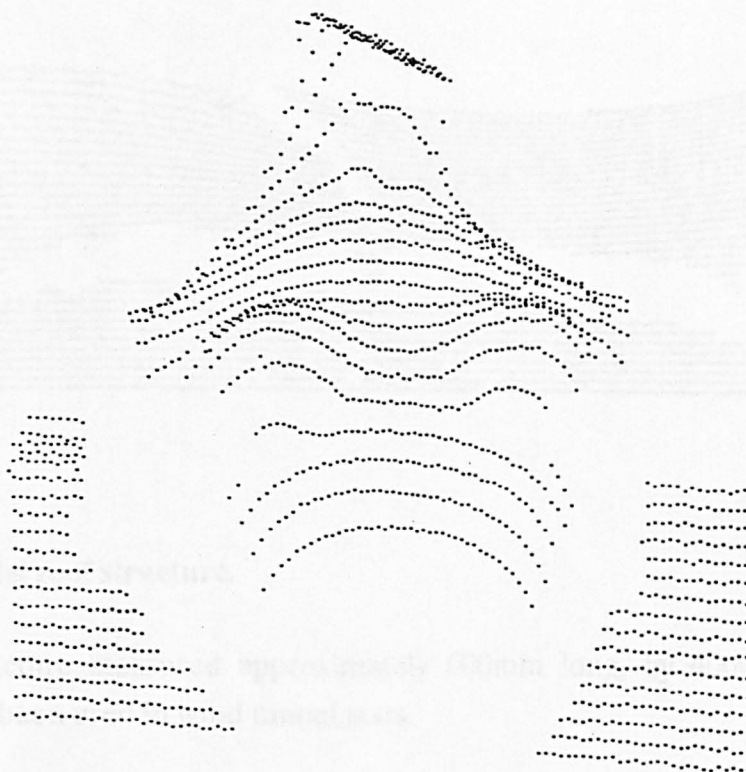


Fig. 4.49. Manikin.

The cross sections of the manikin were obtained from the upper section of a life size manikin.

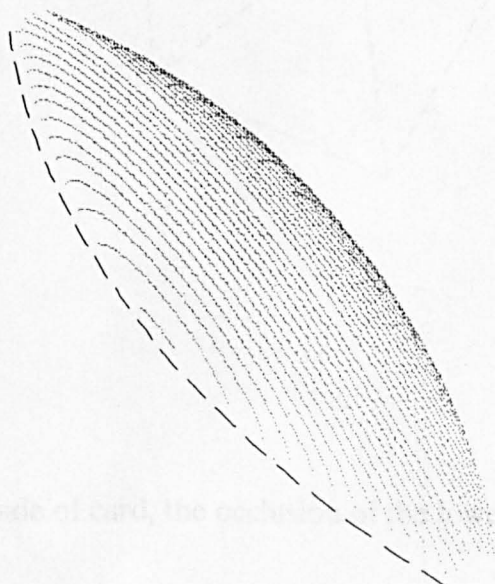


Fig. 4.50. Model boat hull.

The model boat hull measured had dimensions of approximately 1.2 metres long, by 200mm wide. Only half of the hull was measured, as it was symmetric about its centre axis, the full hull shown is constructed from the reflected image of the hull.

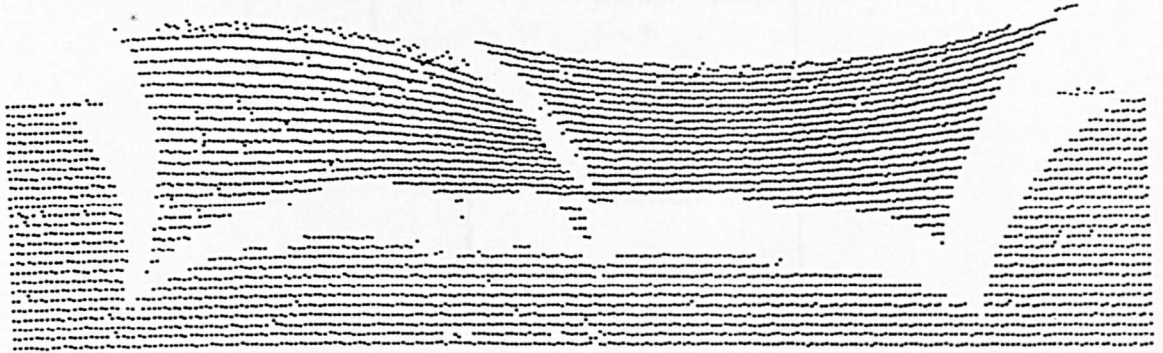


Fig. 4.51. Model roof structure.

The roof structure measured approximately 600mm long, by 400mm wide. The structure had been used in wind tunnel tests.

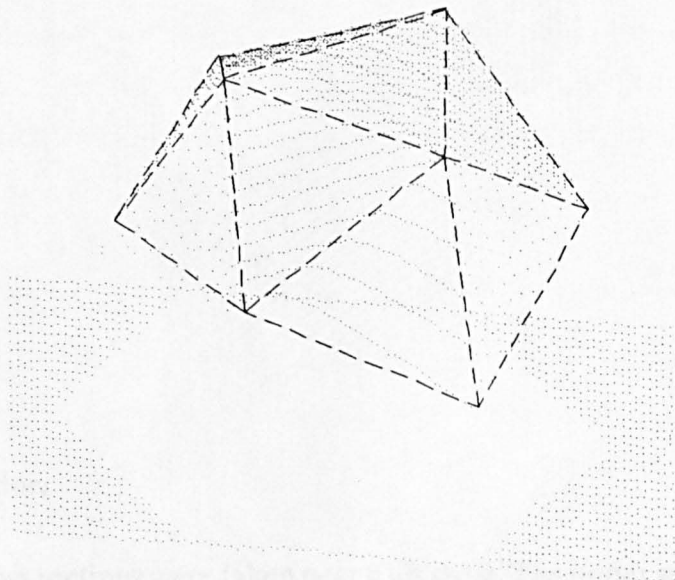


Fig. 4.52. Polyhedron.

The polyhedron was made of card, the occlusion of the lower surfaces can clearly be seen.

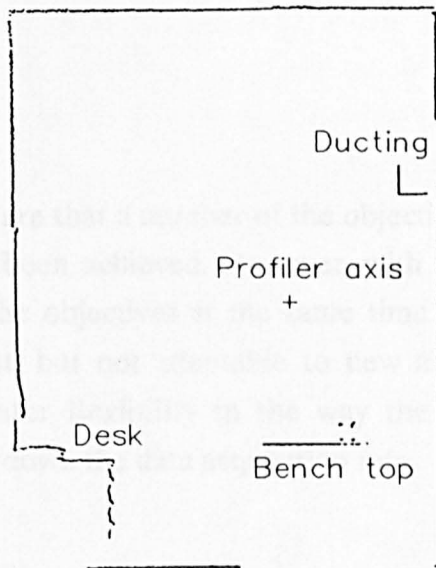


Fig. 4.53. Laboratory.

The Laboratory cross section shows a number of artifacts which are recognisable, the bench, desk, ducting, roof, floor and walls.

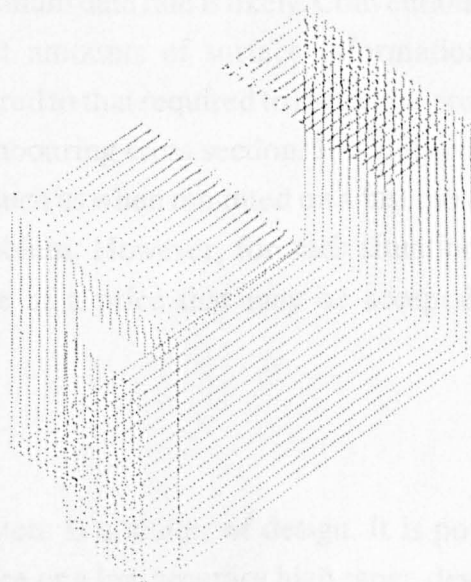


Fig. 4.54. Corridor.

The corridor cross sections were taken near a lift shaft. The upper section, where there are no dots, is because the profiler was too close to the roof and out of range.

4.7. CONCLUSIONS.

4.7.1. Introduction.

The conclusions reached are that a number of the objectives set at the beginning of the research period had been achieved. However, with each prototype it was not possible to meet all of the objectives at the same time. For instance, the second prototype was the fastest, but not adaptable to new algorithms, while the third prototype provided greater flexibility in the way the data was processed, but consequently this slowed down the data acquisition rate.

4.7.2. Speed.

The absolute speed of the triangulation system is dependent upon the line scan rate of the CCD camera, this rate is then dependent upon the size of the array and its architecture. If it is assumed that the design maximises this rate, as with Prototype II, then the rate may be in excess of 10kHz. In the case of the Prototype II, 0.8 kHz was easily achieved, so a maximum data rate is likely. Conventionally measurement at such a fast rate permits vast amounts of surface information to be collected in an insignificant time compared to that required to locate the profiler with respect to some arbitrary datum or neighbouring cross section. It is only when the system is used in unusual circumstances, such as when mounted on a fast moving train, that such a data rate may become a problem. However, for such situations, there are methods of increasing the data rate at a price that may be acceptable for these specialised applications.

4.7.3. Accuracy.

The accuracy of the system is a matter of design. It is possible to construct a high accuracy low range device or a low accuracy high range device. However, it has been shown that an increase in accuracy by subpixel techniques of 3 times is not unreasonable. 6000 pixel chips are available giving an effective 18,000 measurement positions resolved over a given range. This allows an accuracy of 0.3 mm over a range which is great enough to take in road and rail tunnels, sewers, corridors, rooms etc.

4.7.4. Dimensions and non-linearity.

The dimensions of the profiling system are important in so far as a small size makes the measurement system portable, stable, and light. It is not possible to construct a

system as small as a piece of EDM, because of the fundamental triangulation geometry. However, the system has been reduced to a size which fulfils some of the conditions, further improvements are possible by correcting the non-linearity as described in chapter 6.

4.7.5. Reliability.

The design which has evolved is simple, and relatively robust. Consideration has been given to the means of rotation, the tripod mounting, the location of the measurement axis, the retention of the laser and camera. Further improvements have been outlined in chapter 5 to reduce systematic errors.

4.7.6. Measurement of cross sections.

The objective of measurement of cross sections has been fully met with each of the prototypes with increasing reliability and accuracy. Provided the surface to be measured is reasonably accessible, and not either mirror-like, or transparent, the cross section of the surface can be obtained. This can be extended to the measurement of structures whose size is much greater than the range of the profiling device itself by good surveying procedures.

5. ANALYSIS OF ERRORS.

5.1. SYNOPSIS.

This chapter deals with all of the errors that are of importance to the collection of data for cross sections of structures. Error analysis is of great importance in understanding the performance of the measuring system and the quality of the measurements achieved. Some errors have fundamental limits, if the errors due to the various sources are down to that limit, there is no point in expecting any better results. Other errors are accepted as compromises of cost or as a trade off for other desirable features such as speed and convenience.

The errors that result from the use of the triangulation technique in specialised environments such as industrial inspection have not been analysed as these are beyond the scope of this thesis.

The topics covered in this chapter are:

- (i) intrinsic triangulation errors, and
- (ii) survey errors.

The errors are quantified in this chapter. Results from tests carried out to verify the predicted accuracy are given in chapter 6.

5.2. INTRODUCTION.

An error of measurement is the difference between the true position of a point in space compared to that given by a measuring system or by a combination of measuring systems. The errors that are of first importance in the context of this thesis are those of the triangulation system itself, however, this measuring system will generally be

used in conjunction with other measuring systems such as theodolites and/or tapes, hence the interaction of these systems will also be considered.

Errors in measurement may for convenience be divided into two groups, distance measuring errors and the errors in determining the spatial coordinates of measured points.

The errors relating to a measured cross section will also be related to the axis of the measuring system in the plane of measurement. The global errors in locating these points will be considered separately. In both groups there will be systematic and random errors, the systematic errors can be estimated and, in many cases, a correction can be made, the random errors are best treated statistically.

All measuring systems are subject to error. It is necessary to identify the possible sources of these errors and assess their magnitude and likely consequences when attempting to determine the efficacy of the system. To avoid the temptation to exaggerate the accuracy achieved, the various errors, where identified, have been analysed both empirically and theoretically.

5.3. INTRINSIC TRIANGULATION ERRORS.

5.3.1. Introduction.

There are many sources of error in triangulation systems which reduce the maximum measurement resolution available for a given configuration. In many instances a solution can be found which is the result of compromises of cost, speed, and convenience. However, a full understanding of all the contributing sources of error is necessary if a given design is to be 'optimised'. An optical triangulation system is made up of mechanical and optical components, some of which are amenable to design considerations such as choice of laser, sensor or materials and others which are beyond the capabilities of the designer to adjust, such as reflectivity of the surface to be measured and nature of the medium through which light is transmitted and received, e.g. air.

The errors that relate to the camera are considered followed by the errors external to the camera.

It is obvious from the geometry of the optical triangulation system shown in Fig. 5.1, that the sensor resolution and chosen range of measurement will determine the

accuracy of measurement. This accuracy will be inversely proportional to the range of measurement. In fact, the desired range of measurement may be obtained with a number of differing configuration parameters, which will affect the accuracy or range of measurement. Hence, for a specified combination of accuracy, sensor resolution or range of measurement, the remaining parameters must be carefully chosen to minimise the gross error in distance measurement.

These errors will be analysed in this section, first the errors that occur within the camera will be examined and second the errors external to the camera.

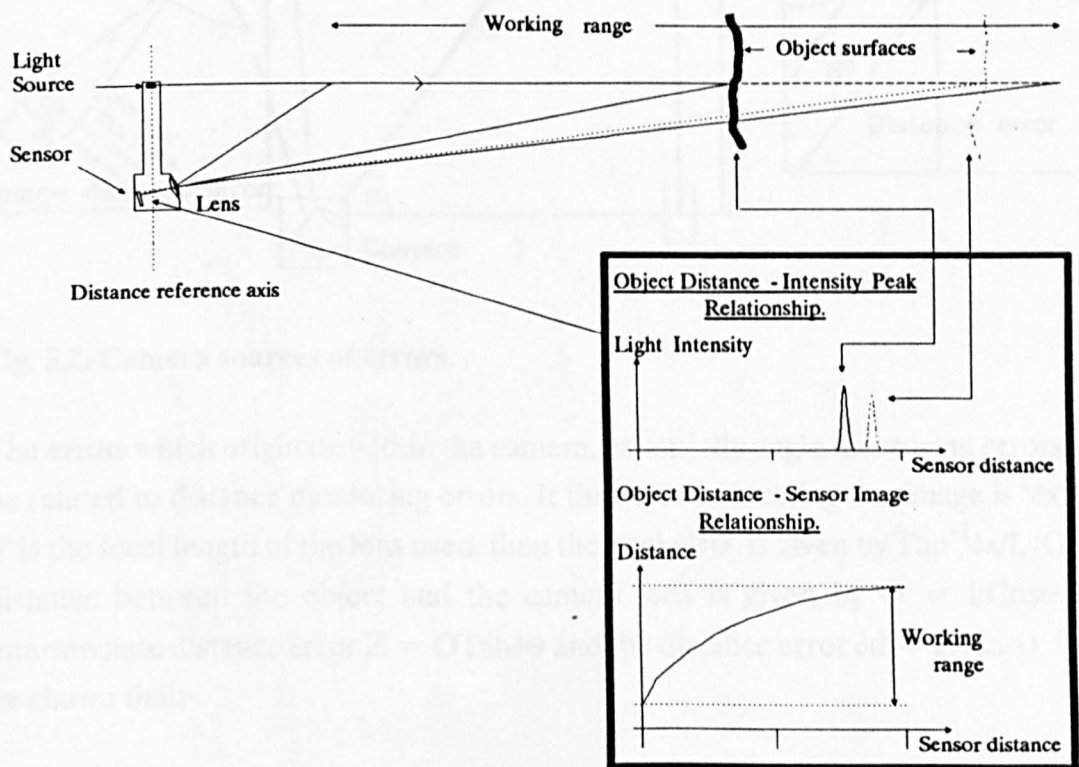


Fig. 5.1. The general optical triangulation system.

5.3.2. Camera errors.

5.3.2.1. Introduction.

The measuring system uses a lens and sensor for angle measurement, these components make up a camera which will have characteristic errors of measurement due to temperature changes and image processing and modelling limitations. These errors are illustrated in Fig. 5.2. The effect of each of these errors is analysed in this section.

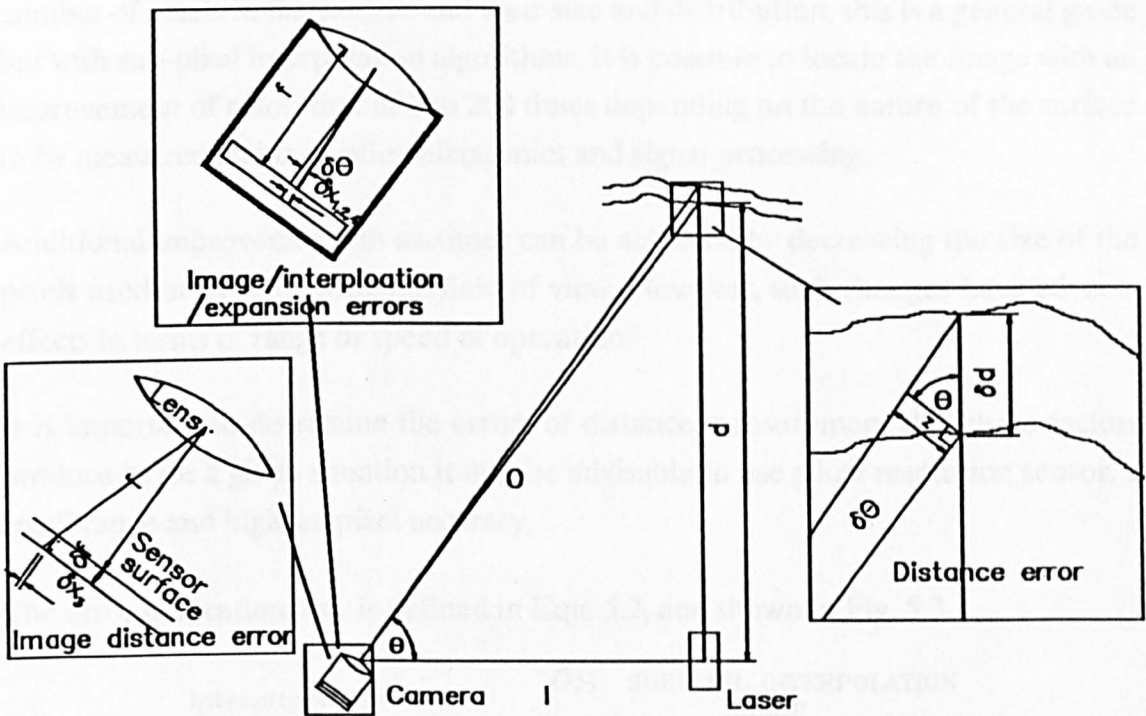


Fig. 5.2. Camera sources of errors.

The errors which originate within the camera, essentially angle measuring errors, can be related to distance measuring errors. If the error in locating the image is ' δx ' and ' f ' is the focal length of the lens used, then the angle ' $\delta\theta$ ' is given by $\text{Tan}^{-1}\delta x/f$, ' O ' the distance between the object and the camera lens is given by $O = p/\text{Cos}\theta$, the intermediate distance error $Z = O \text{Tan}\delta\theta$ and the distance error $\delta d = Z/\text{Cos}\theta$. It can be shown that:-

$$\text{Equ. 5.1.} \quad \delta d_n = \delta x_n / f \text{Cos}^2\theta$$

By determining δx_n for each of the sources of error the total distance measuring error can be evaluated.

5.3.2.2. Location of image with respect to CCD linear array.

The reflections from the surface to be measured are incident on the sensor to form an intensity distribution that has an approximately Gaussian distribution in the absence of any other competing sources of light. This process has been described in chapter 3. The precision with which this Gaussian intensity peak can be located with respect to the sensor determines one of the fundamental limitations of the resolution of the system as a whole. It may appear that the resolution will be determined by the

number of pixels in the camera and their size and distribution, this is a general guide but with sub-pixel interpolation algorithms, it is possible to locate the image with an improvement of resolution of 2 to 200 times depending on the nature of the surface to be measured and the optics, electronics and signal processing.

Additional improvements to accuracy can be achieved by decreasing the size of the pixels used or by narrowing the field of view. However, such changes have adverse effects in terms of range or speed of operation.

It is important to determine the errors of distance measurement that these factors produce as for a given situation it may be advisable to use a low resolution sensor, a small range and high subpixel accuracy.

The error in location, δx_1 , is defined in Equ. 5.2, and shown in Fig. 5.3.

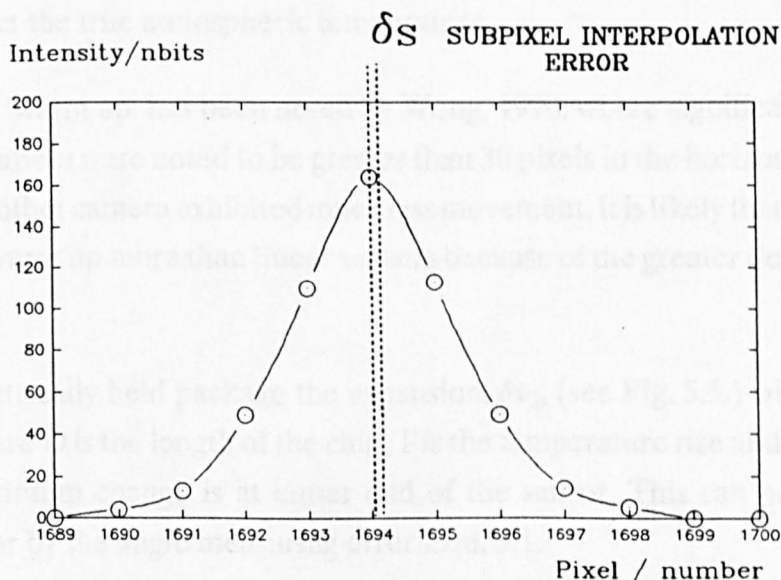


Fig 5.3. Image location error.

Where D is the sensor length, n the number of pixels and δs is the accuracy of sub-pixel interpolation.

Equ. 5.2.
$$\delta x_1 = (D/n)\delta s$$

Currently available linear sensors have 256 - 6000 pixels.

A survey (West, 1990) of the techniques available for subpixel accuracy shows that all gave improvements in resolution of between 2 - 200 times but are affected by noise

and abnormal reflectivity variations that can distort the true position of the subpixel estimation.

5.3.2.3. Sensor position changes with temperature.

The sensor is mounted on a printed circuit board which is held in the camera/lens housing. It is assumed that the camera unit cannot move in relation to the laser, but that it is possible for the CCD sensor itself to expand with temperature. As the sensor is constructed on a silicon substrate, the chip package is designed to expand at the same rate so that undesirable stresses are not allowed to build up within the chip. The printed circuit board will also be designed with a similar coefficient of expansion for the same reason. The coefficient of expansion of silicon α_{sil} is $2.6 \times 10^{-6} \text{K}^{-1}$ at 293 K (20°C) and the possible external temperature range over which the sensor is likely to be operated is 0 to 30°C , however the chip itself will warm up during use, hence, it will not reflect the true atmospheric temperature.

The effect of ‘warm up’ has been noted by Wong, 1990, where significant distortions for an area camera were noted to be greater than 30 pixels in the horizontal direction. However, another camera exhibited much less movement. It is likely that area cameras sensors will warm up more than linear sensors because of the greater density of active elements.

For a symmetrically held package the expansion, δx_2 , (see Fig. 5.5.) will be given by Equ. 5.3, where D is the length of the chip, T is the temperature rise and it can be seen that the maximum change is at either end of the sensor. This can be related to a distance error by the angle measuring error Equ. 5.1.

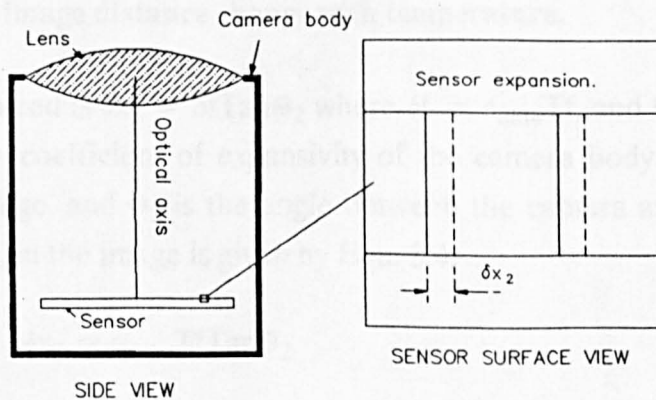


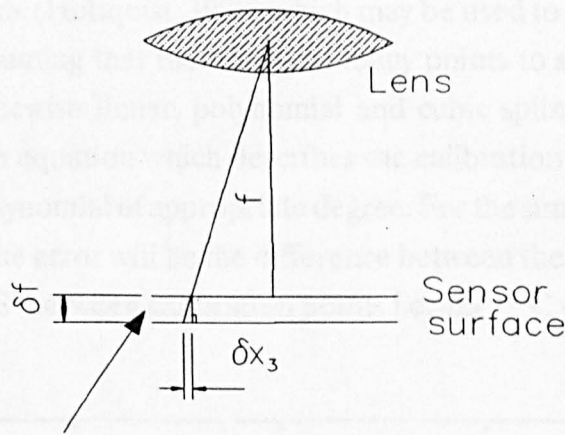
Fig. 5.5. Expansion of the sensor.

Equ. 5.3. $\delta x_2 = (D/2)a_{sil}T$

The analysis of errors caused by the sensor expanding and moving must be taken into account, the expansion may be small because of the small coefficient of expansion, but care must be taken to ensure that the sensor mounting permits only minimum movement.

5.3.2.4. Change in camera image distance with temperature.

The camera/lens system will expand or contract with temperature changes. This will affect the focus on axis, but off axis it will alter the position of the image with respect to the sensor chip and hence introduce an error in distance measurement as shown by Fig. 5.6.



Change in position of sensor surface due to camera body expansion.

Fig. 5.6. Camera image distance change with temperature.

The error introduced is $\delta x_3 = \delta f \tan \Theta_2$ where $\delta f = a_{cam} T f$, and f = focal length of the lens, a_{cam} = coefficient of expansivity of the camera body material, T is the temperature change, and Θ_2 is the angle between the camera axis and the sensor. Hence the effect on the image is given by Equ. 5.4.

Equ. 5.4. $\delta x_3 = a_{cam} T f \tan \Theta_2$

This error is greater for larger sensors, and will vary linearly from the optical centre of the sensor.

5.3.2.5. Interpolation errors from calibration data.

To use the system for distance measurement, data are collected from the image location algorithm and related to the distance from the measuring system axis by means of an interferometer or other high accuracy measuring system. As there are 'n' pixels and with a sub-pixel interpolation limit of 'p' then there are 'np' possible positions of calibration points which can be measured. However, as n is typically greater than a thousand and p may be greater than ten there will often be a very large number of measured data points which could be collected. It is preferable, therefore, to either characterise the data by a single function such as a polynomial or to interpolate with a reduced data set. Both of these methods will cause errors if the model of the system characteristic does not perfectly match the true data.

The numerical methods (Hultquist, 1988) which may be used to interpolate between calibration points, assuming that there are too many points to store for direct "look up" methods, are piecewise linear, polynomial and cubic spline interpolation, and direct evaluation of an equation which describes the calibration curve such as a least squares best fit of a polynomial of appropriate degree. For the simple case of piecewise linear interpolation, the error will be the difference between the calibration curve 'C' and the straight line 'S' between calibration points i.e. $\delta x_4 = C - S$, see Fig. 5.7.

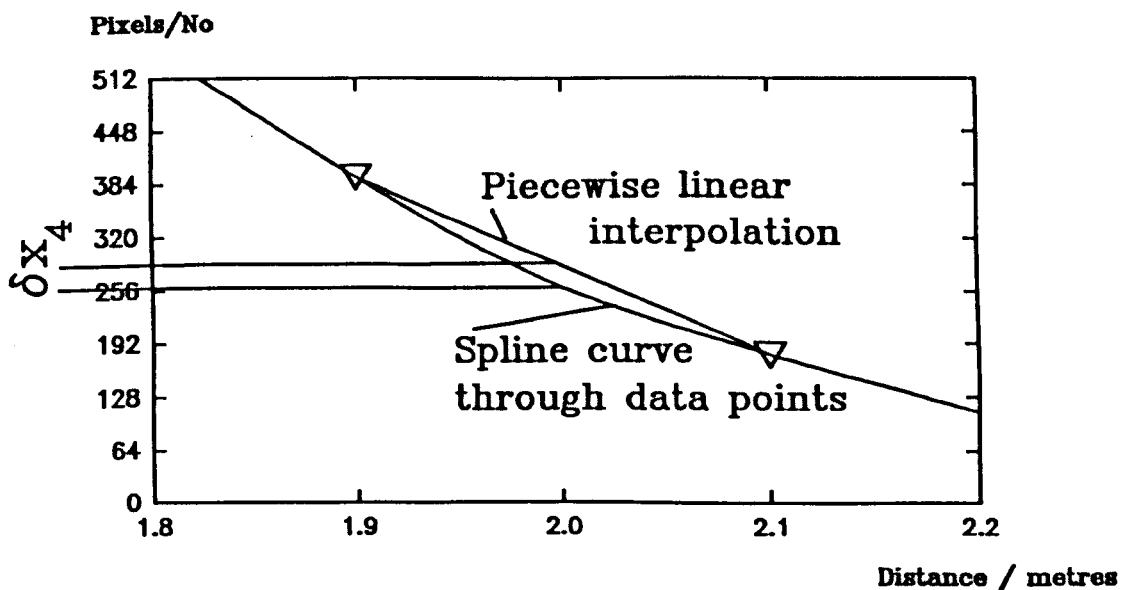


Fig. 5.7. Internal error sources.

The error curve will oscillate between the correct value at the calibrated points to a maximum error at some point between these calibrated points. Again, this error can be related to a distance measuring error by use of Equ. 5.1. The source of error here

is more complex than this simple picture, there are additional factors such as noise and laser pointing errors that influence the calibration and interpolation process, these are covered in detail in chapter 6.

5.3.2.6. Conclusion.

The errors that occur within the camera have been analysed and quantified. The analysis pinpoints the places where changes can be made to minimise errors, such as in the choice of the camera body material, and where they cannot, such as the material used for the sensor.

5.3.3. External errors.

5.3.3.1. Introduction.

The remaining analysis of intrinsic triangulation errors concentrates on the factors which are outside of the camera angle measuring system such as the transmission medium, laser pointing stability, base line expansion and image distortion. These errors are both random and systematic in nature and each will be analysed with reference the effect on distance measuring accuracy, as shown by Fig. 5.8.

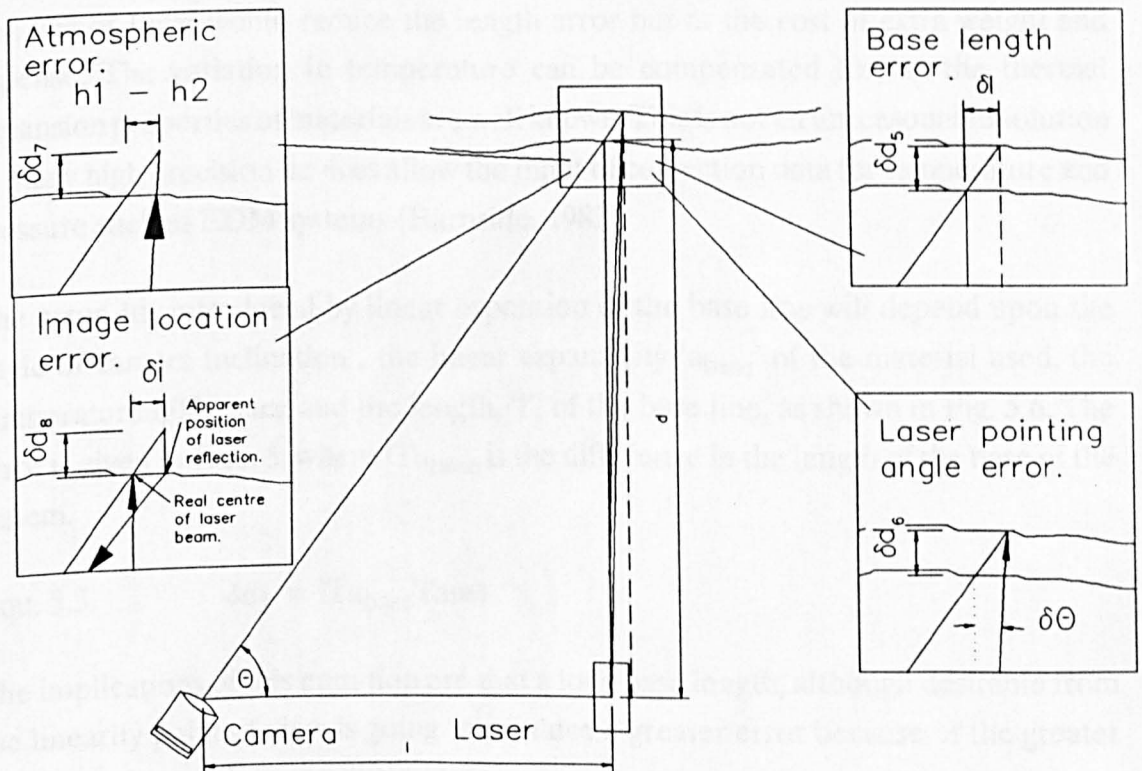


Fig 5.8. External error sources.

5.3.3.2. Triangulation arm length change.

The optical triangulation system is constructed from a laser, sensor and lens which are mechanically held in a fixed orientation with respect to each other and the measurement axis, however, there is always the possibility of change due to temperature or stress. The measurement process relies upon a calibration at a specific time and subsequent interpolation. There is an implicit assumption that the system is still in the same configuration as it was at the time of calibration, this may not be the case, due to temperature changes or other influences.

A major source of error is likely to be variations of to the length of the base of the triangulation triangle due to the thermal expansion of the material over its operating temperature range. It is assumed that the design is such that the camera and the laser are not able to change in orientation with respect to each other. The expansion of a material is equal to length times temperature change times 'a', where 'a' is the coefficient of linear expansivity. (The coefficients for steel, aluminium and Invar are 15, 23 and $0.9 \times 10^{-6}K^{-1}$, respectively.)

In the case of the test system, aluminium was used for strength, cost, lightness. The majority of testing was done in the laboratory where the temperature was controlled. The use of Invar would reduce the length error but at the cost of extra weight and expense. The variation in temperature can be compensated for, as the thermal expansion properties of materials are well known. This is not an unreasonable solution as many high precision devices allow the input of correction data for temperature and pressure such as EDM systems (Burnside, 1982).

The error δd_5 introduced by linear expansion of the base line will depend upon the angle of camera inclination, the linear expansivity ' a_{base} ' of the material used, the temperature difference and the length, 'l', of the base line, as shown in Fig. 5.6. The error is given by Equ. 5. where lTa_{base} is the difference in the length of the base of the system.

$$\text{Equ. 5.5.} \quad \delta d_5 = lTa_{base} \text{Tan}\Theta$$

The implications of this equation are that a long base length, although desirable from the linearity point of view is going to produce a greater error because of the greater difference in length over a given temperature range.

5.3.3.3. Laser pointing stability.

The operation of the triangulation scheme depends critically on a light source providing a small collimated beam to illuminate a measurement position on an object, and upon the pointing stability of the source. A laser provides such a source which will illuminate a small portion of the object with minimal beam wander.

Lasers characteristically have low pointing angle variations over time, but they do exist and as such have to be taken into account. Two types of laser, the diode and gas laser could be used in this application as both provide a highly collimated light source. The sensor used in the system has a peak sensitivity and quantum efficiency in the near infra-red. Hence only HeNe lasers (632.8nm) and visible wavelength laser diodes (670nm) are appropriate. Both of these lasers are well developed technologies providing reliability and cheapness.

For the optical triangulation scheme to operate successfully the light source must be able to illuminate accurately the point of measurement on the structure being surveyed. The laser must satisfy the following conditions:

- (i) **Low beam divergence.** The divergence of the laser beam is very small, but exists due to diffraction. The amount of divergence is greater for a small size beam compared to that of a larger beam, again because of the laws of diffraction. However, the smallest beam size is not essential for accurate distance measurement although a larger beam has two disadvantages: lower signal to noise ratio, and less spatial resolution in the plane perpendicular to the beam.
- (ii) **High directional pointing stability.** The system is calibrated with initial conditions of temperature and warm up time, interpolation then takes place and errors will result if there is a lack of reproducibility of the laser beam position.
- (iii) **Power output stability and variability.** These requirements allow measurements to a wider range of surface reflectances and allows prediction of the exposure level based on the past exposure level which would not be possible if the power output changed between exposures.

(iv) High reliability. The system will be used in a range of temperatures, humidity and pressure, and also for long periods of time. The laser must be reliable if the system is to be trustworthy.

(v) Low cost. Each component in an optical system will contribute to the overall cost and the laser is likely to be a significant cost in the development of the system.

A comparison of performance of a HeNe laser and a typical diode laser is made in Table 5.1. (Smith, 1989; D.O. Industries, 1989; N.E.C., 1990)

	He-Ne	Diode	Units
Divergence	0.7 - 2	1.2	mrad
Pointing stability	< 0.01	< 0.1	mrad
Lifetime	> 10,000	> 50,000	hours

Table 5.1. Laser performance comparison.

As in the case of the other errors, the pointing error can be translated into a distance measurement error. The error introduced through pointing error is given by Equ. 5.6, and shown in Fig. 5.8, where $\delta\theta$ = pointing error of the laser.

$$\text{Equ. 5.6.} \quad \delta d_6 = 1. \sin(\delta\theta \sin\theta) / \cos(\delta\theta \sin\theta + \theta) \cos\theta$$

The pointing stability of the laser used in the Prototype III did exhibit some significant pointing errors. At a distance of 3.3 metres, a base length of 0.7 metres and an angle θ of 78° , the difference between two sets of subpixel measurements, one with the laser close to the target and the other mounted in the prototype caused 50% - 200% larger errors depending on the algorithm used. The error component which appears to be due to the pointing stability can therefore be identified and analysed separately from the errors due to other factors as these were the same in each case. The difference in the standard deviation of the centroid algorithm subpixel measurement for one thousand trials was $0.062 - 0.042 = 0.020/\text{pixel}$. The dimensions of the pixels were $13\mu\text{m}$ so the error was $0.020 \times 13\mu\text{m} = \pm 0.26\mu\text{m}$. The focal length of the lens used was 50mm so the angular error $\delta\theta_{\text{cam}}$ can be calculated and is 0.006 mrad for one standard deviation, multiplying this by three will include 99.7% of the errors, assuming a Normal Distribution (Cooper, 1974), which, corrected for the angle difference the

camera angle and laser, makes the error $\delta\Theta_{\text{las}} = \pm 0.0183$ mrad which using Equ. 5.6. gives an error of ± 0.29 mm due to the laser pointing stability alone.

The laser pointing error can cause significant measuring errors, the pointing error attributed to the laser of ± 0.0183 mrad is a factor of five less than that given by the manufacturers of laser diodes and a factor of two greater than that given by manufacturers of HeNe lasers. If this factor is coupled with that of the increasing effect of this error at greater distances, the HeNe laser would appear to have a significant advantage over the diode laser. However, there are other factors which affect these decisions such as weight, cost, ease of modulation, operating voltage and current, size, and warm up time. A study (Kwiecien, 1985) in Poland showed that the warm up period gave significant variations in the position of the laser beam as it emanated from the laser tube of a gas laser, regular oscillations of up to 0.2 mm were recorded over the initial minute of operation with more consistent, but equally large trends emerging over a longer period of up to 26 minutes. If a diode laser is used because of the warm up problems of the HeNe laser then, because the major cause of the error in pointing is caused by thermal expansion, it is important that any laser is mounted with a good heat sink to minimise the effects due to temperature changes.

5.3.3.4. Temperature, pressure and humidity gradients.

The laser beam and the reflected light all pass through the medium air before entering the camera. During this period it is possible for the light to encounter temperature, pressure or humidity gradients which can affect the direct path of the light to the camera, so giving a false reading. A phenomena which may be recalled to justify this from personal experience is the sight of a ship sailing along the horizon some distance from the perceived water/sky boundary because of the different paths of the light from near to sea level compared to those just above it.

To study the effects of temperature, pressure and humidity an equation is required to quantify the problem. A commonly used formula (Burnside, 1982) for the calculation of the refractive index of air is shown in Equ. 5.7.

$$\text{Equ. 5.7. } (n - 1) \times 10^{-6} = N = 103.49(P - E)/T + (86.26/T)(1 + 5748/T)E$$

Where n = refractive index, P = pressure (mmHg), E = water vapour pressure (mmHg) and T is the temperature in Kelvin and the carbon dioxide content of air has been ignored. This formula is accurate to better than 1 part in 10^6 which is satisfactory for this work.

To analyse the effect of changes in the refractive index of the transmission medium it is important to realise that constant changes will make no difference to the measuring system but, where there is a temperature, pressure or humidity gradient this will affect the measurement process. To analyse the effects of the individual components it is desirable to compute the relative change in refractive index with respect to temperature, pressure and humidity. Typical input parameters are $P = 760$ mmHg, $T = 293\text{K}$, $E = 7.6$ mmHg, and the rate of change of each of these is:

$$dN/dP = +0.35 \text{ units/mm Hg,}$$

$$dN/dT = -1.22 \text{ units/mm Hg,}$$

$$dN/dE = +5.72 \text{ units/mm Hg.}$$

Where N is short for $(n - 1) \times 10^{-6}$.

It is now possible to calculate the change due to each of these parameters over a given range. With these values the variation in position of the laser beam and hence a distance error due to the inhomogeneities of the transmission medium can be computed. However, it must be noted that these effects are much more prominent over large distances of propagation, a study (Harrison, 1972) notes that "The potency of such gradients may be appreciated by noting that a temperature gradient (often termed lapse rate) normal to the reference axis of only $0.1^\circ\text{C}/\text{metre}$ will cause a ray of light to deviate from a straight path by about 50mm over a range of 1km.". In some circumstances conditions exist where temperature gradients could be more severe, for example deep gold mines in South Africa have rock temperatures as high as 63°C (Times, 1990).

The deviation of a laser beam has been derived for temperature, pressure and humidity gradients (Harrison, 1972) with the simplifying assumption that the gradient normal to the direction of the beam is constant over the entire path length. The deviation of the beam is given by 'h' in the following equations:

$$\text{Equ. 5.8.} \quad h_{\text{temp}} = (L^2/2)(n_a - 1)(T_s P/P_s T)(dT/dR)$$

$$\text{Equ. 5.9.} \quad h_{\text{pres}} = (L^2/2)(n_a - 1)(T_s P/P_s T)g_{p_{as}}$$

$$\text{Equ. 5.10.} \quad h_{\text{humid}} = (L^2/2)(n_a - 1)(T_s(1 - a)/P_s T)(dP_w/dR)$$

as defined by Fig. 5.7. and the variables and constants in Table 5.2.

h = deviation of laser beam.

L = distance between laser and object.

$(n_a - 1) = 277 \times 10^{-6}$ @ wavelength 633 nm.

T_s = atmospheric temperature at standard conditions, 288.15K.

T = atmospheric temperature absolute.

P_s = atmospheric pressure at standard conditions, $1.013 \times 10^5 \text{ N/m}^2$.

R = radius of curvature of refracted ray.

g = gravitational acceleration, 9.81 m/s^2 .

$\rho_{as} = 1.22 \text{ kg/m}^3$.

$(1 - a) = 0.16$.

P_w = partial pressure of water vapour.

Table 5.2.

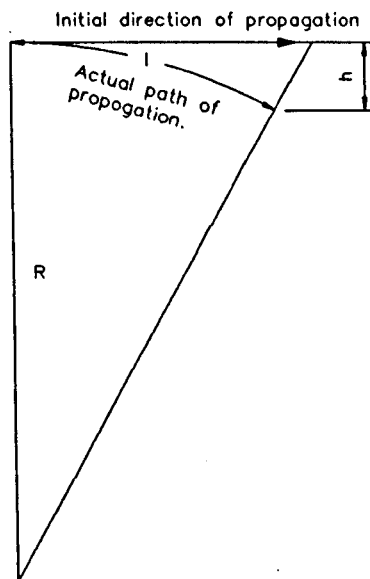


Fig. 5.9. Refracted ray diagram.

Hence, the effect of temperature, pressure and humidity gradients can be estimated. Under normal conditions, temperature is the largest contributor to the deviation of the beam from a straight line, with pressure the next largest followed by humidity. Harrison, 1972, found that there was no significant humidity gradient in tests conducted at Queen Mary reservoir breakwater and at grass site at Wisley airfield, but, Robinson, 1965, has reported humidity gradients between tarmac and an irrigated lawn. However, as the deviation caused by humidity is small, the effect is ignored in this analysis. By inserting a distance of 5 metres at standard temperature and pressure into Equations 5.8, & 5.9, the deviation can be calculated for temperature and pressure and are shown in Table 5.3.

Parameter	Gradient	Deviation / mm
Temperature	1°/m	0.012
Pressure	9.8 m/s ²	0.00041

Table 5.3.

The calculations show that although pressure is a significant factor over distances of greater than fifty metres the effect over five metres is minimal and can be ignored.

If the worst case is taken for temperature where the measuring system is suspended in a mine shaft with ventilating updraught and warm wall surfaces then the temperature gradient will be normal to the line of propagation of the laser beam and at an angle to the surface/camera ray return path, see Fig. 5.10.

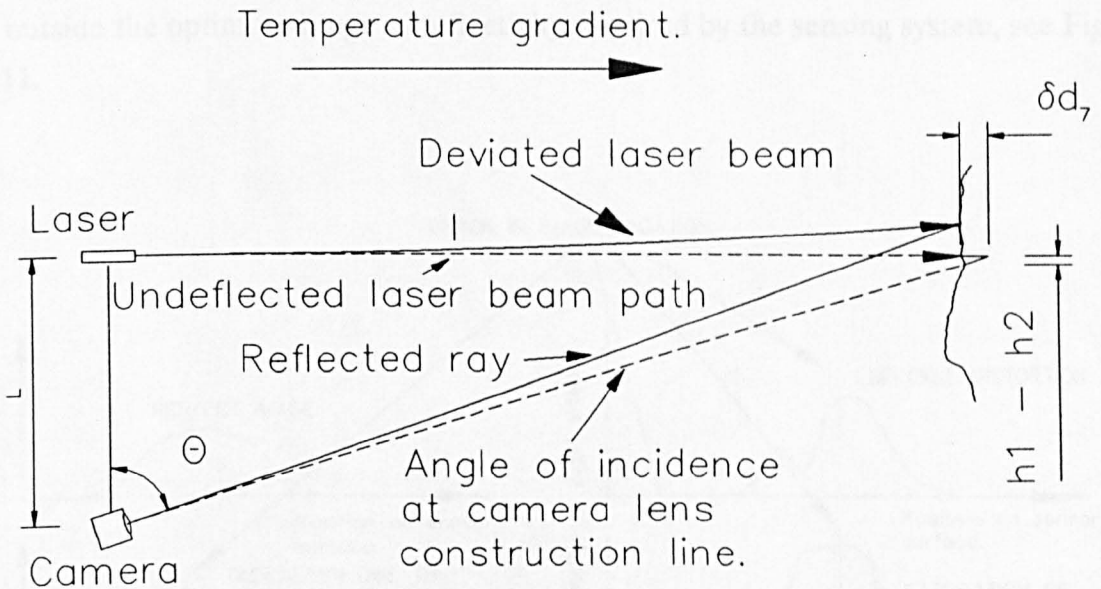


Fig. 5.10. The deviation of the laser and reflected rays due to temperature.

It is apparent from this figure that there are two effects on the measuring system, first, the measurement takes place to a point that is displaced from where it is expected to be in the subsequent analysis of the data making the measurement indeterminate as the orientation of the surface is not known, and second, a measurement error occurs because of the differing angles that the two rays make to the temperature gradient.

This measurement error δd_7 is equal to the difference of the deviation of two rays deviation h_1 and h_2 multiplied by the tangent of the angle θ the camera ray makes with the base line. The path length of the camera ray is given by Pythagoras from the

distance of the target from the base line and the base line length itself. Hence, with simplification, the error is shown in Equ. 5.11.

$$\text{Equ. 5.11.} \quad \delta d_7 = 0.5C(L^2(1 - \sin\theta) - L^2\sin\theta)\tan\theta(dT/dR)$$

Where $C = (n_a - 1)(T_sP/P_sT)$

The error increases if the base of the triangulation triangle is increased and is negligible for small values which yield camera/base angles of greater than 80° , but the indeterminate position of the measurement remains.

5.3.3.5. Image location problems.

The image location with respect to the CCD array can cause errors if the surface to be measured has sharp discontinuities either in form or contrast, has laser speckle or is outside the optimum range of reflectivity required by the sensing system, see Fig. 5.11.

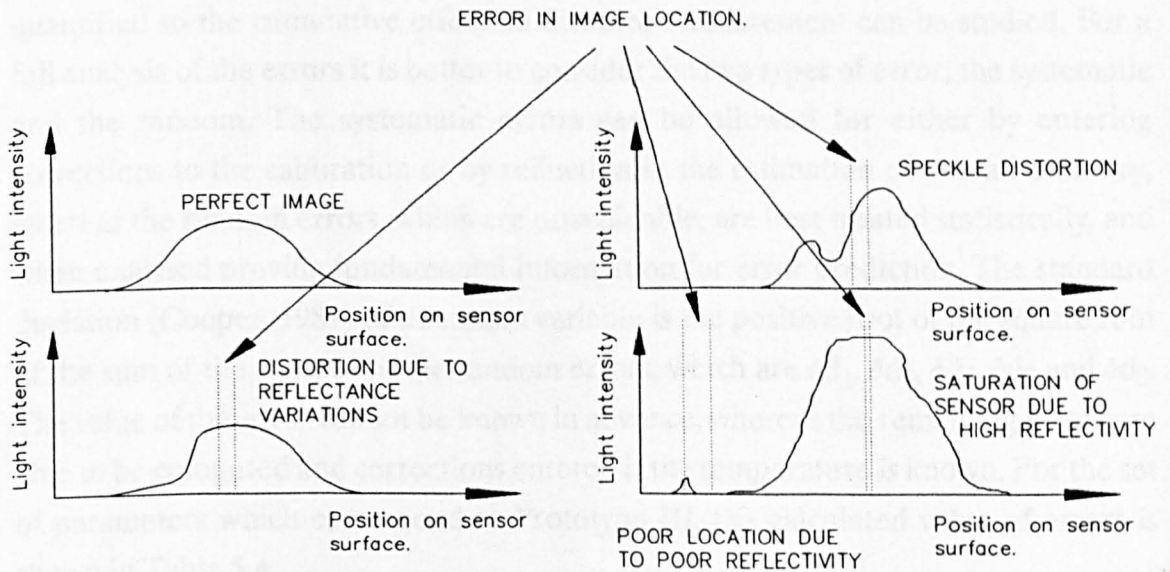


Fig. 5.11. Image location errors.

Some errors, such as the reflectance variation, can be partially eliminated by the *a priori* knowledge of what the image should look like at a given distance. However, if too little or too much light is imaged on the sensor then the sensor system will itself

distort the image either by quantising or by saturation of the sensor. Hence, if a perfect image is not formed then the subpixel algorithm will record the position of the image distorted by an error factor, which will result in an error of measurement which can be estimated by drawing the imaging error 'δi' onto the surface to be measured as shown in Fig. 5.6, and Equ. 5.12.

Equ. 5.12. $\delta d_g = \delta i \tan \theta$

5.3.3.6. Conclusion.

The errors that occur outside the camera have been analysed and quantified. The analysis pinpoints the places where changes could be made to minimise errors such as the choice of laser and where they cannot such as reflectivity of the measurement surface and the temperature gradient in the environment where measurement takes place.

5.3.4. Results of error analysis.

The internal and external errors of the complete triangulation system have been quantified so the cumulative effect on distance measurement can be studied. For a full analysis of the errors it is better to consider the two types of error, the systematic and the random. The systematic errors can be allowed for either by entering corrections to the calibration or by reduction in the estimation of overall accuracy, whereas the random errors, which are unavoidable, are best treated statistically, and when analysed provide fundamental information for error prediction. The standard deviation (Cooper, 1989) of a random variable is the positive root of the square root of the sum of the squares of the random errors, which are δd_1 , δd_4 , δd_6 , δd_7 and δd_8 . The value of this error cannot be known in advance, whereas the remaining errors are able to be computed and corrections entered if the temperature is known. For the set of parameters which correspond to Prototype III, the calculated value of errors is shown in Table 5.4.

Error name		Error type		Distance error ranges / mm		
		Random	Systematic	Min distance	Camera axis	Max distance
Sensor expansion	δd_2		✓	0.03	-	0.7
Camera expansion	δd_3		✓	0.07	-	1.9
Base expansion	δd_5		✓	0.14	0.25	0.9
Image location	δd_1	✓		0.05	0.12	1.3
Interpolation	δd_4	✓		0.02	0.04	0.45
Laser pointing	δd_6	✓		0.02	0.45	5.1
Atmospheric	δd_7	✓		0.00001	0.0003	0.0013
Surface problems	δd_8	✓		0.13	0.24	0.85
Statistical standard deviation of random error.				0.14	0.525	5.35

Table 5.4. Theoretical errors in distance measurement.

The parameters that were used in this analysis are given in Table 5.5.

<p> $l = 0.7\text{m}$, the length of the base of the triangulation triangle. $f = 0.05\text{m}$, focal length of lens. $\theta = 53.6, 67.6, 83.3$ degrees, the angle between measurement base and the measurement points at minimum, camera axis and maximum distance. $\theta_2 = 14$, half the angular field of view. $a_{cam} = 15 \times 10^{-6}$, the expansivity of the camera body. $a_{base} = 15 \times 10^{-6}$, the expansivity of the base line. $a_{sil} = 2.6 \times 10^{-6}$, the expansivity of silicon. $D = 26.62$ m, sensor length. $n = 2048$, the number of pixels. $T(\text{base}) = 10^\circ$, the temperature range of the base. $T(\text{camera}) = 10^\circ$, the temperature range of the camera. $T(\text{sensor}) = 20^\circ$, the temperature range of the sensor. $\delta s = 0.1$, the subpixel accuracy. $C-S = 0.43\mu\text{m}$, the difference between the calibration and the interpolation. $\delta\theta = 0.1\text{mrad}$, the pointing stability of the laser diode. $dT/dR = 1.0$, the temperature gradient. $\delta i = 0.1$, the error in image location. </p>

Table 5.5.

The calculated errors shown in Table 5.4. are likely to be the maximum encountered as the values used are extremes. It should be expected that when using the system where some of these parameters such as temperature is constant or measures have been taken to ensure a better response, then better results will consistently be obtained.

For a number of calibration and interpolation tests carried out over a variety of distances, and a configuration with parameters approximately the same as used for the analysis in Table 5.4, an average standard deviation of 0.361mm was obtained which compares favourably with the predicted value. Further analysis of this is carried out in the chapter 6.

The conclusions of this work are that when designing an optical triangulation measuring system with minimum errors for a selected range, the variable parameters require careful consideration as several configurations are possible. For a comprehensive analysis of a given design a computer simulation of the results is desirable where errors can be assessed and "trade offs" made between the competing parameters. A Computer Aided Design (CAD) system has been developed to model various configurations to assess non-linearity, range and dimension, this is the ideal place for the error analysis work to be included to allow all the effects of altering parameters to be taken into account. This CAD system is described in chapter 6.

5.3.5. Conclusion.

The practical testing of the prototype was carried out on an optical bench with an interferometer integrated into a computer controlled calibration and interpolation system. A number of tests were carried out with several hundred measurements per test. The interferometer provided the means of assessing the error in each measurement and standard deviations for the data were computed. These results are discussed in chapter 6. An important point to note is that the error measurement system obeyed the Abbe principle which states that measurements are best taken along the measurement axis like a micrometer rather than remote from it as with a pair of Vernier callipers. Hence, the measurements were taken along a mutual axis for minimum errors in the measurement.

All of the factors that contribute to the errors of measurement have been analysed. Important information about the origins of large errors can be found and, if possible, steps taken to reduce them to acceptable levels. Furthermore, comparisons can be

made between predicted errors and actual errors to see whether there are other factors influencing measurement and to see of further precautions need to be made.

5.4. TRIANGULATION SURVEYING ERRORS.

5.4.1. Introduction.

A configuration favourable to the production of a general surveying system incorporating optical triangulation is for the measuring system to rotate about the camera/laser axis so that the laser pointer describes a cross section when viewed from a position perpendicular to this measurement plane. The advantage of this arrangement is described later but clearly this is not the only configuration that could be used to collect spatial data. However, certain structures, such as tunnels benefit from this configuration.

Measuring the distance from an optical triangulation system to a structure is effected by means of mechanically holding the measuring system while a measurement is made. When a number of measurements are required to a multiplicity of positions on the structure surface and this procedure is repeated at number of locations, the measuring errors of each of these procedures will be accumulated; these have been covered in the previous section.

There are two further classes of error that require investigating, first the errors in relating the individual points that make up a cross section to each other, and second those that relate to the accuracy with which the cross sections are located one to another. The first errors concern the mechanical design of the apparatus that holds the measuring system and the second are related to the method of surveying required to locate the cross sections. In detail these errors are:

- (i) **Mechanical errors:** (a) eccentricity in the rotation axis due to the measuring and rotation axes not being coaxial, (b) angular measuring errors caused by the rotation system or angle measuring system, (c) bearing errors and backlash caused by lack of fit of the bearing used to provide the rotation of the measuring system, and (d) deviation errors if the laser does not describe a true plane.

(ii) **Survey errors:** (a) Angle of orientation errors with respect to verticality, (b) Position errors with respect to tunnel or structure locally, and (c) Positional errors with respect to the method of surveying used to coordinate cross sections or to relate to the surveying datum.

The errors will be analysed in this order in the next section.

5.4.2. Mechanical errors.

5.4.2.1 Introduction.

The errors particular to the triangulation system have been covered in section 5.3. The errors that result from the use of this system, essentially mechanical errors, are covered in this section. The design must limit these errors to acceptable limits, in the context of a standard deviation of 0.3 mm from the measuring system, the additional errors should, ideally, not be more than one tenth of this figure except in the case of angular errors, in which case errors which approach this value would not be unreasonable.

5.4.2.2. Laser alignment errors.

The laser profiler consists of a fixed laser source emitting a collimated beam of light normal to the axis of rotation of the measuring arm which impinges on the surface under inspection. Thus, for credible results, the laser source must be correctly fitted to the axis of rotation.

The laser can be calibrated at any suitable angle to the axis of rotation that fulfils the condition of always being in the same plane as the sensor active area when traced back through the imaging system into the object space. However it is possible that instead of the beam tracing out a plane it traces out the surface of a cone with a conic section for the profile, see Section AA in Fig. 5.12. When the beam is not perpendicular to the axis, which in turn must be horizontal, the profile will be an irregular conic section, making it impossible to determine the correct surface coordinates.

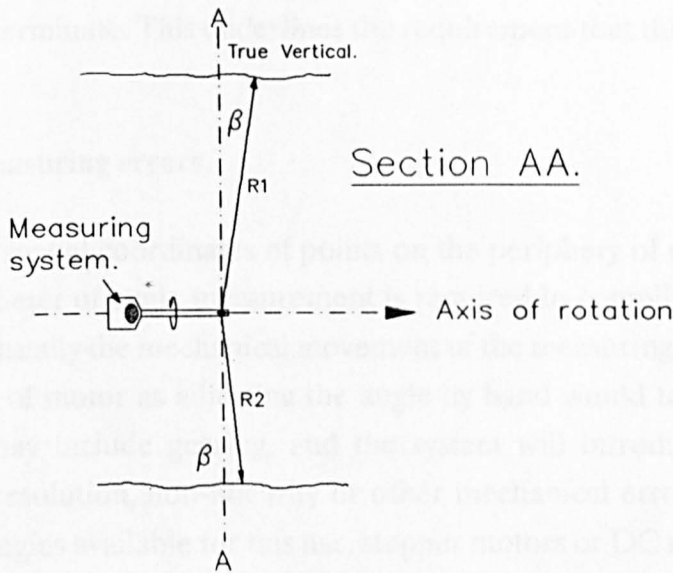


Fig. 5.12. Laser conic section.

A procedure that was adopted to set up the laser to ensure that it was perpendicular to the axis of rotation was achieved by ensuring that the laser impinges on three points which are on the same line one of which requires a rotation through 180° of the measuring arm as shown in Fig. 5.13.

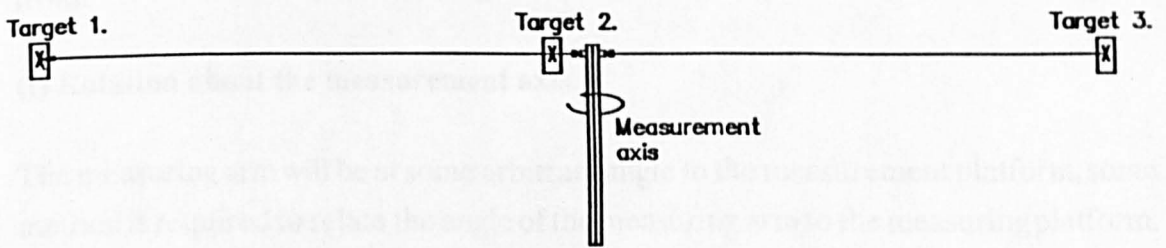


Fig. 5.13. Setting up procedure for rotation of the laser in a plane.

The error that occurs in distance measurement will differ with distance from the measuring axis. If the surface to be measured is parallel to the measuring axis it is possible to compute the error in the measurement which will consist of a small error in distance and an error in the spatial coordinates of the measured point as the system as a whole will compute the position as being on a plane perpendicular to the measuring axis and on the optical axis of the laser system. However, if the surface to be measured is not parallel to the measuring axis it is not possible to compute the error in distance measured as there is no *a priori* knowledge of the surface and hence

the error is indeterminate. This underlines the requirement that this parameter is set up correctly.

5.4.2.3. Angle measuring errors.

To measure the spatial coordinates of points on the periphery of cross sections, the additional parameter of angle measurement is required to compliment the distance measurement. Usually the mechanical movement of the measuring system is effected with some form of motor as adjusting the angle by hand would take too long. This motor system may include gearing, and the system will introduce errors due to backlash, poor resolution, non-linearity or other mechanical errors. There are two suitable technologies available for this use, stepper motors or DC motors and optical encoders. The characteristic errors associated with each of these motors can be gained from the manufacturers literature, and simple "in service" checks.

The position at which the measurement takes place relative to the complete mechanical system must be established. The system may be assumed to be level by some initialising procedure such as those standard for the use with the conventional theodolite or level. This platform will be level to the accuracy provided by the spirit bubble and will contribute an error which must be added to the errors that accrue from:

(i) Rotation about the measurement axis.

The measuring arm will be at some arbitrary angle to the measurement platform, some method is required to relate the angle of the measuring arm to the measuring platform. This starting angle may be determined either by some predetermined starting point, or by reference to a spirit bubble of known sensitivity, say, 10" per graduation, which is mounted on the measuring arm, see Fig. 5.14.

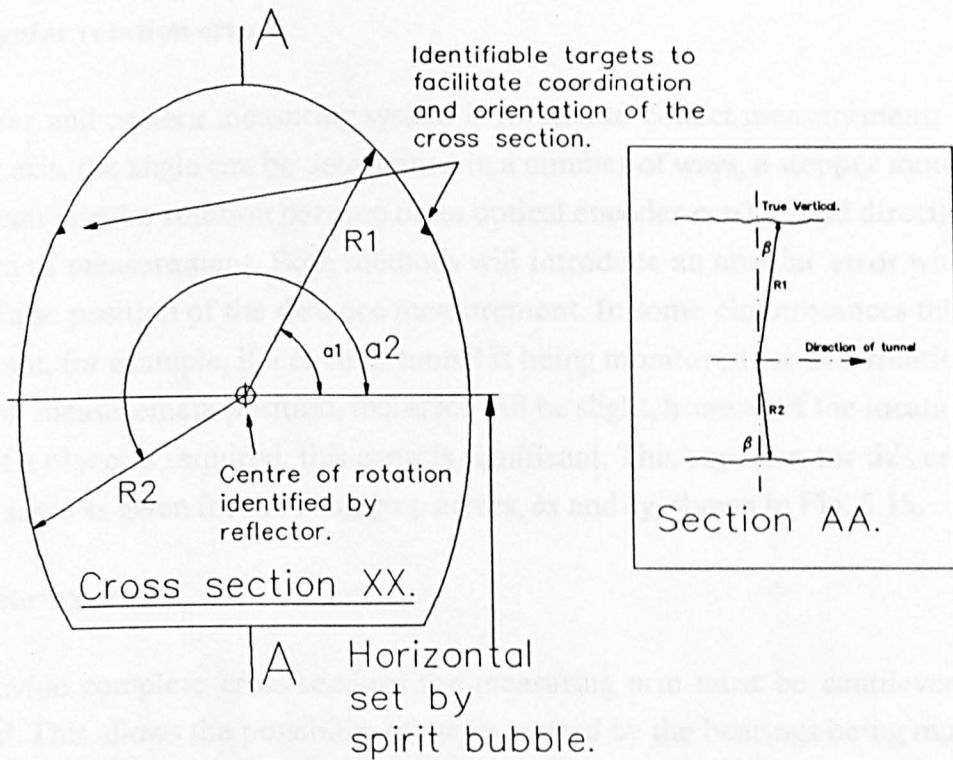


Fig. 5.14. Establishing a starting angle.

The measuring arm can then be adjusted to this degree of precision. This procedure leads to a error of $\delta x = R \cdot \cos(\delta\alpha)$, $\delta y = R \cdot \sin(\delta\alpha)$ where R is the radius from the central measurement position (R will vary point to point), see Fig. 5.15.

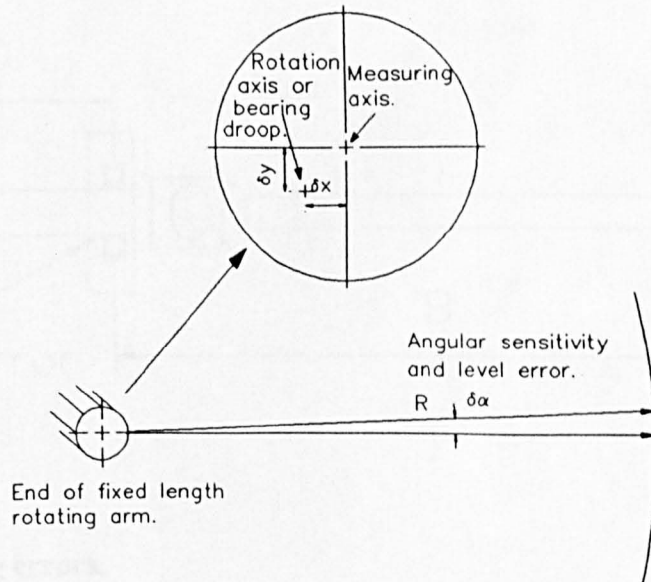


Fig. 5.15. Starting position error.

(ii) Angular rotation errors.

The laser and camera measuring system is rotated to collect measurements from a central axis, the angle can be determined in a number of ways, a stepper motor gives a constant angular rotation per step or an optical encoder can be read directly at the position of measurement. Both methods will introduce an angular error which will give a false position of the distance measurement. In some circumstances this is not important, for example, if a circular tunnel is being monitored for deformation from a central measurement position, this error will be slight, however if the location of an edge of a object is required, this error is significant. This equation for this error will be the same as given for the setting up errors, δx and δy , shown in Fig. 5.15.

(iii) Bearing errors.

To provide complete cross-sections the measuring arm must be cantilevered and rotated. This allows the possibility of errors caused by the bearings being more than desirable because of wear or lack of fit. The bearings would be designed to minimise this error but it must be a part of the error analysis. Fig. 5.16. shows the configuration of the bearing in relation to the measurement arm. the error in profile centre position will be given by $\delta x = (B + D/2) \cdot \tan(2E/D)$ and $\delta y = (B + D/2) \cdot \tan(2E/D)$.

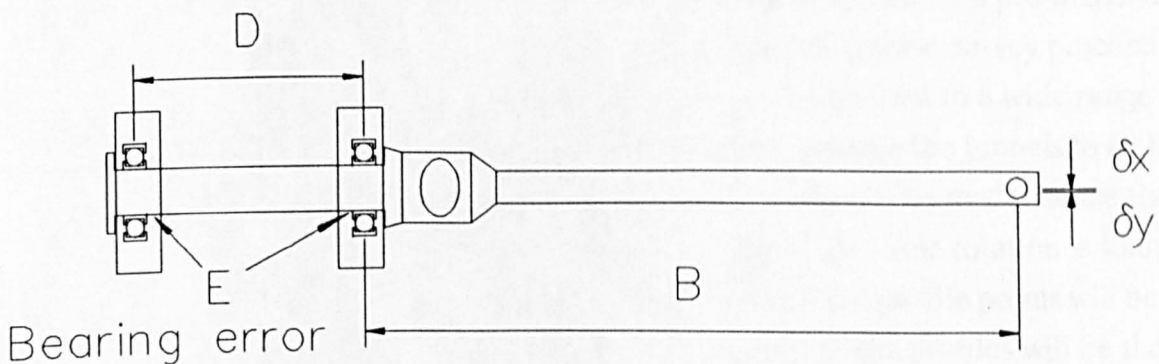


Fig. 5.16. Bearing errors.

5.4.2.4. Eccentricity.

The axis of rotation and the axis of measurement may not be coaxial which gives rise to a systematic eccentricity error. This error can also be written as $\delta x, \delta y$, see Fig. 5.15.

5.4.2.5. Summary.

The sum of all the errors covered in this section must be considered as contributing to errors in the spatial coordinates of the measured points. Some of these errors can be minimised in the design stage, others are susceptible to operator error. It should be possible for a good design to minimise these errors to the desired order of magnitude.

5.4.3. Survey errors.

5.4.3.1. Local errors.

The rotating laser profile measuring device is portable and can be arranged to indicate and measure a profile at almost any attitude and orientation. Thus, the profiler can measure the internal profile of a tunnel or ship-hull or the external shape of a building or clay model of a car. The positions of the profiles may be fitted to appropriate pre-marks, alternatively the position of the laser line may be marked on the subject. In both cases, marks on a tunnel wall, ship side, building face or clay surface will need to be surveyed to fix their position relative to a national or local control system.

Often tunnel profiles are required as part of a structural surveillance programme so that repeated measurement of the same profiles is necessary. In this situation, it is essential that the profile can be guaranteed to be vertical and that the pre-marks are identified in the resultant measured profile. Thus providing good survey practice is maintained the coordinates of the pre-marks may be determined to a wide range of accuracies. The survey operation can involve a traverse through the tunnels to fix the control stations from which observations to the pre-marks can be made, hence their coordinates determined. Providing the starting point of the laser rotation is known i.e. and in a vertical plane, the derived coordinates for all the profile points will be to the same coordinate system. Thus the errors in location of the profiles will be those normally associated with control surveys. See Fig. 5.17.

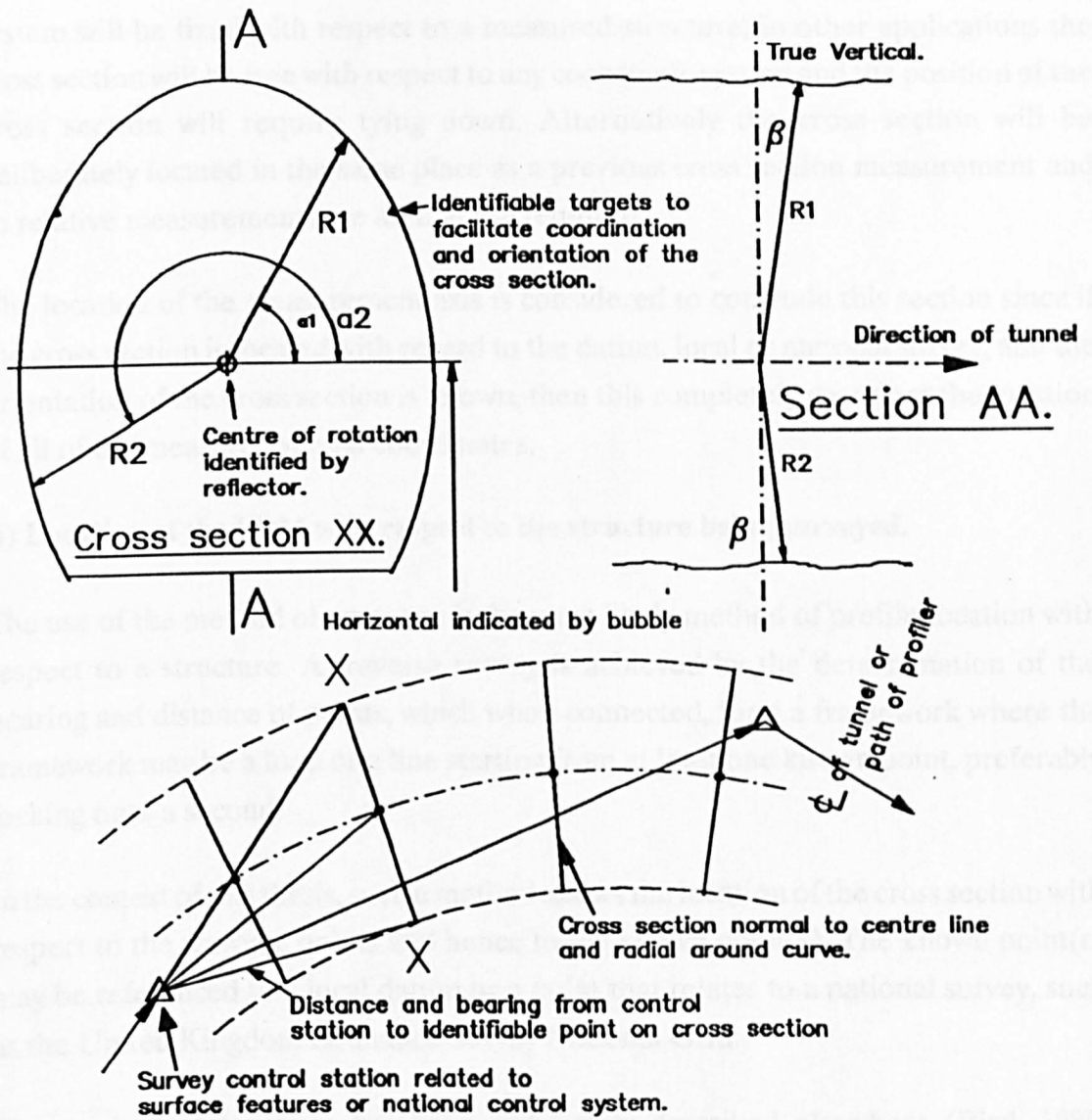


Fig. 5.17. Survey errors.

It is beyond the scope of this thesis to consider other cases where other schemes and associated errors would exist, such as surveying mine shafts, car bodies or rail tunnels at high speed. However, the successful use of this system of measurement in situations requiring regular cross sections is considered as it raises special problems, these are considered in the next section.

5.4.3.2. Cross section location errors.

The cross section measuring system will provide the spatial coordinates of a cross section at a given position, but this information is useless unless the spatial coordinates of that position and the orientation of that cross section is known. The position of the cross section may be determined in a number of ways, sometimes the measuring

system will be fixed with respect to a measured structure, in other applications the cross section will be free with respect to any coordinate system and the position of the cross section will require tying down. Alternatively the cross section will be deliberately located in the same place as a previous cross section measurement and so relative measurements are all that are required.

The location of the measurement axis is considered to conclude this section since if the cross section is located with regard to the datum, local or national survey, and the orientation of the cross section is known, then this completely describes the location of all of the measured spatial coordinates.

(i) Location of the EDM with respect to the structure being surveyed.

The use of the method of traverses is the most likely method of profile location with respect to a structure. A traverse survey is achieved by the determination of the bearing and distance of points, which when connected, form a framework where the framework may be a loop or a line starting from at least one known point, preferably locking onto a second.

In the context of this thesis, such a method allows the location of the cross section with respect to the traverse points and hence to the known point(s). The known point(s) may be referenced to a local datum or a point that relates to a national survey, such as the United Kingdom Ordnance Survey National Grid.

The method of traverses has been adequately described elsewhere (Bird, 1989, Garner, 1976, Manual of photogrammetry, 1980) and it is sufficient to note that the accuracy of the traverse is initially a function of the methods and equipment used which can be improved statistically by multiple observations. Hence, the accuracy is, to an extent, only limited by cost.

The method of traverses provides a means of locating the cross section, this will entail further errors to be added to those of the traverse as multiple measurements are not to be preferred because of the time involved. This error will depend on the procedure adopted, the operator and the equipment used. It is likely that the error in locating the centre of the cross section will exceed the errors inherent in the cross section measurement. This is not as bad as it at first seems because the data are generally required for different purposes, the cross section data for deformation analysis and the location of the cross sections for wriggle surveys, inventory or quantification. The accuracies for a wriggle survey are less rigorous than for deformation analysis.

(ii) Location of the measurement axis with respect to the EDM.

The measurement axis can be determined with a piece of Electronic Tacheometry equipment by mounting a prism on the end of the measuring arm, see Fig. 5.18.

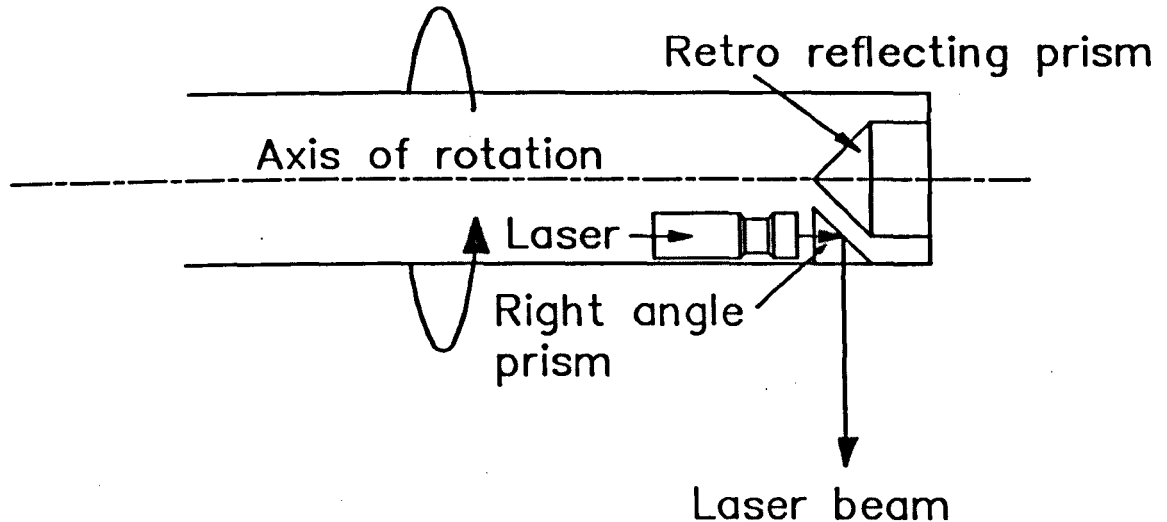


Fig. 5.18. Location of the measuring axis.

The location of the prism can be determined with the EDM and related to the general survey. An offset is required to correct for any displacement of the measurement plane of profiler, however designs could be implemented without the requirement for this offset which would obviate the necessity for being as close to the measurement axis with the EDM to avoid additional errors.

(iii) Orientation of the cross section with respect to the EDM or structure.

Having located the centre of the measuring axis with respect to another survey system there remains a number of further restraints that are required to fully constrain the cross sections location.

(a) **Verticality.** The cross section has not been so far constrained with respect to verticality. The adjusting of the platform so that this is the case is a trivial matter with the built in spirit bubble. The verticality is then fixed to the accuracy of the spirit bubble, typically 30" per division.

(b) **Horizontal orientation.** The orientation of the cross section plane can be at any angle to the traverse station unless the position is further constrained. This

constraint can occur in a number of ways, but because of the constraints already imposed it is only necessary for the cross section to be located in one more place at the same level as the measuring axis.

The location of a point on the profile can take place at any time while the system is set up. This can be achieved simply by rotating the laser beam until it is at 90° from the vertical and marking the position that the laser impinges on the surface. An EDM prism can then be held on that position and measurements taken together with an allowance for the prism offset. For increased accuracy this procedure could be repeated at a further rotation of 180° . The measurements can be made with EDM and theodolite or better with an Electronic Tacheometer.

A further technique which may be employed is the retrospective fixing of these parameters by the method ensuring that each profile cross section is perpendicular to the wall surface. This would be a reasonable approach where the tunnel is nearly straight and the saving in surveying time was important. However, this method would not locate the cross sections as accurately as the previous method.

5.5. CONCLUSIONS.

The analysis of all of the error sources has taken place for the case of measurement of cross sections of such structures as sewers, rail and road tunnels. All of the errors have been analysed to establish the cause of the error and where possible to quantify it. This analysis allows the choice of the correct components in the design of the optical triangulation technique a surveying instrument and identifies the errors that will be added to overall errors from the use of the system as a surveying tool. Further analysis is required if other structures are to be surveyed and additional techniques devised.

6. RESULTS.

6.1. SYNOPSIS.

This chapter describes the results of a number of tests that were carried out to investigate the performance of the optical triangulation measuring system. The results presented are a direct result of the experience gained from the prototypes described in chapter 4, and the desire to minimise the errors described in chapter 5.

This chapter is divided into the following sections:

- (i) calibration tests,
- (ii) subpixel resolution tests, and
- (iii) correction to triangulation non-linearity.

The results show that an advance to the technology associated with optical triangulation systems has been achieved, this is as a result of a greater understanding of the calibration, interpolation and imaging processes, together with a new opto-mechanical design for correction of the undesirable non-linearity characteristic.

6.2. INTRODUCTION.

Optical triangulation measuring systems have been shown, in chapter 4, to be able to collect data appertaining to full, or partial, cross sections of structures with speed, accuracy, and efficiency. The errors associated with using this type of measuring system in a surveying process have been analysed in chapter 5. However, the problems of occlusion and non-linearity have not been dealt with, these are now analysed in this chapter.

Extensive calibration tests were carried out to analyse the performance of the measuring system with specific tests on the subpixel accuracy achieved. Further work

is reported which concerns a correction to the non-linearity of the triangulation scheme and the software that was developed for testing.

6.3. CALIBRATION TESTS.

6.3.1. Introduction.

The triangulation system described in this thesis is a device for measuring distance so traceability to national, and ultimately international, measurement standards needs to be considered. All commercially produced distance measuring instruments, from tapes to interferometers, should be able to show the path back to these standards if the measurements performed are to be meaningful. However, for the purposes of research and development, such stringent measures are not so necessary if other precautions are taken. In the context of the research described in this thesis an interferometer was used to calibrate and check the measurement process that had an inherent accuracy, linearity and repeatability, far better than possible from the triangulation measuring system. Hence, the task of ensuring traceability of the calibration, although important, was not considered essential at this stage because of the inherent stability and accuracy of the interferometer.

6.3.2. Calibration test rig

The theory of operation of the interferometer having been described in appendix 1, the physical calibration rig is now described. The aim was to produce a stable method of calibrating the triangulation system. The method had to be automatic because of the quantity of information involved. A Hewlett Packard interferometer was identified as a means of accurate measurement, a calibration rig was made incorporating this and other essential components described in the following sub sections.

6.3.2.1. Optical benches.

Two, three metre optical benches, were obtained and butted together to form a six metre run, these were then placed on three stable wooden benches that were connected together. The benches were fixed via an optical table to a granite optical bench of considerable weight which was three metres long and perpendicular to the other optical benches. This arrangement ensured that the minimum of external influences would affect measurements that would be taken from the granite bench,

where the triangulation system was to be mounted, to the six metre optical benches where the target trolley was to be moved.

The six metre optical benches were levelled, straightened and squared to the granite bench by the use of a laser, target and tape measure. The optical bench had adjustable feet for height adjustment, the maximum error was thought to be approximately a millimetre, which was sufficiently accurate to allow the trolley to traverse the whole length of the bench without going out of alignment with the interferometer.

6.3.2.2. Trolley.

The trolley was made of Aluminium with roller bearing wheels appropriately spaced to ensure that they would allow the trolley to move along the six metre bench. The mechanical design of the trolley is shown in Fig. 6.1.

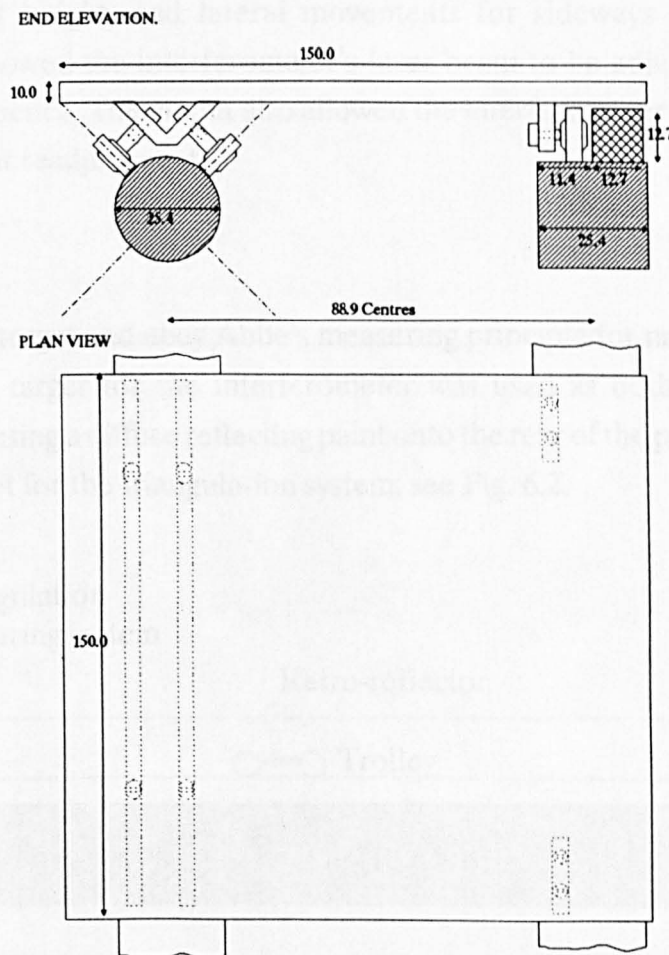


Fig. 6.1. Trolley design for target movement.

The trolley was connected by some lightweight waxed cord to a 'v' pulley mounted on a stepper motor at one end of the bench, and a jockey pulley at the other. The stepper motor could then move the trolley from one end of the optical bench to the other.

6.3.2.3. Interferometer.

The interferometer was required to measure the distance between the triangulation system and the target. The interferometer was mounted at one end of the trolley bench and the triangulation system at the other. The interferometer could be zeroed, this meant that the data from the interferometer would be in the right sense and only missing an easily measured offset to obtain the distance from the triangulation measurement axis to the target.

The interferometer was securely mounted on two optical mounts which had adjustments for height, and lateral movements for sideways adjustments. This arrangement allowed the interferometer's laser beam to be adjusted to be parallel with the trolley bench. The mount also allowed the interferometer to be removed and replaced without readjustment.

6.3.2.4. Target.

To simplify the target and obey Abbe's measuring principle for minimum errors, the retro-reflecting target for the interferometer was used as both targets. This was achieved by painting a diffuse reflecting paint onto the rear of the prism case and using that as the target for the triangulation system, see Fig. 6.2.

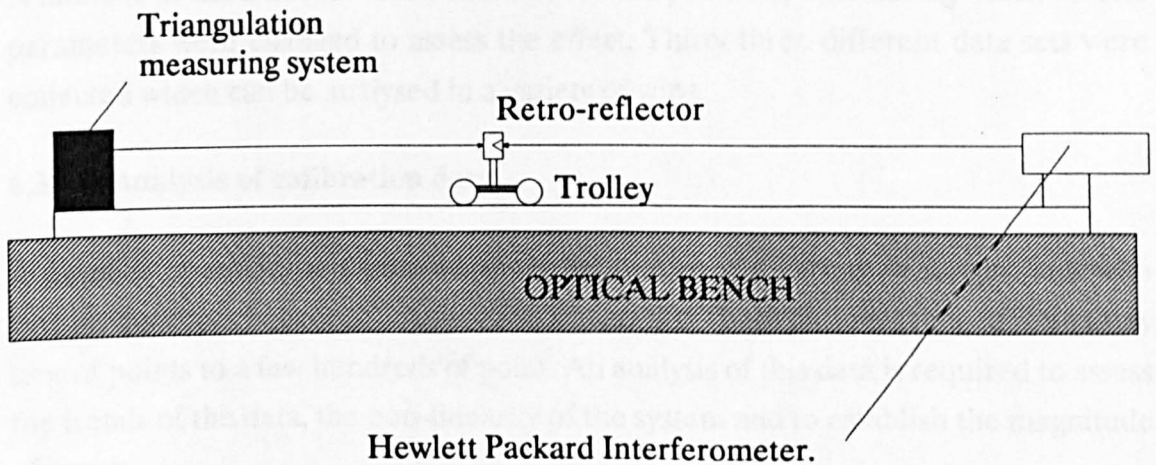


Fig. 6.2. Configuration of the calibration system.

6.3.2.5. The prototype mount.

The prototype was securely fixed to the granite bench which was levelled and securely located on the floor of the laboratory. This was achieved with a heavy multi-axis bracket that allowed all of the adjustments necessary to ensure that the prototype was in the correct orientation.

6.3.2.6. Atmospheric conditions.

The atmospheric conditions in the laboratory, though not ideal, were not sufficiently varied to alter the triangulation measurements, and if temperature or pressure corrections were required for the interferometer, these could easily be entered into the system in the form of a correction factor.

6.3.3. Calibration procedures.

The programming methods to collect the intensity data from the CCD camera, the basis of triangulation measurements, has been described in chapter 4 in the section covering software for Prototype III. A number of different procedures were adopted to analyse the performance of the triangulation system. These varied from multiple measurements at each measurement point, a piecewise method of analysing the data due to the problems of non-linearity, and random measurement positions for the interpolation measurement.

6.3.4. Calibration results.

A number of calibrations were carried out over a period of time during which several parameters were changed to assess the effect. Thirty three different data sets were collected which can be analysed in a variety of ways.

6.3.4.1. Analysis of calibration data.

A number of calibration tests were carried out, over a variety of ranges, and with various distances between the measurement points. These data sets ranged from a few tens of points to a few hundreds of point. An analysis of this data is required to assess the trends of the data, the non-linearity of the system and to establish the magnitude of errors.

The data from CALIB2 is shown in Fig. 6.3, with the residuals from a least squares best fit of a polynomial of degree four to this data. The effect of fitting a polynomial to the data can be seen in the residual data oscillating either side the mean error with the characteristic number of inflections of a fourth degree polynomial superimposed on the noise. This shows that a polynomial is not the best method of calibration for this data.

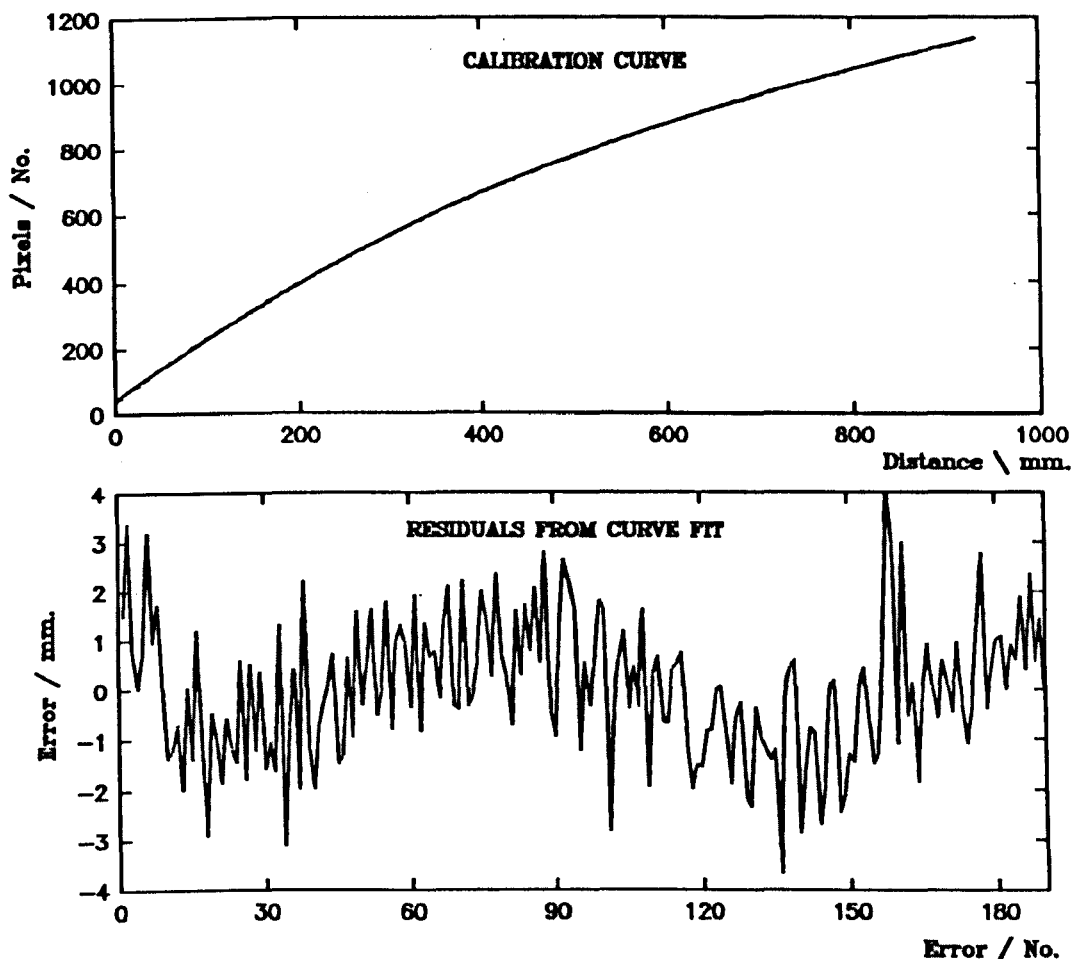


Fig. 6.3. Calibration data from CALIB2 and line fit error data.

The standard deviation for the residual error data was 1.4mm, which is poor considering that the data was collected at close range. The magnitude of the error is partly explained by the method of analysis by a polynomial curve fit but this still left a large random error element which it was thought could be improved by better programming and calibration methodology. Improvements in the data acquisition method were achieved by:

- (i) averaging the centroid data over a number of calibration samples,

- (ii) adjusting the centroid algorithm by better thresholding to gain a more suitable window to compute the centroid,
- (iii) improving the interferometer data collection hardware and software to eliminate spurious data being collected, and
- (iv) allowing a longer period of time between the target trolley stopping and the data being collected.

These changes gave an overall improvement to the error data collected in the set CALIB6 shown in Fig. 6.4.

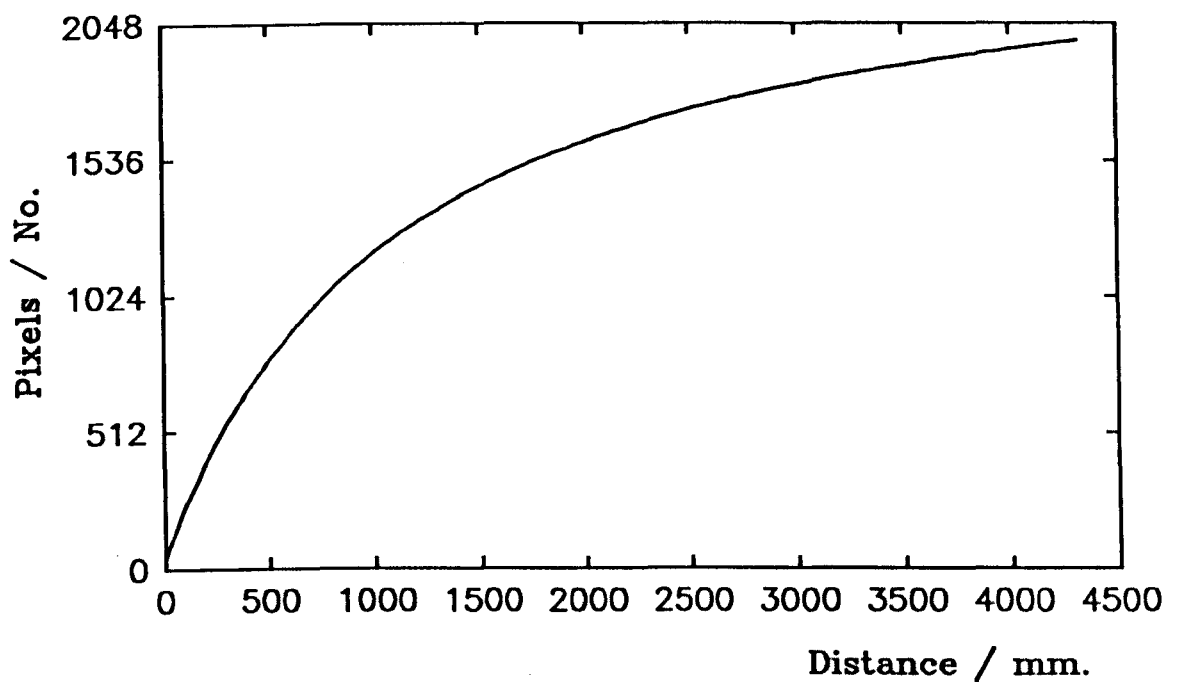


Fig. 6.4. Calibration curve for CALIB6.

To eliminate the problem of a poorly fitting polynomial experienced in the previous example shown Fig. 6.3, ten polynomial curves were fitted to successive data points and the residuals noted. These residuals are shown in Fig. 6.5, where no oscillation of the error data can be attributed to the poor fit of a single polynomial.

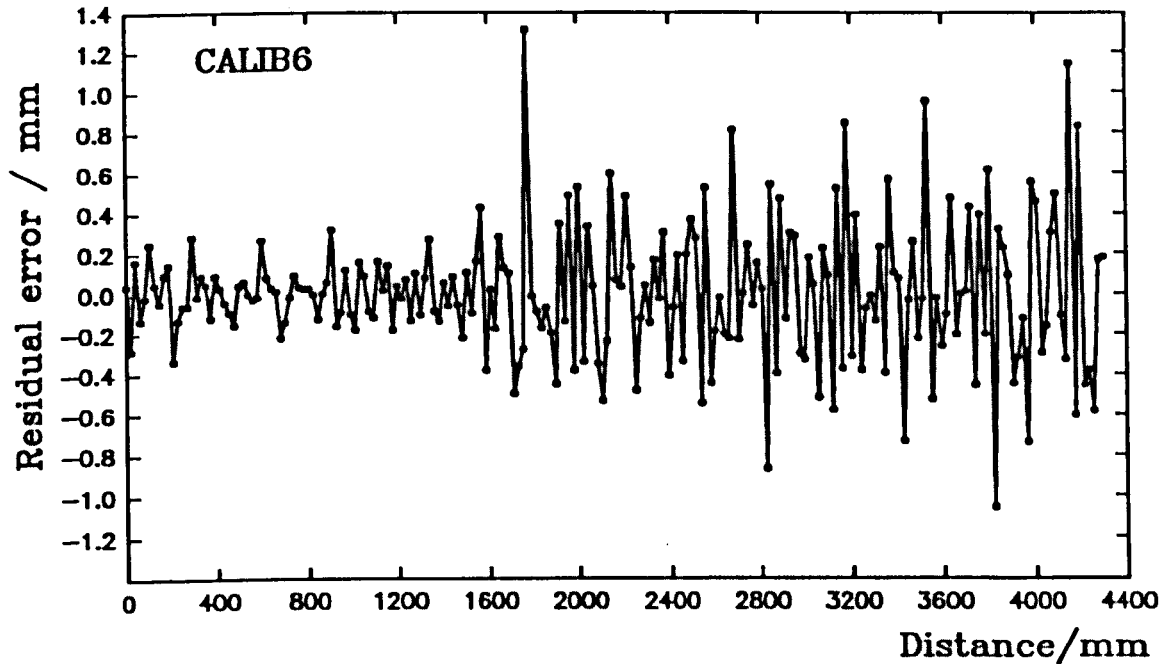


Fig. 6.5. Residuals from curve fitting algorithm on CALIB6 data.

The standard deviation of the error data was 0.33mm. It can be seen here that the errors increase at greater distances from the measuring axis as would be expected from the non-linearity of the system. However, this does not illustrate any trends in the data collection process, so it is desirable to find some alternative way of estimating the performance of the system. The method that was perceived to be the best at characterising the performance of the system was to use the subpixel accuracy, because this is independent of the non-linearity of the system and, all other factors being equal, will be the same for the whole range of measurement. To compute the subpixel accuracy the gradient of the calibration curve was computed for successive pairs of calibration points, this was then multiplied with the error data to give the subpixel accuracy achieved at successive calibration points. The subpixel accuracy is given with respect to pixels and is independent of the size of the sensing elements. The subpixel accuracy for the same data set is plotted in Fig. 6.6.

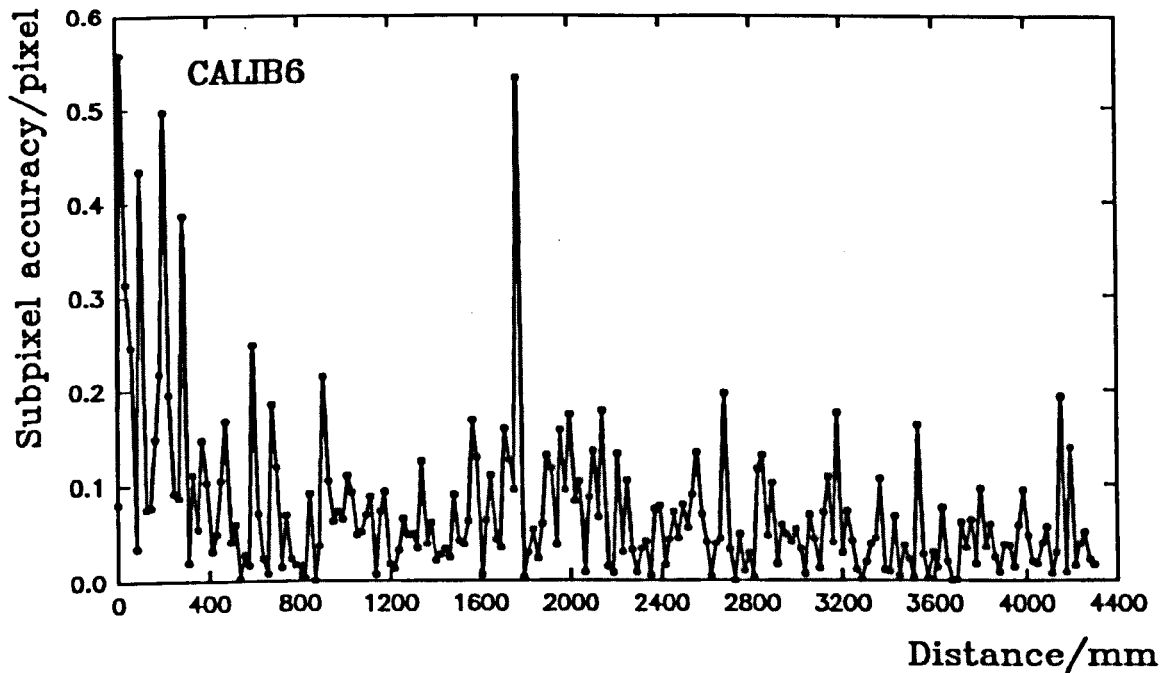


Fig. 6.6. Subpixel accuracy plot for CALIB6.

The graph shows some interesting features which can only be explained by knowledge of the way in which the system was set up. The errors close to the measuring axis are greater than those from about one metre to the end of the range, which appear to be roughly equal. The explanation is that the camera was out of focus at the close ranges which resulted in a large, speckle affected image, which was not suitable for accurate measurement due to the random nature of the speckle pattern. The errors do show a tendency to oscillate, but no conclusion can be reached at this stage as there is not enough data on which to base any judgment. The standard deviation for the subpixel accuracy was 0.085 pixels which compares favourably with other data collected to demonstrate subpixel accuracy.

The analysis of the subpixel accuracy and calibration data illustrates a problem that was not noticed in the calibration trials. The calibration data was not representative of a mean of measurements because the averaging only took place over a short time-scale, and there was no smoothing between calibration points. If the procedure had been adopted, that has been demonstrated in the improvements shown in the analysis of CALIB2 and CALIB6, then the overall accuracy achieved in the interpolation trials would have been substantially improved. In fact, using local data

for piecewise linear interpolation resulted in errors larger than those shown for the calibration data analysis.

6.3.4.2. Large calibration data file CALIB4.

To provide greater statistical accuracy of measurement a calibration test was initiated which collected data at closer intervals than before, every 20 mm. This data was stored in the file CALIB4, the result of which are shown in Fig. 6.7.

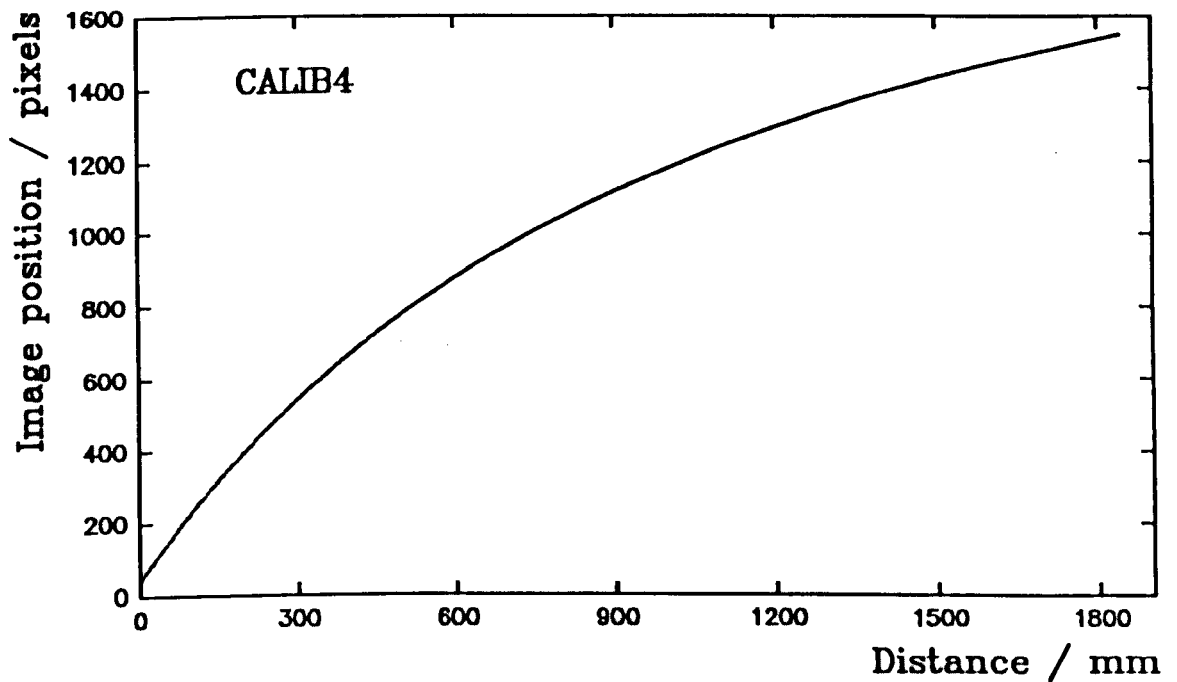


Fig. 6.7. Calibration plot of CALIB4.

This data was analysed by putting twelve separate curves through the data at successive ranges. The plot of the residuals, see Fig. 6.8, shows clearly the problem mentioned in 6.3.4.1. of the poor image formation at close range.

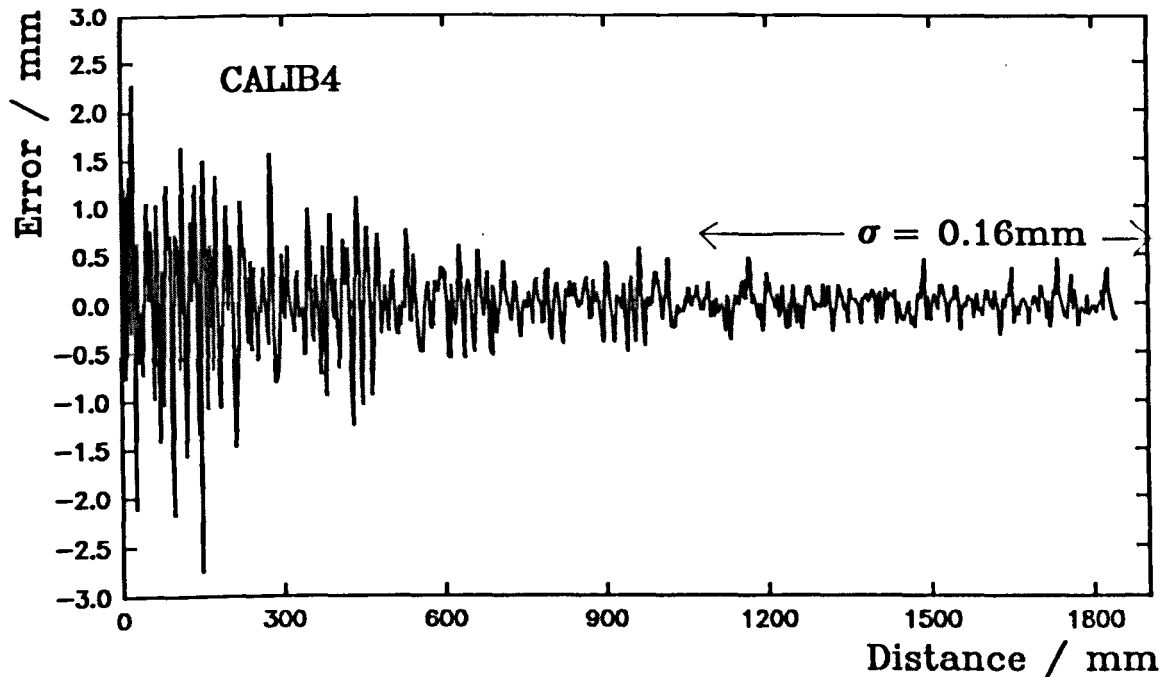


Fig. 6.8. Plot of residuals after curve fit.

The standard deviation, computed over the whole range was 0.44mm, a high figure because of the influence of the poor accuracy of the close range measurement. The standard deviation over the range 1000 mm to 1900 mm was 0.16mm, this is the figure that could be expected, over the whole range, if the Schleimplug condition were implemented in the camera optics.

6.3.4.3. Fitting an appropriate curve to the data.

The calibration data, which is collected at discrete points, must be interpolated to provide information for intermediate points. The method of using a polynomial of appropriate degree was considered in the previous section and was also used in Prototype I & II. Once the parameters of that curve are defined, it can be used to provide interpolation data, however, this method is inadequate for the following reasons:

- (i) a curve is not likely to fit the underlying function perfectly at all points over its range,
- (ii) a single curve will not take account of local variations such as lens distortion and sensor imperfections.

(iii) If a curve is found to fit the data over the whole range, then it is likely to require a large number of parameters and be computationally complex.

Instead of using a polynomial, there is a further method which requires evaluating, that of fitting a single curve defined by the derived equation for the triangulation system. To test this method the calibration data, CALIB6 was chosen, and the Ji curve (Equ. 3.8.) was fitted with a least squares algorithm to the data and the residuals plotted. Fig. 6.9. shows the results.

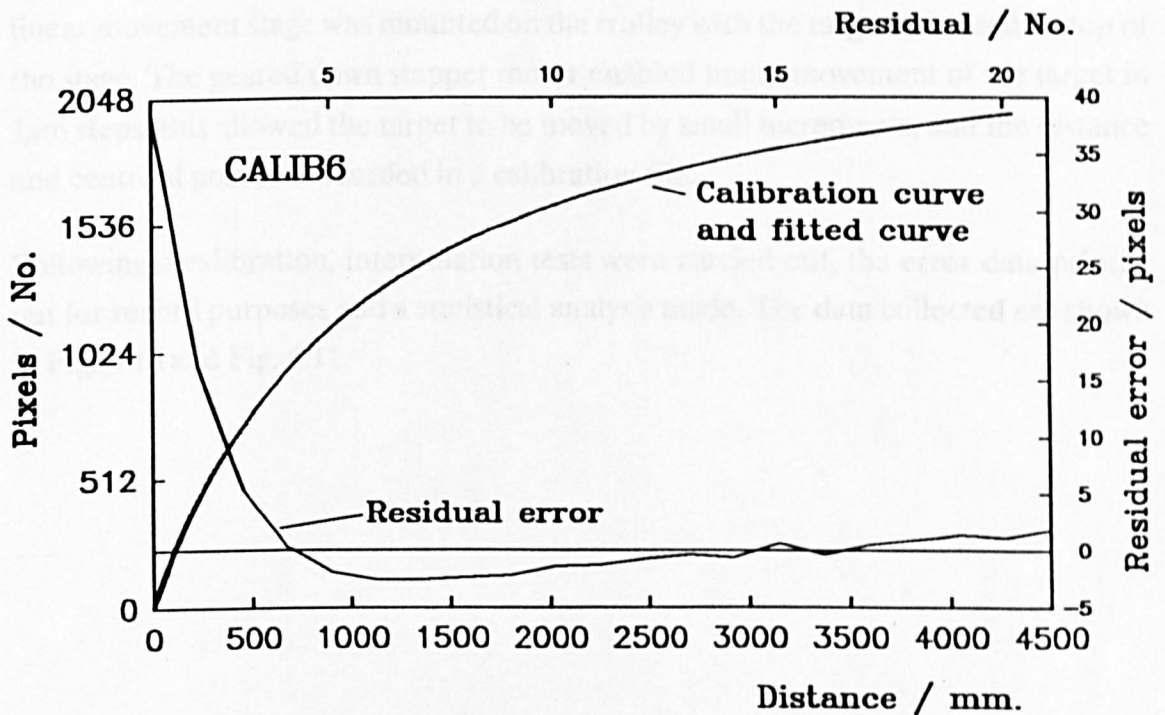


Fig. 6.9. Ji curve fitted to CALIB6.

The curve fits reasonably well for most of the latter section of the data, but does not fit so well at the start, furthermore, the error is significant, even where the curve is a good fit to the data. The disadvantages of this approach are the same as for the polynomial, the curve is not able to follow local deviations, and for a good fit the relationship has to be good over the whole range. In conclusion, this method is not suitable for use in calibration and interpolation, where the method of applying short curves fitted to small sections of the data appears to be a better method.

6.3.4.4. Analysis of data collected over a small range.

The previous tests dealt with an appropriate means of interpolating between the calibration points, and showed that with an appropriate method, the characteristic curve underlying noisy calibration data could be obtained. An analysis of the errors attributable to noise in the system was required, so measurements were taken over a very small range, where the characteristic change of the image with object position could be modelled as linear.

To test out the maximum accuracy and resolution available, a stepper motor driven linear movement stage was mounted on the trolley with the target mounted on top of the stage. The geared down stepper motor enabled linear movement of the target in $1\mu\text{m}$ steps, this allowed the target to be moved by small increments, and the distance and centroid position recorded in a calibration file.

Following a calibration, interpolation tests were carried out, the error data printed out for record purposes and a statistical analysis made. The data collected are shown in Fig. 6.10 and Fig. 6.11.

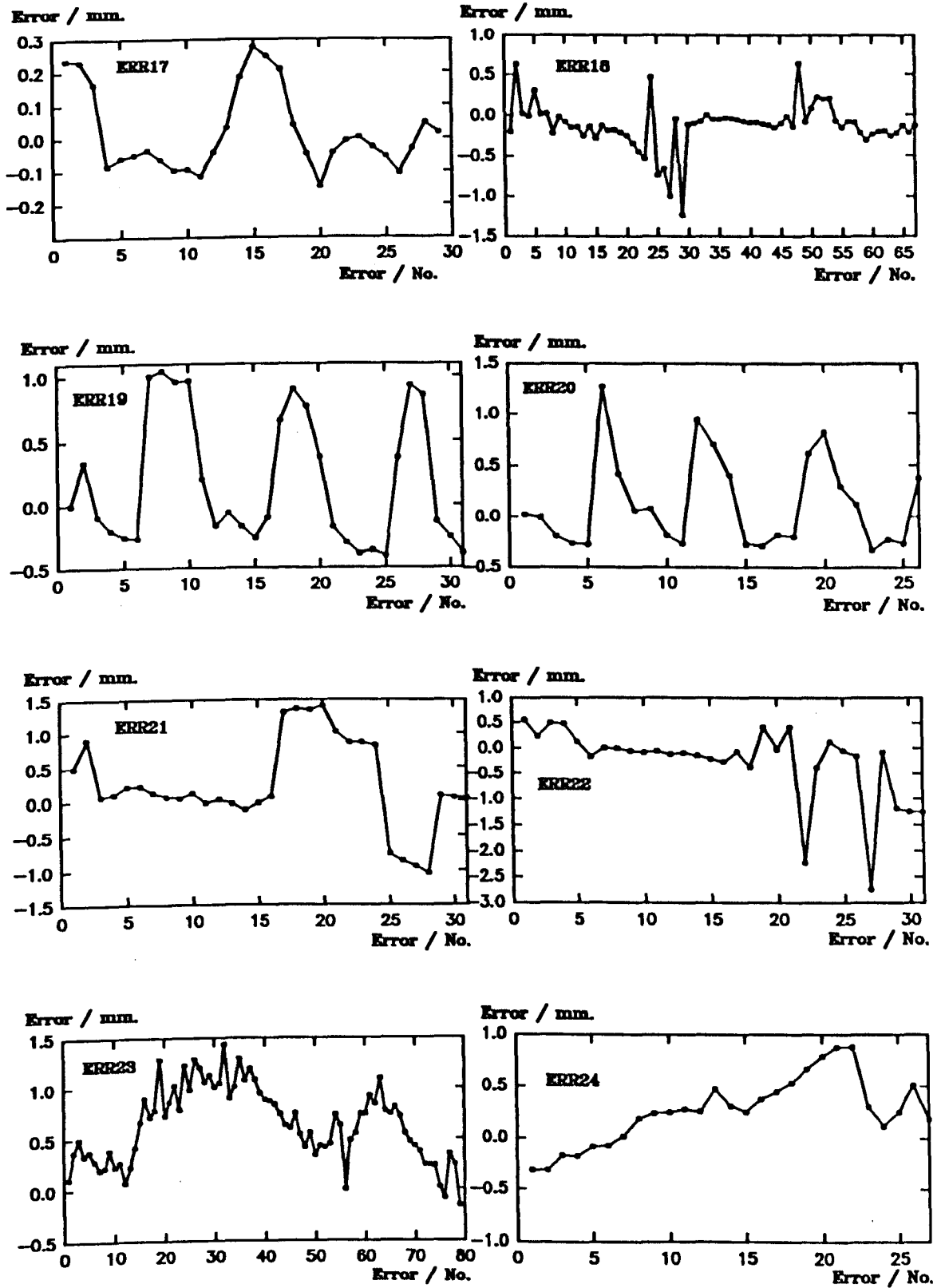


Fig. 6.10. Error sets ERR17-ERR24.

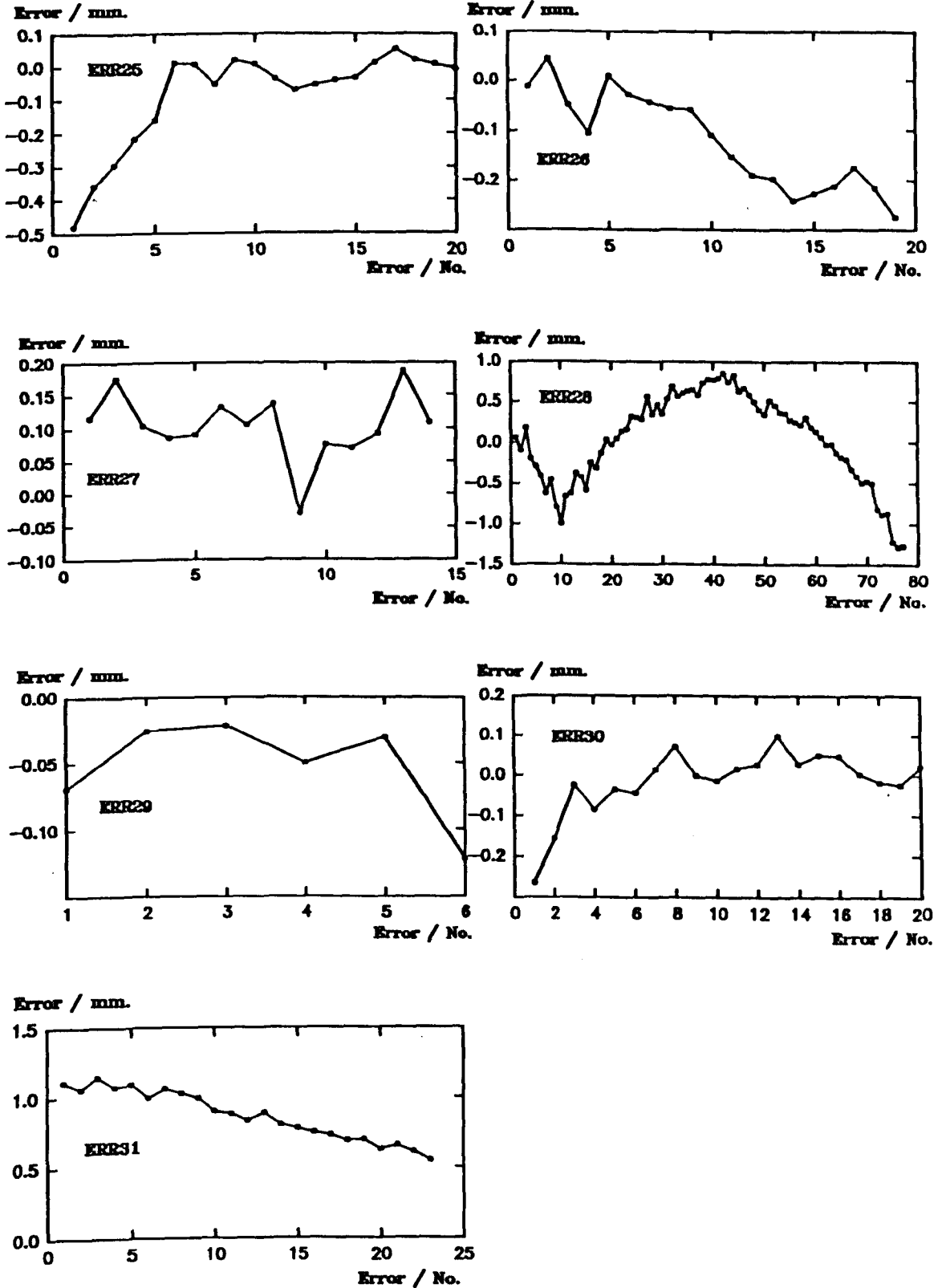


Fig. 6.11. Error sets ERR25-ERR31.

An analysis of this data can be made by reference to the data sets ERR18, and ERR23, which were collected at a distance of 2.5 and 3.5 metres from the profiler axis respectively.

(i) ERR18.

This set of data shown in Fig. 6.12, clearly shows the problem of using the calibration data directly with a piecewise linear interpolation.

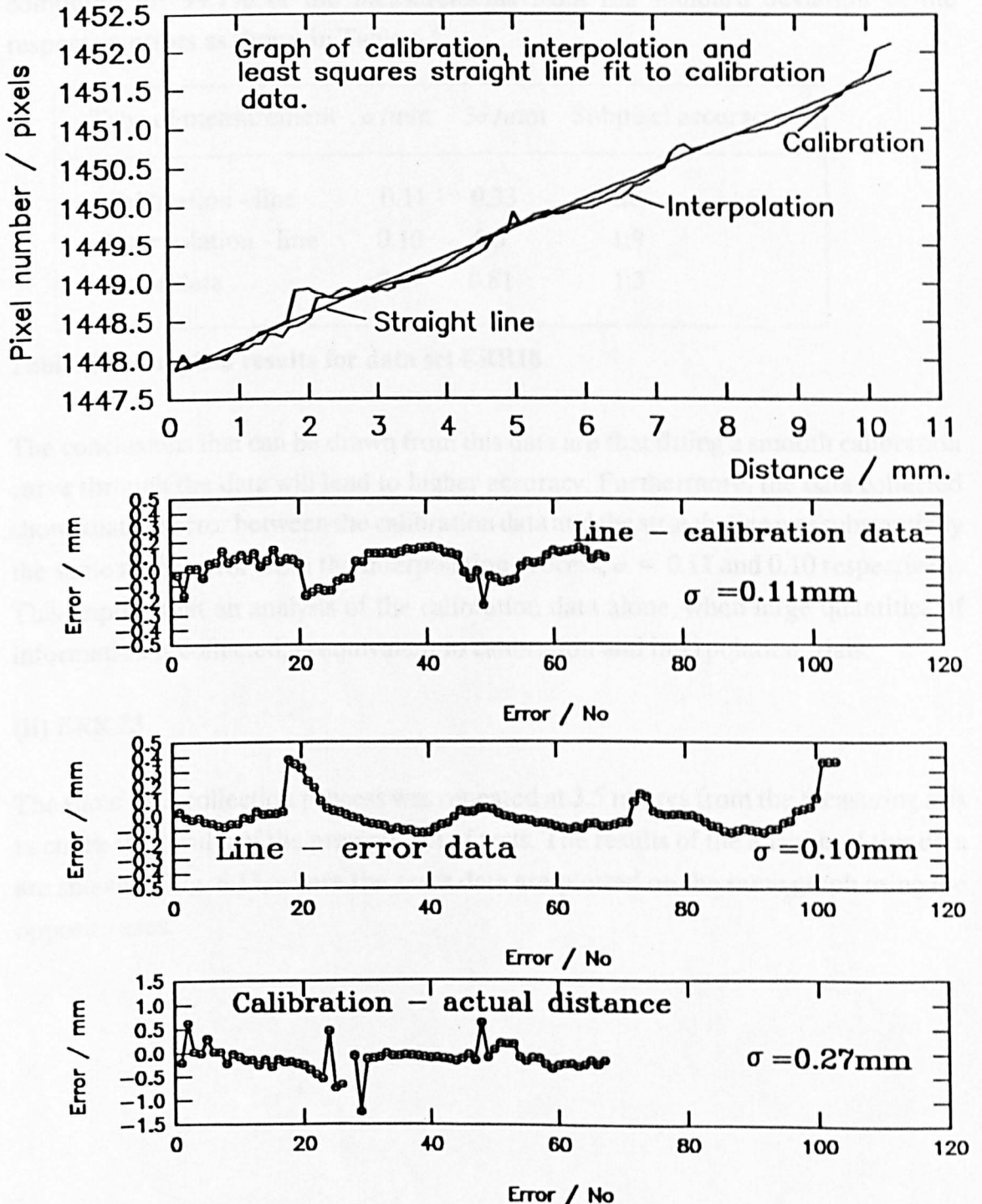


Fig. 6.12. ERR18, calibration and interpolation and error data at 2.5 metres.

The lower three graphs in Fig. 6.12, are all plots of different errors. The top shows the discrepancy between the least squares best fit line through the calibration data and the calibration data itself. The middle shows the difference between the interpolation data and the straight line. The lower shows the error data computed at the time of data collection, the difference between the calibration data and the interpolation data. The slope computed for the straight line fit was 0.378 pixels per mm, which equates to an average distance of 2.64mm between pixels, hence, the subpixel accuracy can be computed for 99.7% of the measurements from the standard deviation of the respective errors as shown in Table 6.1.

Type of measurement	σ /mm	3σ /mm	Subpixel accuracy
Calibration - line	0.11	0.33	1:8
Interpolation - line	0.10	0.3	1:9
Error data	0.27	0.81	1:3

Table. 6.1. Subpixel results for data set ERR18.

The conclusions that can be drawn from this data are that fitting a smooth calibration curve through the data will lead to higher accuracy. Furthermore, the data collected shows that the error between the calibration data and the straight line was substantially the same as the error from the interpolation process, $\sigma = 0.11$ and 0.10 respectively. This implies that an analysis of the calibration data alone, when large quantities of information is collected, is equivalent to calibration and interpolation trials.

(ii) ERR 23.

The same data collection process was repeated at 3.5 metres from the measuring axis to check the results of the previous set of tests. The results of the analysis of this data are shown in Fig. 6.13, where the error data are plotted on the same graph using the opposite axes.

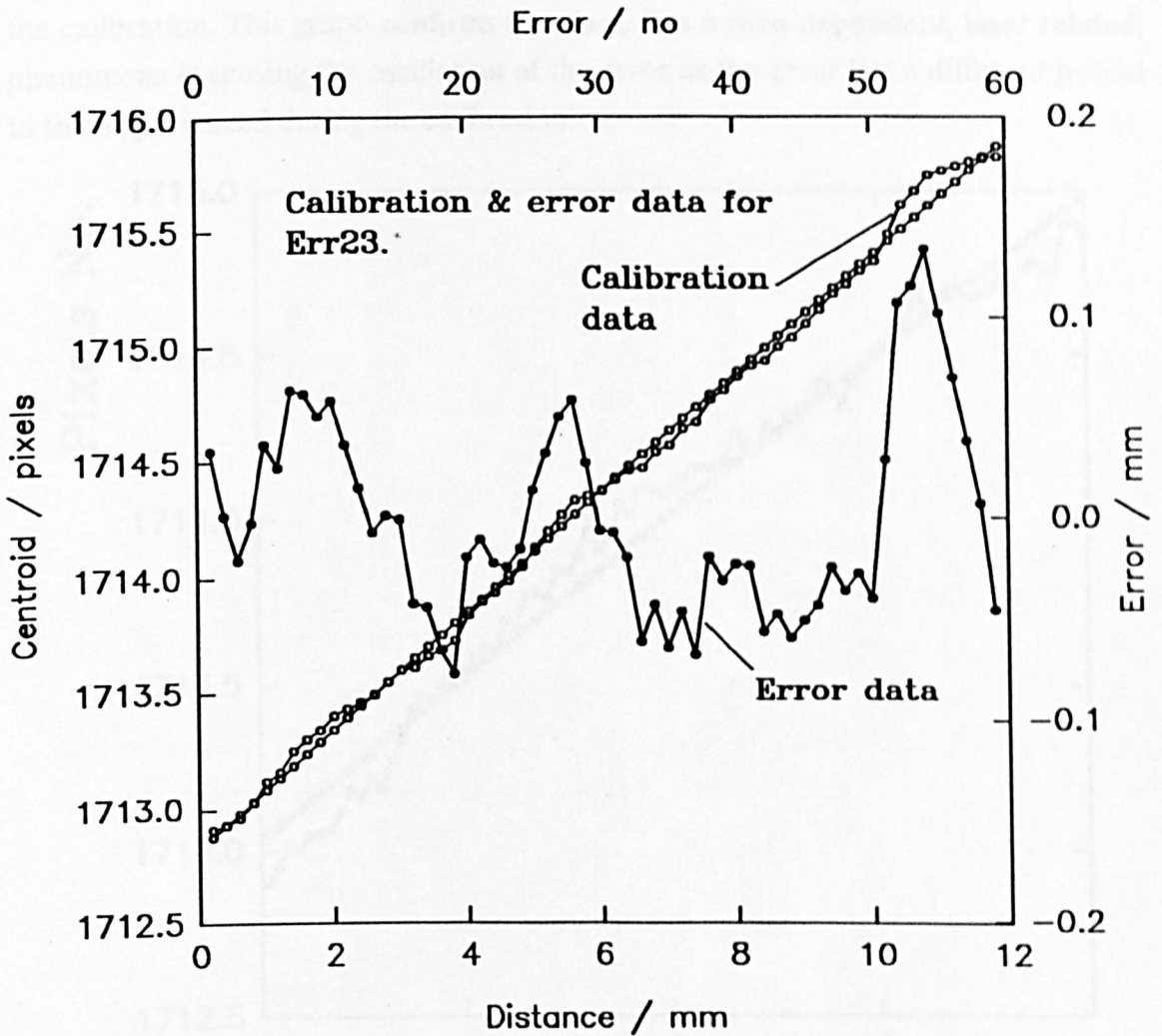


Fig. 6.13. ERR23, calibration, interpolation and error data at 3.5 metres.

There are two interesting features of this graph, first, the error appears to be smaller than in the previous case and second, the same oscillation of the data appears, which is not expected from a random noise process such as introduced by the camera or the electronics. An explanation of the cause of the error oscillation may be (a) an error in the programming of the subpixel algorithm as, in Fig. 6.12, the error appears to coincide with the pixel spacing, or (b) a time related phenomena such as small changes in the position of the laser image. The first explanation is disproved by this second set of data where the correspondence with the pixel spacing is not apparent. The second explanation, a laser pointing instability, is more plausible as this would cause a non-random error which appears characteristic of the data analysed so far.

Fig 6.14, shows the fitting of a straight line to the interpolation data collected after the calibration. This graph confirms the view, that a time dependent, laser related, phenomena is causing the oscillation of the error as the error has a different period to that experienced during the calibration.

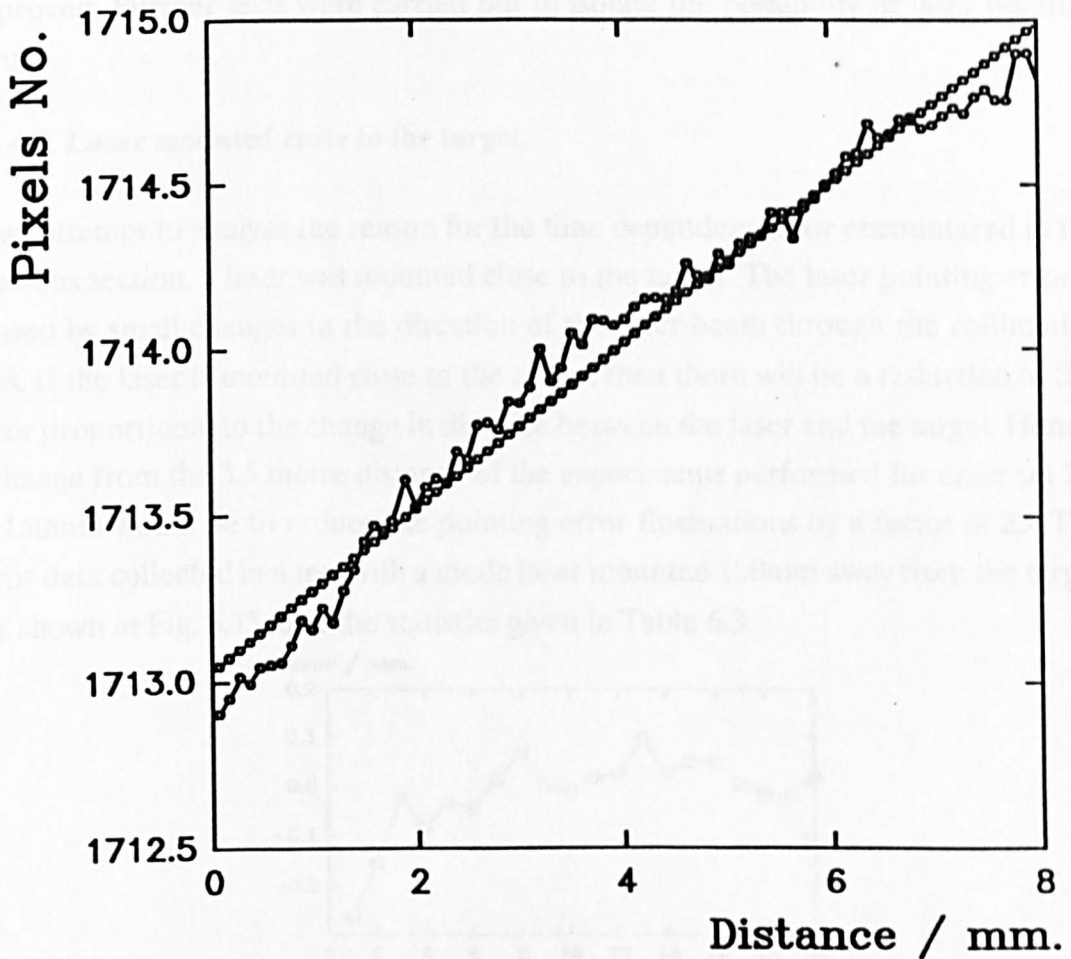


Fig. 6.14. ERR23 data showing interpolation data and best fit straight line.

The data was analysed in the same way as the data given in Table 6.1. and the results shown in Table 6.2.

Type of measurement	σ / mm	3σ / mm	Subpixel accuracy
Calibration - line	0.05	0.15	1:27
Interpolation - line	0.08	0.24	1:17
Error data	0.37	1.11	1:4

Table. 6.2. Subpixel results for data set ERR23.

The increase in accuracy at this distance is likely to be caused by better beam conditioning as the image of the laser beam reflections would be smaller at this distance with less speckle problems. However, it still apparent that, if the problem of the oscillating error can be reduced, then the accuracy could be substantially improved. Further tests were carried out to isolate the possibility of laser pointing error.

6.3.4.5. Laser mounted close to the target.

In an attempt to analyse the reason for the time dependent error encountered in the previous section, a laser was mounted close to the target. The laser pointing error is caused by small changes in the direction of the laser beam through the collimating lens. If the laser is mounted close to the target, then there will be a reduction in this error proportional to the change in distance between the laser and the target. Hence, a change from the 3.5 metre distance of the experiments performed for error set 23, to 150mm would be to reduce the pointing error fluctuations by a factor of 23. The error data collected in a test with a diode laser mounted 150mm away from the target are shown in Fig. 6.15, and the statistics given in Table 6.3.

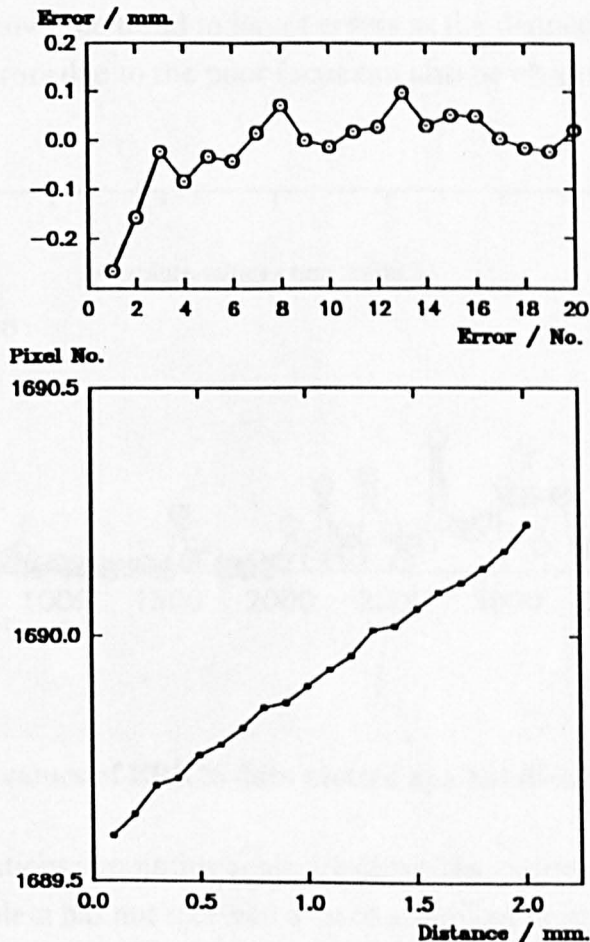


Fig. 6.15. ERR30, error data with laser 150 mm from target.

The increase in accuracy at this distance is likely to be caused by better beam conditioning as the image of the laser beam reflections would be smaller at this distance with less speckle problems. However, it still apparent that, if the problem of the oscillating error can be reduced, then the accuracy could be substantially improved. Further tests were carried out to isolate the possibility of laser pointing error.

6.3.4.5. Laser mounted close to the target.

In an attempt to analyse the reason for the time dependent error encountered in the previous section, a laser was mounted close to the target. The laser pointing error is caused by small changes in the direction of the laser beam through the collimating lens. If the laser is mounted close to the target, then there will be a reduction in this error proportional to the change in distance between the laser and the target. Hence, a change from the 3.5 metre distance of the experiments performed for error set 23, to 150mm would be to reduce the pointing error fluctuations by a factor of 23. The error data collected in a test with a diode laser mounted 150mm away from the target are shown in Fig. 6.15, and the statistics given in Table 6.3.

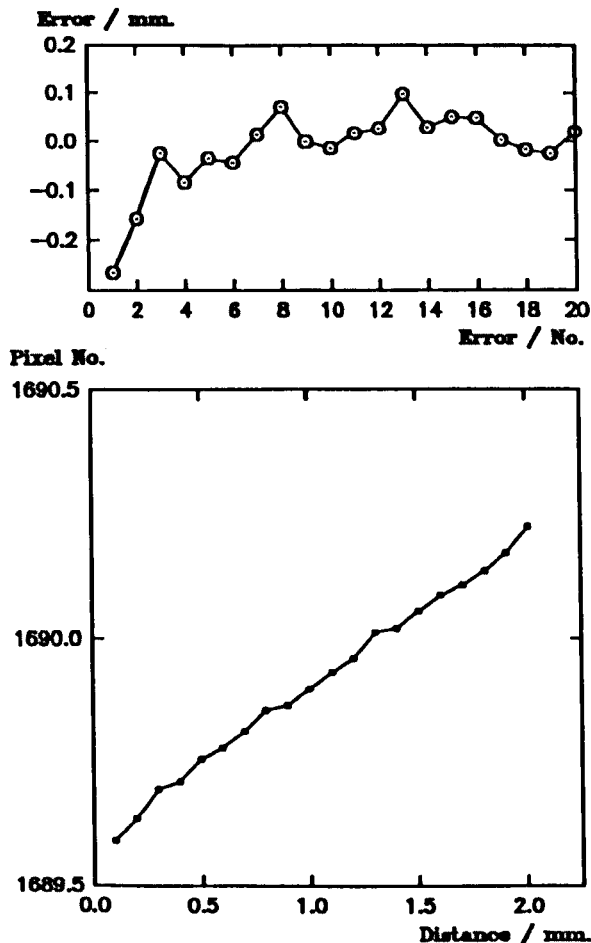


Fig. 6.15. ERR30, error data with laser 150 mm from target.

Type of measurement	σ /mm	3σ /mm	Subpixel accuracy
Calibration - line	0.01	0.03	1:92
Interpolation - line	0.009	0.027	1:123
Error data	0.04	0.132	1:25

Table 6.3. Subpixel results for data set ERR30.

The significant improvement in the subpixel accuracy shows that the fluctuations in the data collected with the laser at longer distances was caused by laser pointing stability errors. This set of data confirms what is noted in the following section on subpixel accuracy, that these errors are the reason that none of the measurements made with the diode laser on the measuring axis were close to the expected theoretical accuracy. The data shown here, however, is close to what should be expected for a the image processing that is used.

Confirmation that the laser was a source of errors is shown in Fig. 6.16, where the absolute values of the data set ERR16 are plotted. A second order polynomial is fitted to the data which shows the trend to larger errors as the distance between the target is increased. The errors due to the poor focus can also be observed at close range.

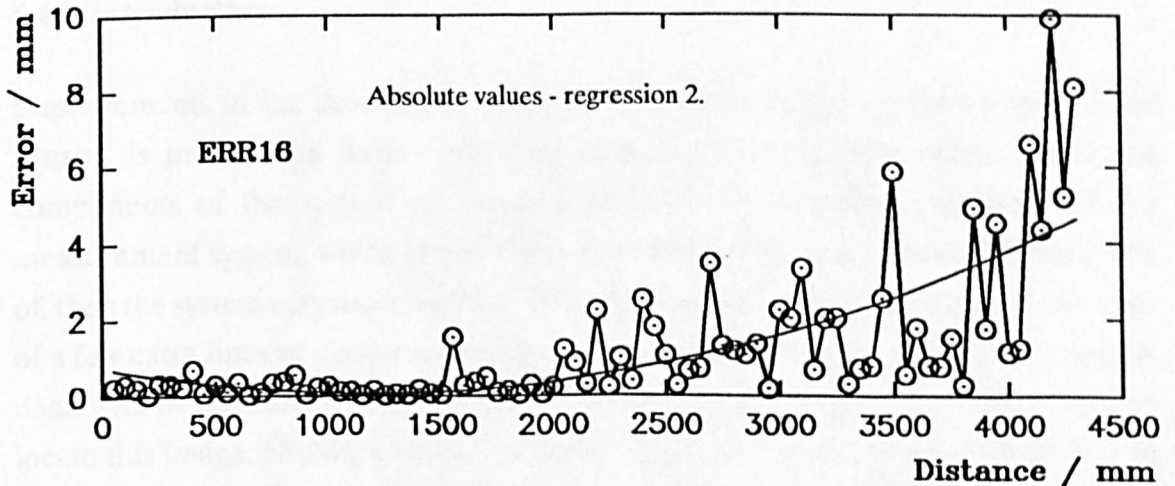


Fig. 6.16. Absolute values of ERR16 data plotted against distance.

The angular fluctuations in pointing angle are caused by temperature variations in the laser chip, the problem has not received a lot of attention, even by the manufacturers of the lasers, so it is difficult to obtain independent information on the likely time

dependency and magnitude of the problem. The laser beam angular variation will be more significant at longer distances from the laser, hence, in this context, will cause greater measuring errors at larger distances.

6.3.5. Conclusion and interpretation of results.

A number of significant problems have been identified which adversely affect the overall accuracy of the measurement system such as focus and laser pointing stability. Data has been collected which was able to identify the problems and quantify them.

The method of calibration of the triangulation system has been developed and the results analysed. The underlying accuracy of the triangulation system was shown to be good with subpixel accuracy routinely achieved, however, care is required in the calibration procedure if random and statistical quantifiable effects are involved.

A high degree of reliability has also been demonstrated in the triangulation measurement system both in terms of the large number of measurements that were taken, and the reliability of the measuring accuracy over long periods of experimentation.

6.4. SUBPIXEL ACCURACY TESTS.

6.4.1. Introduction.

Improvements in the accuracy of location of the laser image on the surface of the sensor, is one of the most rewarding areas for development, when all of the components of the system are fixed. Indeed, if the underlying accuracy of the measurement system, which is exploited with subpixel accuracy, were not made use of, then the system may measure to an order of magnitude less accurately, for the sake of a few extra lines of program code. In the case of prototype III, where the image is dealt with by software, it is comparatively easy to change the algorithm that is used to locate this image. Hence, a number of additional tests were conducted to analyse in detail this subject. It must be noted that the subpixel accuracy achieved will still be a function of the surface that is to be measured, its reflectivity and spectral characteristic may fool the algorithm, therefore this aspect has also to be taken into account.

6.4.2. Discussion of methods for subpixel accuracy.

A number of techniques have been used to obtain image location to greater than pixel accuracy. Often the improvements in accuracy have been driven by the requirement for higher performance from a given sensor when no alternatives are available. Some examples are:

(i) ROSAT star tracker (Lange, 1986), the centroid method was used to improve the angular resolution of the ROSAT star tracker where the angular resolution required was much higher than that given by the pixel dimensions of the 385x288 pixel sensor.

(ii) Target location with camera on theodolite (Huang, 1990), a centroid method is used to accurately locate the position of targets which are circular. Further improvements were obtained with the use of subpixel movement of the camera with respect to the target. Subpixel accuracies of 0.01 pixel were achieved.

(iii) Steel strip width measurement (Li, 1987). The position of the edges of steel strips have been measured for many years using line scan cameras, subpixel edge detection methods have enhanced the accuracy achieved so enabling the same cameras to be used.

(iv) Image registration of satellite images (Gotashby, 1986). Features that occur in one satellite image are required to be matched to those acquired in another, which may be in a different format and of resolution. The rotational, scaling, and translation parameters, are achieved by windowing selected objects and computing the centres of gravity of these objects.

(v) High resolution camera (Lenz, 1990), the principle used to obtain subpixel accuracy, and hence a high resolution image, is to move the sensing element by subpixel distances in a raster scan by piezo electric actuators. The 500 x 291 pixel elements of the sensor used in this way produce an image of resolution 3000x2300.

(vi) Subpixel speckle displacement measurement (Oulamara, 1988). Electronic Speckle Pattern Interferometry (ESPI) measures displacement of rough surfaces, correlation techniques are used to measure the displacement of the speckle patterns and, hence, build up a surface profile of the object being inspected.

The methods used in edge detection would, at first sight, appear to have no relevance to the the task of locating the image of a gaussian peak. However, a first step in finding the position of an edge is often achieved by taking the first order differential of the digital image intensity map, whereupon the step edge, blurred and modulated by the imaging process, is very similar in profile to that of a Gaussian curve. The nominated edge is then the computed centroid position. The connection between area processes and the linear processes is strong, as many of the area processes are explained in the literature for the one dimensional case.

Because of the strong synergy between all of these areas, a study was required to establish the best method in this particular case. No comprehensive survey was found that covered the range of techniques available and so a survey was conducted (West & Clarke, 1990) that sought to categorise techniques, and supply information concerning the likely accuracy that might be achieved. The conclusions reached by the study of this subject were that a number of candidates were available, which would require extensive testing to discover which was the most desirable for the task. A specification for the algorithm was decided as follows:

- (i) insensitive to noise,
- (ii) computationally simple,
- (iii) subpixel accuracy,
- (iv) capable of distinguishing the desired image, and
- (v) able to give an error report when poor results are expected.

It is likely that any such algorithm would have more than one stage.

To study this requirement in the context of a triangulation system, a number of simulated and real trials were set up to test out the reliability of these algorithms. The candidates that were thought to be most likely to be useful in this context have been described in chapter 3, and are the centroid, weighted centroid, Vernier and interpolation methods.

6.4.3. Discussion of performance of subpixel methods.

To determine which subpixel method is best suited for an optical triangulation application requires analysis. Ideally, a theoretical analysis can be made such as that conducted by Havelock, 1989, but he notes that the approach of a number of papers dealing with the theory of problems due to quantisation is inadequate. He develops a theoretical analysis, using the concept of 'locales', for the problem of determining the subpixel accuracy of the centroid of a 2-D object after sampling and quantisation. Locales are the allowed positions of the centroid of image which the algorithm will report. The number of locales increases with the number of quantisation levels. He mainly considered noise free cases, but did present some results on the effect of noise on the results.

In this section trials are performed on both simulated and real data pertinent to optical triangulation. Although meaningful results can be obtained for such effects as quantisation, noise and spatial resolution, it is not possible to directly translate the subpixel accuracy to measurement accuracy. To do so would ignore laser pointing stability, environmental effects, speckle, surface irregularities in form and contrast, and mechanical instabilities. However, if the ideal image location error is known, then a comparison between ideal accuracy and that achieved in practice is possible, and a large factor in the overall error of a triangulation system has been quantified.

6.4.4. Experiments with simulated data.

Simulated data was generated from the equation of a Gaussian distribution as a real continuous function. The continuous distribution was then sampled at regular points with each group of samples starting at a number of different positions varying by a known subpixel amount (1000 points over one pixel spacing) before digitisation. Then each of the three methods were used to compute the location of the spot for the 1000 instances at various quantisation levels, signal to noise ratios and spatial resolutions.

The first set of trials allowed analysis of the effect of noise in the form of quantisation and random noise to take place. The real value at each sample position was quantised into a discrete number of levels: 256, 128, 64, 32, 16, 8, and 4, then the difference between the known centre of the centroid and the computed position of the centroid was noted. This resulted in one thousand trials for each quantisation level. In addition to the quantisation noise, random noise was added with the maximum noise level being equal to $1/256$, $1/128$, $1/64$, $1/32$, or $1/16$ of the maximum signal level. Again 1000

trials took place for each noise level. The standard deviation of the errors was computed and these values are plotted in Fig. 6.17, for the centroid method, Fig. 6.18, for the weighted centroid method and Fig. 6.19, for the Vernier method.

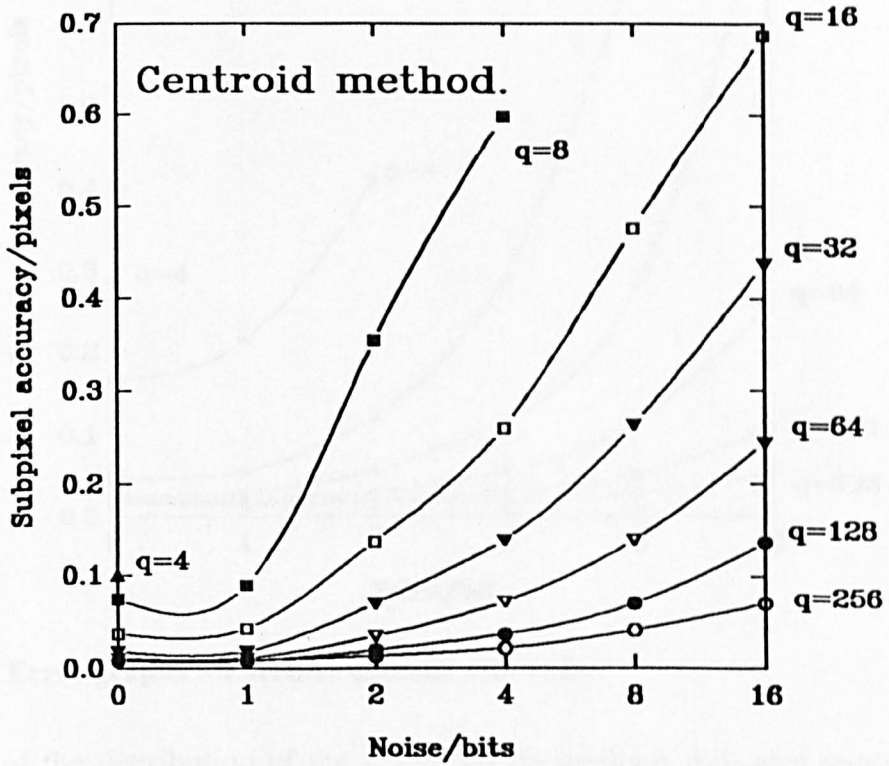


Fig. 6.17. Error graphs for centroid method with noise.

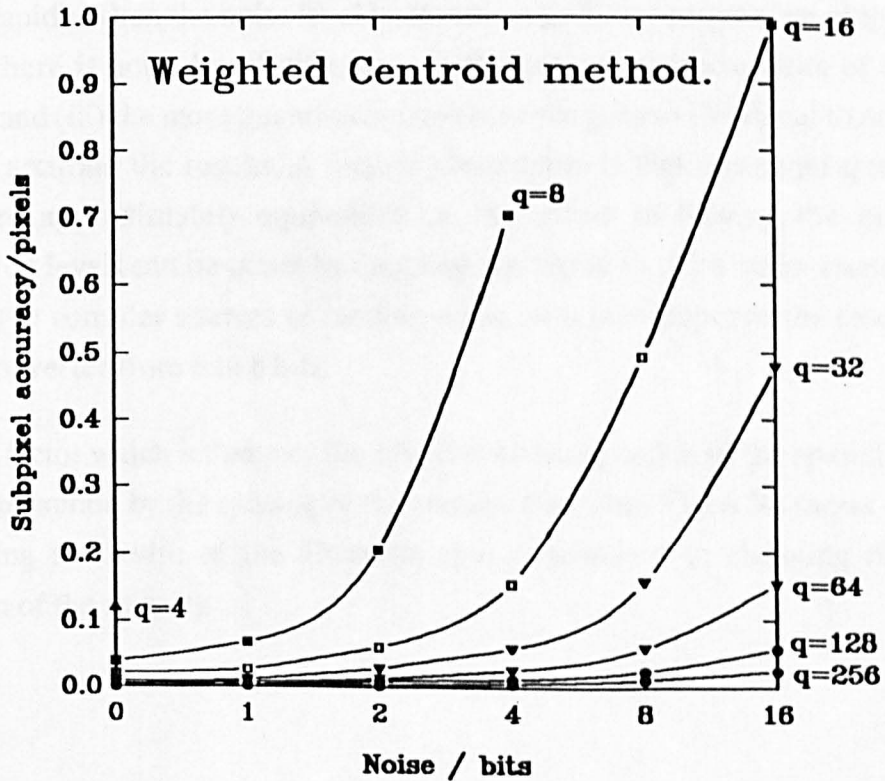


Fig. 6.18. Error graphs for weighted centroid method with noise.

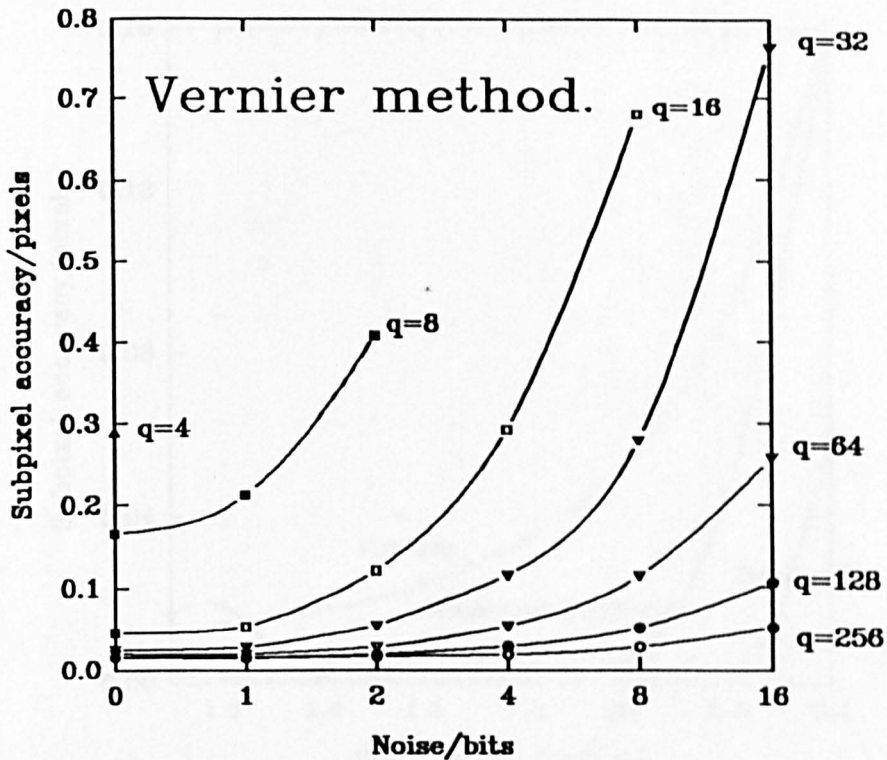


Fig. 6.19. Error graphs for vernier method with noise.

Analysis of the distribution of the errors for all methods indicates approximately Gaussian distributions. Certain observations can be made from this data: (i) the errors increase rapidly when the noise level becomes a significant proportion of the sample size, (ii) there is not a lot of difference in the general characteristics of the three methods, and (iii) the more quantisation levels, or the greater the signal to noise ratio, the more accurate the results. A further observation is that noise and quantisation effects are approximately equivalent i.e. the effect of halving the number of quantisation levels can be offset by doubling the signal to noise ratio. Hence, it is as important to consider sources of random noise, as it is to improve the resolution of an A-D converter from 6 to 8 bits.

A further factor which influences the subpixel accuracy is that of the spatial sampling width, determined by the spacing of the sensing elements. Fig. 6.20, shows the result of changing the width of the Gaussian spot (equivalent to changing the spatial resolution of the sensor).

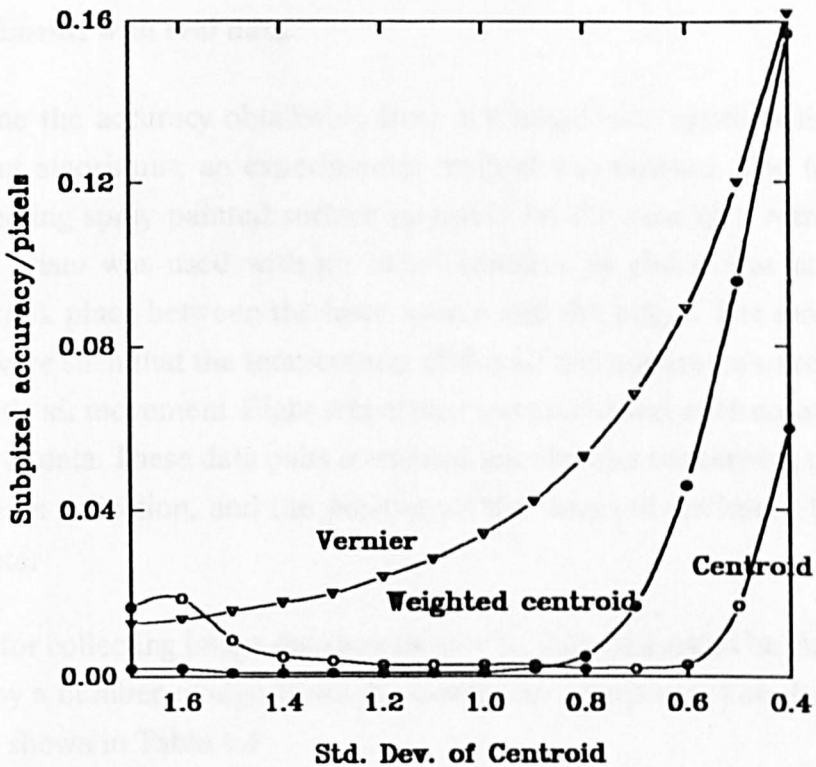


Fig. 6.20. Errors caused by changes in spatial resolution.

The x-axis (horizontal axis) indicates the standard deviation of the Gaussian spot with a value of 1.0 means that the spot was spread across approximately 6 pixels. For all three methods used in this experiment, the accuracy improved as the image size increased. For the two centroiding methods, the accuracy quickly reaches a minimum as the image size is increased. At small image sizes all methods gave poor results. The weighted centroid was worse because the spot was only represented by, at most, 3 pixels and the outer two pixels had little effect, as they were of much lower amplitude than the centre pixel. As each pixel value was weighted by itself the centre pixel had a disproportionate large effect.

The conclusions that may be reached are that random noise and quantisation are equivalent sources of error so a reduction in either is desirable, but not at any expense. The conclusion concerning spatial resolution is easier to define with the width of the Gaussian shaped image required to be over a certain threshold depending on the method used for subpixel accuracy. A width of four pixels or more is satisfactory for the centroid method.

6.4.5. Experiments with real data.

To determine the accuracy obtainable from a triangulation system using subpixel measurement algorithms, an experimental method was devised. The target was a diffuse reflecting spray painted surface mounted on the rear of a retro-reflecting prism. The prism was used with an interferometer to check that no unwanted movement took place between the laser source and the target. The environmental conditions were such that the temperature of the air and apparatus were stable, and there was little air movement. Eight sets of data were collected, each consisting of 900 - 1000 pairs of data. These data pairs contained information concerning the image of the laser beam reflection, and the position of the target as indicated by the laser interferometer

The reason for collecting image data was to provide data that could be analysed, post collection, by a number of algorithms for comparison purposes. The data sets were collected as shown in Table 6.4

Data set	Distance/image(μm)	No/distance	Total distance moved/ μm
1	1	1	900
2	10	10	900
3	10	10	900
4	40	10	3600
7	-	1000	-
8	-	1000	-

Table 6.4. Subpixel data sets.

(i) Analysis of data sets 1-4.

The purpose of the collection of these sets of data was to establish the subpixel accuracy possible when the optics were optimised, and attempt to isolate any other sources of error. The data collected in each of these tests was over the same distance as sets 1-3, and over a greater distance in 4, with the same overall distance from the measuring axis (approximately three metres). The four graphs are shown in Fig. 6.21-24, illustrate the variation of the position of the centroid of the reflected image. The use of the centroid method would not give significant differences to the other methods which could have equally well been used.

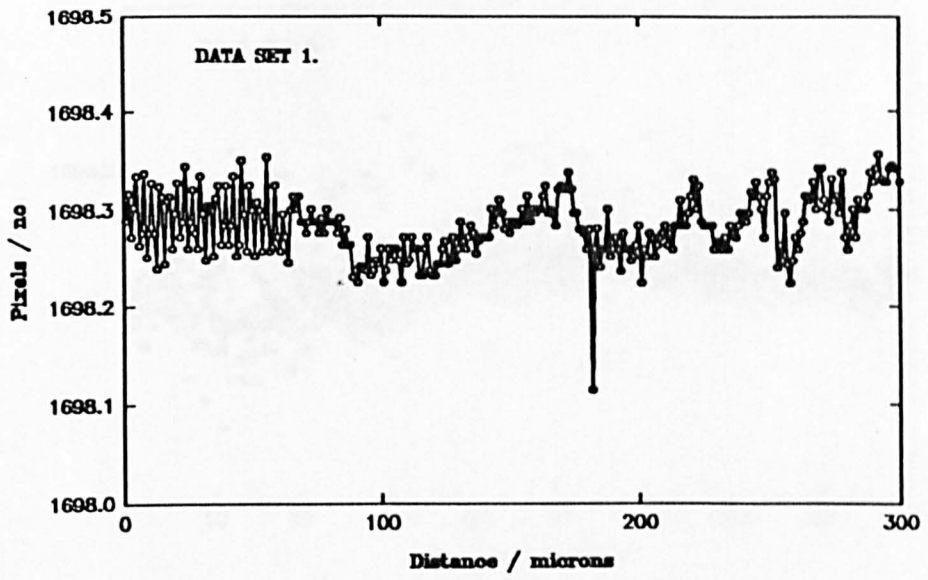


Fig. 6.21. Data set 1.

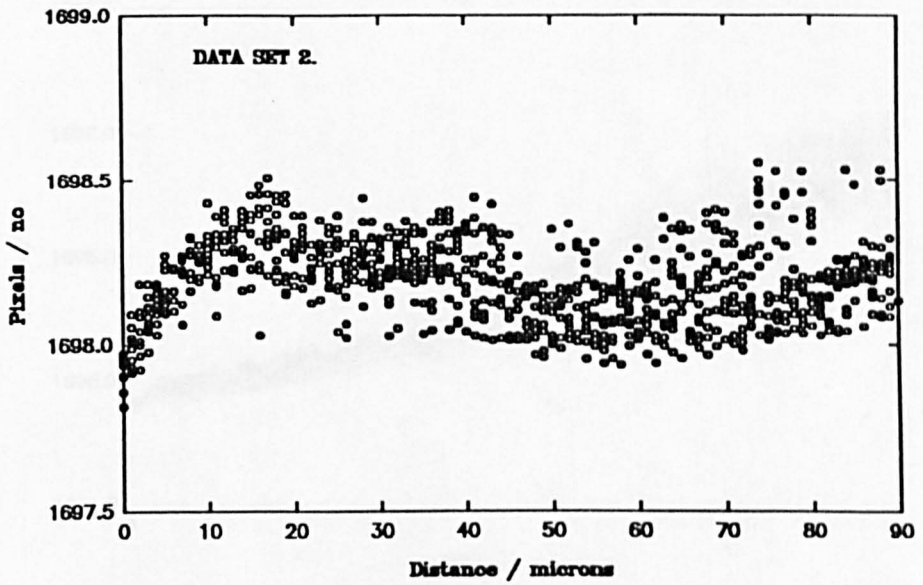


Fig. 6.22. Data set 2.

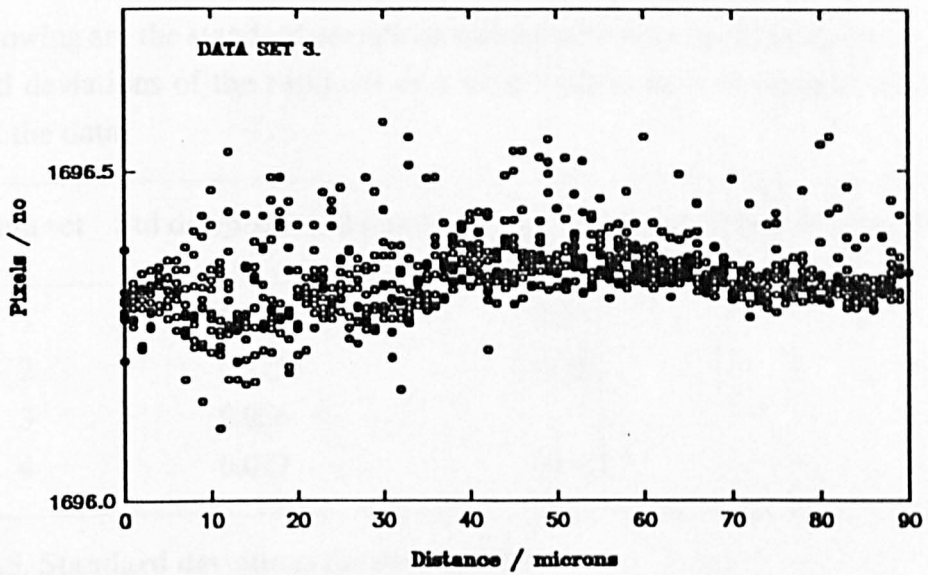


Fig. 6.23. Data set 3.

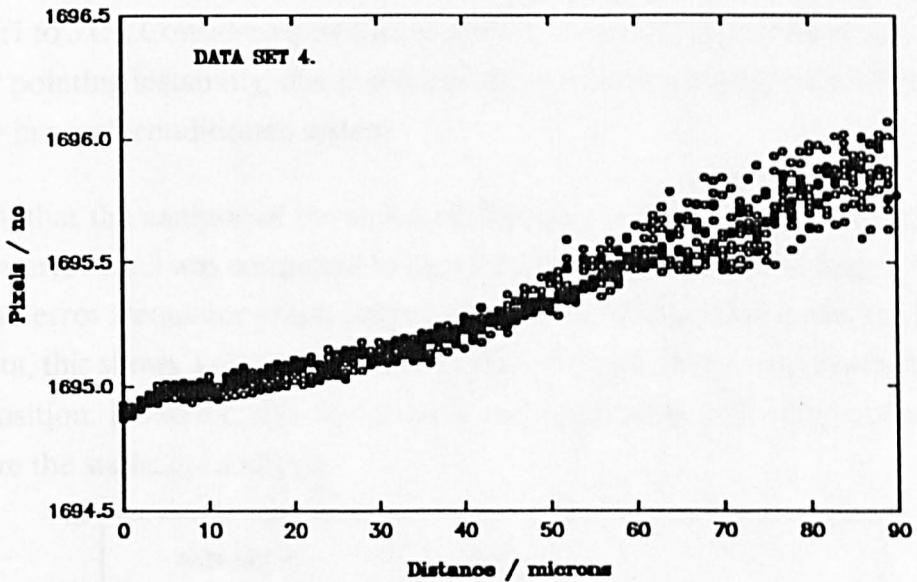


Fig. 6.24. Data set 4.

These graphs exhibit some interesting features:

- (1) there is a significant proportion of what appears to be random noise,
- (2) the data is not always self consistent, there are changes in the quantity of noise and the direction of trends in the centroid data measurement,
- (3) only the last of these data sets shows a consistent difference due to the movement of the target, and
- (4) subpixel accuracy is shown in all sets of data.

The following are the standard deviations obtained from each of the data sets and the standard deviations of the residuals of a least squares best fit straight line plotted through the data.

Data set	Std dev/pixels (all data)	Std dev/pixels (residuals or best data)
1	0.371	0.031
2	0.125	0.123
3	0.056	-
4	0.077	0.032

Table 6.5. Standard deviations for data sets 1-4.

From this analysis it can be shown that all of these data sets show subpixel accuracy from 2.7:1 to 31:1. Considering that a proportion of the errors may be attributable to the laser pointing instability, this shows that there is an underlying possibility of high accuracy in a well conditioned system.

To check that the analysis of the standard deviation was valid, the error frequency graph for error set 3 was computed to check that it was Gaussian in shape. Fig. 6.25, shows the error frequency graph plotted with a best fit Gaussian curve fitted to the same data, this shows a close fit except for slightly more errors away from the +/- 1 sigma position. However, this deviation is not considered sufficient to completely invalidate the statistical analysis.

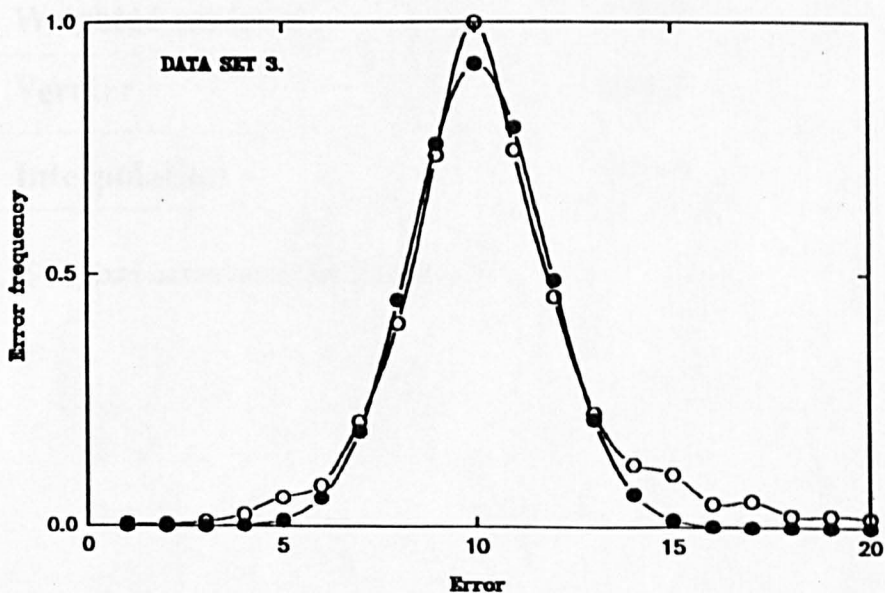


Fig. 6.25. Error frequency for data set 3.

(ii) Analysis of data sets 7-8.

The last two sets of data collected allowed the possibility of isolating two further sources of error, the movement of the target, and the pointing stability of the laser. For data set 7, the laser and camera were mounted 3 metres from the target, and for data set 8, the laser was moved to be 150 mm. from the target (the camera was kept in the same position). The purpose of moving the laser was to ascertain if errors were occurring because of the laser pointing instability and environmental effects. Unlike the simulated data, the target reflection was not allowed to move for these trials but left stationary. This was to remove the effect of changes in the speckle pattern on the results as it would be a stationary pattern. In fact the speckle had little effect on the data at the distance of the tests. It was hoped that the errors in the results would then be related to sampling resolution, quantisation and noise.

Table 6.6, and Table 6.7, show the results for the four methods for the two data sets. In addition to the three techniques already investigated, interpolation was also used. For both, the system produces subpixel accuracy. The best method for both data sets was the Vernier method, with the other three giving similar results. There is obviously an effect associated with the laser distance from the target as concluded in the previous chapter as the subpixel accuracy is higher when the laser is closest to the target.

Method / Data set 7.	Standard deviation/pixel
Centroid	0.062
Weighted centroid	0.068
Vernier	0.052
Interpolation	0.074

Table 6.6. Subpixel accuracies for data set 7.

Method / Data set 8.	Standard deviation/pixel
Centroid	0.042
Weighted centroid	0.043
Vernier	0.017
Interpolation	0.042

Table 6.7. Subpixel accuracies for data set 8.

The increase in subpixel accuracy for the set of data with the laser mounted close to the target is improved by nearly a factor of two.

To further analyse the data contained in data sets 7 and 8 with respect to the influence of the laser beam position, the data was analysed to test the validity of a statistical interpretation of the data based on a Normal Distribution. This distribution is the result of processes that are random such as noise, atmospheric fluctuations, etc. If the distribution is not Gaussian then these statistics are not applicable and the process may not be random, or other statistical analysis applied. To analyse the data a histogram of the data was plotted by adding up the number of measurements that fell in equal ranges over the spread of the measurements. A Gaussian curve was then fitted to this data to estimate how good the fit was.

Fig. 6.26, shows the histogram for data set 7 with a least squares best fit of the superimposed Gaussian curve which clearly shows that the curve does not convincingly fit this data.

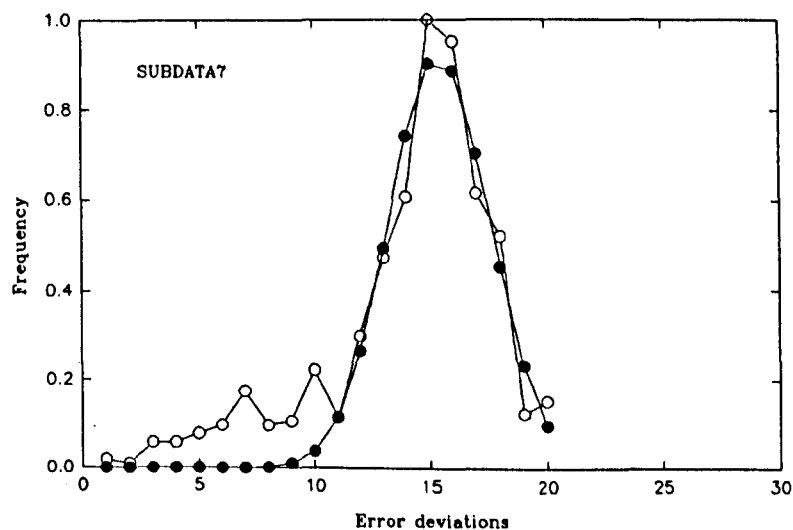


Fig. 6.26. Gaussian curve fit to data set 7.

The data for set 8 is plotted in Fig. 6.29. It would appear from this plot that the distribution of this data is nearer to a Gaussian curve.

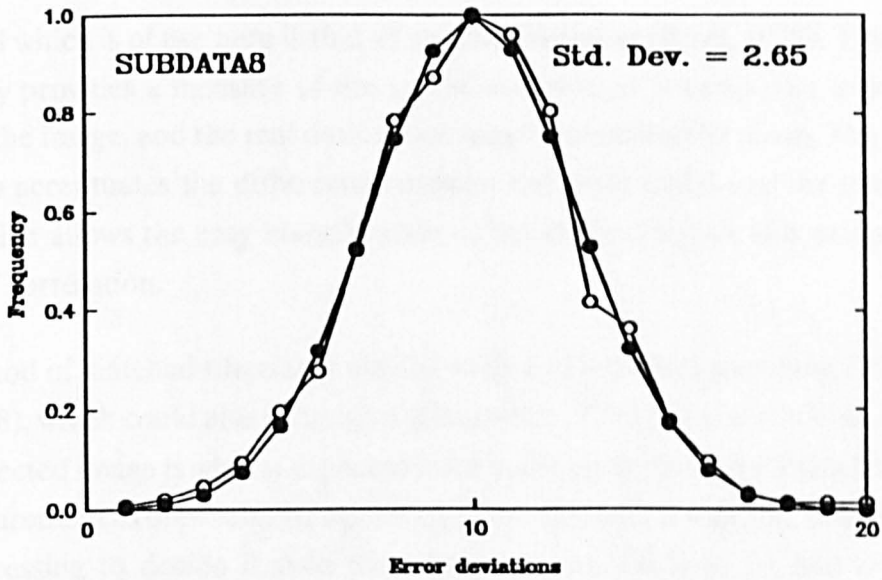


Fig. 6.29. Gaussian curve fit to data set 8.

It may be concluded from this evidence, that a process was occurring in data set 7 that was not completely random, at least not in the time scale of the investigation. The major difference between the two data sets is the distance from the target of the laser, hence, it may therefore be concluded that the laser beam does wander, and is not a random process, giving a less accurate measurement than would be the case with a perfectly stationary laser beam.

The subpixel accuracy achieved with the laser close to the target, is as predicted for the system, which includes the noise sources of quantisation and the camera/sensor electronic noise. Hence, a figure for subpixel accuracy under these conditions of greater than 1:20 is possible, if the problems of non uniform surface form and reflectivity are ignored. This conclusion is reinforced by the fact that this was not the highest subpixel accuracy achieved, which compares favourably with the predicted maximum from the simulation study.

6.4.6. Image problems.

All of the discussions so far have ignored the problem of surface roughness and reflectivity variations, assuming a plane diffuse surface. This will rarely be found in practice and such variations will adversely affect the measurement accuracy. However,

it is possible to gain some information about the characteristics of a surface by analysing the reflected image:

A method which is of use here is that of matched filtering (Pratt, 1978). This method essentially provides a measure of the spatial correlation between the known, ideal shape of the image, and the real data, which may be obscured by noise. The resultant waveform accentuates the difference between the ideal signal and the surrounding noise, which allows the easy identification of the desired signal, if it exists, and the degree of correlation.

The method of matched filtering is similar to that of template matching (Tian, 1986; Slud, 1988), which could also be used in this context. The prime aim is to check to see if the reflected image is what is expected from a diffuse surface. A method of flagging the measurement as unreliable, if a poor image is returned, is a simple way of allowing post processing to decide if such measurements are likely to be bad or whether features, such as an edge can explain why the image is degraded.

A simple form of matched filtering was implemented in the programs for identification of the laser image in the presence of noise, which was useful when such noise was expected to be a problem.

6.4.7. Conclusions.

This section has discussed methods for obtaining subpixel measurements in the triangulation system using a laser and solid state 1-D sensor. Although there have been many methods proposed for subpixel measurement, many are not suitable in this 1-D application. There are five categories of technique of which centroiding, interpolation and correlation are the most applicable. Most of the techniques were capable of obtaining an accuracy better than 0.1 pixel, and in some cases better than 0.05 pixels. Three methods were chosen from the literature and compared using both simulated and real data. Subpixel accuracy was achieved for each of the methods with accuracy specified statistically as the standard deviation of the error between the known position and the measured position.

The data collected also shows that the laser pointing stability has an important bearing on the best accuracy that can be achieved.

6.5. CORRECTION TO TRIANGULATION NON-LINEARITY.

6.5.1. Introduction.

One of the major problems that is fundamental to the way a typical triangulation system operates, is that of the non-linearity of resolution and accuracy. The disadvantages of the non-linearity have been shown in the development of the prototypes which were simple triangulation devices, when the base length was minimised the non-linearity was the major problem encountered.

This undesirable feature may in some circumstances be an advantage if, say, inaccurate long range measurements were required or accurate short range measurements. However, this problem can only in part be alleviated by adjusting the available parameters such as the focal length of the lens and the length of the base of the measurement triangle.

In an attempt to solve this problem a partial solution was arrived at through discussion with a colleague at the University. This solution can in some circumstances linearise a triangulation system, or at least minimise its worst effects. The theoretical derivation of the use of this method is described here, with some theoretical results.

6.5.2. Discussion of solution to non-linearity.

To correct the inherent non-linearity of the triangulation scheme a number of solutions are possible:

(i) The sensor could be made with a continuously variable resolution that counteracts the effect of the smaller angle changes at longer distances from the measurement base line. This scheme would certainly provide a linear measuring system, however there would be problems:

- (a) fabrication of such a device would be difficult, expensive and not necessarily possible, and
- (b) the light sensitivity of the sensor would be a problem, this is normally constant and so smaller sensor elements, which generate less charge, will also receive less light as the target object will be further away.

(ii) Correct the non-linearity of the imaging system by effectively spreading out the bundle of rays that come from the further distances and compressing those that come from closer distances. This manipulation of the characteristics of the imaging system would linearise the system in this limited case.

Of the two solutions outlined, only the second is a reasonable choice, but a non-linear optical element is required. Non-linear optical elements are sometimes used to correct for problems in the optics of systems and to produce wanted effects such as the large viewing angles achieved, at the cost of distortion, by a fish eye lens. However, a simpler solution is to use a prism (as discussed in 3.4.1.) which has non-linear characteristics which can be applied in this case.

The normal use of this characteristic of prisms is to determine the angle of minimum deviation of a beam of monochromatic light in order to calculate its wavelength. However, there are a number of reasons why the characteristics of a prism are particularly useful in this context:

- (i) a prism is a planar system, this is useful because the triangulation system is also planar,
- (ii) monochromatic light is not dispersed through the prism, while white light causes blurring of images which is not a problem to the sensor, and
- (iii) the characteristic light bending of the prism is not linear.

The deviation angles for seven prism refractive indices are calculated and plotted in the graph shown in Fig. 6.28, which clearly shows the non-linearity inherent in these optical elements.

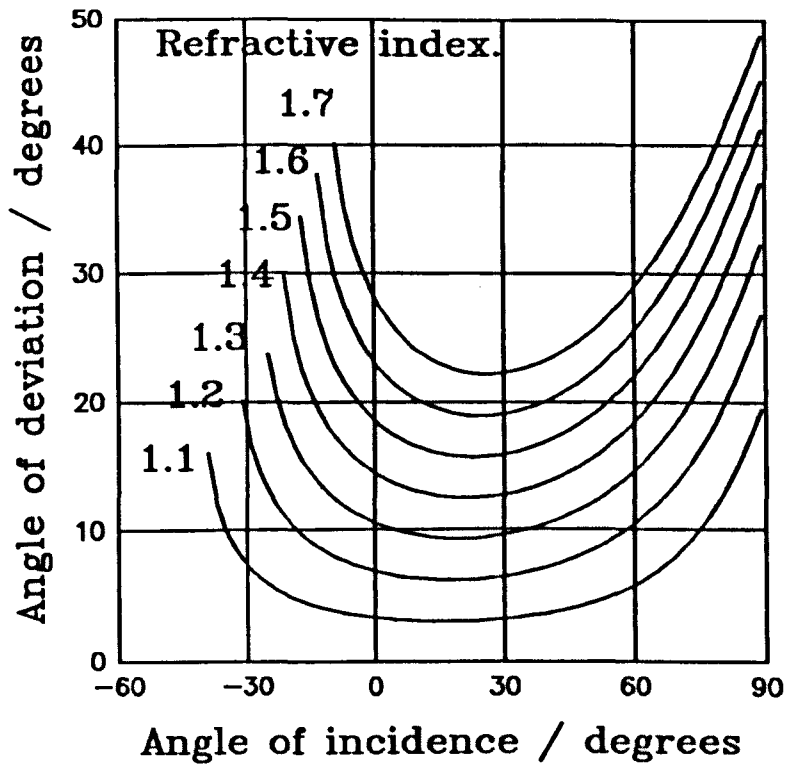


Fig. 6.28. Angular deviation for seven refractive indices.

The prism may be a suitable element to use in the correction of the non-linearity of the system, but testing was required following a theoretical analysis before this could be reliably established.

6.5.3. Application to the triangulation system.

The triangulation measuring system uses standard optics with some optional modifications to measure distance. There are many parameters that can be manipulated to provide the required end result. This may be a measuring system with limited range, but high accuracy, or large range, and limited accuracy.

To pick the correct components requires the an understanding of the geometry and the computation of the effect of each component. The use of a computer program to predict the response to changes in the physical parameters is preferred, as it allows rapid testing compared to what is possible when each change has to be laboriously set up by hand and many readings taken. To achieve this requires an equation linking all of the components together so that the results can be plotted for a each change in the parameters. In such a way it should be possible to predict a configuration for a particular task prior to bench testing.

6.5.4. Derivation of an equation for the corrected system.

An equation is required that links the position of the image of the laser on the CCD chip, with the distance from the target. This equation needs to take in to account the physical parameters of focal length, chip length, triangulation base length, measurement starting distance, and prism parameters. The equation is derived by considering each part of the path of a light ray from the target to the sensor.

6.5.4.1. Angle between object and first element.

Before the light can be of any use to the sensor it must first be conditioned by some optical element to redirect, change its characteristic, or focus it onto the sensor. Elements that could be used range from mirrors to optical filters, all of these elements will pass on information to the sensor about the angle of incidence of a 'ray' from the object (the laser spot). To correct for the inherent non-linearity in the optical configuration a prism is proposed as an initial element. However, if parameters of zero refractive index, or a small apex angle were included, then this element would have no effect and so could then be considered as a null element. This will allow the effect of this element to be isolated from the rest. The configuration of the first part of the system is shown in Fig 6.29.

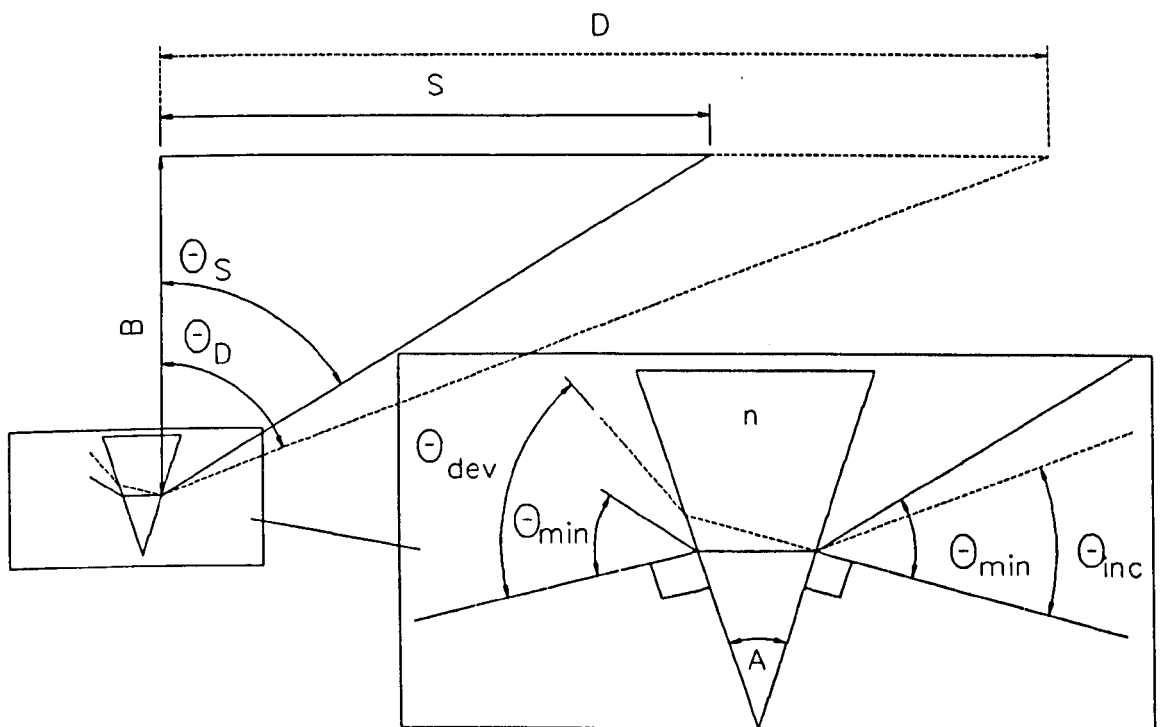


Fig. 6.29. Triangulation configuration diagram number 1.

To analyse the system it is useful to define the angle Θ_{\min} that the normal to the prism face makes with a line drawn between the prism face, and the distance 'D' from the base line measured along the path of the light source, 'S' defines the shortest distance to be measured.

The problem to be solved is to relate 'D', the distance from the base of length 'B', to the position on the sensor where the image is formed. If this is measured from one end of the sensor, this can be defined as 'd'.

The path of a ray will be traced through the system elements starting from the image of a reflected laser beam at the minimum distance 'S' and continuing until: the image can no longer be formed on the sensor, the prism reaches a position where a grazing angle is formed between the prism and the incident ray, or where increasing the distance from the target does not achieve a significant increase in incident angle.

It must be noted here that no account is taken of such factors as: (i) decreased efficiency of transmission through the prism at angles close to the grazing angle because of increased reflection at the glass/air interface, (ii) the diminished light reflected from an object at a great distance, or (iii) the spread of the laser beam. These factors can be introduced later, if required.

If the prism is inclined so that the angle of Θ_{\min} is that of a ray that goes through the prism at the angle of minimum deviation then this will ensure that the non-linear effect of the prism will be used to greatest effect. Consideration of the geometry of the prism establishes that this angle is given by Equ. 6.1.

$$\text{Equ. 6.1. } \Theta_{\min} = d_{\min}/2 + A/2$$

where d_{\min} can be derived from Equ. 3.17. as Equ. 6.2.

$$\text{Equ. 6.2. } d_{\min} = 2 \cdot \sin^{-1}((n \cdot \sin(A/2)) - A$$

where 'A' = apex angle and 'n' = refractive index of the prism.

Hence, the angle of Θ_{inc} will initially be at an angle Θ_{\min} and reduce in value with increasing 'D'. The value of Θ_{inc} is evaluated with reference to Fig. 6.29. where it can be seen that $\Theta_{\text{inc}} = \Theta_{\min} - (\Theta_D - \Theta_S)$, where $\Theta_D = \tan^{-1}(D/B)$ and $\Theta_S = \tan^{-1}(S/B)$. Putting these equations together gives Equ. 6.3.

$$\text{Equ. 6.3. } \Theta_{\text{inc}} = \Theta_{\min} - \tan^{-1}(D/B) + \tan^{-1}(S/B)$$

6.5.4.2. Angle of exit from first element.

Equ. 6.3, satisfactorily describes the variation in angle between the minimum distance to be measured, and the maximum distance defined by the parameters and conditions already set. The subsequent change in angle as the incident light wave is refracted by the prism at its two interfaces has been described in section 3.4.1.1. Using the results given there and substituting for the variables which are most descriptive of this case Equ. 3.14, becomes Equ. 6.4.

$$\text{Equ. 6.4. } \theta_{\text{dev}} = \sin^{-1}(\sin(A)(n^2 - \sin^2(\theta_{\text{inc}}))^{1/2} - \sin(\theta_{\text{inc}}) \cdot \cos(A))$$

6.5.4.3. Orientation of the sensor to the prism.

As with the setting up of the initial angle that the prism makes with the start of the measuring range, it is also desirable to use the known characteristics of the prism to set up the angle of the lens and consequently to the sensor. This position is defined by the ray at θ_{min} being coincident with the start of the sensor, where the sensor is configured so that an increase in distance from the base will result in the image of the reflected laser beam being imaged a distance 'd' from the starting point, as defined in Fig. 6.30.

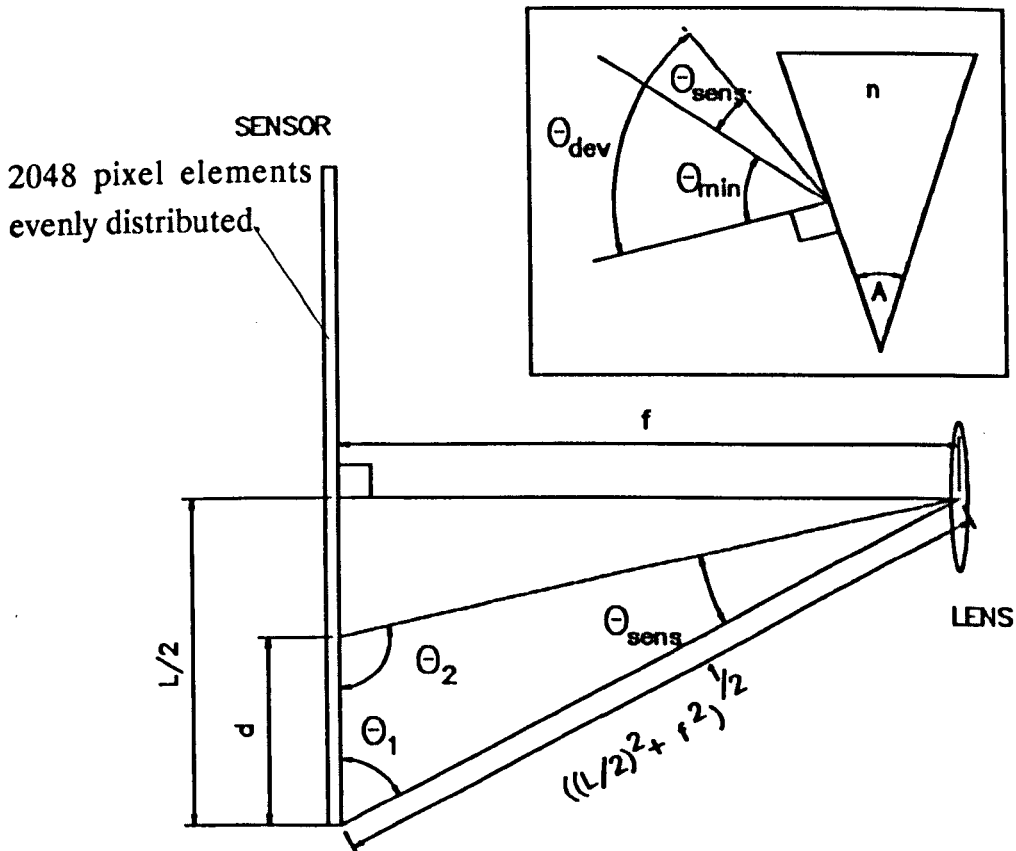


Fig. 6.30. Lens and sensor configuration.

The sensor is required to be parallel to the lens and in a position where its perpendicular bisector is at distance 'f' from the lens centre. Furthermore, the lens/sensor system is required to be at such an angle to the prism that the minimum deviation ray intersects the end of the sensor. In this configuration it is now possible to define 'd' as the distance from the end of the sensor, and obtain an equation linking 'd' to 'D' as required.

From the inset in Fig. 6.30. $\theta_{\text{sens}} = \theta_{\text{dev}} - \theta_{\text{min}}$, and from the main diagram in Fig. 6.30, the angle $\theta_1 = \tan^{-1}(2f/L)$, and $\theta_2 = 180 - (\theta_{\text{sens}} + \theta_1)$. Using the relationships $a/\sin(A) = b/\sin(B) = c/\sin(C)$, where a,b, & c are lengths of the sides of a triangle, and A,B,& C are their corresponding angles, 'd' can be written (Equ. 6.5.) in term of known constants and variables to give the relationship between 'd' and 'D'

$$\text{Equ. 6.5. } d = \sin(\theta_{\text{dev}} - \theta_{\text{min}}) \left((L/2)^2 + f^2 \right)^{1/2} / \sin(180 - \theta_{\text{dev}} + \theta_{\text{min}} - \tan^{-1}(2f/L)) - L/2$$

6.5.4.4. Analysis of the triangulation correction equation.

The equation linking the position of the image of the reflected laser light, from a surface distance 'D' away from the base line, which is imaged a distance 'd' from the optical axis of the sensor/lens combination, has been derived.

By entering appropriate values into this equation and varying the distance to be measured it is possible to characterise the performance of the system as a whole. Furthermore, if the equation is put into a computer program it is then possible, at will, to alter any of these variables and note the effect. It is also possible to include more than one prism element in the system or, by appropriate adjustment of the values used, create a prism of null effect by making its refractive index the same as for air.

6.5.5. Testing of correction to linearity.

To analyse the derived equation it is possible to plot the relationship between what will be the sensor output, and the distance of the measuring axis from the surface to be measured. The plotted information can then be compared to a ideal linear plot or a plot without the correction to the linearity provided by the prism.

The equation was placed into the transformation section of the software graph package 'Sigmaplot 4.0' from where data concerning a number of regular intervals of distance could be tabulated, and input into the equation with the resultant positions on the sensor placed alongside. Following the transformation, the data could be plotted

on screen and the process repeated for differing values of the variables, such as the focal length of the lens, and the prism apex angle.

Following the creation of the data an analysis of the data could take place using another feature of the software package where an equation, in this case the equation of a straight line, could be fitted by the least squares method to the data, and the residuals plotted. This method produces clear indication of the points deviating from a straight line, their magnitude and where they occur.

Six trials took place where the corrected and uncorrected relationships were arranged to have the same range and the same starting distance, hence, a plot of the residuals provides a good comparison. The first three sets used the ranges 1- 2m, 1-3m, and 1-4m, with a base length of 1m and the second three sets used the same ranges with a 0.5m. base length. These results are shown in Fig. 6.31 - Fig. 6.36.

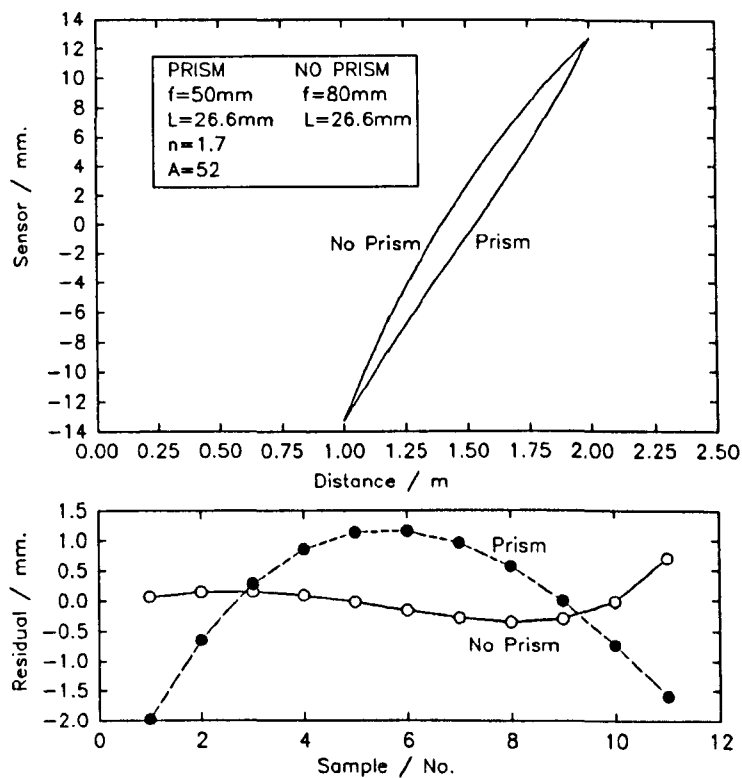


Fig. 6.31. Range 1-2 metres, 1 metre base length.

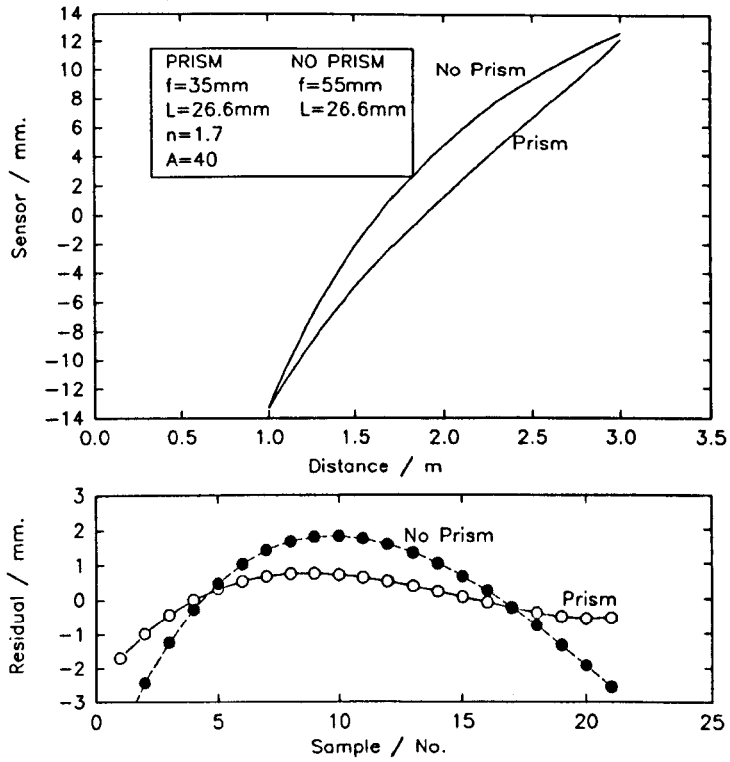


Fig. 6.32. Range 1-3 metres, 1 metre base length.

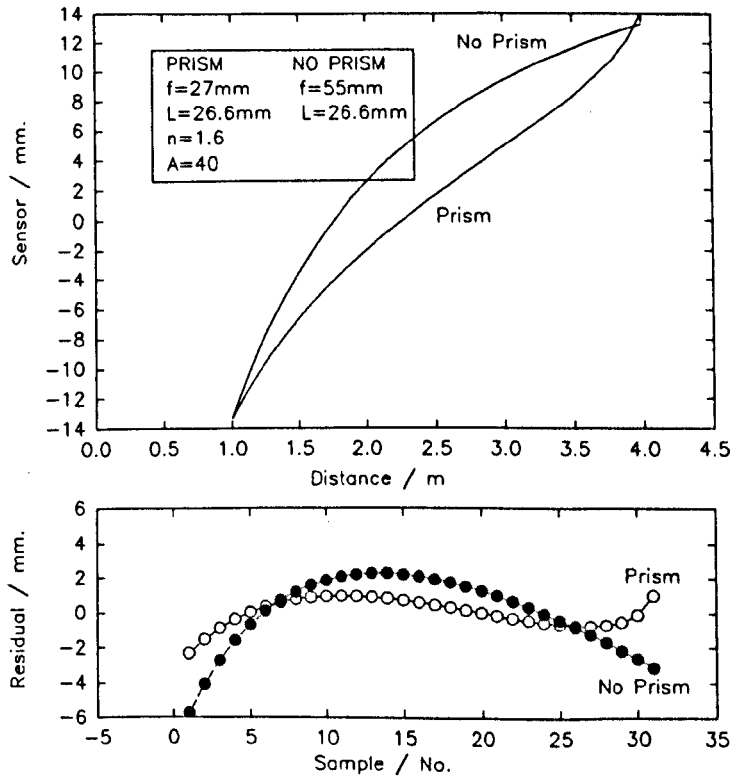


Fig. 6.33. Range 1-4 metres, 1 metre base length.

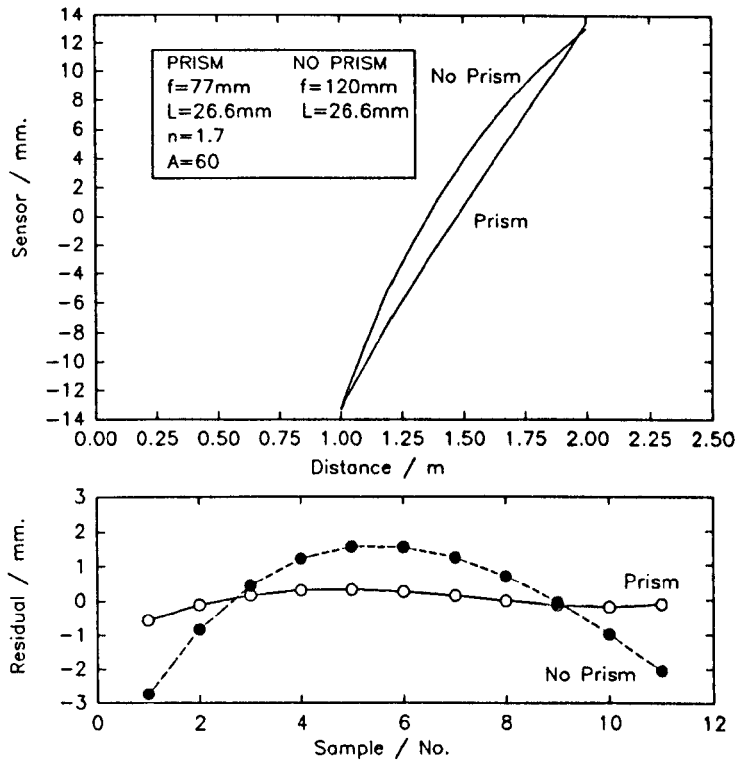


Fig. 6.34. Range 1-2 metres, 0.5 metre base length.

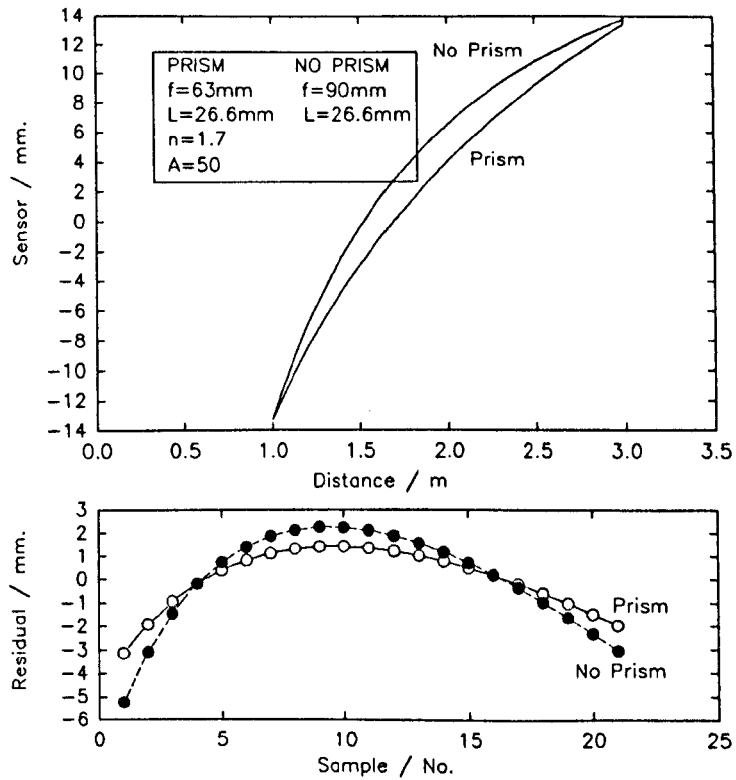


Fig. 6.35. Range 1-3 metres, 0.5 metre base length.

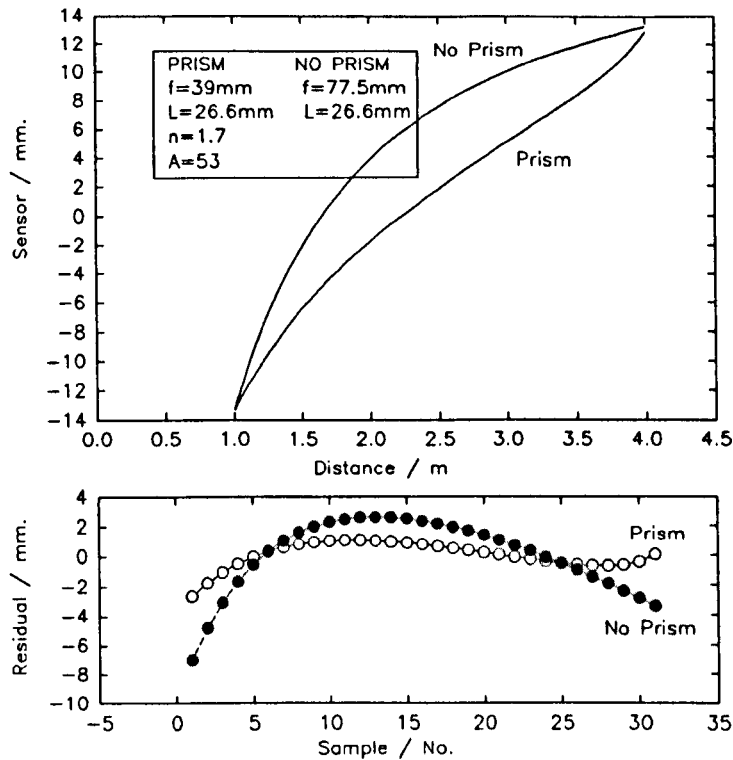


Fig. 6.36. Range 1-4 metres, 0.5 metre base length.

6.5.6. Summary of the correction method.

A number of conclusions can be drawn about the data presented here.

(i) In each case the use of the prism was able to significantly improve the linearity of the system because of the correction applied.

(ii) Both systems are amenable to design for a particular range, although the non corrected system has, for a desired base length, only the focal length available for adjustment, whereas the corrected system also has the parameters of the apex angle and the refractive index. These additional parameters allow the system to be adjusted for best results. For instance, Fig. 6.35, was not best adjusted, while Fig. 6.36, achieved better linearity, with a greater range, because of better use of the available parameters. The process of adjustment was trial and error assisted by an understanding of the role of the parameters in improving the performance.

(iii) The linearity correction is not exact, and in some cases, over correction can take place, however, this may be desirable if the overall linearity is improved.

(iv) The method described in this section can usefully be employed to provide a better design of triangulation system which will have better characteristics than one without this feature. It is not a solution to all of the problems of triangulation systems, but it may find a place as a method of regularising the use of this technique.

6.5.7. Limitations of large apex angle prisms.

Two problems are inherent in use of prisms, first, for large apex angles the angle of view is limited, and second, as the angle of incidence nears the grazing angle then there is a loss in light transmission due to a high proportion of reflection, rather than refraction, taking place at the glass/air interface. Hence, it is preferable to use a smaller apex angle, however, this will not result in such a strong correction because the non-linearity decreases with apex angle and refractive index.

The same degree of non-linearity correction, without resorting to large angle prisms, may be achieved by using two, or more, prisms in series so that deviated light from the first prism operates on the second prism which deviates it further. The only modification to the equations derived so far is to define the input to prism two as shown in Equ. 6.6,

$$\text{Equ. 6.6. } \Theta_{\text{inc}} = 2 * \Theta_{\text{min}} - \Theta_{\text{dev}}$$

where Θ_{min} is defined in Equ. 6.1. and Θ_{dev} is defined in Equ. 6.4.

The resulting equations were again placed in Sigmaplot and plotted as shown in Fig. 6.37, where a comparison was made between the two approaches. The two residual plots show that the double prism method was slightly superior to and at least equivalent to the single prism system.

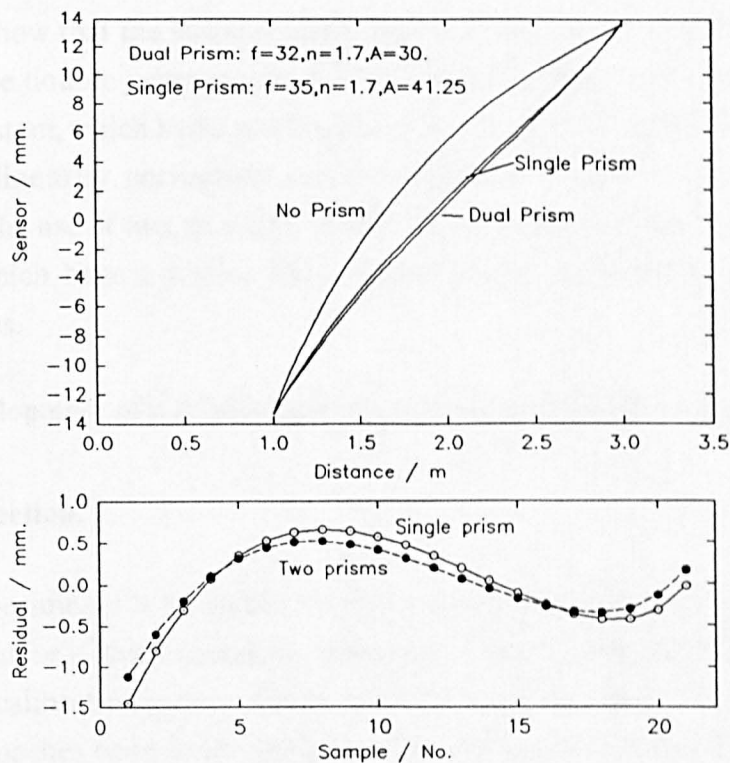


Fig. 6.37. Comparison between double and single prism corrections.

The method of using a least squares best fit of a straight line through the data does not give a clear indication of the degree of correction obtained. A better comparison is made using the residuals for a straight line (an ideal system) constructed between the x,y points -13.33, 1.0 and +13.33, 3.0. The two corrected curves are plotted and the results shown in Fig. 6.38.

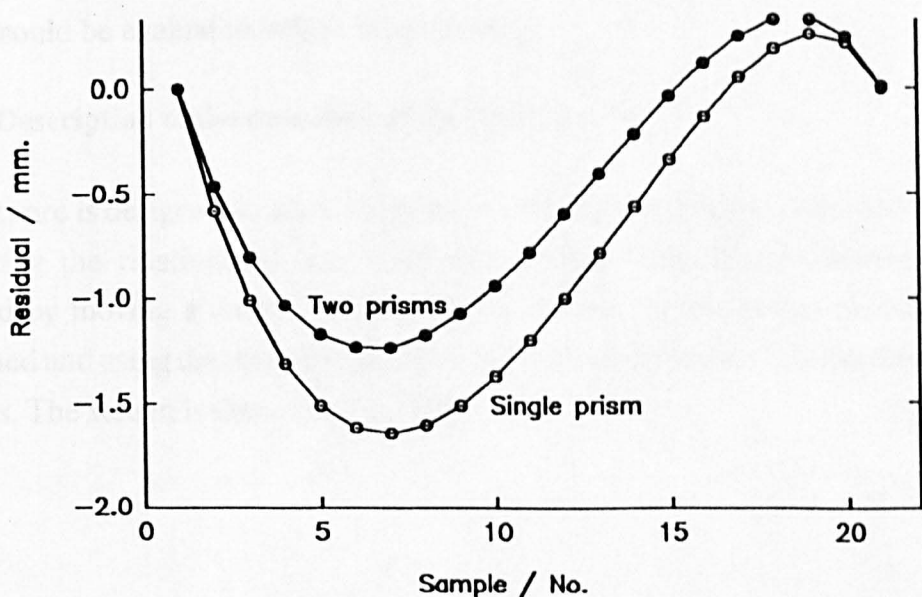


Fig. 6.38. Plot of residuals for linearity comparison.

These graphs show that the single prism achieved a maximum of 6% deviation from linearity and the double prism system 4.7%. Comparing the results with those of the uncorrected system, which had a maximum deviation of 20% from linearity, it is clear that the non-linearity correction method achieves a significant improvement. Furthermore, the use of two, or more, prisms allows for these benefits to be achieved with prisms which have a higher field of view and less problems due to surface reflection losses.

6.5.8. The development of a triangulation computer aided design program.

6.5.8.1. Introduction.

The task of experimentally trying out all of the permutations in a optical triangulation system, to optimise a given design, is enormous, even if, as described in section 6.3, an automated calibration system is built to speed up the process. Traditionally, there were two approaches open to the designer, first, the analysis of the theory to provide simplification and design rules, and second, the inspired or experienced guess at the right sort of parameters which are subsequently tested. It is now generally accepted that the speed and power of computers are able to simulate designs to test a hypothesis before costly experimentation takes place.

A software program was designed to investigate the various configurations to provide a Computer Aided Design (CAD) system for triangulation design. With the incorporation of the error analysis, the complete analysis of the performance of designs could be evaluated before bench testing.

6.5.8.2. Description of the operation of the CAD system.

The software is designed to allow the effect of changes in the parameters to be noted by plotting the relationship between target position and image position. This is achieved by moving a cursor to the position on the screen where the variable is positioned and using the up down cursor to increase or decrease that variable by fixed amounts. The screen is shown in Fig. 6.39.

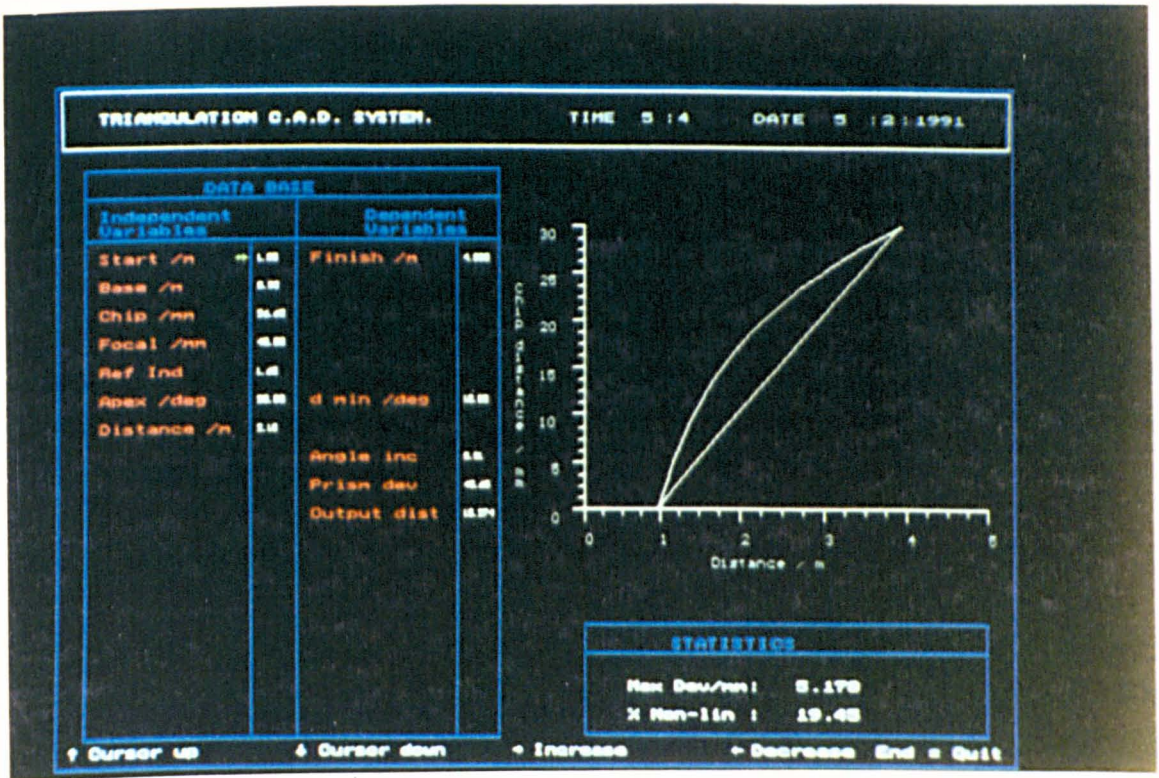


Fig. 6.39. Triangulation CAD screen.

The features shown on the screen are as follows:

(i) Parameter values.

On the left hand side the column of independent variables shows the parameters that can be changed by the user, beside this column are the dependent variables that are changed in response to the parameters selected.

The values of the parameters are stored in a file called 'setup.par' so that the configuration of the previous use of the software is used on the next start up.

Beside one of the parameters is a cursor which can be moved up and down by the up down cursor keys on the keyboard. The values of the variables can be changed by a set amount, different for each variable, either up or down by use of the side cursor keys.

(ii) Calculation of information.

When changes are made to the independent variables a recalculation takes place and the dependent variables are updated.

(iii) Plotting the results.

For each change in the variables, the relationship between the sensor image position and the distance from the sensor is plotted on the right hand screen. This plot uses the equations developed in this section of chapter 6.

A straight line is also plotted with the curve which shows the desired linear result. The maximum deviation of the corrected curve is calculated and the result shown in the lower right hand box marked 'statistics', together with the maximum percentage non-linearity over the range.

6.5.8.3. Conclusion.

This software program facilitated the testing of the design parameters for a triangulation system of the type developed in this thesis. Because of the power of the computer to recalculate the numerous values required to plot out the relationship between image and object distance, this process can save considerable time. Furthermore, because recalculation is so easy, many more permutations of the parameters can be considered before testing the components on the bench.

The software could be further improved to consider the case of two, or more, prisms and enable better plotting of the results, both on screen and by the printer. However, a significant start has been made on what has already proved to be a useful piece of software.

6.6. CONCLUSIONS.

In this chapter the results of three lines of research into the optical triangulation system have been presented and analysed. The conclusions of this work are as follows.

The correction of the linearity of the triangulation system is presented as a novel result of the research conducted for this thesis. The method is essentially very simple and elegant, it conforms to the correction to linearity made in other systems, but is believed to be new to this area. A software program has also been introduced that enables quick calculation and plotting of the relationship between image and object distance for a variety of configuration parameters.

The work conducted to analyse the use of the subpixel algorithms has shown that subpixel accuracy is easily achieved with minimum computational overhead.

However, other features of the overall design can negate the benefits, such as the instability in pointing angle of the laser.

The calibration and interpolation work has shown that the optical triangulation system can be arranged to measure distance over the range 0.9 - 5.0 metres with high accuracy. This accuracy can be improved by careful design. The causes of weakness in the measurement process have also been revealed and analysed.

7. CONCLUSIONS AND SUGGESTIONS FOR FURTHER WORK.

7.1. INTRODUCTION.

This chapter concludes the work of this thesis with a discussion of the salient features of the research, and discusses further work that could be undertaken in this area.

7.2. RESEARCH ACHIEVEMENTS.

This thesis concerns the research conducted into the technique of optical triangulation applied to the task of distance measurement over the range 0.1 to 30 metres. Optical triangulation has frequently been used for distance measurement for accurate, closer range, applications, and over the same range, with less accuracy. However, its use over the specified range, with medium accuracy, has only rarely been considered. As a result, much of the research has concentrated on the analysis of the mechanical and electro-optic triangulation configuration, with the aim of reducing the inherent errors in these systems for surveying applications.

As a result of the research conducted for the thesis three papers have been published at International conferences, and one at a National conference. A patent has been filed concerning the correction of the non-linearity of the triangulation system.

The correction to the, normally ill conditioned, triangulation system is an elegant solution to this problem, and a major result of this research. In addition, three prototypes were designed, built, and tested, which were demonstrated to numerous organisations for consideration. The third prototype was tested for Thames Water Plc and shown to be transportable and battery powered. A further contract has been negotiated with North West Water Plc, to develop a system for remote inspection of sewers and water mains.

A system of distance measurement was designed, and tested, which when compared to the commercial equipment that was available during the period of research, achieved a significant improvement in speed, and accuracy of measurement. The measuring technique was tested in a number of prototype designs and also by experimental and simulation work.

7.3. FURTHER WORK.

Optical triangulation is not an ideal measuring technique, it suffers from several limitations such as: (i) a finite speed of measurement, (ii) the requirement for a clear field of view for the camera and light source, (iii) the physical size of the instrument is not insignificant, (iv) there is a dependency on a high intensity light source, and (v) the resolution achieved is finite, so accuracy must be balanced with the required range.

Many of the limitations of the optical triangulation technique are fundamental to its operation and so research is not likely to increase the overall attractiveness of this technique by orders of magnitude. Hence, the alternative techniques of direct measurement by laser techniques, are probably going to be a better long term solution to measurement problems, and, are a better line of research if solutions can be found to the problems of speed and accuracy. However, in spite of the remaining major limitations of optical triangulation, that of occlusion and the associated size of the measuring device, there may be reasons for continued interest because of the variety of suitable applications. Hence, its continued application will be because, over a limited range, the measurement scheme may perform significantly better than the coaxial measurement method for non-contact measurement to non-cooperative surfaces.

There are a number of areas where further development work would appear to be appropriate. This thesis has shown that the technique can already perform better than any commonly available surveying tool over the specified range, accuracy, and the specific tasks for which the equipment has been developed. Hence, further research could be carried out in the following areas:

7.3.1. Investigation into laser beam pointing stability.

The pointing stability of the light source has been shown to exert an undue influence in reducing the accuracy of measurement available to a triangulation system. Consideration of the cause of such pointing errors, and methods of reducing, or

offsetting, its effect are required. Such investigation would repay the effort of the research with increased accuracy of measurement.

7.3.2. Exposure time control.

Structures requiring survey have a wide variation of surface reflectivity, this can lead to a deterioration in the subpixel accuracy which it is possible to achieve. Hence, an automatic exposure control system is desirable. Diodes lasers can be easily modulated to reduce the intensity output, but, if a HeNe laser is used, then this involves additional components which would add to the expense of the complete system.

7.3.3. Temperature compensation.

The variation in temperature which takes place in the surveying environment can adversely affect the measurement accuracy if the magnitude of the effect is unknown and cannot be compensated for. Hence, if the design allows expansion of vital components, such as the measuring axis, then a means of adjustment is required to ensure minimum errors in measurement.

7.3.4. Compact system design.

A fundamental aspect of optical triangulation systems is the problem of increased non-linearity with reduced base length. This thesis has identified a partial solution to this problem by the use of compensating non-linear optics. Further work could be carried out to assess the extent of the benefit that can be achieved, and to consider other non-linear elements.

7.3.5. Hardware implementation of the image processing algorithms.

The algorithms used to obtain subpixel accuracy can be processed by microprocessor, as in the first and third prototype, but this is expensive and inherently limited in speed by the processor. However, the algorithm can be processed in purpose made hardware which will be much cheaper and faster.

7.3.6. Rotation of the measuring system.

One of the fundamental measurements that takes place when measuring a cross section of a structure, is that of angle. It is desirable that this measurement is achieved with the minimum of computational, or operational overhead. Research is required

to test out the reliability of this measurement, especially for the case of a high speed rotation of the measuring axis.

7.4. CONCLUSION.

This thesis describes the research and development of a surveying tool that has a speed and accuracy specification which is superior to that currently available to the engineer, or surveyor, who wishes to measure the cross sections of structures such as tunnels, sewers, and water mains. This technique may advantageously be used to save time taken in survey work, and encourage the survey of structures not normally measured because of cost. The information gathered will be of increasing use to engineers as the technology to manipulate and analyse such data is developed.

Further developments in the technology of sensors, lasers, electronics, displays, mass storage, and optics will mean that the optical triangulation system can be improved, as it has been during the period of research.

APPENDIX 1.

CALIBRATION EQUIPMENT.

3.9.2.1. Introduction.

A test bed was constructed which was used to calibrate the triangulation based measuring system. The test bed consisted of an interferometer, a six metre long optical bench, a motor driven trolley target, and a computer system to interface to all of these components to gather data. The gathered information enabled a number of tests to be carried out which are described in chapter 6.

3.9.2.2. Specification.

The Hewlett Packard interferometer model 5526A was used with the following general specification:

- (i) accuracy 0.2 micron per metre ± 2 counts in last digit,
- (ii) resolution 0.01 micron,
- (iii) range 213 metres,
- (iv) maximum measuring velocity 0.3 metres/sec, and
- (v) compensation for velocity of light variation (humidity/temperature/pressure).

In operation the interferometer measures relative distance from a arbitrary starting point. A HeNe laser beam is directed at a corner cube reflector. This beam cannot be interrupted during the measuring process.

3.9.2.3. Operation.

The block diagram for the interferometer is illustrated in Fig. 3.39.

Hewlett Packard Interferometer.

Block Diagram

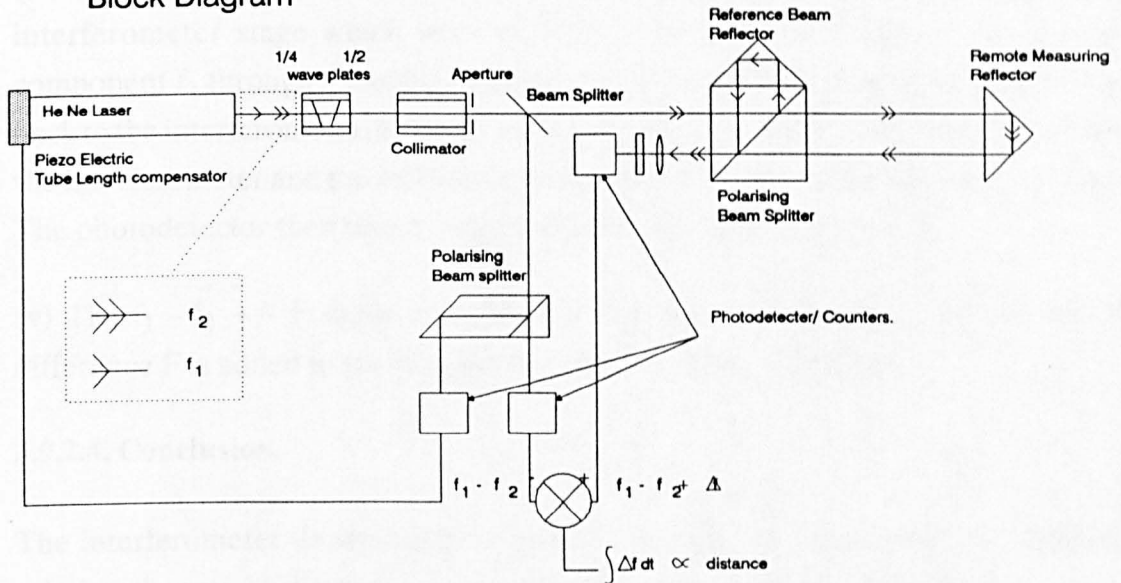


Fig. 3.39. Block diagram of Hewlett Packard interferometer.

The operation is as follows:

- (i) The laser produces a coherent beam of light of approximately 1mW in output power. A cylindrical permanent magnet around the optical cavity of the laser tube causes the laser to resonate at two slightly different frequencies by Zeeman splitting. These two frequencies f_1 and f_2 are of opposite circular polarisation and pass through a quarter wave plate and then a half wave plate which changes the beam to linear vertical and horizontal polarisation.
- (ii) The two orthogonally polarised frequencies pass through a collimating lens/aperture and then pass through the main beam splitter.
- (iii) The small proportion of the beam that is diverted through 90° passes into the lock and reference polarising beam splitter where 80% of f_1 goes in one direction and 20% goes in the other, with the opposite percentages of f_2 going the other direction. The polarising beam splitter changes the polarisations enough so three signals can be

detected: 80% of f_1 , 80% of f_2 and $f_1 - f_2$ for reference. The f_1 and f_2 signals are compared and used to provide an error signal for the Piezo-electric tube length compensator. This enables the laser wavelength to be accurately controlled.

(iv) The largest proportion of the beam from the main beam splitter continues to the interferometer stage which uses another polarising beam splitter to pass one component f_1 through a fixed distance and f_2 through the corner cube reflector and back to the interferometer, hence giving the measuring path. Relative motion between the interferometer and the reflector causes a Doppler shift in the returned frequency. The photodetector then sees a fringe frequency given by $f_1 - f_2 \pm F$.

(v) The $f_1 - f_2 \pm F$ signal is compared with the $f_1 - f_2$ signal reference and the difference F is added to the fringe count accumulated in a register.

3.9.2.4. Conclusion.

The interferometer illustrated here provides a high accuracy device for measuring relative changes in displacement over a reasonable distance. Two disadvantages of this system are: first, that the system cannot give absolute distance because it is a counting system and second, an uninterrupted laser beam with retro-reflector is required. However, within these limitations the system provides an unambiguous result which simple to use and is very useful to anyone wishing to monitor large or small displacements with high accuracy.

REFERENCES.

CHAPTER 1.

Kennie. T.J.M, and Petrie. G, 'Engineering surveying technology.', Blackie and Son Ltd, U.K., pp. 3-5, 1990.

Vancans. N, 'Surveying Equipment, trends in surveying.' Wild Heerbrugg(UK) Ltd. Civil Engineering, Product Profile, 1987.

Jones. M.B, 'New lines in survey equipment.', Tunnels and Tunnelling, November, 1987.

CHAPTER 2.

Amberg, AMT Profiler 2000, Manufacturers literature, Amberg Measurement Technique Ltd, Ausstellungsstrasse 88, PO Box 3131, CH-8031, Zurich, Switzerland.

American, 'Manual of Photogrammetry.', 4th Edition, Published by American Society of photogrammetry. Ed. C.C. Slama, 1980.

Anderson. H, Stevens. D, 'Mono-photographic tunnel profiling.', Close-range photogrammetry & surveying state of the art, Pub. American Society of Photogrammetry, U.S.A., pp. 863-869, 1984.

Anthony. D.M, 'Engineering metrology.', Pergamon press, pp. 170-173, 1986.

Badekas. J, 'Photogrammetric surveys of monuments and sites', Ed J. Badekas, Pub North-Holland/ American Elsevier, 176 pages, 1985.

Bastuheck. C.M, Schwartz. J.T, 'Experimental implementation of a ratio image depth sensor.', Techniques for 3-D machine perception, Ed A. Rosenfield, Elsevier Science Publishers, Holland, pp.1-12, 1985.

Bodlaj. V, Klement. E, 'Remote measurement of distance and thickness using a deflected laser beam.', Applied optics, Vol. 15, No 6, pp. 1432-1436, 1976.

Brady. J.P, Nandhakumar. N, Aggarwal. J.K, 'Recent progress in object recognition from range data.', Image and Vision computing, Vol. 7, No 4, pp. 295-307, Nov 1989.

BritRail, British Rail Tender document, personal communication, 1988,

Browne. M.A, Falkowki. J.L, 'Passive visual tracking for robotic arc welding.', Int. Conf. Optical techniques in process control, pp. 207-216, 1983.

Burnside. C.D, 'Electromagnetic Distance Measurement.', Granada Publishing, 2nd Edition, U.K., 1982.

Chen. Y, Tsai. M, 'A scanning laser range finder with dual receivers.', Journal of Chinese Institute of Engineers, Vol. 10, No 1, pp. 67-74, 1987.

Connel. D.V, 'NPL-Hilger & Watt Mekometer.', Electromagnetic distance measurement., Pub Hilger and Watts ltd, pp. 278-285, 1965.

Deng. T, Bergen. T.L, 'Accuracy of position estimation by centroid', Proc. SPIE Conf. on Intelligent Robots and Computer Vision: Sixth in a series, Vol. SPIE-848, pp. 141-150, 1987.

Developments CRP, 'Developments in close range photogrammetry - 1.', Ed K.B. Atkinson, Pub Applied Science publishers Ltd, London p.v., 1980,

Duda. R.O, Nitzan. D.A, Barrett. P, 'Use of range and reflectance data to find planar surface regions.', IEEE Trans PAMI, Vol. PAMI-1, No3, p. 259-271, 1979.

Eagle, Manufacturers technical information, Eagle 3515-203 precision laser measurement system, Digital Optronics Corporation, Virginia, U.S.A.

Economou, G, Youngquist. R.C, 'Limitations and noise in interferometric systems using frequency ramped single diode lasers.', *Journal of Lightwave Technology*, Vol. LT-4, No 11, pp. 1601-1608, 1986.

Edworthy. M, 'Television measurement for railway structure gauging.', *SPIE*, Vol 654 *Automatic Optical Inspection*, pp. 35-42. 1986.

El-Hakim. S.F, 'A real time system for object measurement with CCD cameras.', *Int. Arc Photogrammetry*, 26(5), pp. 363-373, 1986.

Foo. V.W, 'Automatic shape measurement for tunnel profiling.', *Land and Mineral Surveying*, Vol 7, pp. 350-351, 1989.

Fellows. S, 'Tunnel profiling by photography.', *Tunnels and tunnelling*, May, pp. 70-73, 1976.

Fennel, FET 1 tunnel profile scanner, manufacturers literature, EO Fennel, FÜhrer & Co, MÜhlenbergstr. 21, D-3507 Baunatal 6, West Germany.

Froome. K.D, Bradsell. R.H, 'Distance measurement by means of a modulated light beam yet independent of the speed of light.', *Electromagnetic distance measurement.*, Pub Hilger and Watts ltd, pp. 263-277, 1965.

Garner. J, James. D, Bird. R, 'Surveying.', *The estates gazette Ltd*, London, pp. 25-30, 1976.

Gates. J.W.C, 'Applications of non-conventional imagery', *Developments in close range photogrammetry*, ED K.B. Atkinson, Pub Applied Science publishers Ltd, London, p. 199, 1980.

Goh. K.H, Phillips. N, Bell. R, 'The applicability of a laser triangulation probe to non-contacting inspection.', *Int J. Production Research*, Vol 24, No 6, pp. 1331-1348, 1986.

Gottwald. R, Berner. W, 'A new angle on 3-D coordinate determination.', *Sensor Review*, 7(3), pp. 143-146, 1987.

Grattan. K, Meggit. B, Palmer. A, 'Proposed ranging technique with coherent optical radiation from laser diode using phase shift method.', City University, awaiting publication, 1990.

Grossmann. P, 'Depth from focus.', Pattern recognition letters, 5, pp. 63-69, 1987.

GWI, Graham & White Instruments Ltd, Laser analog displacement sensor LAS-5010, manufacturers literature, 1990.

Hagedorn. H, 'Electronic profile measuring system for tunnels and slopes.', Rock Mechanics, Vol 19, pp. 89-97, 1986.

Haggrén. H, 'Real time photogrammetry as used for machine vision applications.', Int Arch. Photogrammetry. 26(5), pp. 374-382, 1986.

Hall. S.J, 'Vision measurement technology using photogrammetry for quality control in the Aerospace industry.', pp. 77-88.

Hallert. B, 'Photogrammetry - basic principles and general survey.', Mc Graw Hill Book Co, U.S.A., pp. 52-58, 1960.

Handbook NTP, 'Hand book of non-topographic photogrammetry', 1st edition, Pub American society of photogrammetry, 1979.

Hantke. D, Philipp. H, Sparrer. G, 'Precision measurement on position sensitive photodetectors.' Proc Theoretical Metrology, pp. 153-158, 1986.

Harding. H, 'Historical aspects of tunnelling.', Tunnels and tunnelling, January, pp. 53-61, 1972.

Harris. K.D, 'Progress in the application of lasers to distance measurement.', Electromagnetic distance measurement., Pub Hilger and Watts ltd, pp. 391-397, 1965.

Häusler. G, Hermann. J, Wiebmann. H, 'Neue 3D - Sensoren mit nützlichen Eigenschaften.', Optical 3-D measurement techniques, Pub. Wichmann, Ed. Gruen/Kahmen, pp. 57-65, 1989.

Howe. R.D, Kychakoff, 'Optical inverse-square displacement sensor.', Applied Optics, Vol 29 No 10, 1st April 1990, p 1390. (Summary of patent application), 1990.

Hume. K.J, 'A History of engineering metrology.', Mechanical Engineering Publications Ltd, 220 pages, 1980.

Hymans. A.J, Lait. J, 'Analysis of a frequency modulated continuous wave ranging system.', Instn. E.E. Paper No 3264 E, pp. 365-372, July, 1960.

Ishii. M, Nagata. T, 'Feature extraction of three dimensional objects and visual processing in a hand-eye system using a laser tracker.', Pattern Recognition, Pergamon Press, Vol 8, pp. 229- 237, 1976.

Irvine. W, 'Surveying for construction.', Third edition, Mc Graw Hill Book Co, pp. 178-199, 1988.

Jarvis. R.A, 'A perspective on range finding techniques for computer vision.', IEEE Trans on PAMI, Vol PAMI-5, No 2, pp. 122- 139, 1983.

Jarvis. R.A, 'Range from brightness for robotic vision.', 4th Int ROVISEC, pp. 165-172, 1984.

Joynes. G.M.S, Davis. Q.V, 'Movement measurement by modulated lasers using frequency lock loops.', Optics and Laser Technology, pp. 169-174, August 1975.

Kaisto. I, Kostamovaara. J, Manninen. M, Myllya. R, 'Optical range finder for 1.5-10 m distances.', Applied Optics, Vol. 22, No. 20, pp. 3258-3264, October 1983.

Karara. H.M, 'Close-range photogrammetry: where are we where are we headed.', Close-range photogrammetry & surveying state of the art., Pub American Society of Photogrammetry, U.S.A., Proc, pp. 927-934, 1984.

Kawata. Y, et al, 'A precision microwave rangefinder and its application to level measurement in the steel industry', Industrial metrology 1. Elsevier Science publishers B.V. pp. 19-32, 1990.

Kennie. T.J.M, Petrie. G, 'Engineering surveying technology.', Blackie and Son, U.K., 1990.

Kobayashi. T, Shudong. J, 'Optical FM interferometry for range and displacement measurements.', CPEM Digest, 1988.

Kyle. S, Moffit. N, Bethel. J, 'Kern SPACE: Extended Features and Industrial solutions.', Optical 3-D measurement techniques., Ed Gruen & Kahmen, Pub Wichhmann, pp. 206-215, 1989.

Lindsey. N, City University, Personal communication, 1991.

Luhmann. T, 'Image recording systems for close-range photogrammetry.', SPIE Vol. 1395, Conf. Close range photogrammetry meets machine vision., pp. 86-95, 1990.

Maclean. S.G, et. al, 'Vision system development in a space simulation laboratory.', Proc SPIE, Vol 1395 'Close range photogrammetry meets machine vision.', pp. 8-15, 1990.

MDL, MDL profiler, manufacturers literature, Measurement devices Ltd, 3 Old Hall Mews, Colney, Norwich, Norfolk, NR4 7TX.

Mundy. J.L, Porter. G.B, 'A three-dimensional sensor based on structured light.', Three dimensional machine vision, Ed. T. Kanade, Kluwer Academic Publishers.

Nimrod. N, Margalith. A, Mergler. H.W, 'A laser-based scanning range finder for robotic applications.', Robot sensors., Vol 1 vision, Ed A. Pugh, IFS Publications Ltd, Uk, pp. 159-173.

Nitzan. D, 'Three dimensional vision structure for robot applications.', IEEE PAMI, Vol 10, No 3, pp. 291-309, 1988.

O'Connor. B, 'An optical system for determining the positional accuracy of a robot.', Trans Inst. MC, Vol 12, No 2, pp. 85-90, 1990.

Price. W.F, Uren. J, 'Laser surveying.', Van Nostrand Reinhold (International), pp. 155-156, 1989.

Proctor. D.W, Atkinson. K.B, 'Experimental photogrammetric wriggle survey in the Second Mersey Tunnel.', Tunnels and Tunnelling, March. pp. 115-118, 145, 1972.

- Rarity. J.G, et al, 'Experimental demonstration of single photon rangefinding using parametric down conversion.', *Applied Optics*, Vol 29, No 19, pp. 2939-2943, 1990.
- Rioux. M, 'Laser range finder based on synchronised scanners.', *Robot sensors., Vol 1 vision*, Ed A. Pugh, IFS Publications Ltd, Uk. pp. 175-190.
- Rivett. L.J, 'The application of photogrammetry to the measurement of tunnel profiles.', *Cranks and nuts*, Melbourne University Engineering Students Club, 1973.
- Rockset, Photosect 40, Publicity document by Rockset, Rockset International Sales AB, Box 5319, 102-46 Stockholm, Sweden, 1987.
- Rost, Manufacturers data sheet concerning PROTA 2, tunnel profiler, Austria, 1989.
- Rost. R & A, *Surveying Equipment catalogue*, 1990.
- Rüeger. J.M, 'Electronic Distance Measurement.', Pub. Springer-Verlag, Germany, 3rd Edition, 266 pages, 1990.
- Shinohara. S, et al, 'High resolution range finder with wide dynamic range of 0.2m to 1 m using a frequency-modulated laser diode.', *IECON 89, 15th Annual conference of IEEE Industrial Electronics society*, Vol 3, pp 646-651, 1989.
- SIRA, Sira/Brunel, 'Automatic inspection for industrial quality assurance.', course notes, 1988.
- Small. G.W, Hegedus. Z.S, 'Measurement of rail cross-section with solid-state sensor arrays.', *Optics and laser technology*, pp. 43- 47, 1986.
- Smati. Z, Yapp. D, Smith. C.J, 'Laser guidance system for robots.', *4th Int ROVISEC*, pp. 91-101, 1984.
- Stirling. D.M, 'Close range photogrammetry', *Engineering Surveying Technology*, Ed. T.J.M. Kennie & G Petrie, Blackie & Son Ltd, U.K., pp. 311-312.
- Strosche. H, 'Range and accuracy of the EOS Electro Optical Telemeter.', *Electromagnetic distance measurement.*, Pub Hilger and Watts ltd, pp. 287-293, 1965.

Tiziani. H, 'Optical 3-D measurement techniques - a survey.', Gruen & Kahmen Ed. Vienna Sept, pp. 3-21, 1989.

Torlegård, 'An introduction to close range photogrammetry', 'Developments in close range photogrammetry - 1.', Ed K.B. Atkinson, Pub Applied Science publishers Ltd, London, pp. 10-11, 1980.

Tunnels and Tunnelling, Machinery. plant and equipment issue, August, p. 85, 1984.

Tunnels and Tunnelling, Advertisement for 'prota 2', July, p. 55, 1989.

Van den Berg. F.T.M, 'The LAMBDA system: an optical sensor for measuring thickness and distance.', Technical note, Applied Laser Technology bv, Po Box 150, 5720 AD Asden, The Netherlands, 1990.

Verbeek. P.W, et al, 'Range cameras at video speed based on a PSD-array or a CCD-interpolation.', Proc. IASTED, Lugano, June, pp. 67-69, 1985.

Vulylsteke. P, Oosterlinck. A, 'Range-image acquisition with a single binary encoded light pattern.', IEEE Trans PAMI, Vol 12, No. 2, pp. 148-164, 1990.

Warnecke. H.J, Ahlers. R.J, Kim. H, 'New sensor for optoelectronic microprofilometry.', SPIE Vol 849, Automated Inspection and High Speed Vision Architectures, pp. 218-224, 1987.

West. G.A.W, Staines. R, 'Instrumentation for surveying underground structures using image processing.', IMEKO pp. 273- 283, 1989.

Wiese. D.R, 'Laser triangulation sensors: a good choice for high speed inspection.', I & C.S. (U.S.A.), Vol 62, No 9, pp. 27-29, 1989.

Willett. D.C, 'The development of tunnelling and the use of underground space through the ages.', Tunnels and Tunnelling, September, pp. 81-85, 1979.

Wolf. P, 'Elements of Photogrammetry', 2nd Edition, Published by Mc Graw Hill Book Co, U.S.A., p.1, 1983.

CHAPTER 3.

Barbe, 'The charged coupled device.', Optical sensing techniques and signal processing, 1975.

Bobb. M.A, 'Diode-Laser collimators suit communication applications in space', Laser Focus/Electro Optics, No 8, pp. 79- 86, 1988.

Boorland, 'Numerical Methods Toolbox', Boorland International, 4585 Scotts Valley Drive, Scotts Valley, CA 95066, pp. 43-59, 1987.

Bridges. W, 'Optics.', in Newport Catalog - Precision Laser and Optics Products, Pub. Newport Corporation, Fountain Valley, California, U.S.A., pp. N1-31, 1989.

Brook. R.A, Purll. D.J, 'Design of a polaris star sensor using charge-coupled device (CCD) imaging and LSI and microprocessor- based 'signal processing', Proc. SPIE Conf. on Smart Sensors, Vol. SPIE-178, pp. 210-220, 1979.

Castleman. K.R, 'Digital image processing.', publ. Prentice Hall, ISBN 0-13-212365-7, 1979.

Chen. Y, Tsai. M, 'A scanning laser range finder with dual receivers.', Journal of Chinese Institute of Engineers, Vol. 10, No 1, pp. 67-74, 1987.

Deng. T, Bergen. T.L, 'Accuracy of position estimation by centroid', Proc. SPIE Conf. on Intelligent Robots and Computer Vision: Sixth in a series, Vol. SPIE-848, pp. 141-150, 1987.

Doebelin. E.O, 'Measurement systems', applications and design.', pp. 19-36, Mc Graw Hill, Japan, 1983.

El-Hakim. S.F, 'A real time system for object measurement with CCD cameras.', Int. Arc Photogrammetry, 26(5), pp. 363-373, 1986.

Fairchild, 'CCD solid State Imaging Technology.', Manufacturers literature, Fairchild Weston Systems Inc, CCD imaging division, 1801 McCarthy Blvd, Milpitas, CA 95035, U.S.A., 1989.

Gallacher, K.J., Robinson. R.J, UK Patent application, GBB 2173301A, 1986.

- Goh. K.H, 'The applicability of a laser triangulation probe to non-contacting inspection.', *International Journal of Production Research*, Vol.. 24/ No 6, 1331-1348, 1986.
- Gottwald. R, Berner. W, 'A new angle on 3-D coordinate determination.', *Sensor Review*, 7(3), pp. 143-146. 1987.
- Greenspan. D, Casulli. V, 'Numerical Analysis for Applied Mathematics, Science and Engineering.', Addison Wesley, pp. 48- 70, 1988.
- Hagedorn. H, 'Electronic Profile Measuring System of Tunnels and Slopes.', *Technical note, Rock Mechanics and Rock Engineering*, Vol. 19/2, pp. 89-97, 1987.
- Hecht. E, Zajac. A, 'Optics.', Addison Wesley, 4th Edition, 563 pages, 1973.
- Ho. W-H, 'Close-range mapping with a solid state camera', *Photogrammetric Engineering and Remote Sensing*, Vol. 52, No. 1, pp. 67-74, 1986.
- Hopwood. R.K, 'Design Considerations for a solid state image sensing system.', E.G. and G. Reticon, *SPIE Vol. 230, Minicomputers and Microprocessors in Optical Systems*, 1980.
- Hou. H.S, Andrews H.C, 'Cubic spline for image interpretation and digital fitting.', *IEEE Trans. on Acoustics, Speech and Signal Processing*, Vol. ASSP-26, No. 6, pp. 508-516, 1978.
- Hultquist. P, 'Numerical Methods for Engineers and Computer Scientists', Benjamin / Cummings Publishing Co Inc., 1988.
- Irvine. W, 'Surveying for construction.', Mc Graw Hill Book Co, 3rd Ed:156-176, 283 pages, England, 1986.
- Ji. Z, Lue. M.C, 'Design of optical triangulation devices.', *Optics & Laser Technology*, Vol. 21 No 5, pp. 335-338, 1989.
- Jones. R, Wykes. C, 'Holographic and Speckle Interferometry.', Cambridge University Press, 1983.

- Keating. M.P, 'Geometrical, Physical, and Visual Optics.', Butterworths, pp. 360-377, 1988.
- Lake. D, 'Solid State Cameras.', Proc of 4th Int Conf on Robot Vision and Sensory controls. 1984.
- Lange. G, Mossbacher. B, Purll. D.J, 'The ROSAT star tracker', Proc. SPIE Conf. on Instrumentation in Astronomy No. 6, 1986.
- Marescaux. F, 'CCD news letter.', Optimum Vision, Antrobus House, 18 college street, Petersfield, Hants, GU13 4AD , Fairchild Weston, CCD Imaging Division, Paris, May, 1989.
- Melles, 'Optics Guide 2.', Melles Griot, Manufacturers literature, pp. 44-58.
- Meyer-Arendt. J.R, 'Introduction to Classical and Modern Optics.', Prentice Hall, U.S.A., pp. 318-328, 1984.
- Overington. I. Greenway. P, 'Practical first-difference edge detection with subpixel accuracy.', Image and Vision Computing, Vol. 5, No. 3, pp. 217-224, 1987.
- Page, C.J, Hassam. H, 'The orientation of difficult components for automatic assembly.' Robot Sensors Vol. I, Ed A. Pugh, IFS Publications, pp. 191-204.
- Ravich, L.E, 'Charged-Coupled Devices : a primer.', Laser Focus/Electro Optics, June, 1987.
- Salomon. P.M, 'Charge-coupled device (CCD) trackers for high accuracy guidance applications.', Proc. SPIE Conf. on Recent Advances in TV Sensors and Systems, Vol. SPIE-203, pp. 130-135, 1979.
- Sentel, Sentel CB1500 frame card reference manual, Sentel Messtechnik GmbH, W. Germany.
- Schroeder. H.E, 'Practical Illumination concept and technique for machine vision.', Robot sensors Vol. I, Ed A. Pugh, IFS Publications Ltd.
- Smith. A.L.S, 'He-Ne lasers are alive and well', Laser Focus World, July, pp. 75, 1989.

- Smith. M.R, 'Interpolation, differentiation, data smoothing and least squares fit to data with decreased computational overhead.', IEEE Trans. on Industrial Electronics, Vol. IE-32, No. 2, pp. 135-141, 1985.
- Southall. J.P.C, 'Mirrors, prisms and lenses.', Dover Publications, Inc, U.S.A., p. 806, 1964.
- Svelto. O, 'Principles of Lasers.', Orazio Svelto, 2nd Edition, Plenum Press, New York, 1982.
- Tian. Q, Huhns. M.N, 'Algorithms for subpixel registration.', Computer Vision, Graphics and Image Processing, Vol. 35, pp.220- 233, 1986.
- Tiziani. H, 'Optical 3-D Measurement Techniques - a survey.', Int Conf Optical 3-D Measurement Techniques, Vienna/Austria, September, pp. 3-21, 1989.
- Trinder. J.C, 'Precision of digital target location.', Photogrammetric Engineering and Remote Sensing, Vol. 55, No. 6, pp. 883-886, 1989.
- Tunnacliffe. A.H, Hirst, J.G, 'Optics.', The Eastern Press Ltd, G.B., 638 pages, 1986.
- Warnecke. H. J, Ahlers. R. J, Kim. H, 'New sensor for optoelectronic microprofilometry.', SPIE Vol. 849, Automated Inspection and High Speed Vision Architectures, pp. 218-224, 1987.
- Wheeler, J.P, 'The HeNe vs the red diode.', Lasers and optronics, pp. 38-44, Sept, 1990.
- Wiese. D.R, 'Laser triangulation sensors: a good choice for high speed inspection.', I & C.S. (U.S.A.), Vol. 62, No 9, pp. 27-29, 1989.
- Wilson. J, Hawkes. J.F.B, 'Optoelectronics: and introduction.', Prentice Hall International, U.S.A., pp. 174-277, 405 pages, 1983.
- Wolf. P.W, 'Elements of Photogrammetry.', Mc Graw Hill Book Co Ltd, 2nd Edition, pp. 31-33. 628 pages, Singapore, 1983.

CHAPTER 4.

AutoCAD, reference manual, Autodesk Ltd, pp. 395-420, 1989.

Boorland, 'Numerical Methods Toolbox', Boorland International, 4585 Scotts Valley Drive, Scotts Valley, CA 95066, pp. 43-59, 1987.

Chapman. R, 'Introduction to electronics', Lecture notes, City University, 1982.

Clarke, T.A, Lindsey, N, 'Market survey.', internal market survey, City University, London, 1989.

Jones, F.H, Martin. M, 'The AutoCAD database book.', 3rd Edition, Ventana press, 1989.

Gallacher, K.J., Robinson. R.J, UK Patent application, GBB 2173301A, 1986.

Hitachi, Hitachi data sheet.

IBM Technical Reference, IBM Corp, 1984.

Oriel, Oriel Driver/ Control Model no 18548 and rotation stage, manufacturers literature, Oriel Corp, 250 Long Beach Blvd, PO Box 872, Stratford, Conn, 203/377-8282, U.S.A.

Rost, Manufacturers data sheet concerning PROTA 2, tunnel profiler, Austria, 1989.

Sentel, Sentel reference manual, Sentel Messtechnik GmbH, W. Germany.

Sharp, Sharp diode laser application notes.

Sliney. D.H, 'Radiation safety. The maximum permissible exposure levels: our knowledge of the hazards.', Optics and laser technology, Vol. 21, No 4, pp. 235-240, 1989.

Texas, 'Texas Instruments CCD line Imagers.', manufacturers literature, 1988.

Texas.1, 'Linear CCD operation at 10MHz.', Texas Instruments, Application report, pp. 1-9. 1986.

Texas.2, 'CCD Output Signal Processing.', Texas Instruments, Application report, pp. 1-15, 1986.

Toshiba, 'Laser diodes with visible 670 wavelength.', Manufacturers product catalogue, Toshiba Corp, 1-1, Shibaura, Ichome, Minato-Ku, Tokyo, 105-01, Japan.

Vero, 'IBM microcomputer accessories.', manufacturers literature, BICC VERO Electronics Ltd, Electron way, Chandlers Ford, Hampshire, SO5 3ZR, 1989.

CHAPTER 5.

Bird. R.G, 'EDM Traverses measurement, computation and adjustment', Longman Scientific and Technical, England, 1989.

Burnside. C.D, 'Electronic Distance Measurement.', Granada Publishing, 2nd Edition, U.K., 1982.

Cooper. M.A.R, 'Fundamentals of survey measurement and analysis.', Granada Publishing, U.K., 107 pages, 1974.

DO Industries, 'Laser diode products guide.', manufacturers literature, D.O. Industries, Inc, Laser products division, 200 Commerce Drive, Rochester, N.Y. 14623, U.S.A.

Garner. J.B, James. D, Bird. R.G, 'Surveying.', Pub The estates Gazette LTD, London, 1976.

Harrison. P.W, Tolmon. F.R, New. B.M, 'The laser for long distance alignment - a practical assessment.', Proc. Instn Civ. Engineers, 52, 1972.

Hultquist. P, 'Numerical methods for engineers and computer scientists.', Benjamin Cummings Pub. Co. Inc, 1988.

Kwiecien. J, 'The influence of temperature on the results of remote and continuous displacement measurements using a laser in closed premises.', 4th Int. Symposium on Geodetic measurements and deformations, Katowice, pp. 253-262, 1985.

Manual of Photogrammetry, Pub American society of photogrammetry, 4th Edition, pp. 413-452, 1980.

NEC, Product information, 'Gas Laser', 7th edition, NEC Electronics (Europe) GmbH, 1990.

Price. W.F, Uren. J, 'Laser surveying.', Van Nostrand Reinhold (International), pp. 155-156, 1990.

Robinson. G.D, 'Some aspects of the meteorology and refractive index of the air near the Earth's surface.', Int. Soc. Geodesy symposium on Electromagnetic Distance Measurement, pp. 96-103, September 1965.

Smith. A.L.S, 'He-Ne lasers are alive and well.', Laser Focus World, July, pp. 75-86, 1989.

Times, Anglo American Corporation of South Africa, advertisement, The Times, Friday, May 11th, p. 29, 1990.

West. G.A.W, Clarke, T.A, 'A survey and examination of subpixel measurement techniques.', PROC SPIE Vol. 1395, 'Close Range Photogrammetry meets machine vision', pp. 456-463, 1990.

Wong. K.W, Lew. M, Ke. Y, 'Experience with two vision systems.', Proc SPIE, Vol. 1395, Close-range photogrammetry meets machine vision., pp. 3-7. 1990.

CHAPTER 6.

Gotashby. A, Stockman G.C, Page C.V, 'A region-based approach to digital image registration with subpixel accuracy.', IEEE Trans. on Geoscience and Remote Sensing, Vol. GRS-24, No. 3, pp. 390- 399, 1986.

Havelock. D.I, 'Geometric precision in noise-free digital images', IEEE Trans. on Pattern Analysis and Machine Intelligence, Vol. PAMI-11, No. 10, pp. 1065-1075, 1989.

Huang. Y-D, Harley. I, 'CCD camera calibration without a control field.', Proc SPIE Vol. 1395, Close range photogrammetry meets machine vision, pp. 1028-1034, 1990.

Lange. G, Mossbacher. B, Purll. D.J, 'The ROSAT star tracker', Proc. SPIE Conf. on Instrumentation in Astronomy No. 6, 1986.

Lenz. R, 'Calibration of a color CCD camera with 3000x2300 picture elements.', PROC SPIE Vol. 1395, 'Close range photogrammetry meets machine vision.', pp. 104-111.

Li. Y, Young. T.Y, 'Subpixel edge detection and estimation with line scan camera.', Proc. IECON '87, pp. 667-675, 1987.

Oulamara. A, Tribillon. G, Duvernoy. J, 'Subpixel speckle displacement measurement using a digital processing technique', Journal of Modern Optics, Vol. 35, No. 7, pp. 1200-1211, 1988.

Pratt. W.K, 'Digital Image Processing.', John Wiley & Sons, U.S.A., pp. 553-567, 1978.

Slud. E.V, 'Subpixel translation-registration of random fields.', IEEE Trans. on Geoscience and Remote Sensing, Vol. GRS-26, No. 4, pp. 487-490, 1988.

Tian. Q, Huhns. M.N, 'Algorithms for subpixel registration.', Computer Vision, Graphics and Image Processing, Vol. 35, pp.220- 233, 1986.

West. G.A.W, Clarke. T.A, 'A survey and examination of subpixel measurement techniques.', PROC SPIE Vol. 1395, 'Close range photogrammetry meets machine vision.', pp. 456-464, 1990.

GLOSSARY.

1-D	One Dimension.
2-D	Two Dimension.
3-D	Three Dimension.
AM	Amplitude Modulation.
CCD	Charged Coupled Device.
CMM	Coordinate Measuring Machine.
DC	Direct Current.
DOF	Depth Of Field.
DXB	AutoCad binary data exchange format.
DXF	AutoCad ASCII data exchange format.
EDM	Electromagnetic Distance Measurement.
EL	Electro Luminescent.
FM	Frequency Modulated.
FMCW	Frequency Modulated Continuous Wave.
HeNe	Helium Neon.
Hg	Mercury.

IBM PC	International Business Machines Personal Computer.
kV	kilo Volts
k	kilo
LED	Light emitting diode.
LD	Laser Diode.
M	Mega.
m	milli.
mm	milli metre.
mrاد	milli radian.
ms	milli second.
MTF	Modulation Transfer Function.
mW	milli Watt.
n	nano.
ns	nano second.
PSD	Position Sensitive Detector.
RMS	Root Mean Square.